

Design Considerations for Embankment Protection During Road Overtopping Events

Jeffrey D. G. Marr, Principal Investigator

St. Anthony Falls Laboratory

Department of Civil, Environmental, and Geo- Engineering

University of Minnesota

June 2017

Research Project

Final Report 2017-21



To request this document in an alternative format, such as braille or large print, call [651-366-4718](tel:651-366-4718) or [1-800-657-3774](tel:1-800-657-3774) (Greater Minnesota) or email your request to ADArequest.dot@state.mn.us. Please request at least one week in advance.

1. Report No. MN/RC 2017-21	2.	3. Recipients Accession No.	
4. Title and Subtitle Design Considerations for Embankment Protection During Road Overtopping Events		5. Report Date June 2017	
7. Author(s) Jeffrey D. G. Marr, Matthew Hernick, Robert Gabrielson, Sara Mielke		6.	
9. Performing Organization Name and Address St. Anthony Falls Laboratory University of Minnesota 2 SE 3 rd Ave Minneapolis, MN 55414		8. Performing Organization Report No.	
12. Sponsoring Organization Name and Address Minnesota Local Road Research Board Minnesota Department of Transportation Research Services & Library 395 John Ireland Boulevard, MS 330 St. Paul, Minnesota 55155-1899		10. Project/Task/Work Unit No. CTS# 2013034	
		11. Contract (C) or Grant (G) No. (C) 99008 (wo) 50	
15. Supplementary Notes http:// mndot.gov/research/reports/2017/201721.pdf		13. Type of Report and Period Covered Final Report	
		14. Sponsoring Agency Code	
16. Abstract (Limit: 250 words) This report describes the research conducted by the University of Minnesota and project partners on roadway embankment overtopping by flood water. Roadway overtopping is a major safety concern for Minnesota transportation managers because of the potential for rapid soil erosion and mass wasting resulting in partial or complete failure of the roadway embankment. This multi-year research study focused on various aspects of the roadway embankment overtopping. A robust literature survey was performed to identify research, reports and other published knowledge that would inform the project. A field-based research campaign was developed with the goal of collecting data on the hydraulics associated with full-scale overtopping events. Finally, a series of laboratory experiments were conducted at the St. Anthony Falls Laboratory, University of Minnesota to study the hydraulic and erosional processes associated with embankment overtopping and in particular study of three slope protection techniques under overtopping flow. The largest component of the research project was the laboratory hydraulic testing, which focused on bare soil (base case) and three slope protection technologies. A full-scale laboratory facility was constructed to carry out the testing. Three erosion protection techniques were examined including 1) armored sod, 2) turf reinforcement mat, and 3) flexible concrete geogrid mat. Overtopping depths of up to 1-ft were used to determine the failure point of the protection technique and soil on both the 4h:1V and 6V:1H slopes. The full project report details the testing of each protection technique as well as observations and findings made during the testing.			
17. Document Analysis/Descriptors overtopping, embankments, laboratory tests, hydraulics, erosion		18. Availability Statement No restrictions. Document available from: National Technical Information Services, Alexandria, Virginia 22312	
19. Security Class (this report) Unclassified	20. Security Class (this page) Unclassified	21. No. of Pages 216	22. Price

Design Considerations for Embankment Protection During Road Overtopping Events

FINAL REPORT

Prepared by:

Jeffrey D. G. Marr
Matthew Hernick
Robert Gabrielson
Sara Mielke

St. Anthony Falls Laboratory
Department of Civil, Environmental, and Geo- Engineering
University of Minnesota

June 2017

Published by:

Minnesota Department of Transportation
Research Services & Library
395 John Ireland Boulevard, MS 330
St. Paul, Minnesota 55155-1899

This report represents the results of research conducted by the authors and does not necessarily represent the views or policies of the Minnesota Department of Transportation or the University of Minnesota. This report does not contain a standard or specified technique.

The authors, the Minnesota Department of Transportation, and the University of Minnesota do not endorse products or manufacturers. Trade or manufacturers' names appear herein solely because they are considered essential to this report because they are considered essential to this report.

ACKNOWLEDGMENTS

The authors would like to thank the members of the Technical Advisory Panel (TAP) for their support and valuable input. TAP members included J.T. Anderson (Technical Liaison), Alan Rindels (Administrative Liaison), Daniel Sullivan (Administrative Liaison), Mitch Bartelt (Administrative Liaison), Lori Belz, Graig Gilbertson, Andrea Hendrickson, and Dwayne Stenlund. Several members of the technical staff at St. Anthony Falls Laboratory (SAFL) contributed along the course of the project, including the author of the MATLAB code, Chris Milliren. Craig Taylor served as the initial Principal Investigator. Several persons and organizations generously donated materials and/or installation expertise, including Matt Motz and Sean Stallo of Motz Enterprises, manufacturers of Flexamat®, Greg Halvorsen of Brock White Construction Materials, Michael T. Ramy, Jr. of Ramy Turf Products, and Nick Kentros of Tri-State Bobcat, Inc. Special thanks to Luke Riveness, undergraduate student engineering from Bethel University, for his commitment to the laboratory work over the summer of 2015.

TABLE OF CONTENTS

CHAPTER 1: Introduction.....	1
1.1 Roadway Overtopping	1
1.2 Project Objective	2
1.3 Scope of Present Research	5
1.4 Project Team.....	5
CHAPTER 2: Previous Studies and Relevant Literature	6
2.1 Roadway Overtopping	6
2.1.1 Discharge Characteristics of an Embankment-Shaped Weir.....	6
2.1.2 Federal Highway Administration FHWA – RD-86-126.....	6
2.1.3 Federal Highway Administration FHWA-RD-88-181	7
2.1.4 Hydraulic Stability of Conlock and Conlock II Concrete Block Revetment System during Overtopping Flow (St. Anthony Falls Laboratory, University of Minnesota, Project Report No. 369)	8
2.1.5 Hydraulic Stability of Channel Lock™ Concrete Block Revetment System during Overtopping Flow (St. Anthony Falls Laboratory, University of Minnesota, Project Report No. 396)	9
2.1.6 Hydraulic Stability of Hand Placed Positive Interlocking Concrete Block Revetment System during Overtopping Flow (St. Anthony Falls Laboratory, University of Minnesota, Project Report No. 428)	9
2.1.7 Protecting Road Embankments from Overtopping Flow	9
2.2 Additional References.....	9
2.2.1 Stability of riprap and discharge characteristics, overflow embankments, Arkansas River, Arkansas: Hydraulic model investigation	10
2.2.2 Riprap Design for Overtopping Flow	10
2.2.3 Physical Modeling of Overtopping Erosion and Breach Formation of Cohesive Embankments	10
2.2.4 Hydraulics of Embankment Weirs.....	10
2.2.5 Embankment overtopping protection systems.....	11

2.2.6 A Study of Embankment Performance during Overtopping	11
2.2.7 Stabilization of Angular-Shaped Riprap under Overtopping Flows.....	11
2.2.8 Evaluation of Overtopping Riprap Design Relationships.....	11
2.2.9 Enhanced Stone Sizing for Overtopping Flow	12
CHAPTER 3: Laboratory Test Methods	13
3.1 Experimental Setup	13
3.1.1 Test Facility.....	13
3.1.2 Instrumentation	15
3.2 Embankment Stabilization Techniques Tested.....	21
3.3 Experimental Procedures	28
3.3.1 Soil placement and compaction.....	28
3.3.2 Stabilization technique installation.....	28
3.3.3 Tailwater condition	33
3.3.4 Determination of failure.....	34
3.3.5 Point gauge measuring system	34
3.3.6 Flow control and monitoring.....	35
3.3.7 Extended Shoulder Paving or Partial Slope Paving	36
3.4 Summary of Runs.....	38
CHAPTER 4: Laboratory Test Results	39
4.1 Technique 0: Bare Soil	39
4.1.1 Test 1. 4H:1V Slope- Quick Test	39
4.1.2 Test 2. 6H:1V Slope	45
4.1.3 Test 3. 4H:1V Slope with Extended Shoulder Paving- Quick Run.....	51
4.2 Technique 1: Armored Sod	57
4.2.1 Summary of Technique	57

4.2.2 Test 1. 4H:1V Slope- Quick Test	57
4.2.3 Test 2. 6H:1V Slope	63
4.2.4 Test 3. 4H:1V Slope	69
4.2.5 Test 4. 4H:1V Slope with Extended Shoulder Paving	75
4.3 Technique 1A: Armored Sod.....	83
4.3.1 Technique Summary:.....	83
4.3.2 Test 1. 4H:1V Slope- Quick Test	83
4.3.3 Test 2. 4H:1V Slope with Extended Shoulder Paving	90
4.4 Technique 2: Turf Reinforcement Mat with Fiber-Reinforced Matrix	97
4.4.1 Technique Summary:.....	97
4.4.2 Test 1. 4H:1V Slope-Quick Test	97
4.4.3 Test 2. 6H:1V Slope	104
4.5 Technique 3: Flexible Concrete Geogrid Mat	111
4.5.1 Technique Summary.....	111
4.5.2 Test 1. 4H:1V Slope- Quick Test	111
4.5.3 Test 2. 6H:1V Slope	117
4.5.4 Test 3. 4H:1V Slope	123
CHAPTER 5: Field Campaign Summary	130
5.1 Roadway Overtopping Field Monitoring Scope, Procedures, and Equipment.....	130
5.2 Summary of 2013 and 2014 Monitoring Seasons	130
5.3 Field Monitoring Discussion	131
CHAPTER 6: Findings/Discussion.....	133
6.1 Stabilization Technique Performance.....	133
6.1.1 Armored Sod (Techniques 1 and 1A)	133
6.1.2 Turf Reinforcement Mat and Fiber Reinforced Matrix (Technique 2)	134

6.1.3 Flexible Concrete Geogrid Mat (Technique 3)	135
6.1.4 Summary Tables	135
6.2 Failure Mechanisms and Locations.....	142
6.2.1 Failure location:.....	142
6.2.2 Effect of slope continuity, soil contact, and compaction	143
6.2.3 Slope Angle Comparison: 4H:1V and 6H:1V.....	145
6.2.4 Effect of Extended Shoulder Paving (Inslope Paving)	148
6.3 Overtopping Protection Guidance	148
6.3.1 Construction Costs	148
6.3.2 Installation, Maintenance, and Longevity	149
6.4 Limitations of the Research and Applications for Further Study	151
6.4.1 Limitations of the Research.....	151
6.4.2 Applications for further study	151
REFERENCES	153
APPENDIX A: Field site monitoring and inspection reports	
APPENDIX B: Estimated construction costs of selected embankment erosion stabilization techniques	

LIST OF FIGURES

Figure 1.1. Image of spring flooding in Red River Valley. (photo credit, J.T. Anderson)	2
Figure 1.2 Hydraulic flow regimes and overtopping flow zones. Adapted from Clopper and Chen (1988). 3	3
Figure 1.3. Elements of a rural, two-lane roadway (Adapted from McGee et al., 2009, FHWA-SA-09-024))	3
Figure 1.4. Overtopping event on MN TH1 near Oslo, Minnesota, March 21, 2010. “TH 1 at Jct 220 near Oslo 20100321”. Note road signs in yellow circle. Photo by JT Anderson, MnDOT	4
Figure 1.5. Same location, eight days later. Temporary stone fill dumped in some scour holes. Photo by JT Anderson, MnDOT.	4
Figure 2.1 Profile of hydraulic testing facility from Clopper and Chen 1988.....	8
Figure 3.1. Profile view schematic of testing flume, 4H:1V slope. The parallel 6H:1V flume is identical except for the downstream slope angle and length.....	14
Figure 3.2. Flume during construction. Looking downstream from the headbox. The 6H:1V slope is to the left of the center wall, and the 4H:1V slope is to the right of the center wall.	14
Figure 3.3. Perspective view of the flume apparatus with labels. 4H:1V slope is to the right.	15
Figure 3.4. Pump #1 on the model floor.	16
Figure 3.5. SAFL data acquisition carriage scanning pre-flow topography. The laser sheet is projected onto the soil near the bottom of the photo.	18
Figure 3.6. Prepared bare soil slope in the flume.....	19
Figure 3.7.The grainsize distribution for three samples of the flume test soil, plus initial sample.....	20
Figure 3.8. Triangular textural classification chart, from MnDOT Pavement Design Manual, Chapter 3. Data from grainsize analysis plots material in the loam category, indicated with red mark.	20
Figure 3.9. Stabilization techniques tested. Upper left: Technique 1, “Armored Sod” with erosion control blanket; Upper right: Technique 1A, “Armored Sod” with real sod; Lower left: Technique 2, Turf Reinforcement Mat (TRM) with Fiber Reinforced Matrix (FRM); Lower right: Technique 3, Flexible Concrete Geogrid Mat.	22
Figure 3.10. Layers of the armored sod. Image on the left shows the layers of the Erosion Control Blanket. Image on the right shows the plastic geogrid.....	23
Figure 3.11 Bluegrass sod used in Technique 1A.....	24

Figure 3.12 Sod covered with geogrid	24
Figure 3.13. Photo on the left shows the turf reinforcement mat installed on the soil. Photo on the right shows the Fiber Reinforced Matrix being applied.....	25
Figure 3.14. Photo on the left shows the concrete blocks and flexible geogrid underlain by the turf reinforcement mat. In the photo on the right, the turf reinforcement mat is overlaying the soil and the concrete blocks and flexible geogrid is being hoisted into place.	26
Figure 3.15. View looking upslope. Armored sod material wrapped around a piece of lumber and bolted to framing under the shoulder. Once backfilled with soil, the armored sod material on the shoulder would be flipped down to cover the slope.	29
Figure 3.16. Staple pattern for 4H:1V and 6H:1V slopes. Pattern continues to toe of slope, and along any material extended on the surface of the flat runout area.....	30
Figure 3.17. Flexamat® “paved” into the shoulder with Portland cement grout to transition onto the slope. Seam of paving and shoulder sealed with a polyurethane single component sealant (white). Flow is left to right in this image.	31
Figure 3.18. Angle iron fastened to flume wall (left). Flexible concrete geogrid mat installation example with backer rod and spray foam insulation used to fill the void between the Flexamat ® and angle iron resting on top of concrete (right).	32
Figure 3.19. Progressive stages of unprotected embankment erosion under freefall and high tailwater conditions. From Clopper and Chen (1988).	33
Figure 3.20. Point gauge being used on slope to check for erosion and voids in soil beneath erosion control blanket.....	35
Figure 3.21. Point gauge at road crest in use to measure depth of flow over the crest of the model road cross section.....	36
Figure 3.22. Simulated extended shoulder paving in the 4H:1V flume, prior to installation of stabilization materials. A dashed line has been added at the shoulder edge at the top of the slope.....	37
Figure 4.1. Pre-run 4H:1V slope bare soil looking downstream from shoulder.	40
Figure 4.2. 4H:1V Slope mid-run with prevalent channels of flow looking downstream. Less than two minutes of run time.	40
Figure 4.3. Mid-run 4H:1V slope looking upstream. Flow channelized on slope with trough forming on the transition from shoulder to slope.....	41
Figure 4.4. Number of runs within this test with flow rate and duration of time at each flow rate.....	42

Figure 4.5 Topographic difference plot from zero to two minutes of run time, showing prominent channels being carved on slope. Elevation units are in millimeters.....	43
Figure 4.6 Topographic difference plot from zero to eight minutes of run time. Note scour and trough formation at upstream transition from shoulder to slope and primary channel of erosion.....	43
Figure 4.7. (Left). Aerial view of interpolated compaction data on slope interpolated with mid-shoulder starting at zero. The left vertical axis is distance in millimeters from mid-shoulder. Compaction is presented in units of tons per square foot. The white area is the shoulder. The color bar on the right of the figure gives color range for compaction values in tons/ft ² . (Right). Aerial view of scanned slope after eight minutes of run time showing channels of erosion.	44
Figure 4.8. (Left) Initiation of flow on 6H:1V slope looking upstream. (Right) Erosion began immediately with incisional channels forming on slope.....	46
Figure 4.9. Channelized flow and separation form the edge of the shoulder forming trough at the transition.....	47
Figure 4.10. Number of runs within this test with flow rate and duration of time at each flow rate.....	48
Figure 4.11. Topographic difference plot from zero to two minutes of run time. Note the large area of erosion immediately after the shoulder and channels downslope of it.....	48
Figure 4.12. Topographic difference plot from zero to 10 minutes of run time. Only ten minutes of run time has undermined the shoulder.	49
Figure 4.13. (Left). Aerial view of interpolated compaction data on slope interpolated with mid-shoulder starting at zero. Compaction is presented in units of tons per square foot. White area is the shoulder. The color bar on the right of the figure gives color range for compaction values. (Right). Scan of slope after 10 minutes of run time.....	50
Figure 4.14. (Left). Looking upstream at 4H:1V slope with extended pavement (white) before testing. (Right). Looking downstream at flow over 4H:1V slope during 2-4 minute run no prevalent channel on upper slope. Channelization begins on the lower portion of slope.....	52
Figure 4.15. Looking upstream after approximately 25 minutes of run time. Channels and depressions forming, no trough or main channel forming.	53
Figure 4.16. Number of runs within this test with flow rate and duration of time at each flow rate.....	54
Figure 4.17. Topographic difference plot from zero to two minutes of run time.	54
Figure 4.18. Topographic difference plot from two to 22 minutes of run time. Slope now has channels but not as definitive as other runs of bare soil, no primary channel on slope was eroded.	55

Figure 4.19. (Left). Aerial view of interpolated compaction data on slope interpolated with mid-shoulder starting at zero. Compaction is presented in units of tons per square foot. The white region is the extended shoulder. The color bar on the right of the figure gives color range for compaction values. (Right). Scan of slope after 32 minutes of run time..... 56

Figure 4.20. Looking upstream at slope no erosion occurring at 1.1cfs..... 58

Figure 4.21. Start of erosion about ½ way down the slope indicated by the depression leading to a mound that aerated the flow in the center of the flume. Looking downslope from shoulder at mound and hydraulic jump. 58

Figure 4.22. Post flow erosion after 2.7cfs testing. Note the mound near bottom of slope and depression along the left side of the flume looking upstream. Sediment rich water on slope and in tail water indicating erosion occurring on the slope under the ECB. 59

Figure 4.23. Slope with the shoulder at the top of the photo after ECB was removed post-testing. Note the undermining of shoulder and extensive erosion not seen with ECB still in place on previous photos. 59

Figure 4.24. Summary of runs with flow rate and duration. 60

Figure 4.25. Topographic difference plot from zero to 1.5 hours of run time. Minimal erosion on the slope shown here with a depression after the toe of the slope..... 61

Figure 4.26. Topographic difference plot from zero to 1.93 hours minutes of run time. Note large area of erosion on the edge of the slope with soil deposition at the toe of the slope under the ECB. 61

Figure 4.27. Topographic difference plot of bare soil before testing to 1.93 hours of run time with ECB removed. Removing the ECB reveals the extent of erosion that was occurring beneath the ECB. 62

Figure 4.28. (Left) Aerial view of interpolated compaction data on slope. The vertical axis is distance in millimeters from mid-shoulder. Compaction is presented in units of tons per square foot. White area is the shoulder. The color bar on the right of the figure gives color range for compaction values. (Right). Aerial view of scanned slope after eight minutes of run time and ECB was removed showing large depression and channels near pavement edge. 62

Figure 4.29. Running at 1cfs on 6H:1V slope. View from shoulder looking downstream in flume. 64

Figure 4.30. Image of early sign of erosion as a depression 75% of the way down slope caused water to separate from bed. Image is looking downstream near toe of slope with tail-water still draining. 64

Figure 4.31. Flow on slope becoming aerated because of the increasing depth of erosion and separation of the geogrid from the soil. The image shows the formation of a hydraulic jump at bottom of the slope. 65

Figure 4.32. Looking upstream at bare soil post run with treatment removed showing different locations of erosion on the slope.	65
Figure 4.33. Number of runs with flow rate and duration of run time.	66
Figure 4.34. Topographic difference plot from zero to 16 hours of run time. Showing a depression and elevated mound $\frac{3}{4}$ of the way down the slope from the shoulder. Smaller depressions are also on the upper $\frac{1}{4}$ of the slope and at mid-slope	67
Figure 4.35. Topographic difference plot of final bare soil condition vs. initial bare soil condition. Erosional areas are easily identified here because the ECB covering was removed for the scan.....	67
Figure 4.36. (Left). Aerial view of interpolated compaction data on slope. The vertical axis is distance in millimeters from mid-shoulder. Compaction is presented in units of tons per square foot. (Right). Aerial view of final bare soil scanned after the stabilization material was removed from the slope.	68
Figure 4.37. Looking downstream at slope with indications of immediate erosion by murky tail-water during the first test.	70
Figure 4.38. Close up of shoulder and slope transition looking upstream. Note the large depression immediately after the shoulder and mound of soil just downstream.....	70
Figure 4.39. After only a few more minutes of run time the erosion has expanded to nearly the entire width of the transition from shoulder to slope.	71
Figure 4.40. Number of runs with flow rate and duration of run time.	72
Figure 4.41. Topographic difference plot from zero to 30 minutes.	72
Figure 4.42. Topographic difference plot of initial bare soil vs. final bare soil after 30 minutes of testing. The large deposition at toe of slope is the ECB flipped over onto flat area, and not actually soil deposition.	73
Figure 4.43. (Left). Aerial view of interpolated compaction data on slope. Compaction is presented in units of tons per square foot. (Right). Final bare soil scan showing areas of minor erosion.	74
Figure 4.44. Looking upstream at slope with no noticeable erosion. Note the clear tail water.	76
Figure 4.45. Looking upstream after 1.5 hours of run time. Erosion is observed 1.5ft downstream from the shoulder in the form of a depression in river-left half of flume.....	76
Figure 4.46. Looking downstream from the shoulder during 2-4 hour testing period. Note the large area of erosion occurring near the shoulder specifically near the left wall.	77

Figure 4.47. Looking downstream from shoulder near the end of the 4-6 hour run. Note the widespread area of erosion and flow separation from the shoulder hitting an angle where the deepest area of erosion is located.	77
Figure 4.48. Looking upstream at shoulder and slope after stabilization material was removed. Note the remaining soil that was not undermined but close to it after 6 hours of run time.	78
Figure 4.49. Number of runs with flow rate and duration of run time.	79
Figure 4.50. Topographic difference plots from zero to 4 hours of run time.	80
Figure 4.51. Topographic difference plots from zero to 6 hours of run time.	80
Figure 4.52. Topographic difference plot of initial bare soil vs. final bare soil after 6 hours of run time. .	81
Figure 4.53. (Left). Aerial view of interpolated compaction data on slope with mid-shoulder starting at zero. Values measured in tons per square foot. White area is the extended pavement section. (Right). Scan of final bare soil after the ECB was removed.	82
Figure 4.54. Looking downstream from shoulder. Installed sod and geogrid before testing.	84
Figure 4.55. Looking downstream from shoulder. Testing 30-60 min, no noticeable large areas of erosion.	84
Figure 4.56. Looking upstream at toe of slope. Erosion beginning at toe of slope, undermining sod and washing some pieces away. Erosion working up the slope from run-out area.	85
Figure 4.57. Looking upstream from run-out area. Stabilization material removed showing the extent of the erosion starting at the toe of the slope and working up towards the shoulder.	85
Figure 4.58. Number of runs with flow rate and duration of run time.	86
Figure 4.59. Topographic difference plot from zero to 60 minutes of run time.	87
Figure 4.60. Topographic difference plot from zero to 4.5 hours of run time. Note the unchanged upper slope and erosion at the bottom of the slope.	87
Figure 4.61. Topographic difference plot of initial bare soil vs. final bare soil after 4.5 hours of run time. Upper slope to approximately 2500mm downslope still intact.	88
Figure 4.62. (Left). Aerial view of interpolated compaction data on slope with mid-shoulder starting at zero. Compaction measured in tons per square foot. (Right). Plan view of final bare soil scanned after all sod and geogrid was removed from the slope.	89
Figure 4.63. Looking upstream during first two hour run, no noticeable erosion anywhere on slope.	91

Figure 4.64. Aerial view of the slope just past halfway down the slope a large depression formed quickly at the seam of two pieces of sod just minutes before the end of the 2-4 hours testing time.	91
Figure 4.65. During final 4-5.5 hour run, catastrophic erosion took place. Most of the lower slope began eroding under the sod, which had come loose but was held from being washed away by the geogrid and staples.	92
Figure 4.66. Looking upstream at shoulder to slope transition after the geogrid has been removed. Most of the transition is still intact while the areas where there was a seam between the rolled out pieces of sod allowed water to penetrate and erode the slope surface under the sod which was being partly held in place by the geogrid and landscaping staples.	92
Figure 4.67. Number of runs with flow rate and duration of run time.	93
Figure 4.68. Topographic difference plot from zero to two hours of run time showing little visible erosion.	94
Figure 4.69. Topographic difference plot from zero to four hours of testing time. Note the large deposition at the toe of the slope and depression upslope of it.	94
Figure 4.70. Topographic difference plot of initial bare soil vs. final bare soil after 9.5 hours of run time. The upstream slope is still intact. Note that the positive elevation on pavement section is the geogrid that has been flipped back over the surface.	95
Figure 4.71. (Left). Aerial view of interpolated compaction data on slope with mid-shoulder starting at zero. Compaction measured in tons per square foot. (Right). Aerial view of final bare soil scanned after all sod and geogrid was removed from the slope.	96
Figure 4.72. First run on TRM-FRM at 0.89 cfs and 0.5-inches of overtopping.	98
Figure 4.73. View from upstream after 1 hour of run time, note that some of the FRM has been washed away from the surface of the TRM.	98
Figure 4.74. View from upstream during 2.5-3.0 hour run. Note that most of the FRM has been washed away at this point.	99
Figure 4.75. View from downstream after 3.5 hours of run time. Erosion working up the slope from the toe under the TRM.	99
Figure 4.76. Number of runs with flow rate and duration of run time.	100
Figure 4.77. Topographic difference plot from zero to 1.5 hours of run time. Note that there is minimal erosion on the slope.	101
Figure 4.78. Topographic difference plot from zero to 2.5 hours of run time. Erosion and deposition occurring at the toe of the slope.	101

Figure 4.79. Topographic difference plot from zero to 3.5 hours of run time. Extensive erosion at the toe of the slope.	102
Figure 4.80. Topographic difference plot from initial bare soil vs. final bare soil after 3.5 hours of run time. Substantial erosion near the toe of the slope. The large depositional area at 4300 mm is the TRM after being flipped onto the flat run-out area.	102
Figure 4.81. (Left). Aerial view of interpolated compaction data on slope with mid-shoulder starting at zero. Compaction measured in tons per square foot. (Right). Aerial view of final bare soil scanned after TRM and FRM was removed from the slope.	103
Figure 4.82. View from downstream during 0-2 hour run. Minimal erosion noticed. FRM is being washed away while TRM is remaining stapled to the slope.	105
Figure 4.83. View from upstream during 2-4 hour run. Noticeable depression after shoulder along right edge of slope. More of the FRM is being removed from testing.	105
Figure 4.84. View looking upstream after six hours of run time. Almost all of the FRM has been washed away and the depression near the shoulder has gotten deeper.	106
Figure 4.85. View looking downstream after 8.25 hours of run time. The large amount of erosion along right wall represents failure.	106
Figure 4.86. Number of runs with flow rate and duration of runtime.	107
Figure 4.87. Topographic difference plot from zero to four hours of run time. Note that there is little noticeable erosion with the difference plot.	108
Figure 4.88. Topographic difference plot from zero to eight hours of run time. The start of erosion near the shoulder is detected.	108
Figure 4.89. Topographic difference plot from zero to 8.25 hours. Erosion quickly expanded near the top of the slope leading to failure.	109
Figure 4.90. (Left). Aerial view of interpolated compaction data on slope with mid-shoulder starting at zero. Compaction measured in tons per square foot. (Right). Aerial view of final bare soil scanned after TRM and FRM was removed from the slope.	110
Figure 4.91. Image from Run 1 with discharge set at 0.9 ft ³ /s. There was no noticeable erosion over entire 30 min run.	112
Figure 4.92. View looking downstream from the shoulder during 1 to 1.5 hour run with flow of 2 ft ³ /s and overtopping depth of 3 inches. The flow was aerated and very turbulent.	112
Figure 4.93. Looking upstream at slope near end of 1.5 hour run. Aeration near mid-slope and erosion/deposition areas stepping down the slope.	113

Figure 4.94. Number of runs with flow rate and duration of run time.	114
Figure 4.95. Topographic difference plot from zero to 1.5 hours of run time. Note the erosion in a stepped fashion with two depressions and two deposition areas in the middle of the flume.	115
Figure 4.96. Scan of the final bare soil after the Flexamat [®] was removed. Two large depressions are shown here, similar to what is seen in the difference plot of zero vs 1.5 hours of run time, but more prevalent when seen without the Flexamat [®] covering it.	115
Figure 4.97. (Left). Aerial view of interpolated compaction data on slope. Compaction is presented in units of tons per square foot. (Right) Aerial view of final bare soil scanned after Flexamat [®] Plus was removed from slope.	116
Figure 4.98. View from shoulder after Flexamat [®] Plus installation and before testing.	118
Figure 4.99. View from shoulder looking downstream during 10-12 hour run. No noticeable erosion on the slope.	118
Figure 4.100. View from shoulder looking downstream during 22-24 hour run. No noticeable erosion, smooth water surface to about mid-slope.	119
Figure 4.101. Number of runs with flow rate and duration of run time.	120
Figure 4.102. Topographic difference plot from zero to 18 hours of run time. No erosion noticeable on the slope.	121
Figure 4.103. Topographic difference plot from zero to 30 hours of run time. Apparent differences shown are due to concrete blocks shifting downslope of their original resting place.	121
Figure 4.104. (Left) Aerial view of interpolated compaction data on slope with mid-shoulder starting at zero. Compaction measured in tons per square foot. (Right) Aerial view of final bare soil scanned after Flexamat [®] Plus removed from slope.	122
Figure 4.105. View from shoulder looking downstream during first two hour run. Highly turbulent flow but no noticeable erosion on slope.	124
Figure 4.106. View from downstream looking up at slope during 24.35 to 25.33 hour run. Mid-slope mound has been eroded and flat upper slope has stabilized and new mound at toe of slope is causing aeration.	124
Figure 4.107. View from downstream looking up at slope during 4-6 hour run. Note the depression and subsequent aggradation at mid-slope causing aeration.	125
Figure 4.108. View from downstream looking up at slope during 17.25-20.25 hour run. The slope did not drastically change over 10 hours of run time from the first sign of erosion.	125

Figure 4.109. Number of runs with flow rate and duration of run time.	126
Figure 4.110. Topographic difference plot from zero to two hours of run time. No noticeable erosion on the slope.	127
Figure 4.111. Topographic difference plot from zero to four hours of run time. This increments saw a measureable change in slope elevation with a depression at mid-slope and aggradation immediately after.....	127
Figure 4.112. Topographic difference plot from zero to 25.33 hours of run time (end of test).	128
Figure 4.113. Topographic difference plot from initial bare soil vs. final bare soil after 25.33 hours of run time. Note the similarity to the previous figure in the location of the depression and the intact portion of the soil near the shoulder-slope transition.	128
Figure 4.114. (Left) Aerial view of interpolated compaction data on slope with mid-shoulder starting at zero. Compaction measured in tons per square foot. (Right) Aerial view of final bare soil scanned after Flexamat® Plus was removed from slope.....	129
Figure 5.1. Field monitoring site locations on a map of northern Minnesota counties.	131
Figure 6.1. View from above of the bare soil after the ECB was removed post-testing, 6H:1V slope. Note the indicated holes where the staples were holding down the stabilization material. Flow was from right to left.....	144
Figure 6.2. Flexible concrete geogrid mat tested on the 4H:1V slope at 9.90 ft ³ /s and approximately 25 hours of run time. Concrete blocks may be pushed down with a probe rod 3-4 inches before touching the slope surface ¾ of the way down the slope.	145

LIST OF TABLES

Table 3.1. Manufacturers and MnDOT classifications for products used in Techniques 1-3.	27
Table 3.2. List of techniques used to terminate stabilization material for all experiments.	33
Table 3.3. Matrix of slopes and techniques tested. Test completion marked with "X".	38
Table 4.1. Test data for bare soil, 4H:1V slope.	42
Table 4.2. Statistics of compaction on 4H:1V slope for bare soil testing.	44
Table 4.3. Run data for bare soil, 6H:1V slope.	47
Table 4.4. Statistics of compaction on 6H:1V slope for bare soil testing.	50
Table 4.5. Run data for bare soil, 4H:1V slope with extended shoulder paving.	53
Table 4.6. Statistics of compaction on 4H:1V slope with extended pavement for bare soil testing.	56
Table 4.7 Run data for Armored Sod (ECB), 4H:1V slope "quick" run.	60
Table 4.8. Statistics of compaction on 4H:1V slope for ECB testing.	63
Table 4.9. Run data for Armored Sod (ECB), 6H:1V slope.	66
Table 4.10. Statistics of compaction on 6H:1V slope for erosion control blanket testing.	68
Table 4.11. Run data for Armored Sod (ECB), 4H:1V Slope	71
Table 4.12. Statistics of compaction on 4H:1V slope for erosion control blanket testing.	74
Table 4.13. Run data for Armored Sod (ECB), 4H:1V slope with extended shoulder paving.	79
Table 4.14. Statistics of compaction on 4H:1V slope with extended pavement for erosion control blanket testing.	82
Table 4.15. Run data for Armored Sod (1A), 4H:1V slope "quick" run	86
Table 4.16. Statistics of compaction on 4H:1V slope for sod testing.	89
Table 4.17. Run data for Armored Sod (1A), 4H:1V slope with extended shoulder paving.	93
Table 4.18. Statistics of compaction on 4H:1V slope with extended pavement for bare sod testing.	96
Table 4.19. Run data for TRM with FRM, 4H:1V slope "quick" run.	100
Table 4.20. Statistics of compaction on 4H:1V slope for TRM-FRM testing.	103

Table 4.21. Run data for TRM with FRM, 6H:1V slope.	107
Table 4.22. Statistics of compaction on 6H:1V slope for TRM-FRM testing.	110
Table 4.23. Run data for Flexible Concrete Geogrid Mat, 4H:1V slope "quick" run.	114
Table 4.24. Statistics of compaction on 4H:1V slope for Flexamat®-Plus testing.	116
Table 4.25. Run data for Flexible Concrete Geogrid Mat, 6H:1V slope.	120
Table 4.26. Statistics of compaction on 6H:1V slope for Flexamat® Plus testing.	122
Table 4.27. Run data for Flexible Concrete Geogrid Mat, 4H:1V slope.	126
Table 4.28. Statistics of compaction on 4H:1V slope for Flexamat® Plus testing.	129
Table 6.1. Summary of hydraulic conditions at first noticeable erosion and average measured compaction.	136
Table 6.2. Summary of hydraulic data at noted "failure" and final flow.	136
Table 6.3. Initial erosion location and description of the progression of erosion.	138
Table 6.4. Description of slope condition when testing was stopped and predicted result with continued flow.	140
Table 6.5. Comparison of 6H:1V and 4H:1V mid-slope data, Technique 1, Armored Sod.	146
Table 6.6. Comparison of 6H:1V and 4H:1V mid-slope data, Technique 2, TRM with FRM.	147
Table 6.7. Comparison of 6H:1V and 4H:1V mid-slope data, Technique 3, Flexible Concrete Geogrid Mat.	147
Table 6.8. Estimated construction costs of various embankment stabilization techniques.	149
Table 6.9. Comparison of selected properties for tested stabilization techniques.	149

EXECUTIVE SUMMARY

This report describes the research conducted by the University of Minnesota and project partners on roadway embankment overtopping by flood water. Roadway overtopping is a major safety concern for Minnesota transportation managers because of the potential for rapid soil erosion and mass wasting, resulting in partial or complete failure of the roadway embankment. Flooding and overtopping of roadways is a hazard that exists throughout the state, with most recent events occurring in western Minnesota within the Red River Valley, where the topography is flat and roadway surfaces represent the highest elevations. During flooding events, the road surface can act as a broad-crested weir, creating pooled water “upstream” of the roadway. Floodwaters flow across the road surface, over the shoulder, and down the sloped embankment. It is the flow of water down the soil embankment slope and the resulting hydraulic forces on the slope surface that can lead to erosion and failure of the road embankment. The risk to safety and damage to property that results from embankment failure are expensive and slow to repair and many times severely limit access between communities.

This multi-year research study, funded by the Minnesota Department of Transportation and the Minnesota Local Road Research Board, focused on multiple aspects of the roadway embankment overtopping. The project included three primary components. First, a robust literature survey was performed to identify research, reports, and other published knowledge that would inform the project. Second, a field-based research campaign was developed with the goal of collecting data (of which there is presently very little available) on the hydraulics associated with full-scale overtopping events. Third, a series of laboratory experiments were conducted at the St. Anthony Falls Laboratory, University of Minnesota, to study the hydraulic and erosional processes associated with embankment overtopping and, in particular, three slope protection techniques under overtopping flow.

There is a sizeable amount of published literature on overtopping that dates back to the early to mid-20th century. Fundamental work focused on the hydraulics of flow over prismatic embankments without consideration of erosion or bed shear stress. There is also a body of work focused on general soil embankment flow and erosion. For these publications, the focus was on erosion protection methods that mostly examine the use of riprap and developing methods for appropriately sizing the riprap materials. The research team focused most of our efforts on studying published research and reports that examined roadway embankment overtopping. In these reports, which include laboratory and field research, there is good information on hydraulic and erosional processes as well as assessment of some protection techniques. This final project report provides a review of the body of literature associated with embankment overtopping.

The field research component of the project, led by Wenck Associates, involved site monitoring and inspection out of a field office located near the watershed of the Red River of the North. Site monitoring involved recording flood stage at several roadway locations during overtopping events. Post-flood inspections were conducted to evaluate the failure modes observed under natural conditions. Monitoring and inspection field sites were selected based on their likelihood of overtopping and use of scour protection systems, if present. Monitoring seasons included 2013, 2014, 2015, and 2016. In the

2013 and 2014 seasons, three overtopping events were captured. During the remainder of the study, no overtopping events occurred due to low snowfall and precipitation quantities. The field work methods were summarized in a project report along with instrumentation and provided to MnDOT and LRRB such that future field work can be carried out by state transportation agencies directly.

The largest component of the research project involved laboratory hydraulic testing of bare soil (base case) and three slope protection technologies. A full-scale laboratory facility was constructed at the St. Anthony Falls Laboratory. The facility simulated a transverse section of a roadway and included an upstream water supply, the road crest, shoulder, and downstream embankment slope. The research team and technical advisors constrained the project to only look at low tailwater overtopping scenarios. Two slopes were included in the design, 4H:1V and 6H:1V. For each simulation, a soil embankment was created using a silty sand material with a measured composition of 11% clay, 44% silt and 45% sand. Soil was placed in the flume at a depth of 12 inches and was compacted prior to testing. A series of bare soil tests were carried out as a base case of no protection. Three erosion protection techniques were examined including 1) armored sod, 2) turf reinforcement mat, and 3) flexible concrete geogrid mat. Overtopping depths of up to 1 foot were used to determine the failure point of the protection technique and soil on both the 4h:1V and 6V:1H slopes. The full project report details the testing of each protection technique as well as observations and findings made during the testing. Key observations include:

- Bare soil with zero vegetative cover was highly susceptible to erosion during overtopping flows and represent a worst-case situation that should be avoided in practice. New installation should ensure that some vegetation is established prior to the first overtopping event.
- Of the three techniques studied, all approaches reduced the amount of soil erosion, but the flexible concrete geogrid mat provided the greatest protection against high bed shear stresses. Flexible concrete geogrid mat was able to withstand up to 5.7 lb/ft² of bed shear stress. We note that these results are for overtopping immediately after installation. Established vegetation and root growth would likely improve performance of all protection techniques.
- Even under tight control of the experimental variables (e.g., soil composition, soil compaction, installation techniques, and hydraulic variables), a variety of failure locations, timing of failures, and initiation stress were observed. This finding is important—the initiation of erosion, which can quickly evolve into mass failure of an embankment, appears to be linked to small-scale heterogeneities with the soil, the variability in erosion control material, and subtle variability in the final placement of the protection technique.
- The tests revealed that failure of soil occurred in locations where the protection technique physically separated from the soil surface, exposing a direct pathway for water to flow over the soil. Techniques that were not flexible and could not articulate with the soil surface (Technique 1 and 1A) were the worst performers in this regard.
- A common location for failure was the toe of the slope due to low tailwater conditions of the experiments and the location of a hydraulic jump.
- A common location for failure was the upstream transition from the shoulder to the soil slope.

- The tests show a strong correlation between embankment slope and extent of erosion. In most cases, soil protection measures performed better on the 6H:1V slope when compared to the 4H:1V slope.

CHAPTER 1: INTRODUCTION

Erosion and embankment loss resulting from roadway overtopping is a major safety concern for the State of Minnesota. Flooding events occur throughout the state during snow-melt season and after large rainfall events. The risk of failure associated with overtopping events puts people and property at risk from both acute localized failure of the roadway and the loss of transportation connectivity between communities—especially when some rural communities are connected only by one or two roadways. In addition to safety concerns, appropriate repairs after an erosion event require significant time and monetary resources to fix damaged roadway embankments.

Roadway embankment overtopping is widespread in the valley of the Red River of the North in northwestern Minnesota and eastern North Dakota. The region's flat topography is particularly susceptible to frequent overland flooding, leading to roadway embankment overtopping and scour. Flood events in the Red River watershed in the recent past reinforce the need to protect overtopping roadways from scour. According to MnDOT personnel, some stretches of MnDOT highway, which required repair after the 2011 Red River flood, exceeded three miles in length. At this scale, prevention of flooding is not possible; scour prevention countermeasures must be considered.

Flood overtopping of roadway embankments occurs in other areas of Minnesota as well. Possible situations where this may occur include regions of similarly flat topography, embankments restricting flow across wide flood plains where bridges or culverts are undersized relative to the volume of flow or have become plugged, or where roadways parallel to rivers act as levees. Some low-volume road crossings of rivers or streams may be intentionally designed to flood during large, infrequent events (Schall et al. 2012).

1.1 ROADWAY OVERTOPPING

When floodwaters rise and begin to inundate the land, the roadways and embankments begin to function as low head dams or levees. As flood levels rise further, water begins to flow over or “overtop” the roadway, where the roadway begins to behave as a broad-crested weir with the downstream roadway embankment acting as a spillway (Figure 1.1). Overtopping by moving water subjects the paved or gravel travel surface, the subgrade, and the embankment to hydraulic forces not normally considered in roadway design.

As illustrated in Figure 1.2, an overtopped roadway and embankment may experience a range of hydraulic conditions including sub-critical and super-critical flow and hydraulic jumps. If instantaneous shear forces of the moving water exceed the resisting forces of the roadway or embankment materials, there is a high probability that erosion and/or embankment failure will occur. When overtopping events continue for long periods of time (i.e., hours to days), breach or washout of the entire roadway is possible.

Assuming flow perpendicular to the road centerline, the downstream embankment, labeled as inslope or side slope in Figure 1.3, is often subjected to the greatest hydraulic forces and is the most susceptible

to erosion, scour, and eventual failure. At the level of the downstream tailwater, a hydraulic jump typically forms as the flow regime transitions to sub-critical (Figure 1.2). Figure 1.4 and 1.5 illustrate an overtopping event and the resulting scour development at the roadway. In this case, the roadway did not fully fail but did require emergency countermeasure placement during the event.

1.2 PROJECT OBJECTIVE

The objective of this project was to evaluate several cost-effective, commercially available erosion protection treatments. A full-scale testing facility was constructed at University of Minnesota's St. Anthony Falls Laboratory and each treatment was carefully evaluated under a range of test conditions. As explained in the following sections, the current research examines several "soft" design methods using an integrated approach of full-scale physical models and field monitoring.



Figure 1.1. Image of spring flooding in Red River Valley. (photo credit, J.T. Anderson)

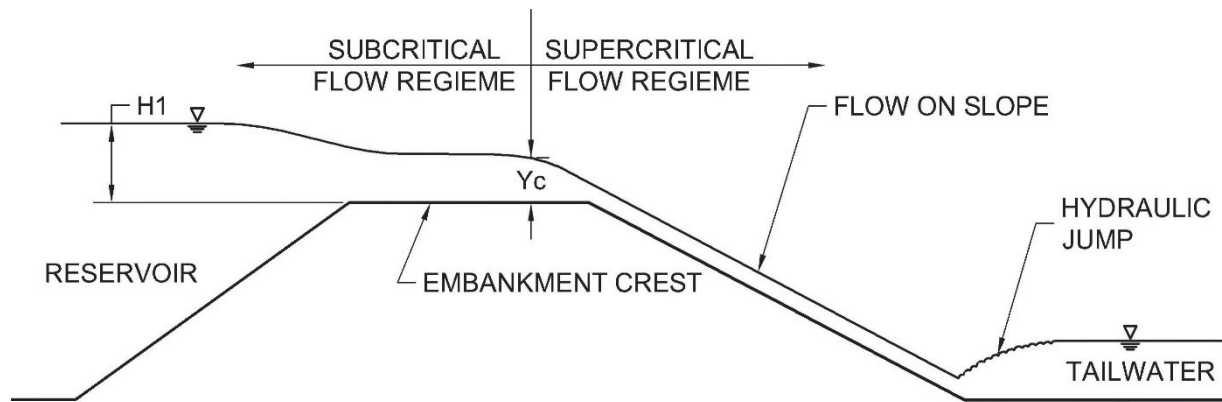


Figure 1.2 Hydraulic flow regimes and overtopping flow zones. Adapted from Clopper and Chen (1988).

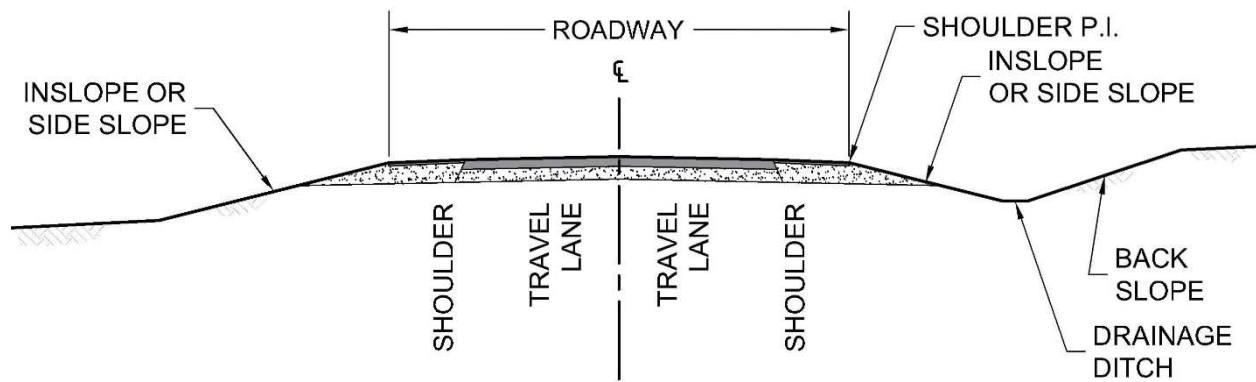


Figure 1.3. Elements of a rural, two-lane roadway (Adapted from McGee et al., 2009, FHWA-SA-09-024)



Figure 1.4. Overtopping event on MN TH1 near Oslo, Minnesota, March 21, 2010. “TH 1 at Jct 220 near Oslo 20100321”. Note road signs in yellow circle. Photo by JT Anderson, MnDOT



Figure 1.5. Same location, eight days later. Temporary stone fill dumped in some scour holes. Photo by JT Anderson, MnDOT.

1.3 SCOPE OF PRESENT RESEARCH

The focus of this research project was to provide laboratory evaluation of several erosion protection approaches typically used or considered for use to protect roadway embankments from hydraulic overtopping events in Minnesota and the upper Midwest. The research approach involved full-scale, physical model testing of three embankment armoring techniques: 1) geogrid-reinforced sod, 2) turf reinforcement mat with hydraulically applied fiber reinforced matrix, and 3) a flexible geogrid concrete mat. All techniques were aimed at protecting embankments during road overtopping events. Physical modeling results were complemented with field monitoring of several sites in northwestern Minnesota where overtopping was likely to occur.

The report is organized in the following sections:

- Chapter 1 - Introduction
- Chapter 2 - Literature Review
- Chapter 3 - Laboratory Test Methods
- Chapter 4 - Laboratory Test Results
- Chapter 5 - Field Monitoring
- Chapter 6 - Research Results and Applications

1.4 PROJECT TEAM

The project was led by a research team at the St. Anthony Falls Laboratory (SAFL), University of Minnesota. SAFL was responsible for literature review, laboratory experiments, and analysis. Wenck Associates was a partner in the project with responsibility for a small numerical modeling effort and coordination of field monitoring.

The project was greatly aided by participation of a Technical Advisory Panel (TAP), which was made up of state agency engineers and scientists from the Minnesota Department of Transportation and the Minnesota Department of Natural Resources. The TAP provided guidance throughout the project on field work, laboratory design, and numerical modeling.

CHAPTER 2: PREVIOUS STUDIES AND RELEVANT LITERATURE

The intent of this project was to examine alternative countermeasure such as vegetation, fabrics, and blankets to protect roadways from overtopping events. The hydraulics of overtopping is well-studied for levees and dams and, to a lesser extent, roadways. Below we provide a summary of relevant roadway overtopping literature that was reviewed and used in developing the design and research plan for this project.

2.1 ROADWAY OVERTOPPING

2.1.1 Discharge Characteristics of an Embankment-Shaped Weir

This report published in 1964 (Kindsvater, 1964) focused on the fluid mechanics problem of water flow over highway embankments and is a compilation of research occurring at Georgia Tech that took place from 1947 through 1958. In total, 936 experiments were conducted on 17 different embankment models. Three Master's Degree theses were produced. The work does not consider erosion but rather focused on developing and validating equations for prediction of discharge, flow depth, and boundary layer development on fixed embankments. Laboratory experiments were undertaken along with careful measurement of flow depth, discharge, and velocity. The work provided important fundamental information that was incorporated into later studies on the topic.

2.1.2 Federal Highway Administration FHWA – RD-86-126

This comprehensive report call *Development of a Methodology for Estimating Embankment Damage Due to Flood Overtopping*, details a research program focused on roadway overtopping. The 1987 study contains a review of literature, a review of available field data from overtopping events in the United States, and laboratory flume studies of overtopping. The information was used to develop mathematical models and design aids for the prediction of embankment damage from overtopping events.

Failure mechanisms – Mass wasting mechanisms such as piping and liquefaction contribute to erosion but are not the primary mechanisms associated with overtopping of the roadway by floodwaters. The initiation of erosion is linked to the elevation of the tailwater. High tailwater results in erosion initiation at the shoulder whereas low tailwater results in erosion initiation at the toe of the slope.

Field data – The project involved collection of embankment damage from 21 sites across the U.S. by a joint force workgroup made up of state agencies, U.S. Geologic Survey, and consultants. The information gathered included geometric information on the embankment, soils, hydraulics of the overtopping event, and summary of damage.

Laboratory test program – The testing program summarized an initial series of tests focusing on bare soil. Two fine-grained soils were studied. A second series of tests focused on protection measures including vegetated cover, gabion mattresses, soil cement, geoweb and Enkamat.

The embankment dimensions used in the study were 6 feet high with 10 to 22 foot crest widths and 3 feet in length with slope aspects at either 2H:1V or 3H:1V. Depths of overtopping tests ranged from 0.5 to 4 feet and test durations lasted from 1 to 20 hours.

The results indicate that soil cement and gabions performed well under all conditions. Geoweb performed poorly and Enkamat performed well at flows less than 1-ft of overtopping. The report provides quantitative results for critical velocity and shear stress for each protection method.

The report provides a considerable amount of information on mathematical modeling of the overtopping processes including numerical model called EMBANK. The model incorporated different relationships for erosion of cohesive soils and used field and laboratory data to calibrate the model. The research team tried to locate the EMBANK model but was not able to locate and it appears the model is not supported.

2.1.3 Federal Highway Administration FHWA-RD-88-181

This comprehensive report titled, *Minimizing Embankment Damage During Overtopping Flow*, by Clopper and Chen (1988) examines the hydraulic and erosional characteristics of embankment overtopping flows through a series of laboratory experiments. Full-scale tests were conducted in a laboratory facility which was four feet wide simulating an embankment height of six feet and crest length of 20-ft (Figure 1.7). The total embankment length was up to 44-ft including crest and side slopes. Two series of tests were performed on bare soil embankments (no protection). Both soils were fine grained with mean grain size (D_{50}) of about 45 micron. 19 separate tests were conducted on the bare soils. Additional series of tests were conducted on six different types of protection. Protection systems included soil cement, gabions, geogrid, Enkamat®, Enkamat® paved with asphalt, and articulated concrete block. The study examined slopes of 2H:1V, 3H:1V and 4H:1V.

The testing protocol involved careful installation of soil embankment material including compaction and final survey. The countermeasures were installed per manufacturer's instructions. Three overtopping depths were examined for each treatment – 1, 2 and 4 –ft (0.30, 0.61 and 1.2 meter) of overtopping depth. Tests were carried out from 4-10 hours depending on the countermeasure treatment. During a test, centerline water surface profiles were captured and 3-point vertical velocity profiles were measured.

Some of the key findings from the study include:

- The tests held volumetric discharge constant for a total length of 4 hours for bare soil and 10 hours for other treatments and, after completion of the test, total bed elevation was recorded. (Note that this method is different from the approach selected in this study).
- The bare soil tests experienced erosion for all test conditions with the greatest amount of erosion occurring under the deeper overtopping discharge, 2-ft and 4-ft (0.61m and 1.2 m).
- The authors describe that for low tail water tests (i.e. freefall), soil erosion was initiated at the toe of the slope and migrated upstream.

- Relationships were developed for an average erosion rate versus bed shear stress for the two bare soils and is based on the total soil eroded over the four hour test period. The erosion rates ranges from 0.0002 – 0.002 ft³/s/ft over bed shear stress from 5 – 40 lb/ft².
- The engineered protection tests demonstrated an ability to protect the soil embankment with bed shear stress ranging from 7-47 lb/ft². Soil cement performed the most consistently but gabion baskets as well as some of the articulated concrete blocks also performed well.
- The authors described the issue of negative pressures that formed at the crest-slope transition. The effect caused mats or blankets placed on the soil to be drawn upward into the flow leaving the soil below unprotected.

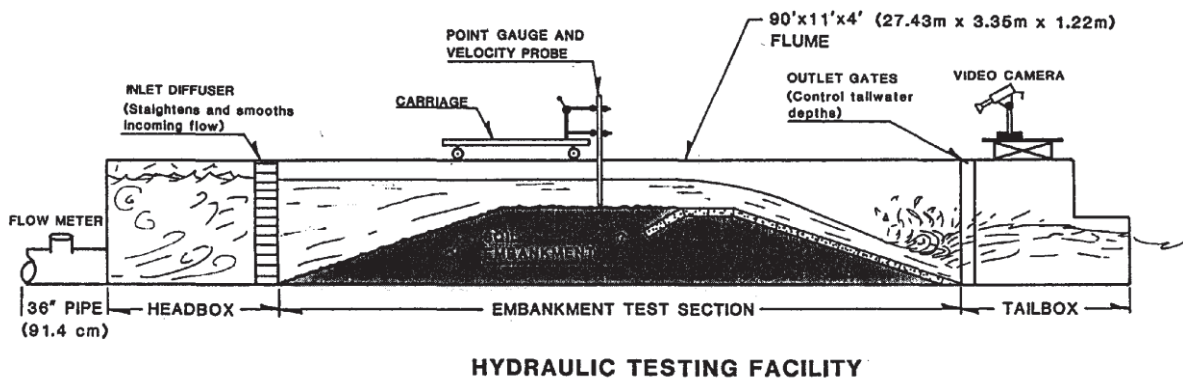


Figure 2.1 Profile of hydraulic testing facility from Clopper and Chen 1988.

2.1.4 Hydraulic Stability of Conlock and Conlock II Concrete Block Revetment System during Overtopping Flow (St. Anthony Falls Laboratory, University of Minnesota, Project Report No. 369)

This project report by Voigt et al. (1998) evaluated the stability of Conlock and Conlock II concrete block revetment systems during embankment overtopping flows. Test protocols utilized the methods outline in FHWA-RD-89-199 (Clopper, 1989). The study used 3H:1V slopes and a low tail water condition. The embankment lateral width (transverse to flow) was 9 feet. Embankment height was 5.5 feet and a maximum overtopping depth of 3.5 feet. The study found the Conlock systems to be stable up to 3 feet of depth and 19 cubic feet per second.

2.1.5 Hydraulic Stability of Channel Lock™ Concrete Block Revetment System during Overtopping Flow (St. Anthony Falls Laboratory, University of Minnesota, Project Report No. 396)

This project report by Morgan et al. (1998) evaluated the stability of Channel Lock™ concrete block revetment system during embankment overtopping flows. The study used 3H:1V slopes and a low tail water condition. Test protocols utilized the methods outline in FHWA-RD-89-199 (Clopper, 1989). The embankment lateral width (transverse to flow) was 9 feet. Embankment height was 5.5 feet and a maximum overtopping depth of 3.5 feet. Tests were performed up to 3.0 feet of overtopping depth generating shear flow of 12.3 lb/ft² and 18.4 ft/s of flow velocity. Placing Enkamat® below the block system reduced the level of erosion.

2.1.6 Hydraulic Stability of Hand Placed Positive Interlocking Concrete Block Revetment System during Overtopping Flow (St. Anthony Falls Laboratory, University of Minnesota, Project Report No. 428)

This report by Morgan et al. (1998) evaluated the stability of hand placed positive interlocking concrete block revetment system during embankment overtopping flows. Test protocols utilized the methods outline in FHWA-RD-89-199 (Clopper, 1989). This study used 2H:1V slopes and a low tail water condition and overtopping depths of 1, 2, 3, and 3.5 feet. Tests found that this system was stable over all overtopping conditions including the maximum of 3.5 feet of approach flow which generated velocities of 17 ft/s and shear stresses of 23.7 lb/ft².

2.1.7 Protecting Road Embankments from Overtopping Flow

This report by Anderson & Lim (2012) provides a summary of three protection methods for roadway embankment overtopping - bituminous pavement, open-cell articulated concrete block, and riprap. The protection was placed on actual roadways ahead of anticipated spring 2011 flooding in the Red River Valley in North Dakota. Sensors were also installed to monitor flow hydraulics. The report identifies good performance for articulated concrete block but limited performance of bituminous pavement on the shoulder and riprap.

2.2 ADDITIONAL REFERENCES

The issues of scour and erosion protection is not a new topic and has a significant body of literature associate with it. Much of the existing literature associated with embankments focuses on the design of riprap protection for larger embankments, levees, dams, and steep gradient slopes as well as specific processes associated with the flood events. A brief summary of the reviewed literature is provide below.

2.2.1 Stability of riprap and discharge characteristics, overflow embankments, Arkansas River, Arkansas: Hydraulic model investigation

The U.S. Army Corps of Engineers Waterways Experiment Station Technical Report No. 2-650 (USACE, 1964) reported the performance of riprap-covered embankments subject to overflow in a series of tests on 1:4 scale models. Embankments with and without paved roadways were subject to overtopping flows. Riprap was most subject to movement in the roadway shoulder region, but smaller riprap could be used beneath the water line without movement. After a failure occurred at the downstream edge of the embankment top, the riprap re-organized into a more stable parabolic shape resembling a flip bucket.

2.2.2 Riprap Design for Overtopping Flow

This journal paper (peer reviewed) from Abt and Johnson (1991) details a series of laboratory experiments used to develop design methods for riprap sizing to provide erosion and fluidization protection during overtopping events. The authors identify the key design parameters for riprap protection of overtopping flow as stone size, hydraulic gradient, and discharge. The experiments utilized two facilities and examined rounded and angular stones of various sizes. Embankment slopes of 1, 2, 8, 10, and 20% and median stone sizes of 1, 2, 4, 5, and 6 in. were examined. The results allowed the authors to generate a relationship for selection of minimum median stone size for angular riprap based on the channel unit discharge and embankment slope. Safety factors were incorporated to account for stone movement versus stone failure and also self-channelization, which resulted in effectively narrowing the flow width of the embankment.

2.2.3 Physical Modeling of Overtopping Erosion and Breach Formation of Cohesive Embankments

This journal article (Hanson et al., 2005) produced by the USDA – Agricultural Research Station, summarizes findings from a series of large-scale overtopping failure tests of cohesive material. The work is motivated by breach and failure of dams rather than roadway embankments but provides interesting insight into the four stages of embankment failure: Stage 1 – initial overtopping forming rills and headcuts; State 2 – migration of a large headcut upstream and widening of the erosion and banks; Stage 3 – crest lowers to a minimum level and upstream water levels decrease; Stage 4 – breach widens.

2.2.4 Hydraulics of Embankment Weirs

Fritz and Hager (1998) examined flow over a fixed embankment weir with 2H:1V slopes. Under the condition of submerged embankment overflow, four flow regimes were identified, in order of increasing tailwater: classical hydraulic jump (A-jump), plunging jet, surface wave, and surface jet are discussed with an emphasis on plunging jets and surface waves. The classical jump at low tailwater was associated with the highest velocities, especially at the slope toe. At intermediate tailwater level, the plunging jet regime was characterized by a forward jet along the downstream embankment slope and bottom, with a region of recirculation or backward flow above the jet, while the surface wave regime exhibited a

recirculation region at the toe of slope below the forward flow at the surface. Under certain conditions, switching between these regimes may occur. The surface jet regime represents a high tailwater condition with a smaller magnitude recirculation at the bottom.

2.2.5 Embankment overtopping protection systems

This journal article by Chanson (2015) reviewed and summarized numerous overtopping protection systems for embankments and earthfill dams as well as their small scale prototypes. Chanson found the most important feature of a successful protection system is the stability of the embankment material. Subsequently the construction must be of good quality with a simple design and adequate drainage to disallow damaging seepage. For embankments higher than 5-10 meters, concrete stepped spillways and precast concrete is well suited for large discharges, however, each spillway should be considered individually given discharge estimates and energy dissipation design. The best proof of design according to Chanson is the successful operation of a prototype.

2.2.6 A Study of Embankment Performance during Overtopping

The technical report by Gilbert and Miller (1991) from the US Army Corps of Engineers focused on literature from 42 different prototype dam failures: 15 of which were overtopped, 26 embankments subjected to overtopping, and reports of centrifuge modeling of embankments and numerical modeling techniques. Using these areas of study, Gilbert and Miller did not conclude a definitive solution for protection, rather they suggest aspects observed which were favorable to reducing erosion and called for the need of further research in this complex field. Highlights of these include having the embankment composed of homogenous and highly plastic soils with minimal irregularities on the surface with vegetation and a shallow slope away from the embankment.

2.2.7 Stabilization of Angular-Shaped Riprap under Overtopping Flows

This paper by Khan and Ahmad (2011) described a review of published equations developed for determination of median riprap size for embankment protection. The authors describe new results derived from multivariable power regression analysis of the 53 published riprap stability tests. The equation, developed for angular riprap, considers unit discharge, bed slope, riprap thickness, and coefficient of uniformity.

2.2.8 Evaluation of Overtopping Riprap Design Relationships

This journal paper by Abt et al. (2013) provides a comparative analysis between published experimental data from overtopping protection tests against 21 published riprap sizing relationships. The authors summarize the various data sets and sizing relationships and performs evaluation of the accuracy of the expressions and determined which expressions are most accurate over the range of slopes, discharges and applications.

2.2.9 Enhanced Stone Sizing for Overtopping Flow

This journal paper by Thornton et al. (2014) continues analysis of laboratory data and development of design equations for selection of riprap material for protection of embankments. In this work, the authors carry out a power regression analysis on 102 overtopping observations from published literature. The analysis expands the variable set to include median stone size, slope, unit discharge, coefficient of uniformity, rock layer thickness, and stone specific gravity.

CHAPTER 3: LABORATORY TEST METHODS

3.1 EXPERIMENTAL SETUP

3.1.1 Test Facility

Laboratory tests were carried out at full-scale (1:1) in a specially designed flume built to mimic a two lane rural road section complete with shoulder and a downstream slope (inslope) constructed of erodible soil, as shown in Figure 3.1. The flume apparatus was constructed on the Model Floor at the University of Minnesota, St. Anthony Falls Laboratory (SAFL).

Described from upstream to downstream, the major sections of the flume were:

1. Headbox
2. 12-foot wide upstream lane at +2% slope
3. Crest (high point) corresponding to the centerline of the road
4. 12-foot wide downstream lane at -2% slope
5. 6-foot wide shoulder at -4% slope
6. Erodible soil slope (25% and 16.67%)
7. Flat runout area
8. End weir
9. Drain box (tailbox)

Within the overall flume structure, two parallel flumes, each three feet wide, allowed study of the effect of the slope angle on scour. Looking downstream, which is to say, perpendicular to the centerline, the right flume was designed for a 25% embankment slope (4 horizontal units per vertical unit, noted hereafter as 4H:1V slope), and the left flume was designed for a 16.67% slope (6 horizontal units per vertical unit, noted hereafter as 6H:1V slope).

The overall flume apparatus was approximately 70 feet long, 8 feet wide, and 6 feet tall. The apparatus was built on a foundation framed out of 2x4 studs and sheeted with ½-inch plywood. The flume walls were constructed out of 2x6 studs and sheeted with ¾-inch plywood. The joists and ledgers that form the flume bottom were constructed out of 2x6 studs and sheeted with ¾-inch plywood. Figure 3.2 is an image of the flume during construction. All construction joints were sealed with a high-quality polyurethane sealant and all wetted surfaces were sealed with epoxy resin paint. Figure 3.1 is an annotated view of the finished test facility.

Mississippi River water from the Upper Pool at St. Anthony Falls was routed through SAFL's Supply Channel to two 40-horsepower Variable Frequency Drive (VFD)-equipped centrifugal pumps (model floor pumps #1 & #3). The pumps discharged to the 7-foot by 10-foot headbox through 12-inch diameter PVC piping. A removable bulkhead was fitted on each of the parallel flumes so that discharge from the headbox was isolated to only the desired flume for each run.

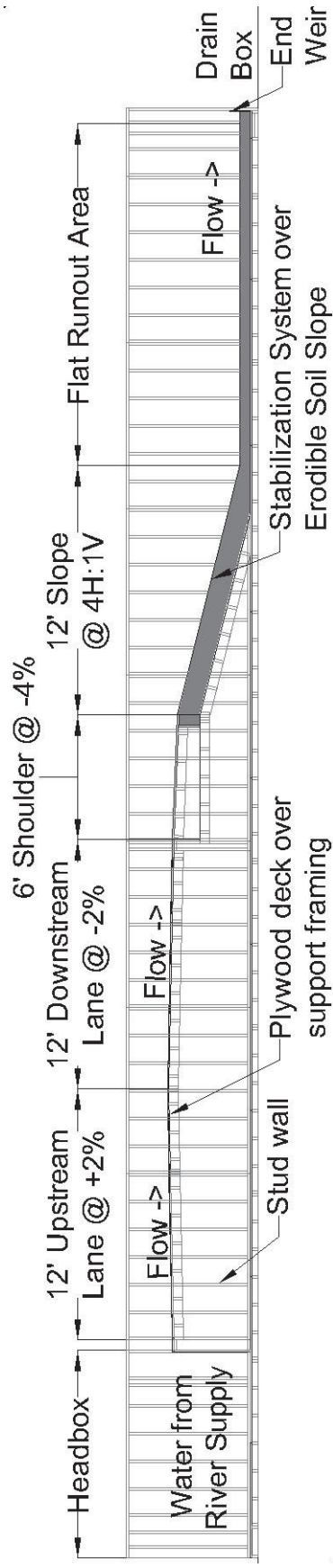


Figure 3.1. Profile view schematic of testing flume, 4H:1V slope. The parallel 6H:1V flume is identical except for the downstream slope angle and length.



Figure 3.2. Flume during construction. Looking downstream from the headbox. The 6H:1V slope is to the left of the center wall, and the 4H:1V slope is to the right of the center wall.

At the beginning of a test run, upon starting the pump, the water filled the headbox until it flowed over the plywood roadway lanes and shoulder, then down the erodible soil embankment slope. At the end of the flat runout section, a 12-inch high fixed weir controlled the tailwater depth on the embankment slope. The weir discharged freely into a tailbox approximately 30-feet by 20-feet by -feet deep. From the tailbox, two 12-inch diameter vertical drains conveyed water to an exit channel on a lower level of the laboratory.

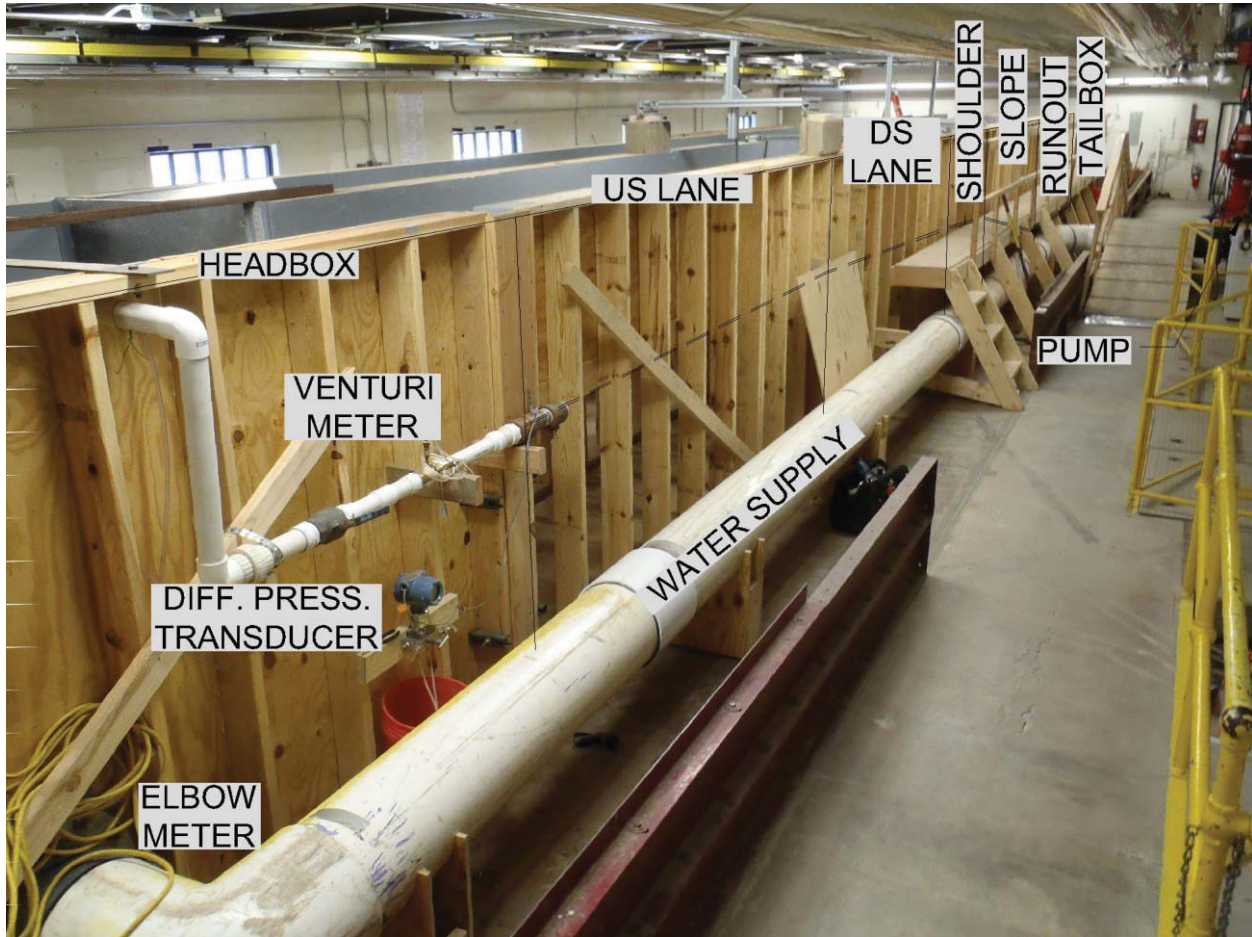


Figure 3.3. Perspective view of the flume apparatus with labels. 4H:1V slope is to the right.

3.1.2 Instrumentation

3.1.2.1 Flow control and metering

For the majority of tests water flow was controlled by the Pump #1 variable frequency drive (VFD) controller and/or a 12-inch butterfly valve. Pump #1 is shown in Figure 3.4. Typically, the flow rate was measured using an elbow meter, which is a differential pressure-type meter having a low pressure tap on the inner radius and a high pressure tap on the outer radii of a 90-degree elbow. A Rosemount model 3051S differential pressure transducer (Emerson Process Management Rosemount, Shakopee,

Minnesota), operating on the same principle as a manometer, displayed differential pressure in inches of water column. The analog pressure signal was converted to a digital signal with a USB 1408FS board manufactured by Measurement Computing, Inc., Norton, Massachusetts. LabView 6i software (National Instruments Corporation, Austin, Texas) running on a Windows PC logged the differential pressure data. Differential pressure was related to flow via a calibration of the elbow meter with the SAFL Weigh Tanks.

A few high-flow tests required additional flow capacity supplied by Pump #3. An elbow meter was installed in the supply piping from Pump #3, but due to consistent air entrainment the differential pressure readings were unreliable. Flow rates for experimental runs using water from Pump #3 are extrapolated based on depth over roadway crest measurements, again calibrated with the SAFL Weigh Tanks.



Figure 3.4. Pump #1 on the model floor.

For very low flows, especially for the bare soil case, tap water was used for testing. Flow was regulated by a ball valve and measured by a Gerand Engineering Model 632 threaded 1-1/2" Venturi meter. Volumetric testing for verification showed excellent correspondence with the manufacturer's curve.

3.1.2.2 Water Depth and Erosion - Point Gauge

A Lory-type A point gauge with a ¼-inch rounded pointer was used to measure flow over the roadway crest at the roadway centerline. The point gauge units are feet, with a Vernier scale precision of 0.001 feet. When surface disturbance prevented more accurate measurement, the point gauge reading was reported to 0.01-foot.

The Lory point gauge was also used to perform a manual topographic survey before and after each test run with several of the stabilization techniques (Erosion Control Blanket, Sod, and Turf Reinforcement Mat) in an attempt to quantify erosion below the surface treatment material. It was found that a ¼-inch

rounded pointer penetrated the stabilization material and the soft soil below too easily, so a 1-inch diameter foot on the point gauge was used along with moderate down pressure in an effort to detect voids where soil had eroded. Measurements were taken on a standard grid at five points across the slope laterally (center, near each wall, and midway between center and wall). This pattern was started at two inches down from the flume shoulder and repeated every three feet, the approximate flume width, along the slope, and flat runout area. These depths were compared among successive runs to determine an average depth of erosion and to evaluate whether or not failure had occurred. It was not possible to implement this method for the Flexible Concrete Geogrid Mat due to the three-dimensional shapes of the blocks.

3.1.2.3 Water Depth - Ultrasonic Sensors

Three ultrasonic sensors from Massa Products Corporation (M-300) were used to measure depth of flow. The Massa M-300 series is capable of collecting elevations from four inches to seven feet precisely with contact-free measurements. The sensors were placed at specific locations including the slope of the embankment several inches from the edge of the shoulder, mid-slope of the embankment, and at the end of the flume in the tail water section. Sensors were mounted perpendicular to the grade below the sensor so as to measure a true depth. Data was collected and averaged over three second intervals and written to a file every 15 seconds for the duration of each run, pre and post-flow.

3.1.2.4 Water Depth and Erosion - Manual Measurements

An aluminum meter stick was periodically used to measure water depth in various places along the flume while testing was in progress to verify and supplement the ultrasonic sensor measurements. Manual measurements were also taken after runs on the embankment slope to gauge the size of erosion events.

3.1.2.5 Erosion - Topographic Scans

A special piece of equipment used in this project was a computer automated data acquisition (DAQ) carriage designed at SAFL. The data carriage was used for topographic scans of the slope before and after each run, with the goal of detecting and quantifying soil movement. The scanning equipment consists of a high-speed camera and continuous laser sheet projected onto the surface of the slope. The overhead carriage traverses the test flume in the longitudinal direction and records bed elevations to the corresponding horizontal coordinates on a 0.002-m x 0.002-m x 0.002-m grid across the test section. Figure 3.5 shows the DAQ carriage scanning the flat runout portion of the flume.

Many examples of topographic scans created by the DAQ carriage follow in Chapter 4. To determine the relative difference in elevation between any two scans, and hence the erosion or deposition of soil, a MATLAB script was written to perform a point-by-point subtraction of subsequent scans. Many examples of the resulting difference maps are also presented in Chapter 4.

3.1.2.6 Soil Compaction

A Humboldt Manufacturing model H-4200 pocket penetrometer was used to measure surface compaction on the soil slope and flat runout area in tons per square foot. A grid similar to the point gauge grid described above was used, except the spacing between longitudinal points was two feet. The pocket penetrometer was used to record the as-compacted values.



Figure 3.5. SAFL data acquisition carriage scanning pre-flow topography. The laser sheet is projected onto the soil near the bottom of the photo.

3.1.2.7 Soil

The original substrate identified for the tests was a well sorted sand that eroded immediately in initial baseline tests. The second soil selected was an organics-rich material but was still determined to be too sandy and thus not representative of fine soils typically encountered in the Red River valley. The researchers worked with the Technical Advisory Panel (See Chapter 1, Project Team) to identify a target ratio for the testing of 20-30% clay (<0.002mm), 30-45% silt (0.002-0.075mm), and 25-50% sand (0.075-2mm). The research team inquired with local vendors to find material within range of this distribution and found a limited number of available bulk options. The material selected was reported by the vendor as 18% clay, 41% silt, and 41% sand, and initial testing showed the actual ratio to be 11% clay, 44% silt and 45% sand. This material was approved by the TAP. The loam soil used for embankment overtopping testing was much more cohesive than both the soils previously trialed. Figure 3.6 is a photo of the graded soil slope in the flume.

The soil was delivered to SAFL in bulk bags of approximately one cubic yard each and stored under tarps before being placed in the flume. A sample was taken for each bag of material delivered, and select samples were analyzed for both grain size distribution and their plastic and liquid limit. The samples analyzed included multiple vendor deliveries and experimental runs as to capture the range of variability.



Figure 3.6. Prepared bare soil slope in the flume.

3.1.2.8 Sieving and Hydrometer tests

The grainsize distribution of each sample was determined according to ASTM standard D422 – 63, using a hydrometer test and sieve analysis to determine the size range. The results of the analyses shown in Figure 3.7 were consistent, reporting an average of 10% clay, 44% silt, and 46% sand. In addition, sporadic pebbles were found in the samples. The clay content was lower than reported by the material supplier, and placed the material in the loam category on the triangular textural classification chart shown in Figure 3.8. In the AASHTO classification of soils, this soil is classified as A-4. In the United Soil Classification System (USCS) this soil is classified as SM, silty sand.

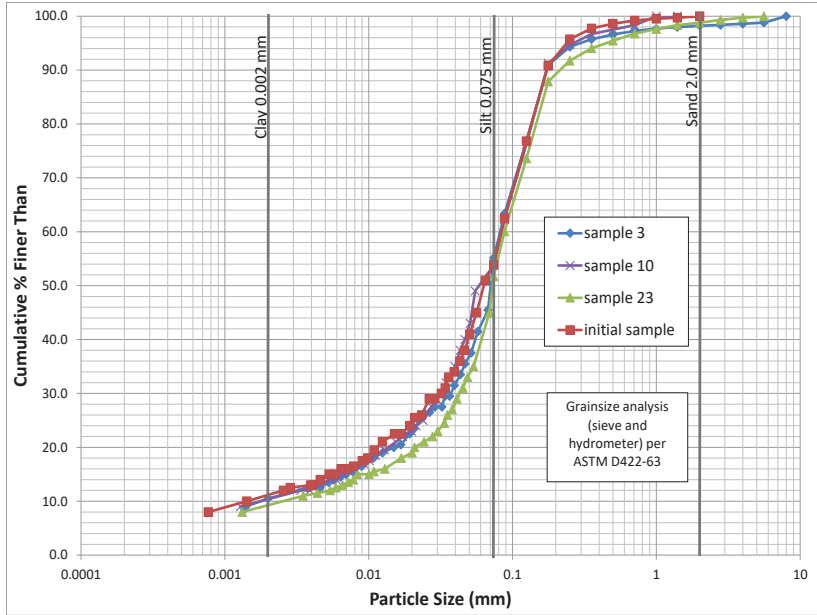


Figure 3.7. The grainsize distribution for three samples of the flume test soil, plus initial sample.

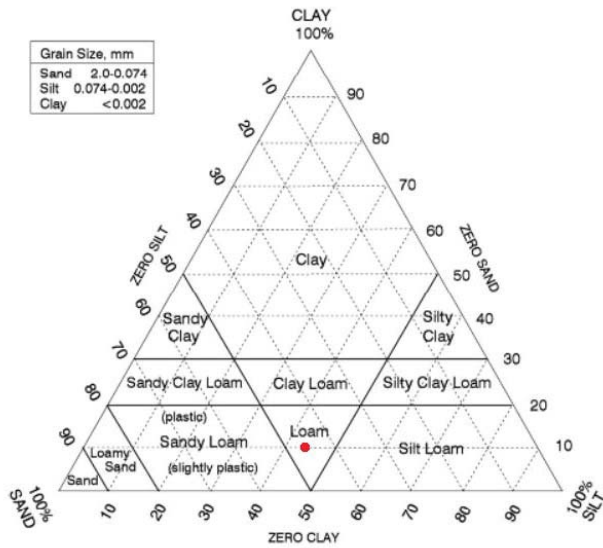


Figure 3.8. Triangular textural classification chart, from MnDOT Pavement Design Manual, Chapter 3. Data from grainsize analysis plots material in the loam category, indicated with red mark.

3.1.2.9 Atterberg Limit Tests

Liquid limit determination tests were performed according to procedures named in AASHTO Designation T89. The liquid limit among the three samples occurred in a range of 19.5 – 20% moisture content.

Plastic Limit and Plasticity Index of Soils determination tests were performed according to AASHTO Designation T90 (MnDOT modified). The results of these tests were inconclusive, indicating that the material behaves in a non-plastic manner.

3.2 EMBANKMENT STABILIZATION TECHNIQUES TESTED

Choosing a stabilization technique for roadway overtopping protection is an optimization problem carried out for a specific site. In other words, for a given site, the engineer is tasked with determining the technique or product that will provide a satisfactory level of stabilization at a minimum total cost and including consideration of site conditions, maintenance requirements, and aesthetic or environmental requirements.

Embankment stabilization techniques may be thought of as falling along a “continuum” or spectrum of protection, from no protection at negligible cost (bare soil) to a very costly impervious hard- armored slope (complete structural concrete slope paving, essentially a spillway). Within these end member examples many stabilization techniques have been developed. Although a full review of embankment stabilization or erosion prevention techniques was beyond the scope of this project, descriptions of and comparative costs for a number of techniques is tabulated in Appendix B and summarized in Table 6.8.

Advances in manufacturing technologies for fibers, polymers, and concrete materials have led to innovations in erosion protection and stabilization techniques. Engineers can now choose from a broad range of products that extend beyond the more traditional choices of slope paving, stone riprap, and vegetation alone. Recognizing the limited scope of the testing program, it was decided that techniques from several points along the “continuum” would be tested in the embankment overtopping flume. The goal of testing these intermediate techniques was to provide designers with information on countermeasure performance, which will help guide selection of an approach.

The Figure 3.9 is a compilation of stabilization techniques tested. Brief descriptions of the manufactured products used in this study are listed in the following paragraphs, including description of the typical installation technique. At the end of this section, specific products used in the tests as well as MnDOT classifications are summarized in Table 3.1. Readily available erosion prevention products were chosen as representative of similarly classified products for testing purposes.

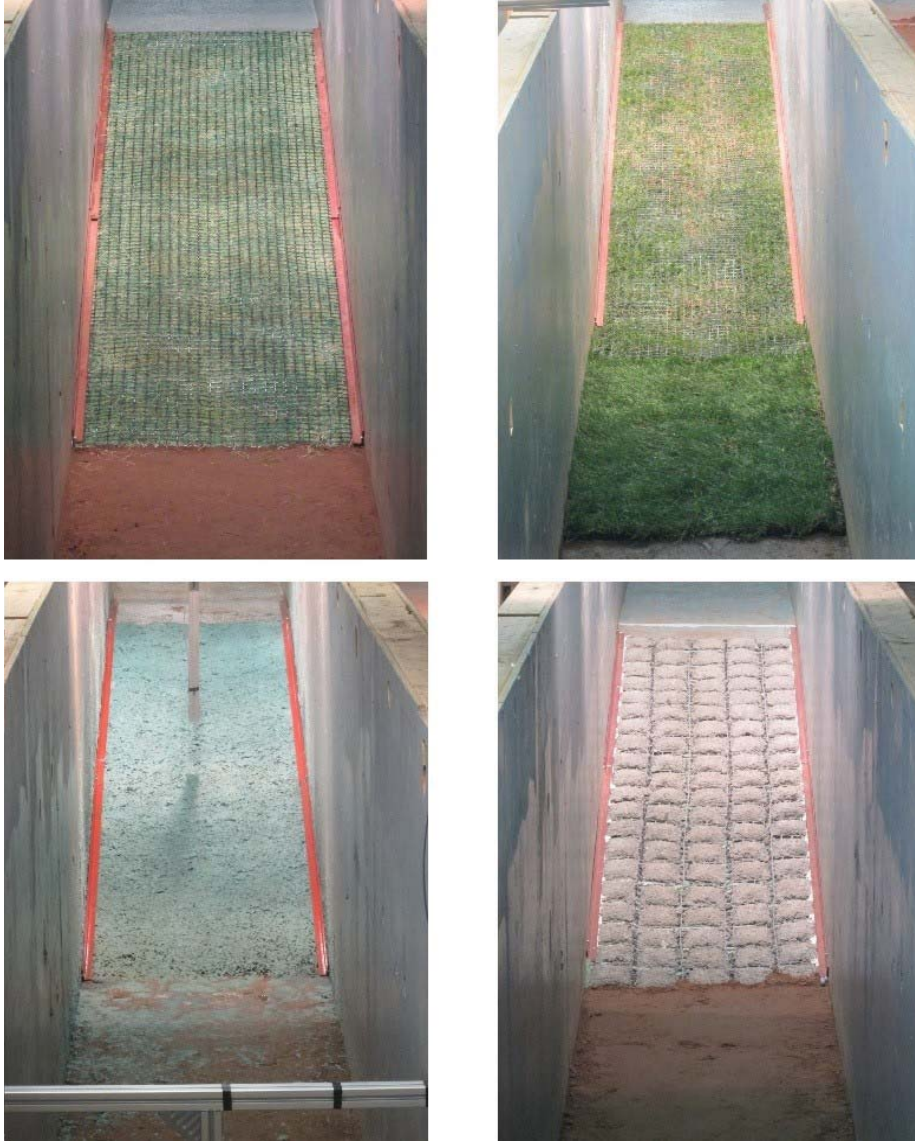


Figure 3.9. Stabilization techniques tested. Upper left: Technique 1, “Armored Sod” with erosion control blanket; Upper right: Technique 1A, “Armored Sod” with real sod; Lower left: Technique 2, Turf Reinforcement Mat (TRM) with Fiber Reinforced Matrix (FRM); Lower right: Technique 3, Flexible Concrete Geogrid Mat.

3.2.1.1 Technique 0: Bare Soil (Control).

No stabilization material present. Three bare soil tests were completed with a loamy soil comprised of silt, fine sand, and clay. The primary goal of the bare soil tests was to understand the soil erosion mechanisms and patterns to be later incorporated into technique testing. Refer to Figure 3.6 for a photo of the bare soil slope.

3.2.1.2 Technique 1: “Armored Sod” (Biaxial Geogrid underlain by Erosion Control Blanket to model vegetation).

This “light”, non-proprietary stabilization technique has not been widely tested. In a field installation a plastic geogrid would be placed either over existing grass as a retrofit application or over newly seeded slopes, and pinned in place with wire U-shaped staples or other anchoring systems. In theory, the geogrid helps to stabilize the root system of the vegetation and allows the vegetation root mat to act as a unit to resist washing away of chunks. The tensile strength of a typical multi-axial geogrid is substantially greater than required for this application, so the geogrid was chosen based on the opening size of approximately 1” x 1.3” and product availability. An alternative to the geogrid is metal chain-link fencing. Due to the difficulties of growing and maintaining healthy vegetation in an indoor laboratory, excelsior (aspen fiber) Erosion Control Blanket (ECB) in contact with the bare soil was chosen as a stand-in for vegetation for this testing. The tests could also be seen as representing a just-installed case where no vegetation has yet taken root.



Figure 3.10. Layers of the armored sod. Image on the left shows the layers of the Erosion Control Blanket. Image on the right shows the plastic geogrid.

3.2.1.3 Technique 1A: “Armored Sod” (Biaxial Geogrid underlain by bluegrass sod)

This variation of Technique 1 utilized standard bluegrass sod obtained from a local nursery in place of the erosion control blanket to better simulate vegetation. Although the sod remained alive and even exhibited some growth during the tests, it did not root into the soil slope.



Figure 3.11 Bluegrass sod used in Technique 1A.

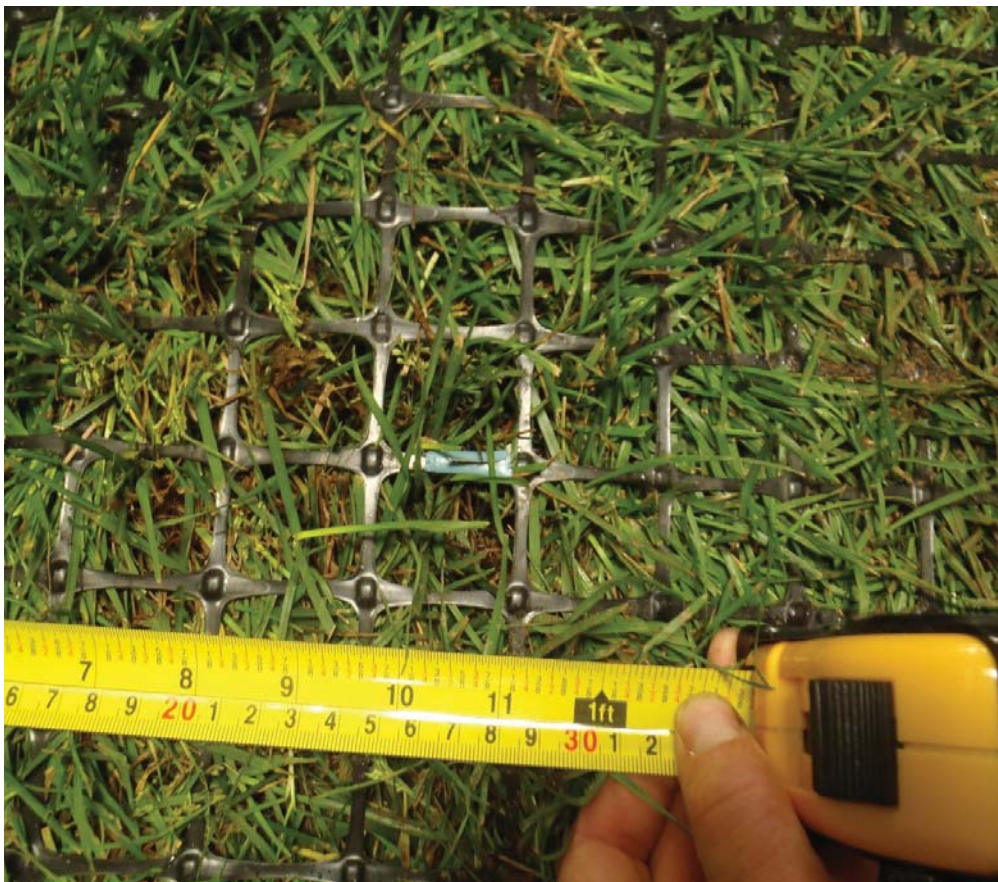


Figure 3.12 Sod covered with geogrid

3.2.1.4 Technique 2: Turf Reinforcement Mat (TRM) with Fiber Reinforced Matrix (FRM)

Turf reinforcement mats are non-degradable, synthetic, three-dimensional mats designed to provide permanent support to vegetation root structure. The particular TRM used for testing (Futerra® 7020 (Formerly Enkamat® 7020), manufactured by Profile Products, LLC, of Buffalo Grove, Illinois) was selected because of the large openings in the mat structure (95% open area) which allow larger legume seeds to penetrate through to the soil surface. This is a desirable property to establish a strong long-term stand of vegetation. The TRM was pinned to the slope with the same U-shaped wire staples used in Technique 1. The Fiber Reinforced Matrix (FRM) was applied over the TRM as a water-based slurry consisting of fibers (typically wood or cellulose), tackifiers, seed, and fertilizer. The FRM used in testing was Flexterra™ High Performance Flexible Growth Medium (HP-FGM®), also manufactured by Profile Products, LLC. The seed and fertilizer were omitted for the laboratory tests.



Figure 3.13. Photo on the left shows the turf reinforcement mat installed on the soil. Photo on the right shows the Fiber Reinforced Matrix being applied.

3.2.1.5 Technique 3: Flexible Concrete Geogrid Mat (Flexamat® Plus)

This product consists of rough-surface concrete blocks cast onto a very flexible but tough polypropylene geogrid such that the geogrid ties the blocks together. This is similar to a cable concrete mat but more flexible. In the tested configuration (Flexamat® Plus), manufactured by Motz Enterprises of Cincinnati, Ohio, the geogrid tied concrete blocks were placed on top of a Recyclex® turf reinforcement mat. The TRM is manufactured from recycled green and brown polyethylene bottles by American Excelsior of Arlington, Texas. Below this layer and in direct contact with the soil is a very light excelsior mat. The weight of the blocks serves to anchor the mat, while the geogrid provides flexibility to conform to the soil surface. It is a much heavier armoring technique than the others tested. In a typical field application, a roll of Flexamat® is unrolled onto a slope by earthmoving machinery.



Figure 3.14. Photo on the left shows the concrete blocks and flexible geogrid underlain by the turf reinforcement mat. In the photo on the right, the turf reinforcement mat is overlaying the soil and the concrete blocks and flexible geogrid is being hoisted into place.

Descriptions of products used for each test, including manufacturer and MnDOT classification are listed in Table 3.1.

Table 3.1. Manufacturers and MnDOT classifications for products used in Techniques 1-3.

Used for Tech	Product Classification	Product Used	Manufacturer	MnDOT Specification and Usage Notes
1, 1A	Biaxial Geogrid	Tensar® BX1100	Tensar International Corporation	Refer to State Aid Division Technical Memo No. 15-SA-02, dated Dec 14, 2015.
1	Erosion Control Blanket (ECB)	Curlex® High Velocity™ (HV)	American Excelsior Company	Category 4 ECB, Wood Fiber, High Velocity, 2-sided net. MnDOT Std. Specification 3885, Table 3885-1
1, 1A, 2	Wire U-Shaped Staples	8" length	(Commodity product)	Used at 3.5 staples per square yard. Refer to MnDOT Std. Spec. section 2575 G.3, and Std. Spec 3885, Table 3885-5. (note a)
1A, 3	Wire U-Shaped Staples	≤6" length	(Commodity product)	(note b)
1A	Bluegrass sod		(Commodity product)	Rolls 24" x approx. 80"
2	Turf Reinforcement Mat (TRM)	Futerra® 7020	Profile Products	Category 3 TRM, MnDOT Std. Specification 3885, Table 3885-6.
2	Hydraulically-applied Fiber-Reinforced Matrix (FRM)	Flexterra™ FGM-HP®	Profile Products	MnDOT Std. Specification 3884, Hydraulic Matrix, B.5. Type Fiber Reinforced Matrix (FRM)
3	Flexible Concrete Geogrid Mat or Tied Concrete Block Mat	Flexamat® Plus	Motz Enterprises, Inc.	MnDOT Special Provision. Pay item 2511, Articular Riprap
3	(part of Flexamat® Plus)	Recyclex® TRM	American Excelsior Company	(between soil and concrete portions of Flexamat®)
(a) 8-inch staples were used in place of 12-inch staples due to slope soil depth limitation.				
(b) Used to anchor bluegrass sod before geogrid installation (Tech 1A) and temporarily anchor underlayment (Tech 3). Shorter staples (≤6" length) were used to anchor products in the flat runoff when applicable due to soil depth limitation.				

3.3 EXPERIMENTAL PROCEDURES

In this section we summarize the procedures for setup, testing, and data collection.

Before starting experiments a plan was developed for installation and testing of the stabilization techniques. This plan was partly based on ASTM Standard D6460-12, which is a standard test for determination of rolled erosion control product (RECP) performance in protecting earthen channels from stormwater-induced erosion.

3.3.1 Soil placement and compaction

The flume design allowed for a soil thickness of approximately 12 inches on the embankment slope and 6 inches on the flat runout area downstream. Refer to Figure 3.1 for dimensions. For the first installation of soil, material was compacted by spreading layers of soil in no more than six inch lifts and tamped using a hand tamper. For each subsequent experiment, soil was removed to at least 2 inches below the lowest scour depth of the previous run and then refilled with soil to a depth sufficient to bring the new stabilization technique to the appropriate depth of the shoulder and angle of the slope.

Once the desired elevation of soil was achieved, a final survey of soil compaction was performed using a Humboldt Manufacturing model H-4200 pocket penetrometer. Soil compaction was measured every two feet starting with the first measurement two inches from edge of the shoulder. Five measurements were taken across the width of the slope at each position, the center of the flume, two inches from each wall, and $\frac{1}{4}$ of the width of the flume from each wall. In rare cases where the compaction was locally very low or highly varied, the slope was repacked and the entire surface was measured again. These compaction measurements were taken for the entire length of the flume unless soil was not present, which was only applicable for the flat run-out area near the end of flume on some runs.

After the compaction data was collected, the slope was scanned using the DAQ carriage on the SAFL's Model Floor. Topographical information was collected for the shoulder, slope and flat run out area of the flume. Once the soil placement and measurements were complete, the slope was loosely covered with plastic sheeting to maintain soil moisture.

3.3.2 Stabilization technique installation

Each stabilization material was installed on top of the compacted soil as per the manufacturer's guidelines. While each technique used similar methods to level and compact the soil, the technique for installing the actual stabilization materials differed per the manufacturer's installation guide as well as the capabilities of the flume and researchers. The blanket, geogrid, and TRM materials for techniques 1, 1A, and 2 were all fastened to the shoulder structure of the flume using similar methods, as illustrated in Figure 3.15. Approximately six inches of plywood at the end of the shoulder was left as an overhang. Underneath this overhang, the framing for the shoulder was used as a fastening point for the various materials. Each of the above mentioned materials was wrapped around a piece of dimensional lumber and fastened to the lumber using a staple gun. The wrapped lumber was then bolted or screwed to the

shoulder's framing to ensure the shoulder to slope transition of the stabilization material was not pulled loose at the top.

This robust fastening simulated a completely reliable anchor near the shoulder. Testing of near-shoulder anchoring systems was not part of the scope due to the 12 inch soil depth limitation of the flume, which is shallower than many anchoring systems, as well as a need to limit the number of variables contributing to embankment failure.



Figure 3.15. View looking upslope. Armored sod material wrapped around a piece of lumber and bolted to framing under the shoulder. Once backfilled with soil, the armored sod material on the shoulder would be flipped down to cover the slope.

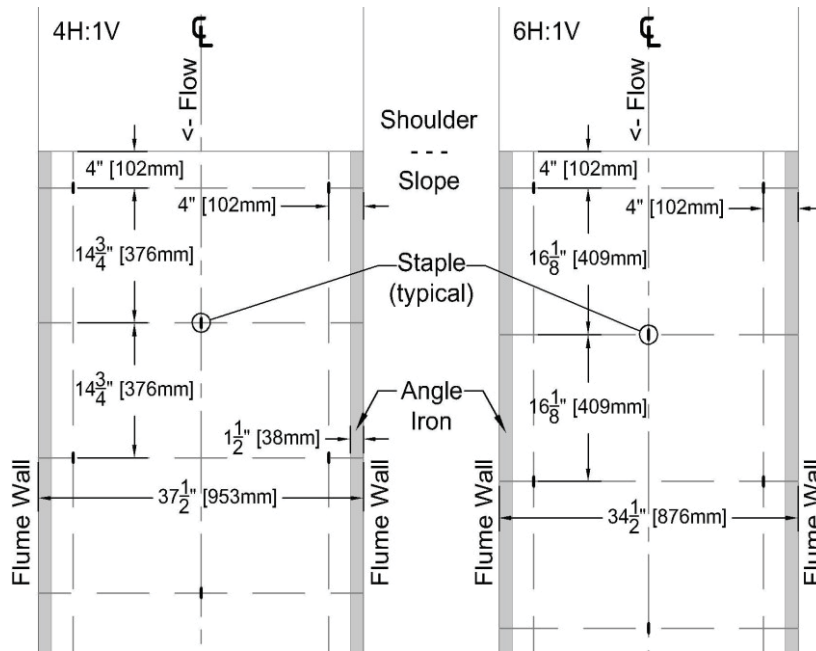


Figure 3.16. Staple pattern for 4H:1V and 6H:1V slopes. Pattern continues to toe of slope, and along any material extended on the surface of the flat runout area.

The material was flipped back and laid on the shoulder while soil was packed underneath the overhang to ensure a level transition from shoulder to slope. Once the soil in the trench immediately downstream of the shoulder was brought to the proper depth and compacted, the stabilization materials were laid on the slope and fastened using the manufacturer's recommended or modified methods to fit the flume width. For techniques 1, 1A, and 2, the mats were fastened using landscaping staples in a pattern of 3.5 staples per square yard with the orientation of the staple being parallel to the flow down the slope and driven in perpendicular to the angle of the slope, as shown in Figure 3.16. The staple density was chosen based on section 2575 G.2 & G.3 and Table 3885-5 of the 2014 Edition of the MnDOT Standard Specifications for Construction.

Technique 3 was fastened to the shoulder by sliding the first line of concrete blocks under the shoulder and grouting over the first exposed concrete block line (see Figure 3.17). The concrete geogrid was not required to be fastened to the slope with landscaping staples.



Figure 3.17. Flexamat® “paved” into the shoulder with Portland cement grout to transition onto the slope. Seam of paving and shoulder sealed with a polyurethane single component sealant (white). Flow is left to right in this image.

Along the flume walls forming the edges of the slope, a piece of angle iron was installed to decrease the edge effect caused by the flume walls and the likelihood that water would flow around and beneath the stabilization materials. For techniques 1, 1A, and 2, the angle iron was fastened to the flume wall resting on top of the slope with minimal downward pressure so as to not serve as additional fastening. Technique 3 required additional measures to reduce edge effect because of the irregular shape of the concrete blocks. To fill the area beneath the angle iron, foam backer rod and spray foam insulation was used in the first 4H:1V slope test run (see right photo, Figure 3.18). In subsequent runs, the Recyclex® TRM underlayment was cut slightly wider than the flume and curled around to fill the space, supplemented with foam backer rod.



Figure 3.18. Angle iron fastened to flume wall (left). Flexible concrete geogrid mat installation example with backer rod and spray foam insulation used to fill the void between the Flexamat[®] and angle iron resting on top of concrete (right).

Three methods were used to terminate the stabilization material after the toe of the slope:

1. Anchor trench – The material was extended beyond the toe of the slope horizontally 18 inches along the flume floor under six inches of compacted soil. This method was devised from manufacturers' recommended techniques and used in a majority of cases. However, the bare soil covering the material was susceptible to erosion, and this technique could not be used in all cases, for example, with the real sod.
2. Extended several feet past toe (partial covering) – The material was extended onto the surface of the flat runout area several feet past the toe of slope with the same anchoring pattern as on the slope.
3. Extended to end of flume (full covering) – The material was extended and anchored all the way to the downstream end of the flat runout area at the downstream weir.

Refer to Table 3.2 for the termination techniques used in the various tests. Note that the run designations "4H:1V quick", "4H:1V", and "6H:1V" refer to the embankment slope, and are described in detail in Section 3.3. Once all of the materials had been fastened on the slope, the embankment was scanned again using the data acquisition carriage, and the experiment could proceed.

Table 3.2. List of techniques used to terminate stabilization material for all experiments.

	Buried in anchor trench at toe of slope	Extended on flat surface several feet	Extended full length of flat runout
Technique 1 Armored Sod (ECB)	4H:1V quick, 4H:1V, 6H:1V		4H:1V ext. paving
Technique 1A Armored Sod (Real Sod)		4H:1V quick	4H:1V ext. paving
Technique 2 TRM FRM	4H:1V quick, 6H:1V		
Technique 3 Flexible Concrete Geogrid Mat	4H:1V quick	4H:1V, 6H:1V	

3.3.3 Tailwater condition

In an overtopping event of a typical road section, such as is simulated in the experimental flume, several locations are susceptible to erosion and failure, including: 1) the toe of the inslope where the embankment meets the surrounding grade or ditch bottom, 2) the transition from the shoulder to the inslope, or 3) the location of a hydraulic jump, if a hydraulic jump forms. Refer to Figure 3.19, reproduced from Clopper & Chen (1988), who note “In general, embankment erosion under freefall (low tailwater) conditions is more severe than when high tailwater is present, all other factors being equal.” All tests reported here were run with a low but variable tailwater, which was set by a fixed height weir with a crest six inches vertically above the toe of slope elevation. This was equivalent to a “freefall” condition.

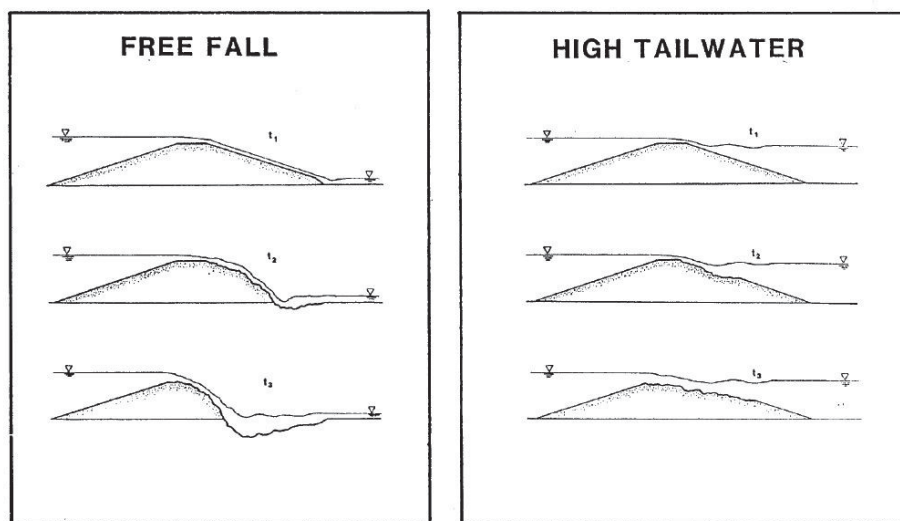


Figure 3.19. Progressive stages of unprotected embankment erosion under freefall and high tailwater conditions. From Clopper and Chen (1988).

3.3.4 Determination of failure

Failure of the soil slope was determined in three different ways.

1. Catastrophic Failure: A catastrophic failure included a mass slope failure or formation of rills deeper than six inches. Rills were measured manually on the slope with either a point gauge or a ruler.
2. Clopper Soil Loss Index: Another failure mode was determined by the Clopper Soil Loss Index (CSLI) when the slope had a soil loss of 0.5 inches, as reference in ASTM 6460-12. The soil loss for the CSLI is calculated as Total Cut (ft³) / Wetted Channel Area (ft²). In practice, a point gauge was used to measure differences of a series of cross sections.
3. BMP Detachment: The third mode of failure was determined by the continuous flow under a surface treatment or loss of contact of surface treatment with the soil.

Assessment of the second and third failure modes proved to be difficult to quantify. Additionally, while a 0.5 inch average soil loss may be classified as a failure from a soil conservation perspective (Erosion Control Technology Council) of an installed erosion prevention practice, if the roadway embankment is still intact, the stabilization technique may be considered to have performed successfully from a structural perspective. Accordingly, the later tests were allowed to run longer in an attempt to detect major failures.

3.3.5 Point gauge measuring system

For each of the techniques of slope stabilization, because of the inherent in situ product characteristics and surface attachment-fastened to the slope, it was not possible to visually determine if the soil was being eroded; to do so mid-test would have required removal of the material and thus invalidate the test. There was potential that erosion had occurred and the stabilization material was bridging a void thereby giving the appearance that soil was undisturbed under the stabilization material. To address this issue, a Lory-type point gauge with a one inch diameter circular foot was used to systematically probe the surface of the slope to check for any voids beneath the surface (Figure 3.20). A coordinate system similar to that created for the penetrometer data was used for the point gauge. Cross sections of the soil surface were measured at stations beginning two inches from the edge of the shoulder followed by three foot increments going downslope. At each station, five measurements were taken with the point gauge: two inches from each wall, the center of the flume, and a quarter of the width of the flume from each wall. These measurements were compared with previous runs to quantify any erosion or deposition. Unfortunately, despite significant effort to maintain consistent procedures, it was challenging to measure soil surface through the erosion protection material. As a result, data from this method had greater variability than expected making quantification of the volume of soil loss difficult.



Figure 3.20. Point gauge being used on slope to check for erosion and voids in soil beneath erosion control blanket.

3.3.6 Flow control and monitoring

Water depth overtopping the crest of the road at the centerline was measured with the Lory-type point gauge (Figure 3.21). A target overtopping depth was set for each run. The depth over the crest was then checked, and the flow adjusted by means of the pump variable frequency drive or valves to reach the desired flow depth.



Figure 3.21. Point gauge at road crest in use to measure depth of flow over the crest of the model road cross section.

3.3.7 Extended Shoulder Paving or Partial Slope Paving

One technique to reduce the erosion of roadway embankments subject to overtopping flow that has been employed by MnDOT in the field is the practice of partially paving the inslope with bituminous pavement. This practice is illustrated in Figures 1.4 and 1.5 and is observed to be partially successful. Apart from construction and maintenance considerations, one favorable aspect of partial slope paving is that the transition point to the “soft” slope is away from the edge of the shoulder, thus reducing the chance of undermining that is detrimental to the roadway. On the other hand, water flowing over the relatively smooth and steep extended pavement will, in theory, be moving faster than if the water were flowing over a rougher, vegetated inslope, potentially causing increased erosion at the downstream edge of the extended paving.

To test the effectiveness of partial slope paving, a sub-series of experiments were run at the end of the testing program. For this series all soil in the upper portion of the 4H:1V slope flume was removed and a 42-inch long simulated pavement made of white colored epoxy painted plywood was fastened so that

the top surface of the plywood was at a 4H:1V slope. Figure 3.22 shows the extended paving just after installation. Stabilization materials were then installed and fastened below this simulated pavement extension in the same manner as described for anchoring below the shoulder.



Figure 3.22. Simulated extended shoulder paving in the 4H:1V flume, prior to installation of stabilization materials. A dashed line has been added at the shoulder edge at the top of the slope.

3.4 SUMMARY OF RUNS

To allow comparisons of performance among stabilization techniques, slope angles, slope modifications, and flow durations, a variety of experimental runs were completed. Test runs were either “quick” or “long” referring the duration of time discharge was held constant. Table 3.4 summarizes the various runs performed.

Because we did not have a priori knowledge of the failure point of an erosion protection treatment, the first run was designed to incrementally step through a series of flows in order to establish the approximate velocity and shear stress condition at which a certain stabilization technique would fail on the 4H:1V slope. These were defined as “quick tests”. Each discharge was held for 30 minutes before raising the flow rate. The same erosion protection techniques were then tested on either the 4H:1V or 6H:1V slope, or both, at flow duration increments of two hours. These tests were defined as “long tests”.

Each quick or long test followed the same procedure for preparation of slope and installation of materials. Each technique tested was run until failure; some of the techniques were run past failure to determine the extent and dynamics of how the slope would erode.

Table 3.3. Matrix of slopes and techniques tested. Test completion marked with “X”.

	Technique 0 Bare Soil	Technique 1 Armored Sod (ECB)	Technique 1A Armored Sod (Real Sod)	Technique 2 TRM FRM	Technique 3 Flexible Concrete Geogrid Mat
4H:1V “Quick”	X	X	X	X	X
4H:1V “Long”		X			X
4H:1V “Ext. Paving”	X	X	X		
6H:1V “Long”	X	X		X	X

CHAPTER 4: LABORATORY TEST RESULTS

In Chapter 4 we provide a summary of the laboratory tests conducted on the four erosion protection techniques selected for this project.

4.1 TECHNIQUE 0: BARE SOIL

4.1.1 Test 1. 4H:1V Slope- Quick Test

4.1.1.1 Summary

This was a baseline test of bare soil only carried out on the 4H:1V slope. Four separate runs were completed with a discharge of 0.09 ft³/s and a total duration of eight minutes. The unit discharge was 0.03 ft³/s-ft. The overtopping depth was small and not measurable.

4.1.1.2 Observations

With no stabilization technique on the surface of the slope, the soil quickly eroded in a manner that correlated with areas of lower compaction. This caused channels to form and perch the remaining areas of higher compaction.

4.1.1.3 Failure Description

Erosion occurred immediately across entire slope. Preferential flow paths were quickly established then deepened by repeated flows. Concentrated erosion occurred immediately downstream of the fixed edge of the “shoulder”, eventually funneling all flow into the deepest preferential path, forming a pattern of cyclic steps, which are similar to pools and chutes, migrating upstream. If the shoulder were not fixed in place, it would most likely have undermined and collapsed.

4.1.1.4 Photographs



Figure 4.1. Pre-run 4H:1V slope bare soil looking downstream from shoulder.



Figure 4.2. 4H:1V Slope mid-run with prevalent channels of flow looking downstream. Less than two minutes of run time.



Figure 4.3. Mid-run 4H:1V slope looking upstream. Flow channelized on slope with trough forming on the transition from shoulder to slope.

4.1.1.5 Test Data

The data collected during these tests are summarized in the following tables and figures. The same format is used for all the runs and so explanation of the information is provided here. Table 4.1 summarizes the primary variables of the test. Figure 4.4 shows the time duration of each run within a test and water discharge for each run. For this test the flow rate was held constant and was turned off after a two minute run to allow a surface scan of the slope. Figure 4.5 and 4.6 are the summary plots derived from surface scans; they are difference plots of two consecutive surface scans and show the change (erosion/deposition) of the slope surface. The color bar on the right of the figure shows the change in the surface and is in millimeters of erosion/deposition. Figure 4.7 and 4.8 are graphs of measured compaction and final surface topography, respectively. Table 4.2 includes summary statistics of the compaction data including the average of the measured values, the standard deviation, coefficient of variability, and maximum/minimum measured values.

Table 4.1. Test data for bare soil, 4H:1V slope.

Bare Soil: 4H:1V Slope			Mid-Slope			
Run end time(min)	Depth Over Crest (ft)	Unit Discharge (ft ³ /s-ft)	Water Depth (ft)	Velocity (ft/s)	Shear Stress, τ (lb/ft ²)	Mannings 'n'
2.0	Not Measured	0.03	Not Measured			
4.0		0.03				
6.0		0.03				
8.0		0.03				

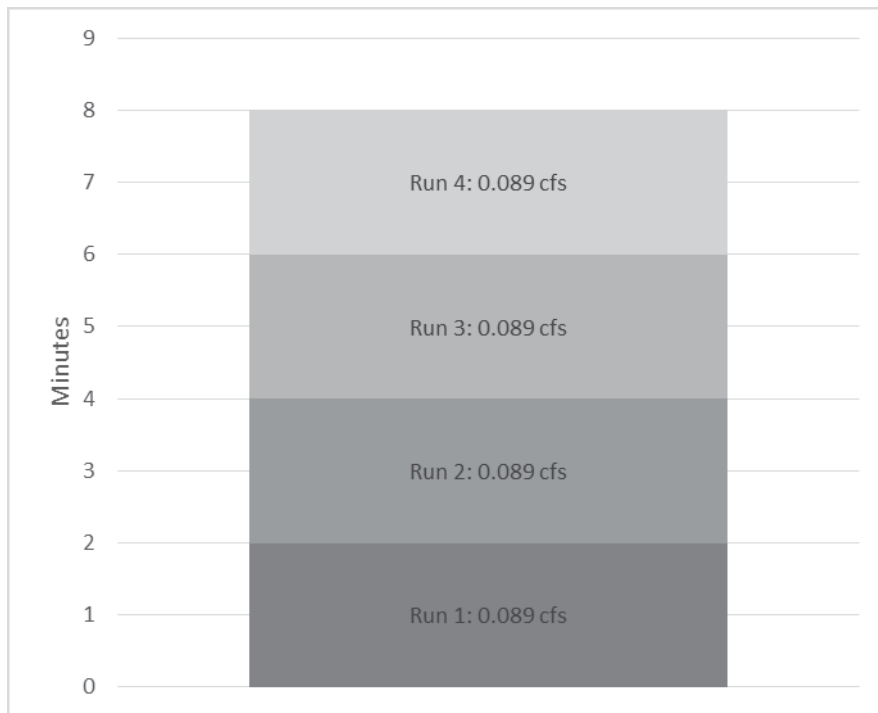


Figure 4.4. Number of runs within this test with flow rate and duration of time at each flow rate.

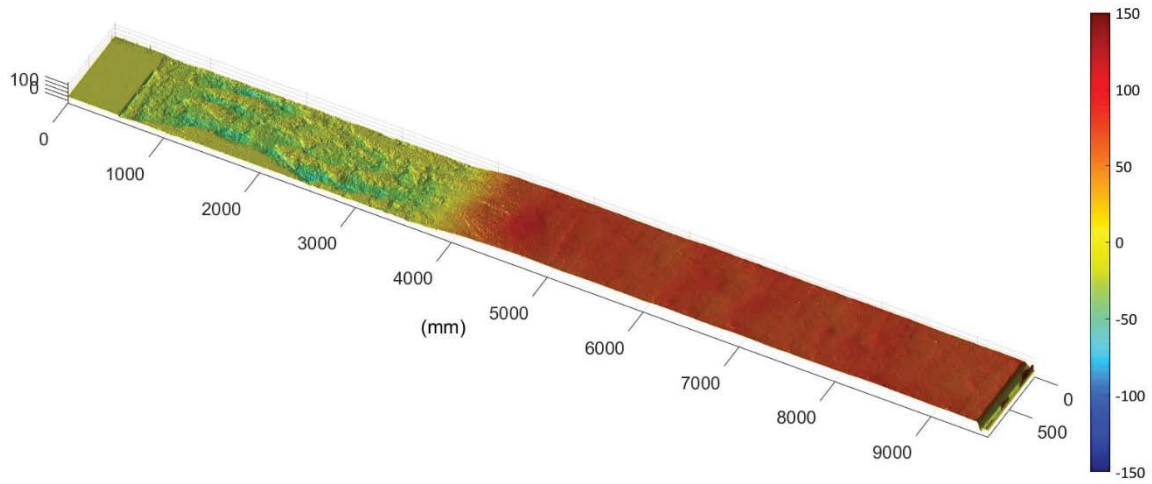


Figure 4.5 Topographic difference plot from zero to two minutes of run time, showing prominent channels being carved on slope. Elevation units are in millimeters.

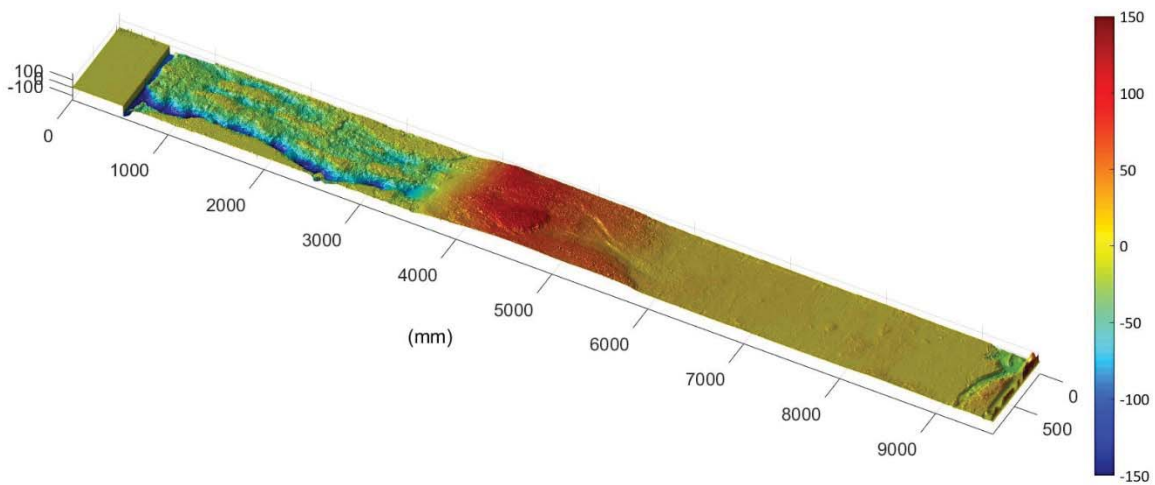


Figure 4.6 Topographic difference plot from zero to eight minutes of run time. Note scour and trough formation at upstream transition from shoulder to slope and primary channel of erosion.

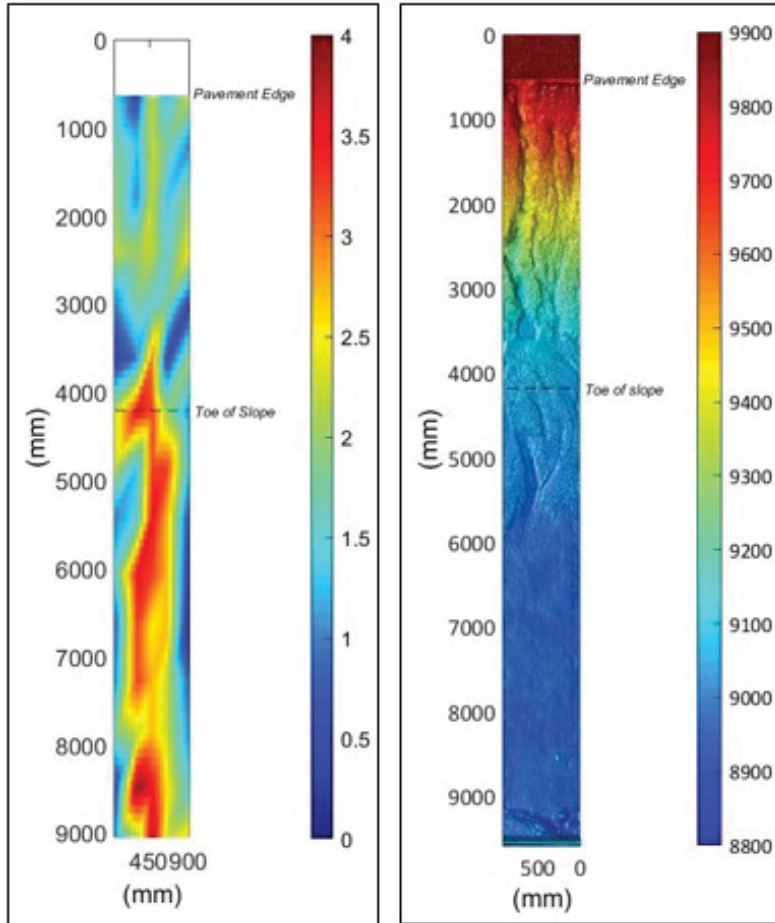


Figure 4.7. (Left). Aerial view of interpolated compaction data on slope interpolated with mid-shoulder starting at zero. The left vertical axis is distance in millimeters from mid-shoulder. Compaction is presented in units of tons per square foot. The white area is the shoulder. The color bar on the right of the figure gives color range for compaction values in tons/ft². (Right). Aerial view of scanned slope after eight minutes of run time showing channels of erosion.

Table 4.2. Statistics of compaction on 4H:1V slope for bare soil testing.

Statistics	On Slope (0-12 feet)		On Flat Run-out (14-28 feet)	
	Tons/SF	psi	Tons/SF	psi
Average	1.71	23.8	2.12	29.4
Std. Dev	0.77	10.7	1.08	15.1
COV	0.45	6.2	0.51	7.1
Maximum	3.50	48.6	4.00	55.6
Minimum	0.25	3.5	0.00	0.0

4.1.2 Test 2. 6H:1V Slope

4.1.2.1 Summary

This test was to examine bare soil on the 6H:1V slope. Total duration of the test was 8 minutes over four runs. Discharge was 0.09 ft³/s or unit discharge of 0.03 ft³/s-ft. The overtopping depth was small and not measurable.

4.1.2.2 Observations

Slope failure was similar to the 4H:1V bare soil test with near-instantaneous erosion of the slope. The location of failure occurred immediately downstream of the shoulder where soil was slightly less compacted than the rest of the slope. The average soil compaction was 0.30 tons/ft² higher on this slope, which may have caused the soil to erode less quickly than the 4H:1V run. Conversely, the largest erosive channel running down the middle of the slope was also where compaction was measured to be the highest (as seen on the penetrometer plot, Figure 3.13).

4.1.2.3 Failure Description

This slope's failure was similar to the 4H:1V slope except that the erosion occurred less rapidly and did not erode as deep into the slope. A trough formed immediately downstream of the shoulder and fed into carved channels that wove down the slope. On the lower half of the slope, several flow paths recombined and erosion was shallower and more prevalent as opposed to one deep prominent channel.

4.1.2.4 Photographs



Figure 4.8. (Left) Initiation of flow on 6H:1V slope looking upstream. (Right) Erosion began immediately with incisional channels forming on slope.



Figure 4.9. Channelized flow and separation from the edge of the shoulder forming trough at the transition.

4.1.2.5 Run Data

Table 4.3. Run data for bare soil, 6H:1V slope.

Bare Soil: 6H:1V Slope			Mid-Slope			
Run end time (min)	Depth Over Crest (ft)	Unit Discharge (ft ³ /s-ft)	Water Depth (ft)	Velocity (ft/s)	Shear Stress, τ (lb/ft ²)	Mannings 'n'
2.0	Not Measured	0.03	Not Measured			
4.0		0.03				
6.0		0.03				
8.0		0.03				
10.0		0.03				



Figure 4.10. Number of runs within this test with flow rate and duration of time at each flow rate.

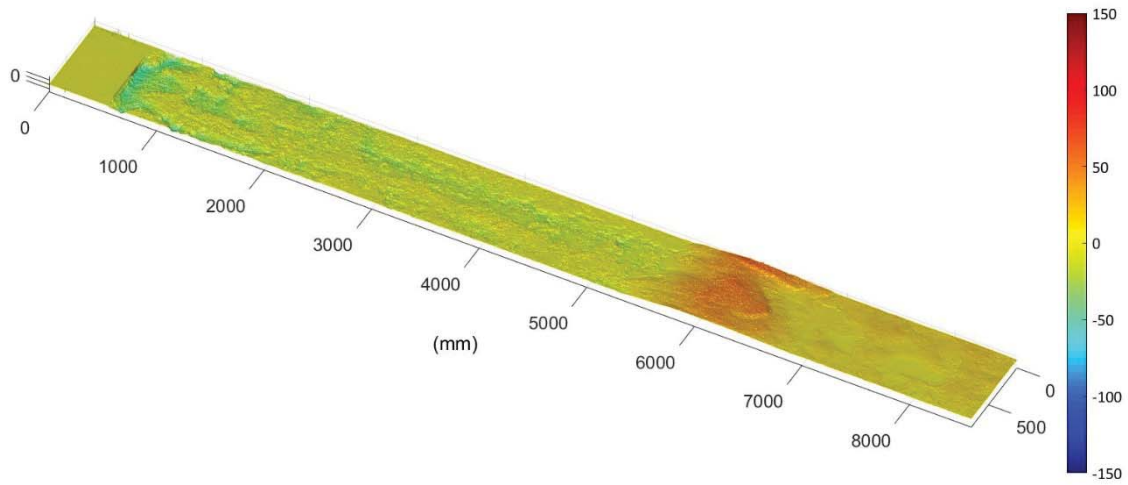


Figure 4.11. Topographic difference plot from zero to two minutes of run time. Note the large area of erosion immediately after the shoulder and channels downslope of it.

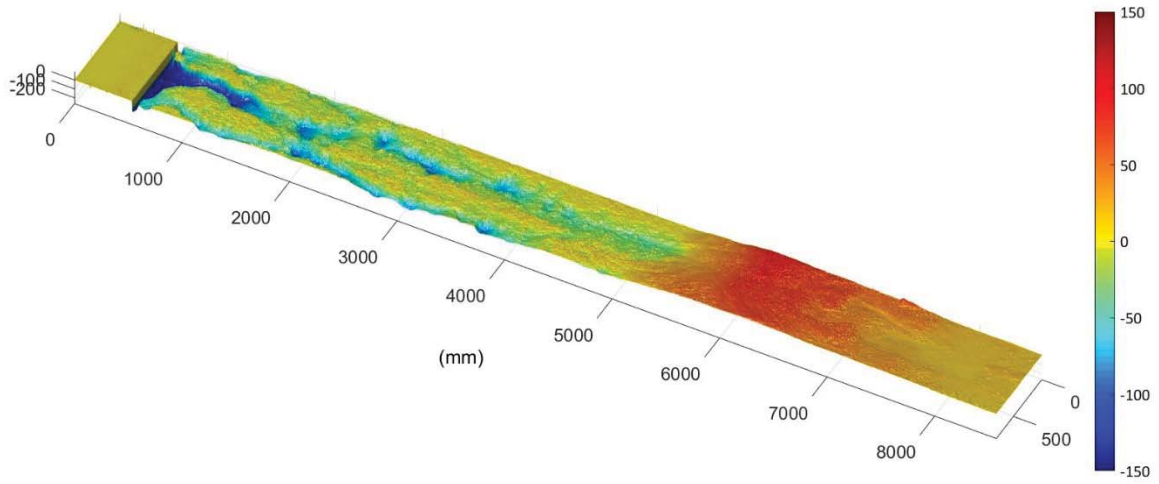


Figure 4.12. Topographic difference plot from zero to 10 minutes of run time. Only ten minutes of run time has undermined the shoulder.

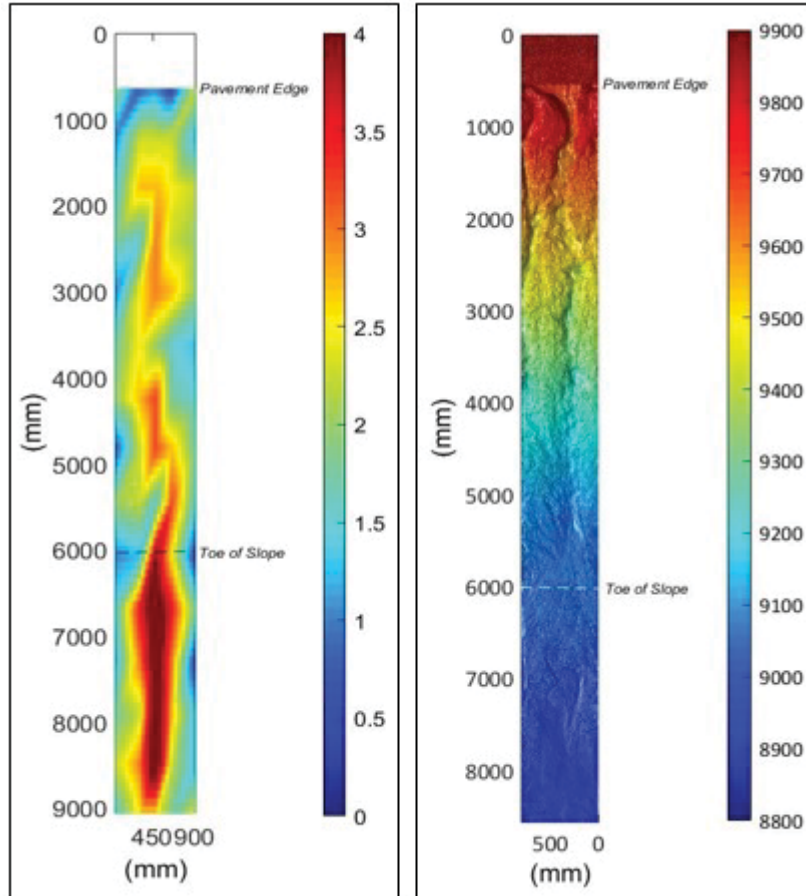


Figure 4.13. (Left). Aerial view of interpolated compaction data on slope interpolated with mid-shoulder starting at zero. Compaction is presented in units of tons per square foot. White area is the shoulder. The color bar on the right of the figure gives color range for compaction values. (Right). Scan of slope after 10 minutes of run time.

Table 4.4. Statistics of compaction on 6H:1V slope for bare soil testing.

Statistics	On Slope (0-12 feet)		On Flat Run out (14-28 feet)	
	Tons/SF	psi	Tons/SF	psi
Average	2.00	27.7	2.54	35.3
Std. Dev	0.78	10.9	1.14	15.9
COV	0.39	5.5	0.45	6.2
Maximum	4.00	55.6	4.50	62.5
Minimum	0.50	6.9	0.50	6.9

4.1.3 Test 3. 4H:1V Slope with Extended Shoulder Paving- Quick Run

4.1.3.1 Summary

The test was a repeat of the Test 1 on the 4H:1V slope however the shoulder was extended with a 42 inch long extension (see Section 2.2). The goal was to observe the impact of the shoulder extension on erosional patterns for the base case of bare soil/no erosion protection. The total duration of this test was 50 minutes carried out over seven runs. Discharge was 0.09 ft³/s equivalent to a unit discharge of 0.03 ft³/s-ft. The overtopping depth was small and not measurable except for that last run, which had an overtopping depth of 0.18 feet.

4.1.3.2 Observations

Testing the 4H:1V slope with the extended pavement resulted in a similar general outcome that rapid and widespread erosion occurred on the bare soil surface at very low discharge. However, some changes in the erosional pattern were documented. Where Test 1 had developed a local scour feature immediately downstream of the shoulder section and channelized erosion on the slope surface, this run did not develop the local scour feature. Because of the extension, the length of the erodible slope section was shorter. The whole erodible section was, more or less, eroded evenly by the event.

4.1.3.3 Failure Description

Both the pattern and intensity of erosion was different for this run than the previous bare soil tests. A local scour feature downstream of the shoulder did not form in this run and erosion near the top of the slope was relatively even and less channelized. One possible reason is that the impact of water onto the slope was at a smaller angle due to the extended shoulder paving (partial slope paving), which conformed to the 4H:1V slope. Channels did form further downslope and eventually grew very deep. This run was continued longer than the previous bare soil runs in order to observe the growth of the failure. In general, this test along with the two other bare soil runs failed at low discharge and were not able to run longer than 60 minutes.

4.1.3.4 Method for calculating velocity, shear stress, and roughness.

An ultrasonic sensor (Massa probe) was positioned perpendicular to the soil slope at mid-slope to record water depth. Before each test run, an ultrasonic sensor recorded the distance from the sensor to the protected slope surface. During the test run the ultrasonic sensor recorded the water surface. Making the assumption of uniform flow the water surface is approximately parallel to the slope. The average water depth for each run was calculated by subtracting the time-averaged sensor distance reading during flow from the time-averaged pre-flow distance for the same run. Since the flume width is known (37.5 inches for 4H:1V slope, 34.5 inches for 6H:1V slope), along with the flow rate and average depth, the bulk or average velocity may be calculated as:

$$V \left(\frac{\text{ft}}{\text{s}} \right) = \frac{Q}{w \cdot d_{\text{avg}}} \quad (1)$$

Maintaining the assumption of uniform flow, assuming the slope, S , of the energy grade line is parallel to the soil slope, and that the frictional effect of the flume walls is small compared with the effect of the bed, the shear stress τ at the slope midpoint is:

$$\tau \left(\frac{\text{lb}}{\text{ft}^2} \right) = \gamma d S \quad (2)$$

Where d is the mid-slope depth and γ is the unit weight of water, taken as 62.4 lb/ft^3 . By inverting Manning's equation, it is possible to solve for the friction factor 'n' at the midpoint. Assuming the hydraulic radius is equal to the depth of flow, with the previously defined variables, the equation is:

$$n = \frac{1.49}{V} d^{2/3} S^{1/2} \quad (3)$$

The calculated values of V , τ , and n are displayed in Table 4.5 and similar subsequent tables. Note that for the majority of bare soil tests, the flow depths were too small and erosion too rapid to make meaningful calculations of these values.

4.1.3.5 Photographs



Figure 4.14. (Left). Looking upstream at 4H:1V slope with extended pavement (white) before testing. (Right). Looking downstream at flow over 4H:1V slope during 2-4 minute run no prevalent channel on upper slope. Channelization begins on the lower portion of slope.



Figure 4.15. Looking upstream after approximately 25 minutes of run time. Channels and depressions forming, no trough or main channel forming.

4.1.3.6 Run Data

Table 4.5. Run data for bare soil, 4H:1V slope with extended shoulder paving

Bare Soil: 4H:1V Slope, Partially Paved			Mid-Slope			
Run end time(min)	Depth Over Crest (ft)	Unit Discharge (ft ³ /s-ft)	Water Depth (ft)	Velocity (ft/s)	Shear Stress, τ (lb/ft ²)	Mannings 'n'
2.0	Not Measured	0.03	Measurements unreliable, too shallow & quick erosion			
4.0		0.03				
6.0		0.03				
10.0		0.03				
22.0		0.03				
32.0		0.03				
50.0	0.18	0.33	0.12	2.85	1.81	0.062

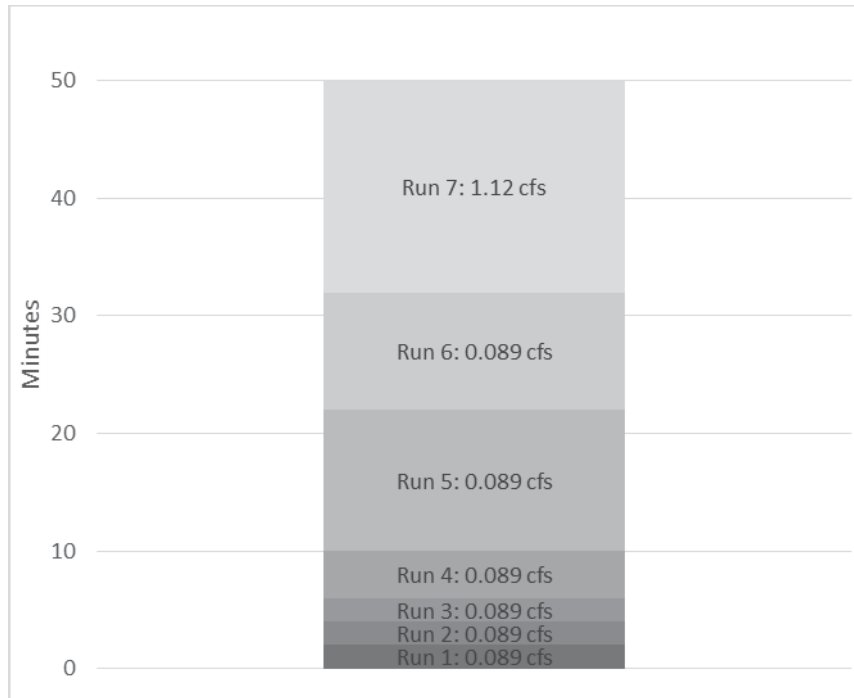


Figure 4.16. Number of runs within this test with flow rate and duration of time at each flow rate.

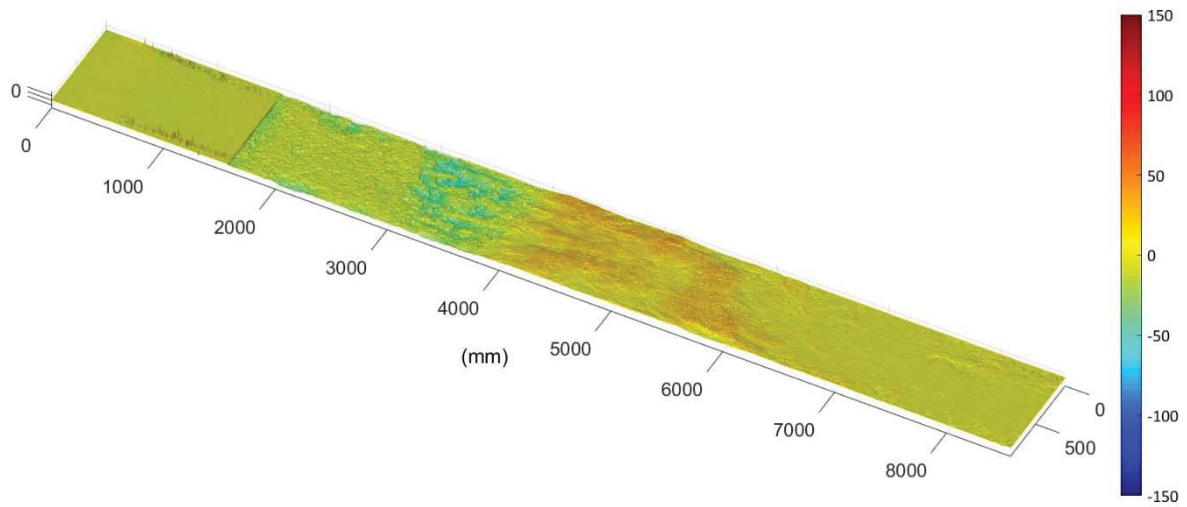


Figure 4.17. Topographic difference plot from zero to two minutes of run time.

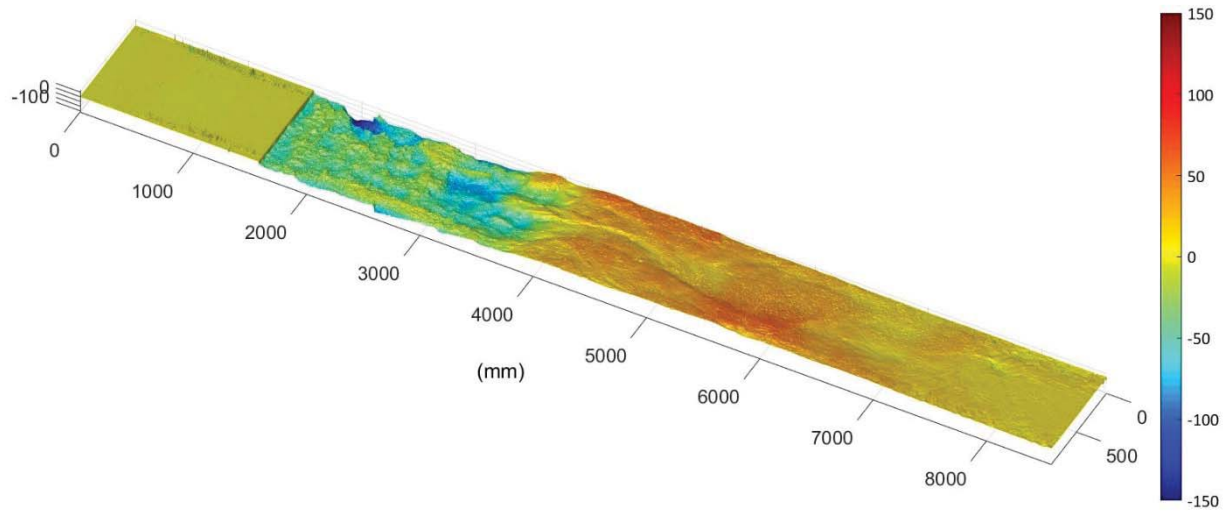


Figure 4.18. Topographic difference plot from two to 22 minutes of run time. Slope now has channels but not as definitive as other runs of bare soil, no primary channel on slope was eroded.

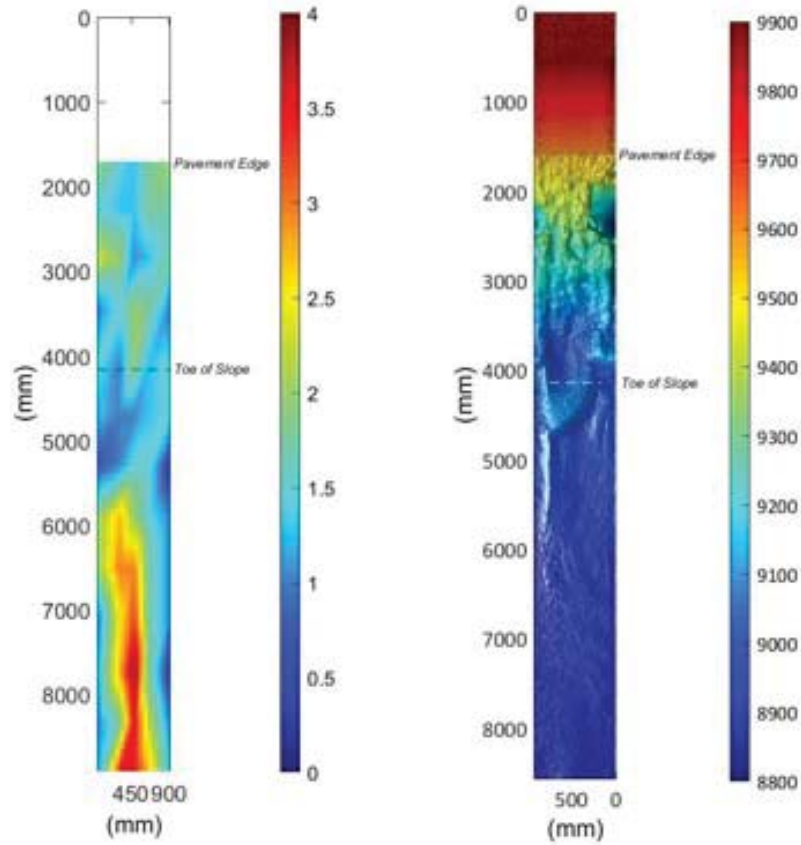


Figure 4.19. (Left). Aerial view of interpolated compaction data on slope interpolated with mid-shoulder starting at zero. Compaction is presented in units of tons per square foot. The white region is the extended shoulder. The color bar on the right of the figure gives color range for compaction values. (Right). Scan of slope after 32 minutes of run time.

Table 4.6. Statistics of compaction on 4H:1V slope with extended pavement for bare soil testing.

Statistic	On Slope (0-9 feet)		On Flat Run-out (9-24 feet)	
	Tons/SF	psi	Tons/SF	psi
Average	1.55	21.5	1.82	25.3
Std. Dev	0.38	5.2	0.94	13.0
COV	0.24	3.4	0.51	7.1
Maximum	2.25	31.3	4.00	55.6
Minimum	1.00	13.9	0.50	6.9

4.2 TECHNIQUE 1: ARMORED SOD

4.2.1 Summary of Technique

This technique did not withstand much flow before experiencing erosion on the slope surface. It performed best on the 6H:1V slope where it endured a flow of 0.37 feet over the crest. All of the 4H:1V slopes experienced slope failure near the transition from paved section to slope. The 6H:1V slope experienced erosion in the middle of the slope in the form of a scour hole and downstream deposition of the scoured material.

4.2.2 Test 1. 4H:1V Slope- Quick Test

4.2.2.1 Summary

This was a baseline test of the armored sod. Failure of the treatment occurred within 2 hours of starting flow. The total test duration was 2 hours with a maximum discharge of 2.7 ft³/s, equivalent to a unit discharge of 0.87 ft³/s-ft. Overtopping depth ranged from 0.03-ft to 0.30-ft.

4.2.2.2 Observations

We observed a large amount of erosion on the right side of the embankment slope. The left edge opposite the erosional area remained intact. A large depositional mound just upstream of the toe of the slope could be a result of the soil that eroded and traveled under the ECB. Burying the ECB at the toe of the slope could have helped to reduce erosion. The erosion that took place along the river-right edge of the flume was unobservable from the surface during the flow event due to the bridging of the stabilization material.

4.2.2.3 Failure Description

The first flow increments were uneventful with little noticeable erosion occurring. Water flowed both on top of the geogrid and through the erosion control blanket. At the end of the third flow step, some visible erosion occurred directly downstream of the shoulder. On the fourth flow step, an erosional scour hole formed just over half way down the slope, with a corresponding depositional mound clearly forming immediately downstream. Both features gradually grew in size and moved slightly upstream, until a large failure occurred within less than five minutes of the start time. Soil from an erosional trench, extending from the road shoulder to 2/3 of the way down the slope, was excavated and was partially retained by the geogrid and erosion control blanket creating a mound just upstream of the toe. On the upper part of the slope the geogrid spanned across the eroded region, while on the lower part of the slope the geogrid protruded upward over the soil mound.

4.2.2.4 Photographs

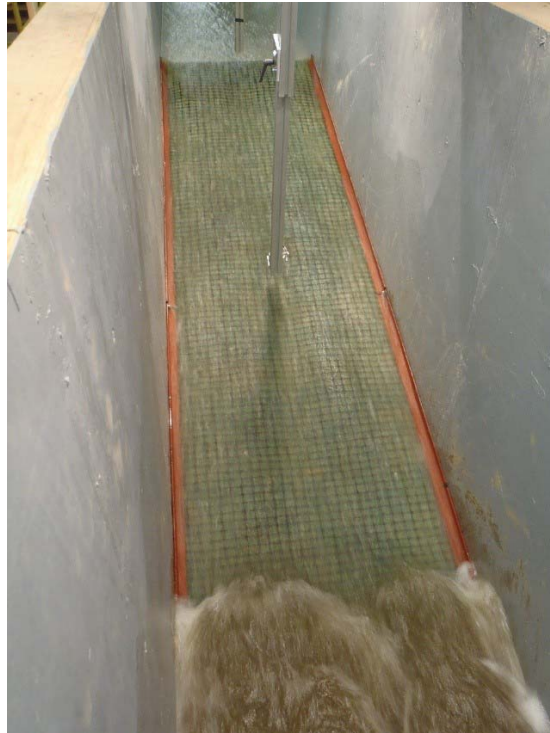


Figure 4.20. Looking upstream at slope no erosion occurring at 1.1cfs.



Figure 4.21. Start of erosion about $\frac{1}{2}$ way down the slope indicated by the depression leading to a mound that aerated the flow in the center of the flume. Looking downslope from shoulder at mound and hydraulic jump.



Figure 4.22. Post flow erosion after 2.7cfs testing. Note the mound near bottom of slope and depression along the left side of the flume looking upstream. Sediment rich water on slope and in tail water indicating erosion occurring on the slope under the ECB.



Figure 4.23. Slope with the shoulder at the top of the photo after ECB was removed post-testing. Note the undermining of shoulder and extensive erosion not seen with ECB still in place on previous photos.

4.2.2.5 Run Data

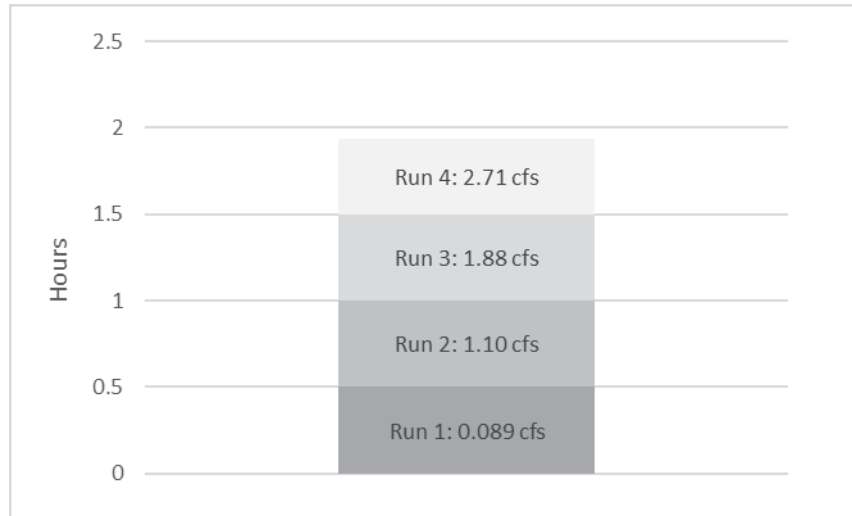


Figure 4.24. Summary of runs with flow rate and duration.

Table 4.7 Run data for Armored Sod (ECB), 4H:1V slope "quick" run.

Tech 1: 4H:1V Slope "quick"			Mid-Slope			
Run end time(hr)	Depth Over Crest (ft)	Unit Discharge (ft ³ /s-ft)	Water Depth (ft)	Velocity (ft/s)	Shear Stress, τ (lb/ft ²)	Mannings 'n'
0.5	0.03	0.03	0.02	1.32	0.34	0.044
1.0	0.17	0.35	0.09	3.78	1.45	0.040
1.5	0.24	0.60	0.12	4.91	1.91	0.037
1.93	0.30	0.87	0.16 **	5.55	2.44	0.039

** Depth, V, τ , from first part of run; later affected by rapid erosion

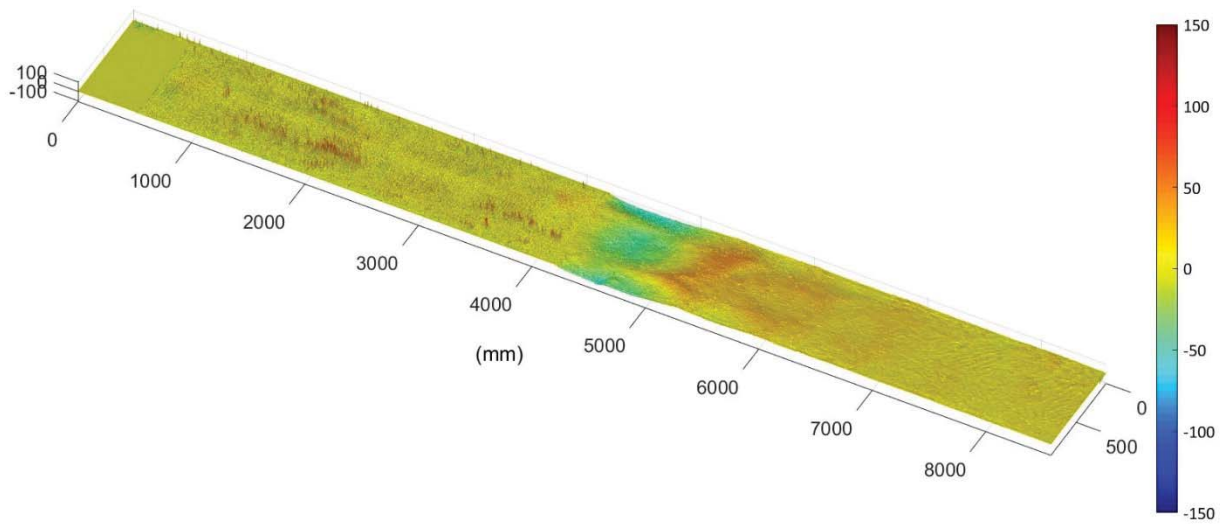


Figure 4.25. Topographic difference plot from zero to 1.5 hours of run time. Minimal erosion on the slope shown here with a depression after the toe of the slope.

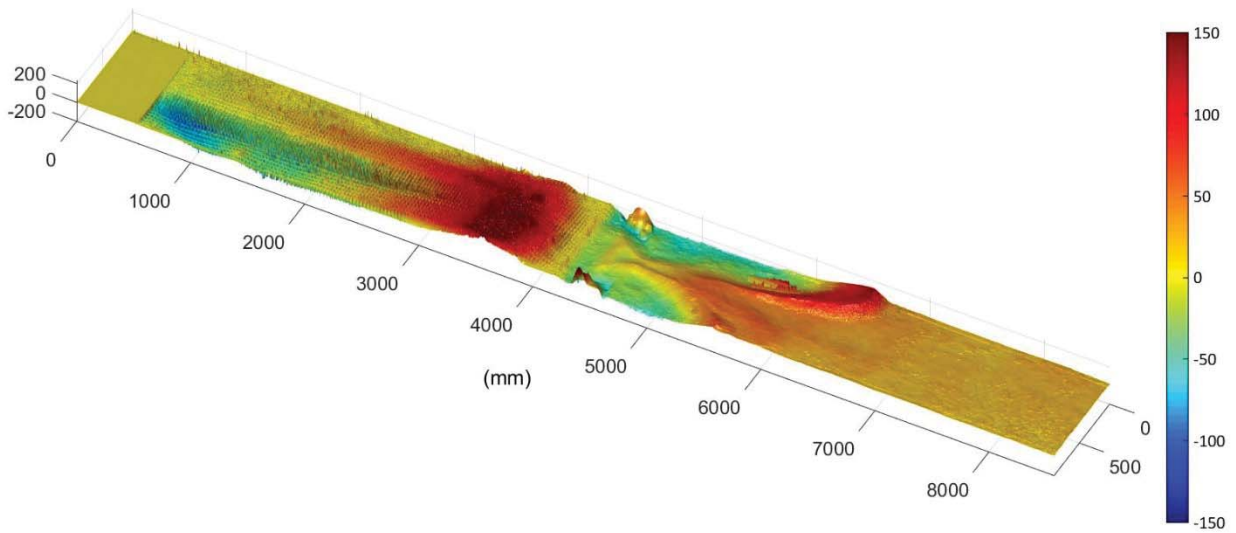


Figure 4.26. Topographic difference plot from zero to 1.93 hours minutes of run time. Note large area of erosion on the edge of the slope with soil deposition at the toe of the slope under the ECB.

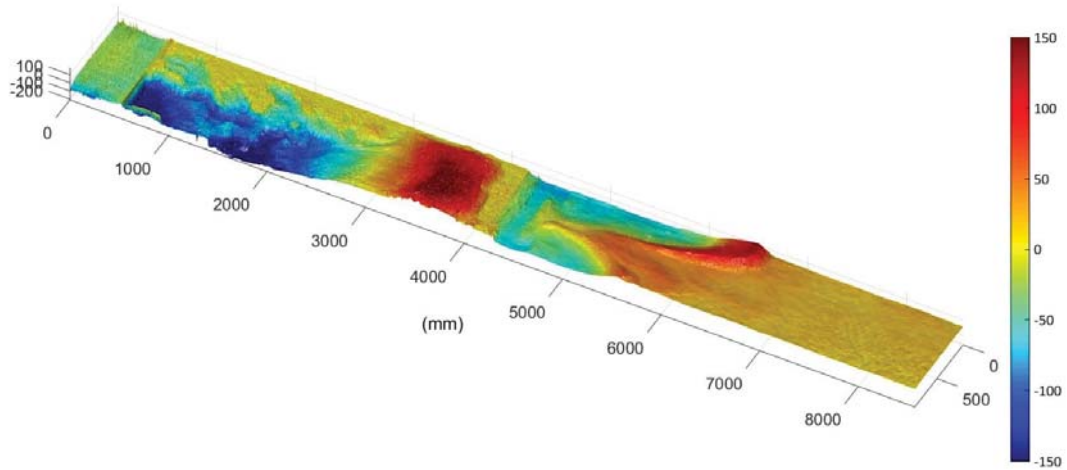


Figure 4.27. Topographic difference plot of bare soil before testing to 1.93 hours of run time with ECB removed. Removing the ECB reveals the extent of erosion that was occurring beneath the ECB.

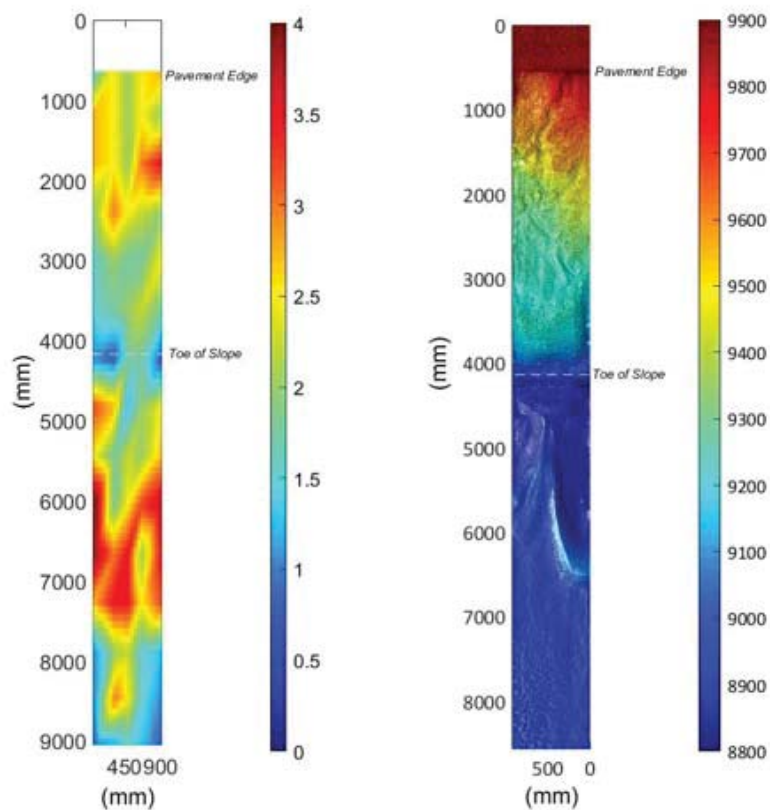


Figure 4.28. (Left) Aerial view of interpolated compaction data on slope. The vertical axis is distance in millimeters from mid-shoulder. Compaction is presented in units of tons per square foot. White area is the shoulder. The color bar on the right of the figure gives color range for compaction values. (Right). Aerial view of scanned slope after eight minutes of run time and ECB was removed showing large depression and channels near pavement edge.

Table 4.8. Statistics of compaction on 4H:1V slope for ECB testing.

Statistic	On Slope (0-12 feet)		On Flat Run-out (14-28 feet)	
	Tons/SF	psi	Tons/SF	psi
Average	2.09	29.1	2.31	32.0
Std. Dev	0.61	8.5	0.97	13.5
COV	0.29	4.1	0.42	5.9
Maximum	3.50	48.6	4.25	59.0
Minimum	0.75	10.4	0.75	10.4

4.2.3 Test 2. 6H:1V Slope

4.2.3.1 Summary

This was a test of the armored sod on the 6H:1V slope using incremental flow tests until failure. The treatment showed early signs of failure after 16 hours of run time. The total test duration was 16 hours with a maximum discharge of 3.36 ft³/s, equivalent to a unit discharge of 1.17 ft³/s-ft. Overtopping depth ranged from 0.17-ft to 0.37-ft.

4.2.3.2 Observations

The tests was terminated as soon as there were signs of erosion and was not allowed to develop deep failures. There does not appear to be a correlation between compaction of the slope and areas of erosion.

4.2.3.3 Failure Description

Similar to the 4H:1V slope “quick” test, there was little erosion during the first initial hours of run time. Through subsequent runs, aerially extensive but shallow erosion increased. Between 10 and 12 hours a small dip and mound was formed on the lower portion of the slope. This zone of erosion grew gradually until the test ended at 16 hours. The test was ended based on calculation of greater than 0.5 inches of soil loss. When the geogrid and erosion control blanket were peeled back, several other shallower areas of erosion were revealed.

4.2.3.4 Photographs



Figure 4.29. Running at 1cfs on 6H:1V slope. View from shoulder looking downstream in flume.

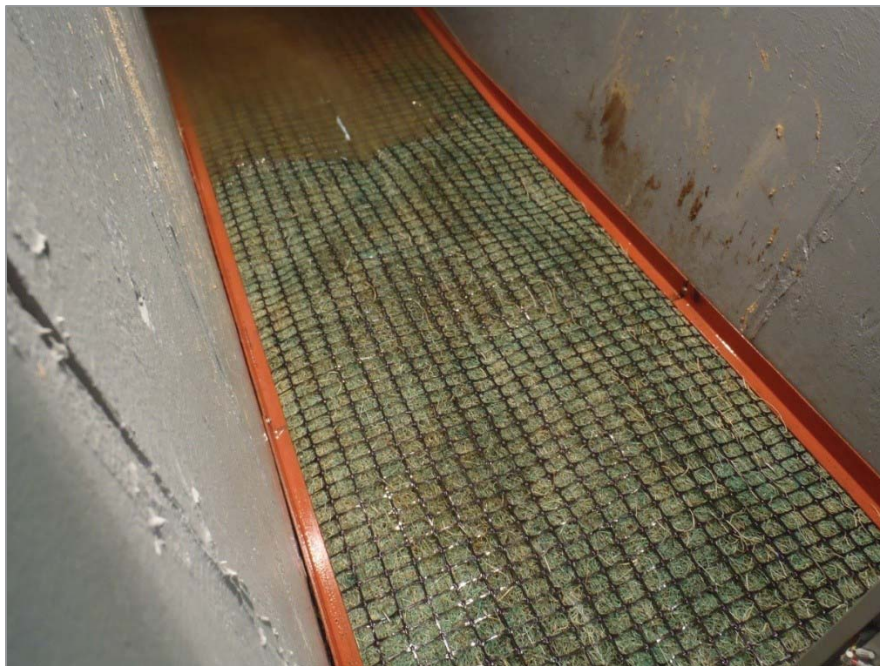


Figure 4.30. Image of early sign of erosion as a depression 75% of the way down slope caused water to separate from bed. Image is looking downstream near toe of slope with tail-water still draining.



Figure 4.31. Flow on slope becoming aerated because of the increasing depth of erosion and separation of the geogrid from the soil. The image shows the formation of a hydraulic jump at bottom of the slope.



Figure 4.32. Looking upstream at bare soil post run with treatment removed showing different locations of erosion on the slope.

4.2.3.5 Run Data

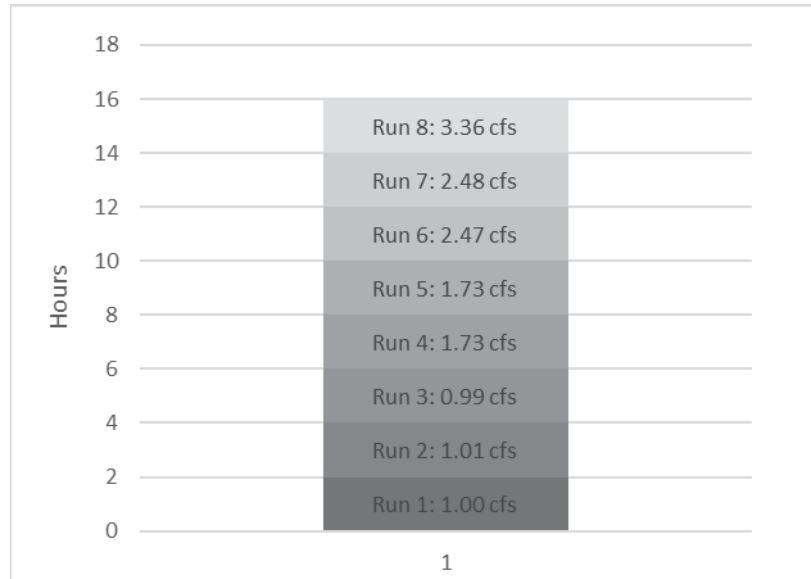


Figure 4.33. Number of runs with flow rate and duration of run time.

Table 4.9. Run data for Armored Sod (ECB), 6H:1V slope.

Tech 1: 6H:1V Slope			Mid-Slope			
Run end time(hr)	Depth Over Crest (ft)	Unit Discharge (ft ³ /s-ft)	Water Depth (ft)	Velocity (ft/s)	Shear Stress, τ (lb/ft ²)	Mannings 'n'
2.0	0.17	0.35	0.10	3.56	1.02	0.036
4.0	0.17	0.35	0.09	3.96	0.93	0.031
6.0	0.17	0.34	0.09	3.94	0.91	0.030
8.0	0.24	0.60	0.12	5.06	1.24	0.029
10.0	0.24	0.60	0.12	5.00	1.26	0.030
12.0	0.30	0.86	0.15	5.68	1.57	0.030
14.0	0.30	0.86	0.17	5.22	1.72	0.035
16.0	0.37	1.17	0.18	6.45	1.89	0.030

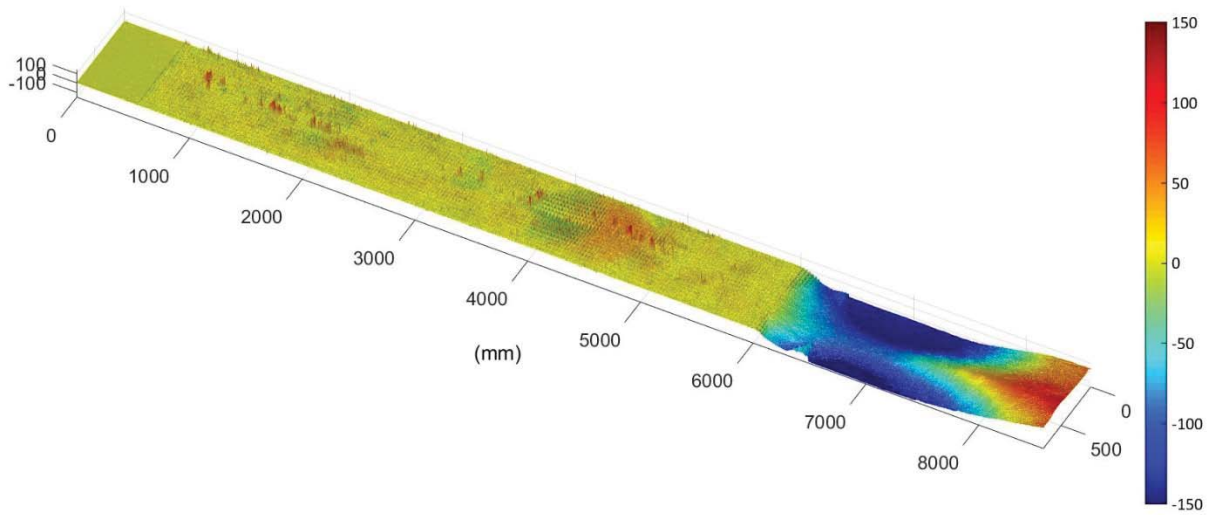


Figure 4.34. Topographic difference plot from zero to 16 hours of run time. Showing a depression and elevated mound $\frac{3}{4}$ of the way down the slope from the shoulder. Smaller depressions are also on the upper $\frac{1}{4}$ of the slope and at mid-slope

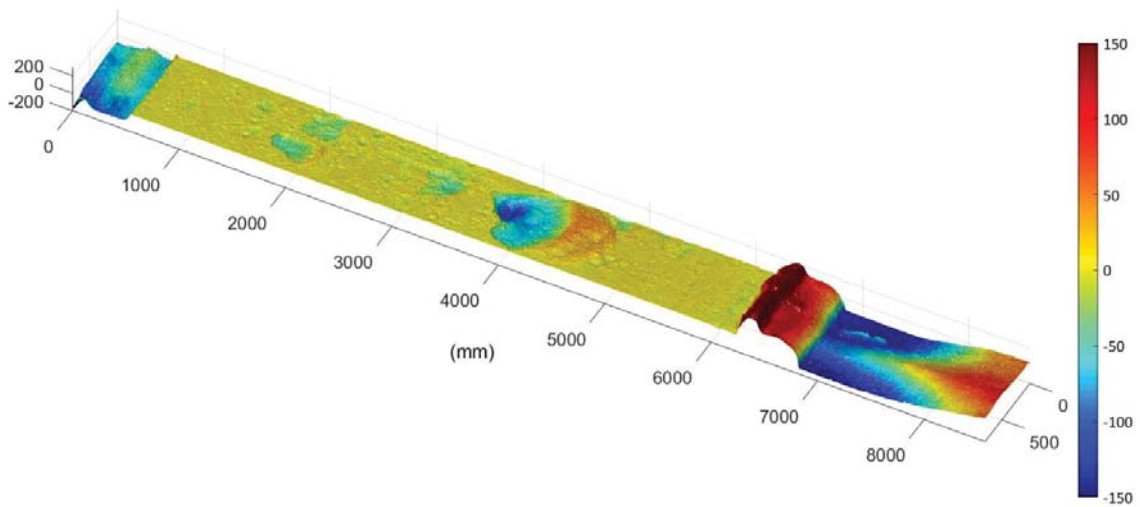


Figure 4.35. Topographic difference plot of final bare soil condition vs. initial bare soil condition. Erosional areas are easily identified here because the ECB covering was removed for the scan.

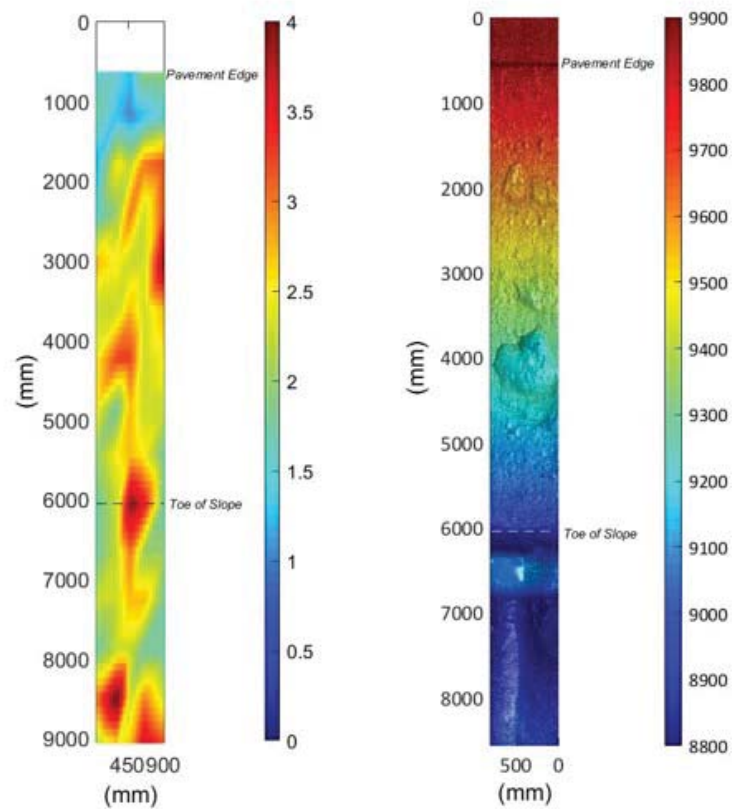


Figure 4.36. (Left). Aerial view of interpolated compaction data on slope. The vertical axis is distance in millimeters from mid-shoulder. Compaction is presented in units of tons per square foot. (Right). Aerial view of final bare soil scanned after the stabilization material was removed from the slope.

Table 4.10. Statistics of compaction on 6H:1V slope for erosion control blanket testing.

Statistic	On Slope (0-12 feet)		On Flat Run-out (14-28 feet)	
	Tons/SF	psi	Tons/SF	psi
Average	2.31	32.0	2.46	34.2
Std. Dev	0.69	9.7	0.65	9.0
COV	0.30	4.2	0.26	3.7
Maximum	4.00	55.6	4.25	59.0
Minimum	1.00	13.9	1.75	24.3

4.2.4 Test 3. 4H:1V Slope

4.2.4.1 Summary

This was a test of the armored sod on the 4H:1V slope and was a repeat of Test 1 to observe repeatability of the performance at a fixed discharge (e.g. a “long test”). Total duration of the test was 0.5 hours, which 1.5 hours shorter than the Test 1. Maximum discharge was 1.10 ft³/s, equivalent to a unit discharge of 0.35 ft³/s-ft. Overtopping depth ranged from 0.17-ft.

4.2.4.2 Observations

Nearly all of the erosion occurred immediately downstream of the shoulder; the remainder of the slope did not experience erosion. Failure at this location caused the research team to end the test quickly. Several factors may have contributed to the immediate, localized failure: 1) there was a small vertical offset in the geogrid at the shoulder edge resulting in a discontinuity at the edge of the slope; 2) the rapid increase in discharge of water (versus the quick test in which we incrementally raise water) and resulting wetting front may have resulted in greater erosion; 3) as part of test protocol, the slope was wetted with a garden hose prior to the start of the run; for this test, the slope was not wetted and this may have contributed to the rapid result.

Compaction may have played a role in stabilization of the slope as the average compaction was higher in this test than other slopes tested with this stabilization technique. With the exception of the upstream shoulder erosion, the slope experienced relatively minor erosion.

4.2.4.3 Failure Description

Almost immediately after the first flow began, erosion initiated just downstream of the shoulder resulting in flow penetrating beneath the geogrid and erosion control blanket. Water was turned off after 30 minutes. Erosion near the shoulder transition was similar to that of bare soil tests characterized by a scour hole immediately downstream of the shoulder.

4.2.4.4 Photographs



Figure 4.37. Looking downstream at slope with indications of immediate erosion by murky tail-water during the first test.

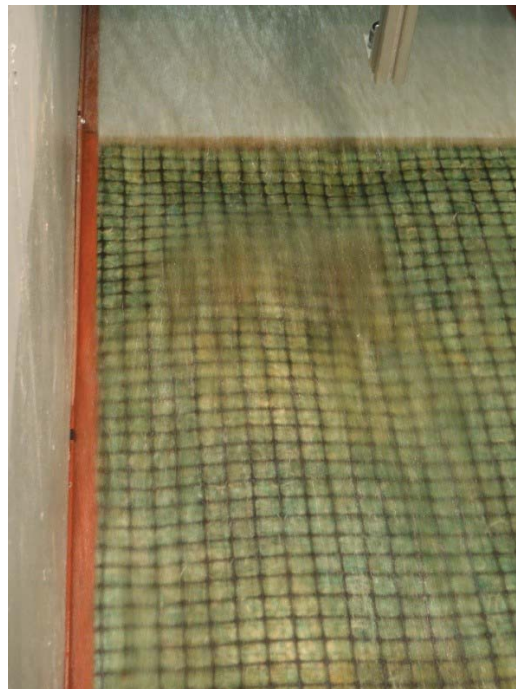


Figure 4.38. Close up of shoulder and slope transition looking upstream. Note the large depression immediately after the shoulder and mound of soil just downstream.

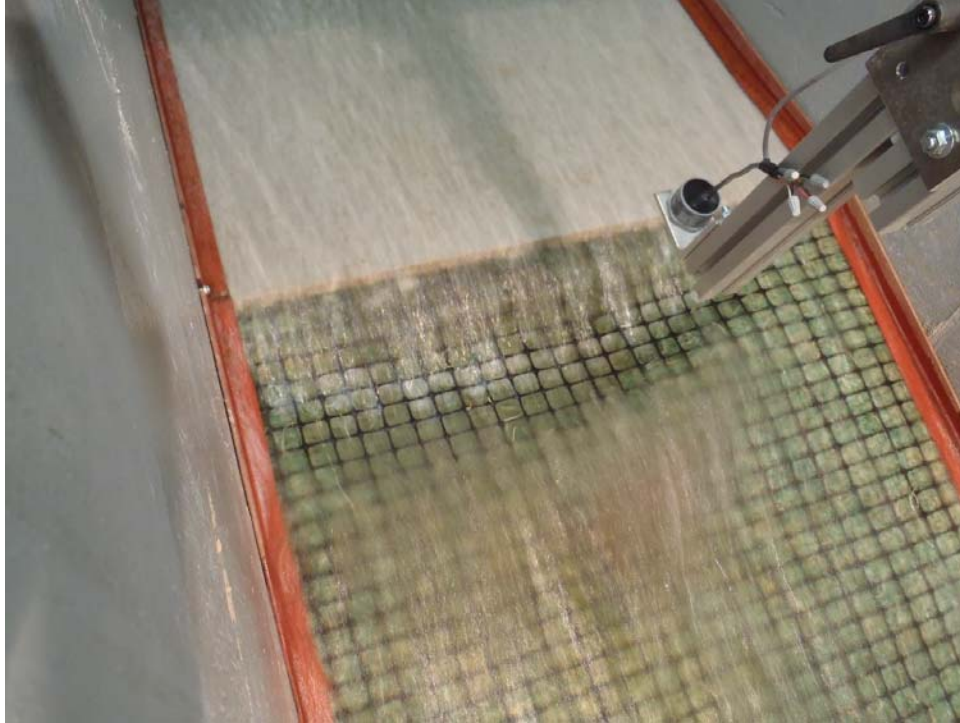


Figure 4.39. After only a few more minutes of run time the erosion has expanded to nearly the entire width of the transition from shoulder to slope.

4.2.4.5 Run Data

Table 4.11. Run data for Armored Sod (ECB), 4H:1V Slope

Tech 1: 4H:1V Slope			Mid-Slope			
Run end time(hr)	Depth Over Crest (ft)	Unit Discharge (ft ³ /s-ft)	Water Depth (ft)	Velocity (ft/s)	Shear Stress, τ (lb/ft ²)	Mannings 'n'
0.5	0.17	0.35	0.11	3.28	1.67	0.051

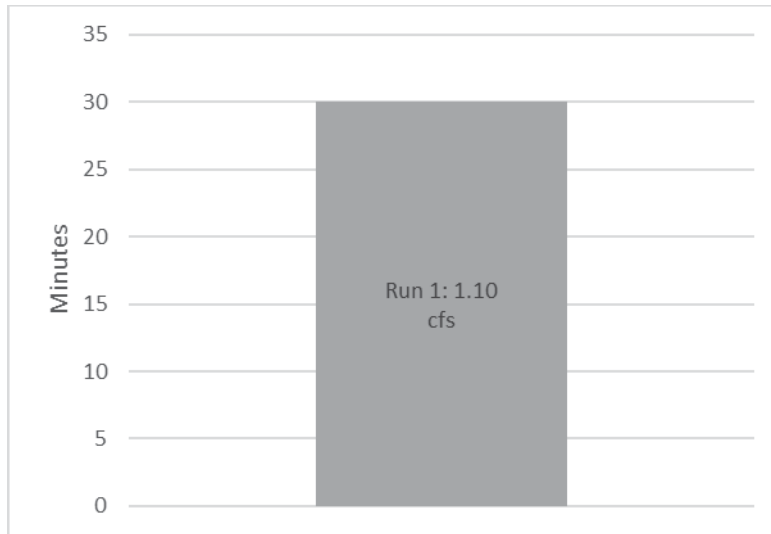


Figure 4.40. Number of runs with flow rate and duration of run time.

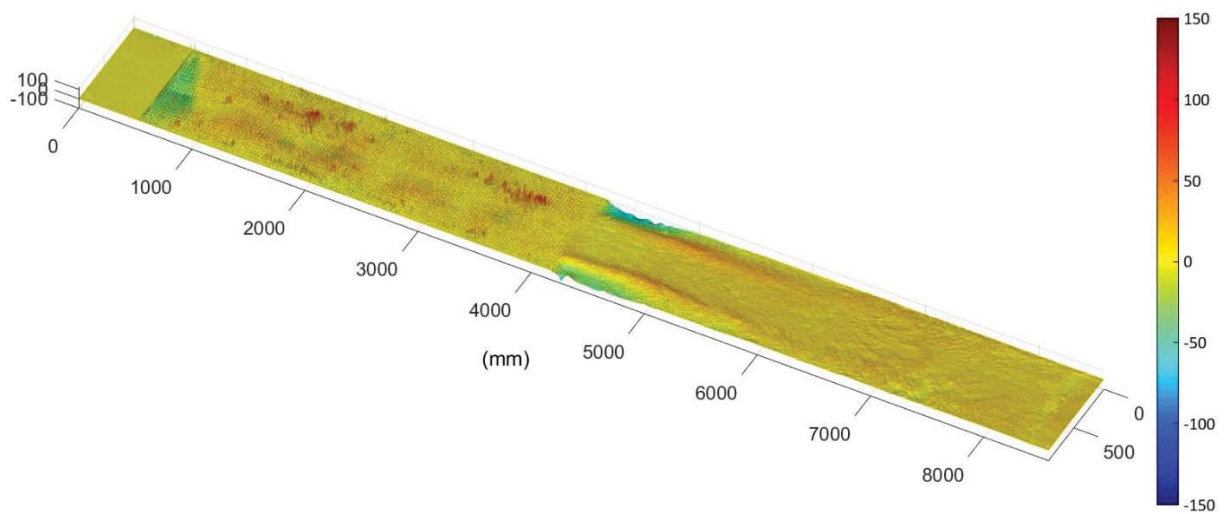


Figure 4.41. Topographic difference plot from zero to 30 minutes.

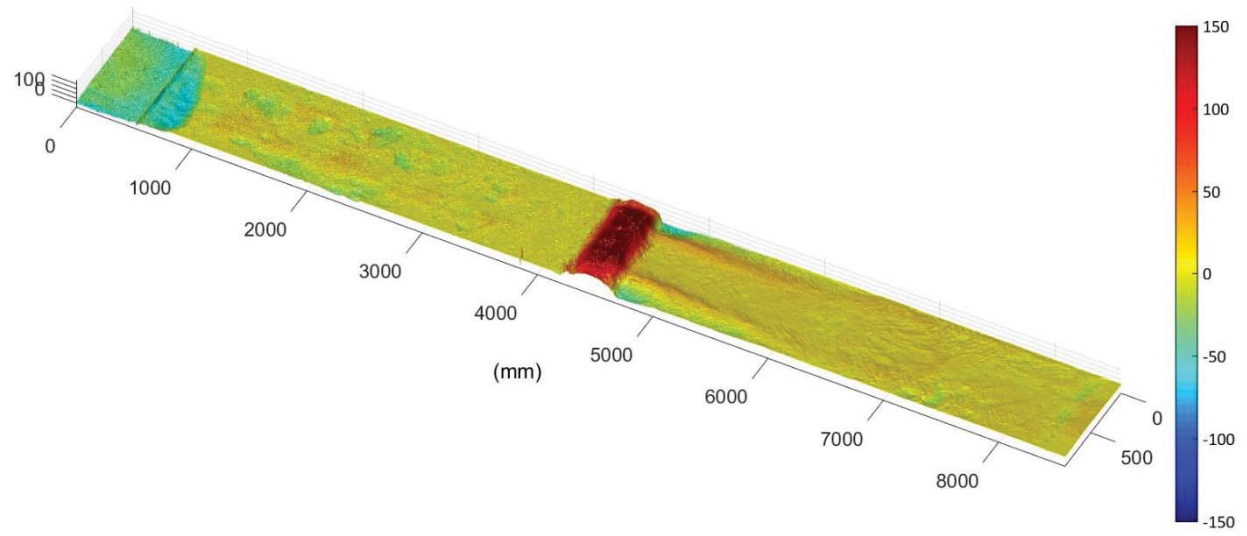


Figure 4.42. Topographic difference plot of initial bare soil vs. final bare soil after 30 minutes of testing. The large deposition at toe of slope is the ECB flipped over onto flat area, and not actually soil deposition.

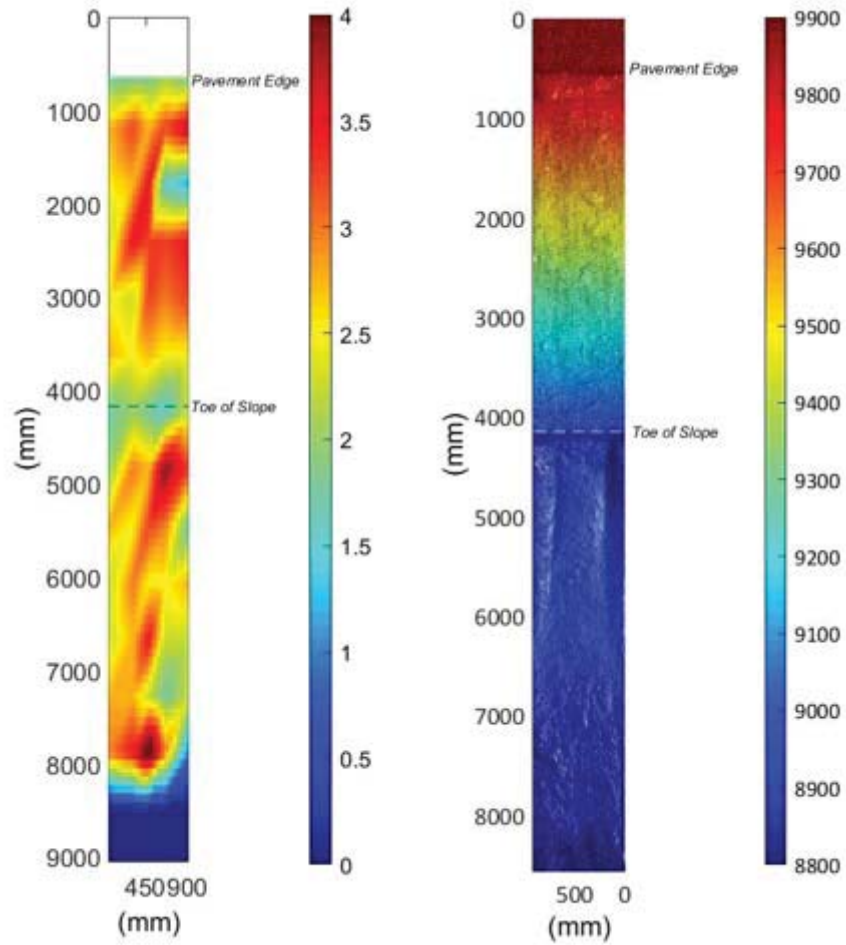


Figure 4.43. (Left). Aerial view of interpolated compaction data on slope. Compaction is presented in units of tons per square foot. (Right). Final bare soil scan showing areas of minor erosion.

Table 4.12. Statistics of compaction on 4H:1V slope for erosion control blanket testing.

Statistic	On Slope (0-12 feet)		On Flat Run-out (14-28 feet)	
	Tons/SF	psi	Tons/SF	psi
Average	2.64	36.7	2.70	37.5
Std. Dev	0.67	9.3	0.69	9.6
COV	0.25	3.5	0.26	3.5
Maximum	3.75	52.1	4.50	62.5
Minimum	1.25	17.4	1.00	13.9

4.2.5 Test 4. 4H:1V Slope with Extended Shoulder Paving

4.2.5.1 Summary

This was a test of the armored sod on the 4H:1V slope with a 42 inch pavement extension on the upper portion of the slope. Total run time was 6 hours and failure was localized at the upstream transition from the paved shoulder to the soil. The total test duration was 6 hours with a maximum discharge of 2.76 ft³/s, equivalent to a unit discharge of 0.88 ft³/s-ft. Overtopping depth ranged from 0.15-ft to 0.30-ft.

4.2.5.2 Observations

The first sign of erosion occurred after 1.5 hours of run time and slowly progressed to 3 hours when a large depression formed near the top of the slope. It is likely that the extension of the pavement aided in the preservation of 4-6 inches of soil immediately downstream of the paved slope section. The erosion moved up the slope towards the top of the paved shoulder, but not nearly as quickly as other tests that experienced slope failures near the pavement. The slope below the failure remained mostly intact, with exception of an area of aggradation of eroded material deposited immediately downstream of the scour hole.

4.2.5.3 Failure Description

Similar to the 4H:1V “quick” test, the bulk of the erosion occurred near the top of the slope. The erosion and resulting mound extended across the width of the flume. Although the upstream eroded face was quite steep and the erosion was deep, the simulated paved edge was not undermined.

4.2.5.4 Photographs



Figure 4.44. Looking upstream at slope with no noticeable erosion. Note the clear tail water.



Figure 4.45. Looking upstream after 1.5 hours of run time. Erosion is observed 1.5ft downstream from the shoulder in the river-left half of flume.



Figure 4.46. Looking downstream from the shoulder during 2-4 hour testing period. Note the large area of erosion occurring near the shoulder specifically near the left wall.



Figure 4.47. Looking downstream from shoulder near the end of the 4-6 hour run. Note the widespread area of erosion and flow separation from the shoulder hitting an angle where the deepest area of erosion is located.



Figure 4.48. Looking upstream at shoulder and slope after stabilization material was removed. Note the remaining soil that was not undermined but close to it after 6 hours of run time.

4.2.5.5 Run Data

Table 4.13. Run data for Armored Sod (ECB), 4H:1V slope with extended shoulder paving.

Tech 1: 4H:1V Slope, Partially Paved			Mid-Slope			
Run end time(hr)	Depth Over Crest (ft)	Unit Discharge (ft ³ /s-ft)	Water Depth (ft)	Velocity (ft/s)	Shear Stress, τ (lb/ft ²)	Mannings 'n'
2.0	0.15	0.30	0.06 **	4.90	0.95	0.023
4.0	0.15	0.30	0.11 **	2.68	1.74	0.064
6.0	0.30	0.88	0.31 **	2.89	4.76	0.117

** Depth, V, τ , from first part of run; each run later affected by erosion



Figure 4.49. Number of runs with flow rate and duration of run time.

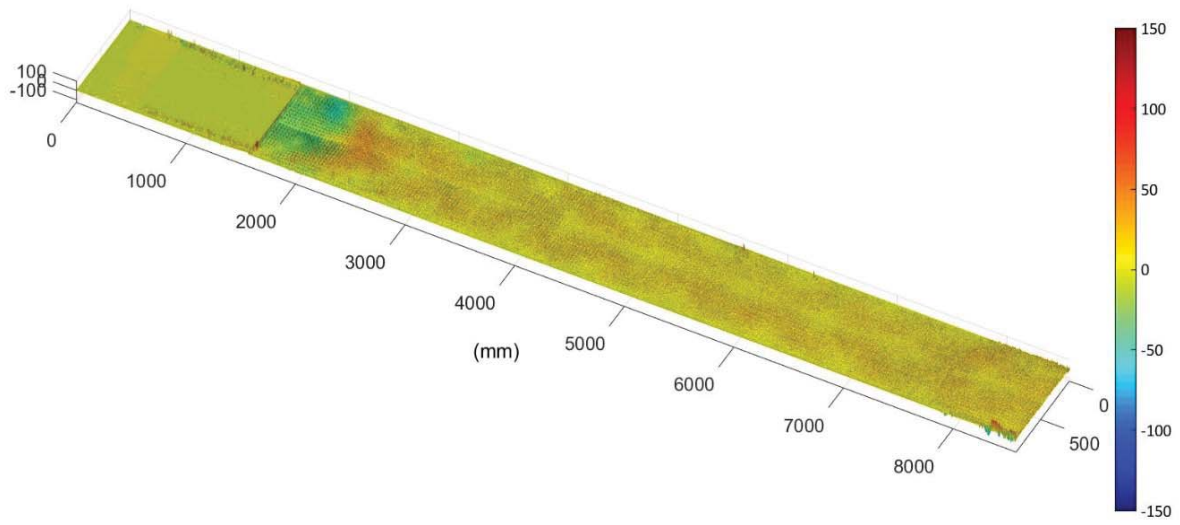


Figure 4.50. Topographic difference plots from zero to 4 hours of run time.

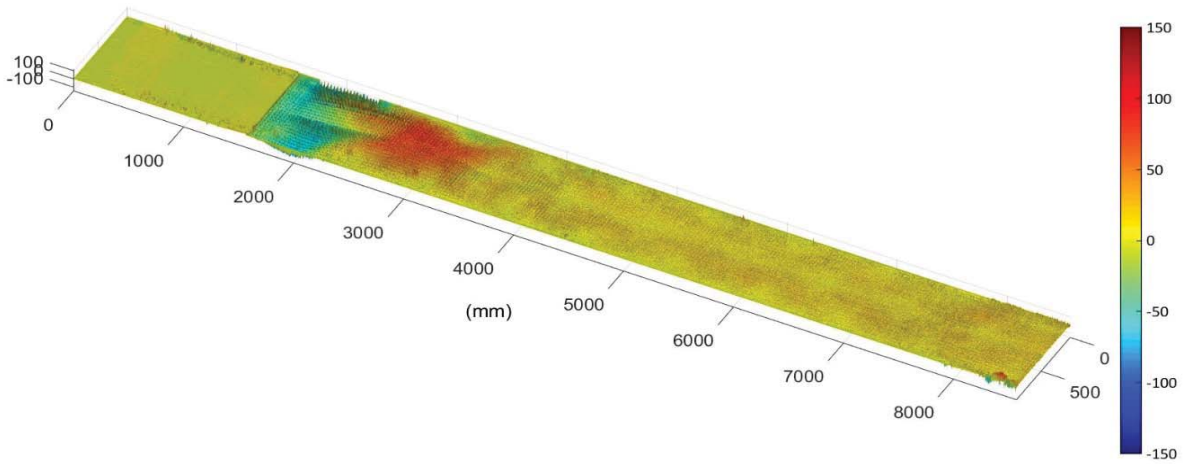


Figure 4.51. Topographic difference plots from zero to 6 hours of run time.

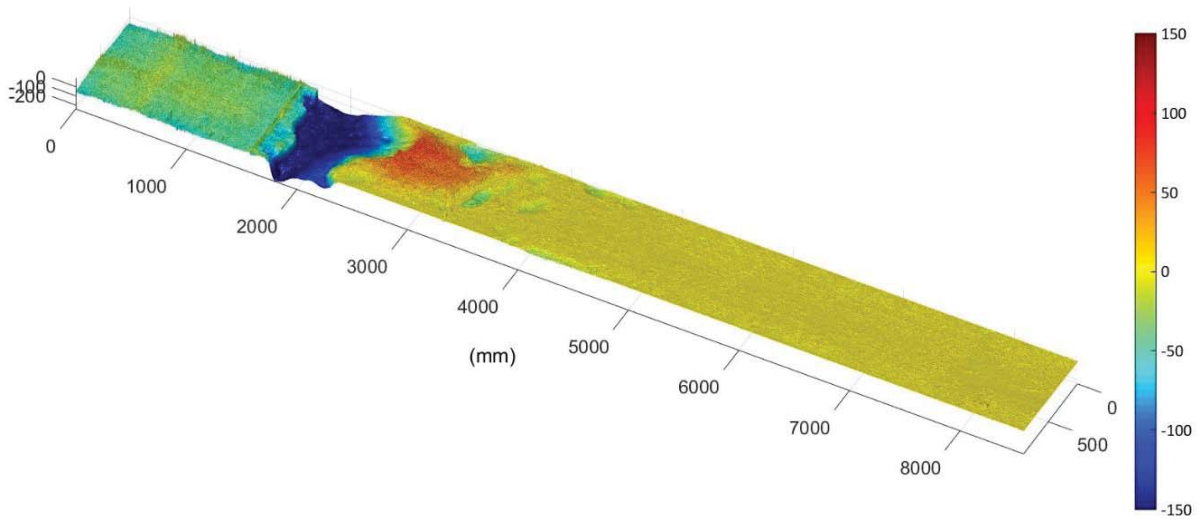


Figure 4.52. Topographic difference plot of initial bare soil vs. final bare soil after 6 hours of run time.

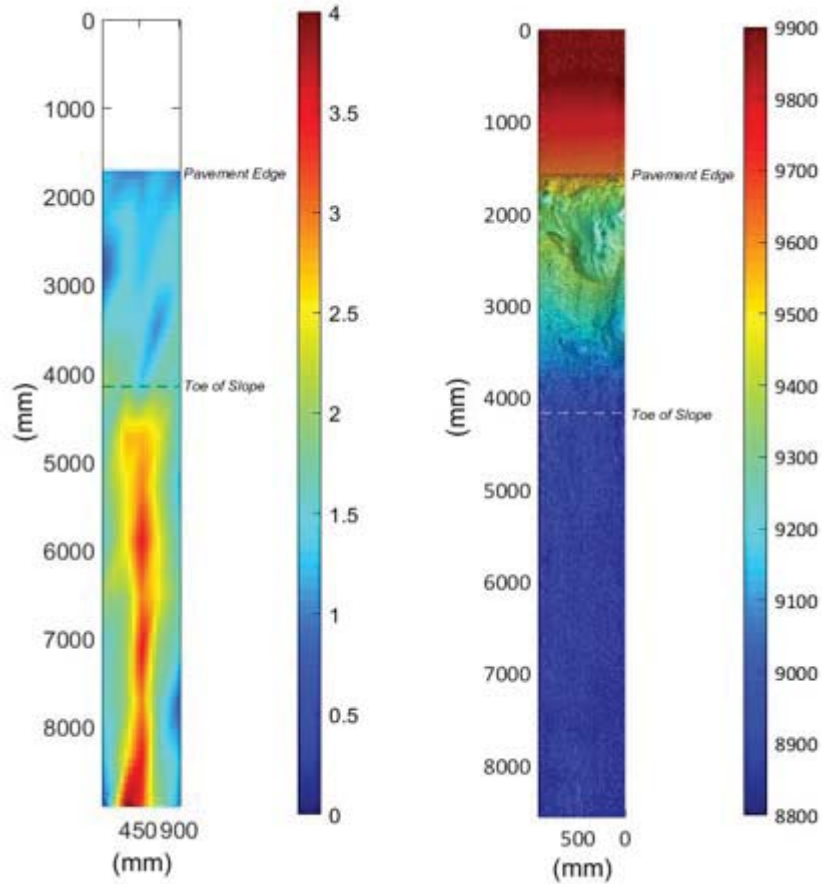


Figure 4.53. (Left). Aerial view of interpolated compaction data on slope with mid-shoulder starting at zero. Values measured in tons per square foot. White area is the extended pavement section. (Right). Scan of final bare soil after the ECB was removed.

Table 4.14. Statistics of compaction on 4H:1V slope with extended pavement for erosion control blanket testing.

Statistic	On Slope (0-9.5 feet)		On Flat Run-out (9.5-26 feet)	
	Tons/SF	psi	Tons/SF	psi
Average	1.37	19.0	2.16	30.1
Std. Dev	0.48	6.6	0.84	11.6
COV	0.35	4.8	0.39	5.4
Maximum	2.00	27.8	4.00	55.6
Minimum	0.75	10.4	0.75	10.4

4.3 TECHNIQUE 1A: ARMORED SOD

4.3.1 Technique Summary:

This stabilization technique was effective as long as sod was kept in contact with the slope. There were no instances in which the soil under the sod was eroded unless the water was diverted to flow between the underside of the sod and the top of the soil slope. This can be seen in both tests that were completed on the 4H:1V slope; when the tests were complete and the sod was removed, there was little to no erosion where the sod had not been disturbed.

4.3.2 Test 1. 4H:1V Slope- Quick Test

4.3.2.1 Summary

This was a baseline test of the armored sod using commercially available bluegrass sod placed under the geogrid. The “quick” test indicates a testing protocol that quickly swept through a range of flow discharges with the goal of identifying the threshold of failure. Total duration of the test was 4.5 hour over 9 runs. Maximum discharge was 13.35 ft³/s, equivalent to a unit discharge of 4.27 ft³/s-ft. Overtopping depth ranged from 0.03-ft to 0.85-ft.

4.3.2.2 Observations

Erosion initiated at the toe of the slope and from that location upstream towards the shoulder. Other than the migrating knickpoint, the rest of the slope remained well intact even when the depth over the crest exceeded 0.80 ft. It was noted that the sod that ran out past the toe of the slope was not fastened as well as the sod that was located on the slope. This may have been a factor in why the sod was eroded away from the toe of the slope. If this test had run longer, the erosion would have continued up the slope.

4.3.2.3 Failure Description

Although the sod did not root, it remained alive through the test and exhibited some growth. In this test, a progressive failure began at the flat run-out area and moved upstream. Sod pieces on the flat run-out area were washed away and soil was eroded to the floor. The soil beneath the sod at the toe of the slope was undermined, though the sod flexed to partly cover the eroding soil surface. Above the obvious eroded area, the soil was completely intact.

4.3.2.4 Photographs



Figure 4.54. Looking downstream from shoulder. Installed sod and geogrid before testing.

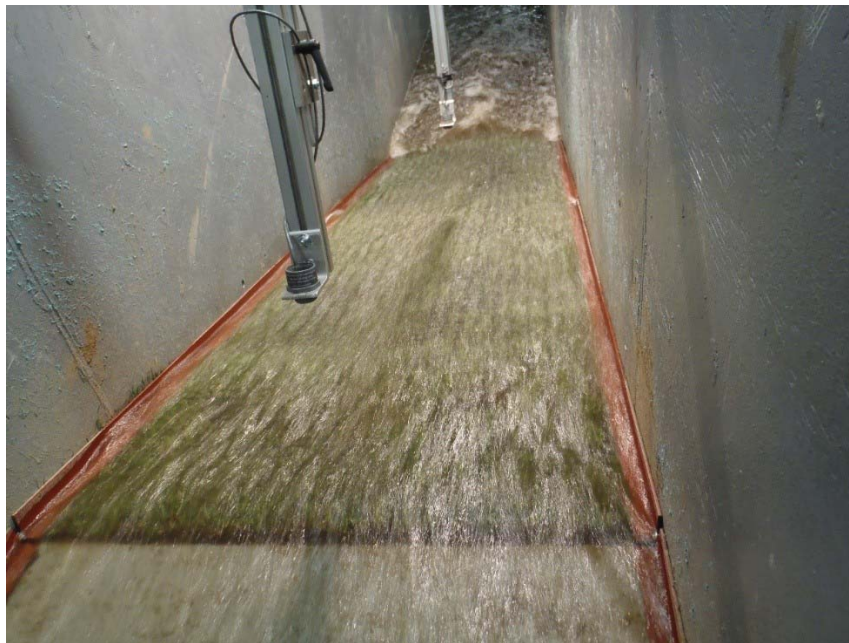


Figure 4.55. Looking downstream from shoulder. Testing 30-60 min, no noticeable large areas of erosion.



Figure 4.56. Looking upstream at toe of slope. Erosion beginning at toe of slope, undermining sod and washing some pieces away. Erosion working up the slope from run-out area.



Figure 4.57. Looking upstream from run-out area. Stabilization material removed showing the extent of the erosion starting at the toe of the slope and working up towards the shoulder.

4.3.2.5 Run Data

Table 4.15. Run data for Armored Sod (1A), 4H:1V slope "quick" run

Tech 1A: 4H:1V Slope "quick"			Mid-Slope			
Run end time(hr)	Depth Over Crest (ft)	Unit Discharge (ft ³ /s-ft)	Water Depth (ft)	Velocity (ft/s)	Shear Stress, τ (lb/ft ²)	Mannings 'n'
0.5	0.03	0.03	0.01	2.39	0.19	0.016
1.0	0.17	0.37	0.06	6.21	0.92	0.018
1.5	0.24	0.62	0.09	7.00	1.39	0.021
2.0	0.40	1.36	0.15	8.78	2.41	0.024
2.5	0.50	1.92	0.18	10.67	2.80	0.022
3.0	0.70	3.19	0.28	11.46	4.34	0.028
3.5	0.79	3.82	0.34	11.39	5.24	0.032
4.0	0.87	4.49	0.37	12.00	5.84	0.032
4.5	0.85	4.27	0.32	13.15	5.07	0.027

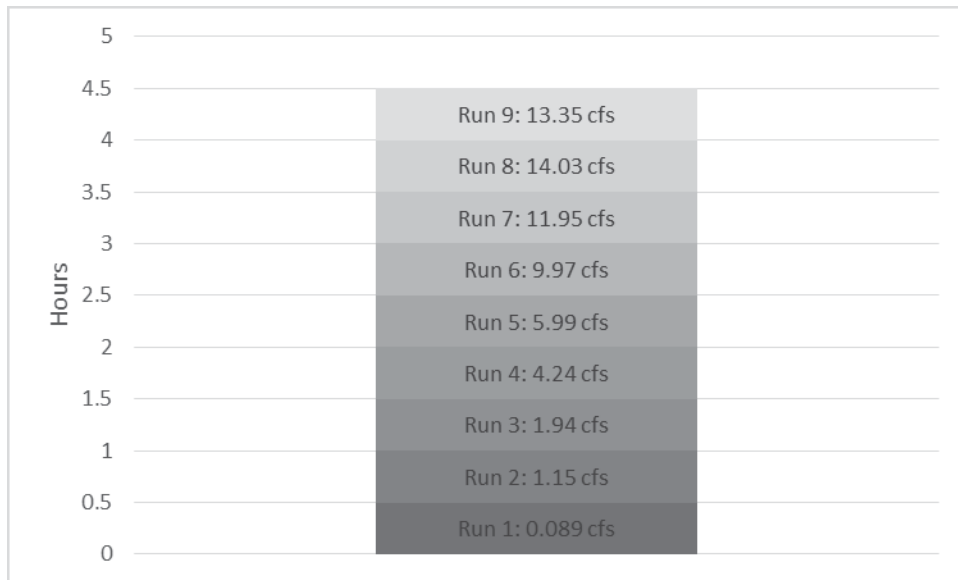


Figure 4.58. Number of runs with flow rate and duration of run time.

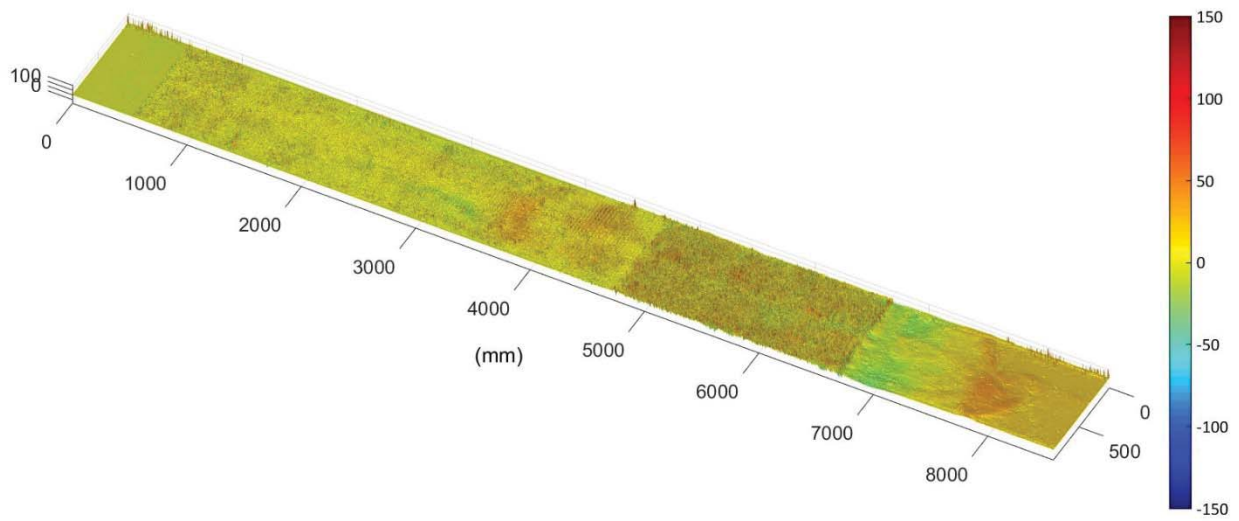


Figure 4.59. Topographic difference plot from zero to 60 minutes of run time.

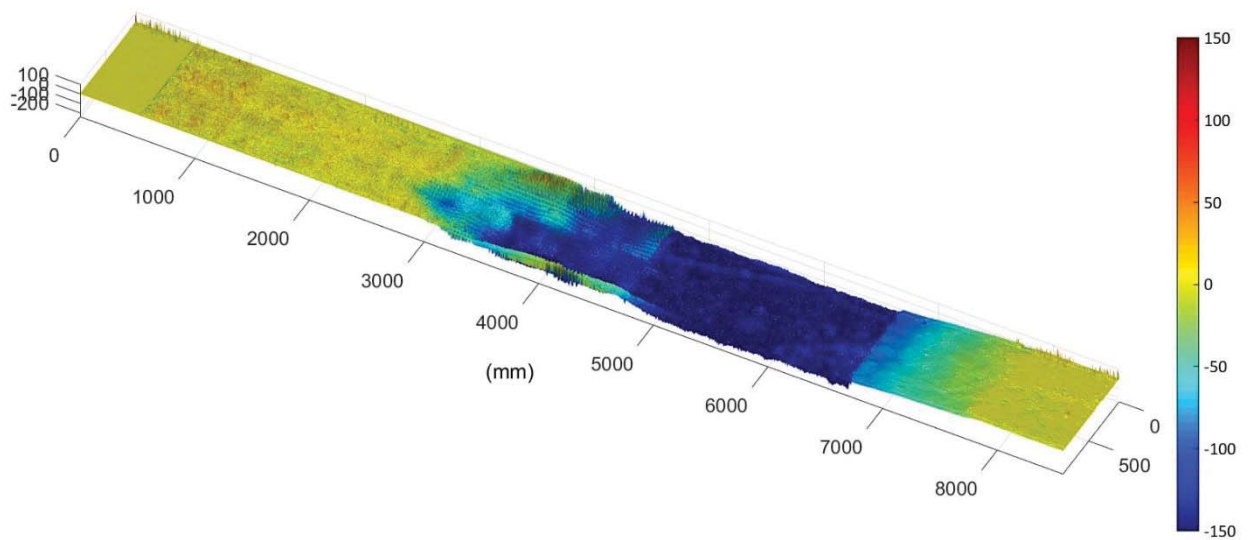


Figure 4.60. Topographic difference plot from zero to 4.5 hours of run time. Note the unchanged upper slope and erosion at the bottom of the slope.

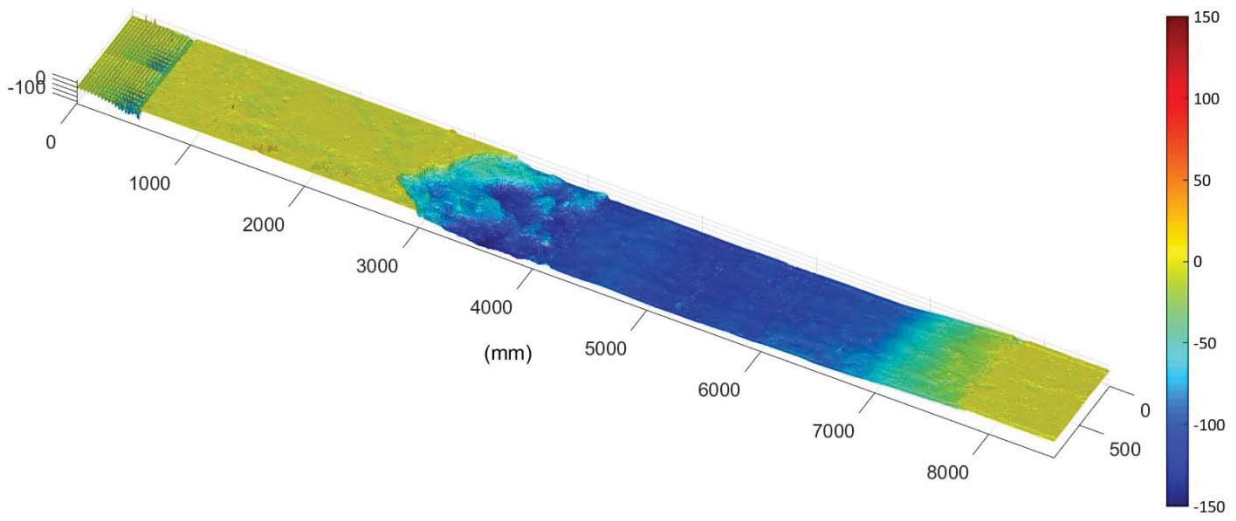


Figure 4.61. Topographic difference plot of initial bare soil vs. final bare soil after 4.5 hours of run time. Upper slope to approximately 2500mm downslope still intact.

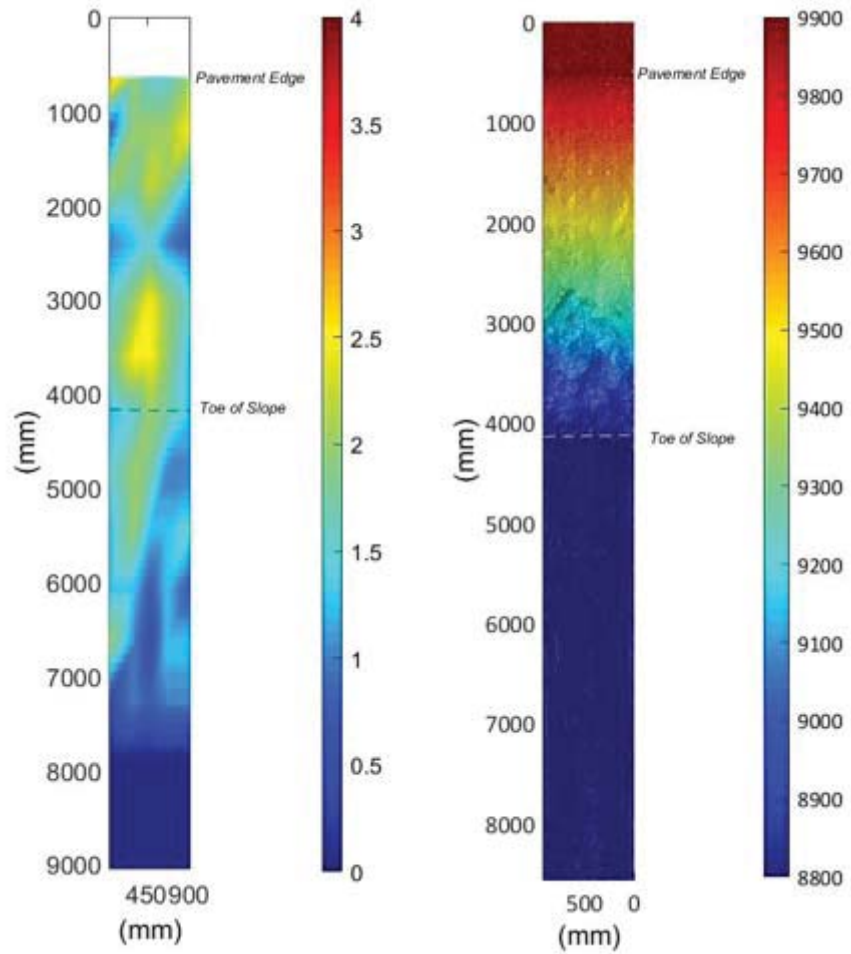


Figure 4.62. (Left). Aerial view of interpolated compaction data on slope with mid-shoulder starting at zero. Compaction measured in tons per square foot. (Right). Plan view of final bare soil scanned after all sod and geogrid was removed from the slope.

Table 4.16. Statistics of compaction on 4H:1V slope for sod testing.

Statistic	On Slope (0-12 feet)		On Flat Run-out (14-28 feet)	
	Tons/SF	psi	Tons/SF	psi
Average	1.75	24.3	1.20	16.7
Std Dev	0.53	7.3	0.42	5.8
COV	0.30	4.2	0.35	4.9
Maximum	3.00	41.7	2.00	27.8
Minimum	0.75	10.4	0.50	6.9

4.3.3 Test 2. 4H:1V Slope with Extended Shoulder Paving

4.3.3.1 Summary

This was a test of the armored sod with real grass on the 4H:1V slope with a 42 inch pavement extension on the upper portion of the slope. It will be compared with the other armored sod with real grass test (Test 1) without the pavement extension to assess its effectiveness. The total test duration was 9.5 hours over three runs. Maximum discharge was 2.8 ft³/s, equivalent to a unit discharge of 0.90 ft³/s-ft. Overtopping depth ranged from 0.15-ft to 0.30-ft.

4.3.3.2 Observations

The upper portion of the slope, just downstream of the paved section, was unaffected by the flow – even for the highest flow rates. The separation between sod pieces was observed at the lower flow however no large erosion was detected. At 4 hours discharge was increased from 0.15-ft of overtopping to 0.3-ft of overtopping resulting in initiation of erosion and failure. The erosion that did occur was substantial and we believe it was exacerbated by flow penetrating between the seams of two adjacent sod mats. Once flow penetrated the sod layer, the soil was quickly washed out and failure of the slope proceeded.

The area where the erosion was initiated had a higher measured compacted level than other areas of the slope suggesting that, at high flows, compaction may have a smaller role in initiation of erosion.

4.3.3.3 Failure Description

In contrast to the 4H:1V “quick” test, the slope first began to erode at a butt joint between sod pieces about halfway down the slope after more than two hours. This erosion was relatively localized until the flow step increase, when it expanded greatly. Similar to the 4H:1V “quick” test, soil eroded from beneath the sod before the sod washed away. At the end of the test a small section of sod near the top of the slope was still intact, as well as the soil beneath.

4.3.3.4 Photographs



Figure 4.63. Looking upstream during first two hour run, no noticeable erosion anywhere on slope.



Figure 4.64. Aerial view of the slope just past halfway down the slope a large depression formed quickly at the seam of two pieces of sod just minutes before the end of the 2-4 hours testing time.



Figure 4.65. During final 4-5.5 hour run, catastrophic erosion took place. Most of the lower slope began eroding under the sod, which had come loose but was held from being washed away by the geogrid and staples.



Figure 4.66. Looking upstream at shoulder to slope transition after the geogrid has been removed. Most of the transition is still intact while the areas where there was a seam between the rolled out pieces of sod allowed water to penetrate and erode the slope surface under the sod which was being partly held in place by the geogrid and landscaping staples.

4.3.3.5 Run Data

Table 4.17. Run data for Armored Sod (1A), 4H:1V slope with extended shoulder pavement.

Tech 1A: 4H:1V Slope, Partially Paved			Mid-Slope			
Run end time(hr)	Depth Over Crest (ft)	Unit Discharge (ft ³ /s-ft)	Water Depth (ft)	Velocity (ft/s)	Shear Stress, τ (lb/ft ²)	Mannings 'n'
2.0	0.15	0.32	0.11	2.98	1.66	0.056
4.0	0.15	0.30	0.09	3.28	1.43	0.046
9.5	0.30	0.90	0.12 **	7.51	1.86	0.024

** Depth, V, τ , from first part of run; later affected by rapid erosion

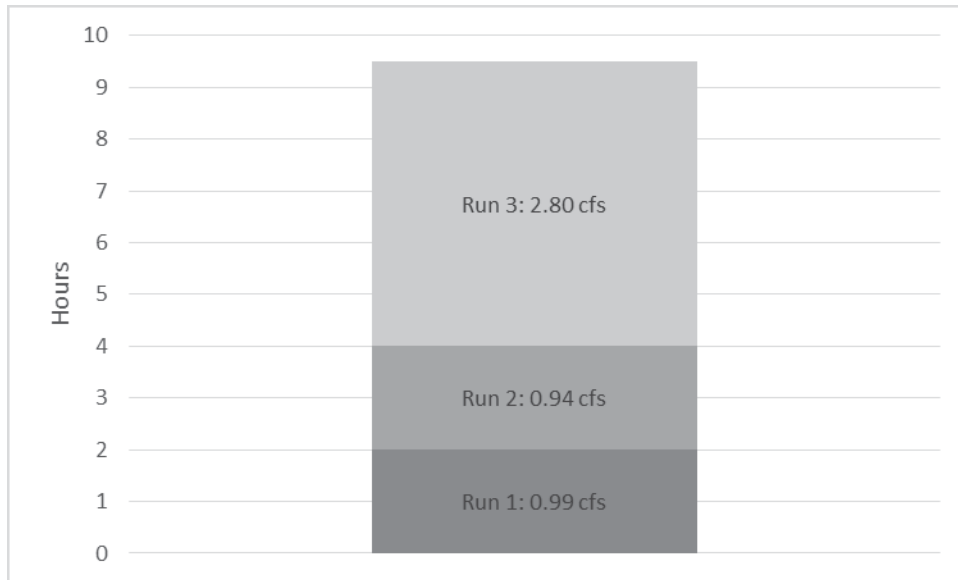


Figure 4.67. Number of runs with flow rate and duration of run time.

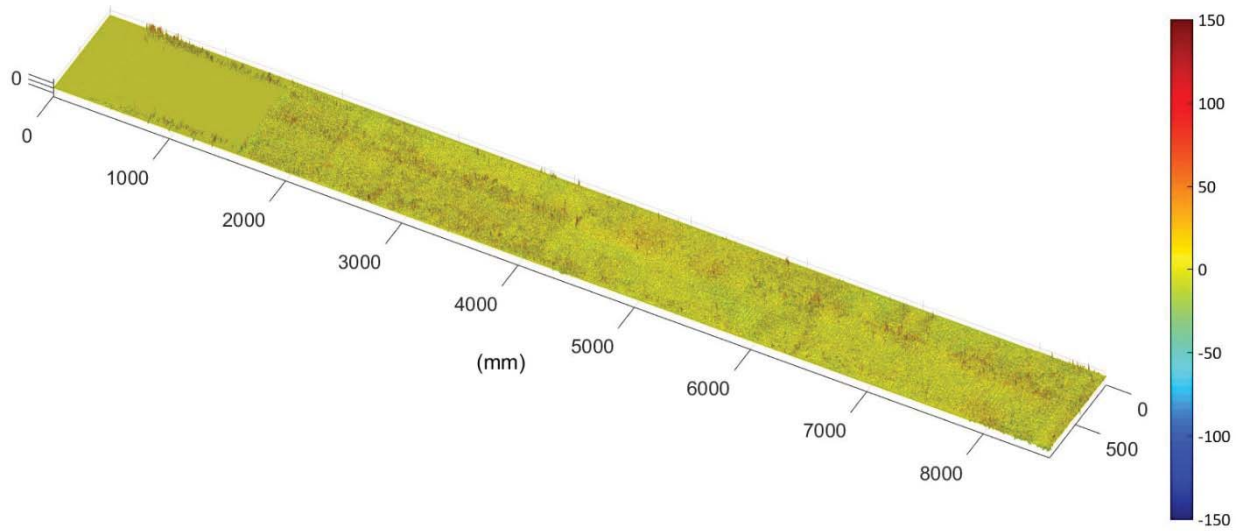


Figure 4.68. Topographic difference plot from zero to two hours of run time showing little visible erosion.

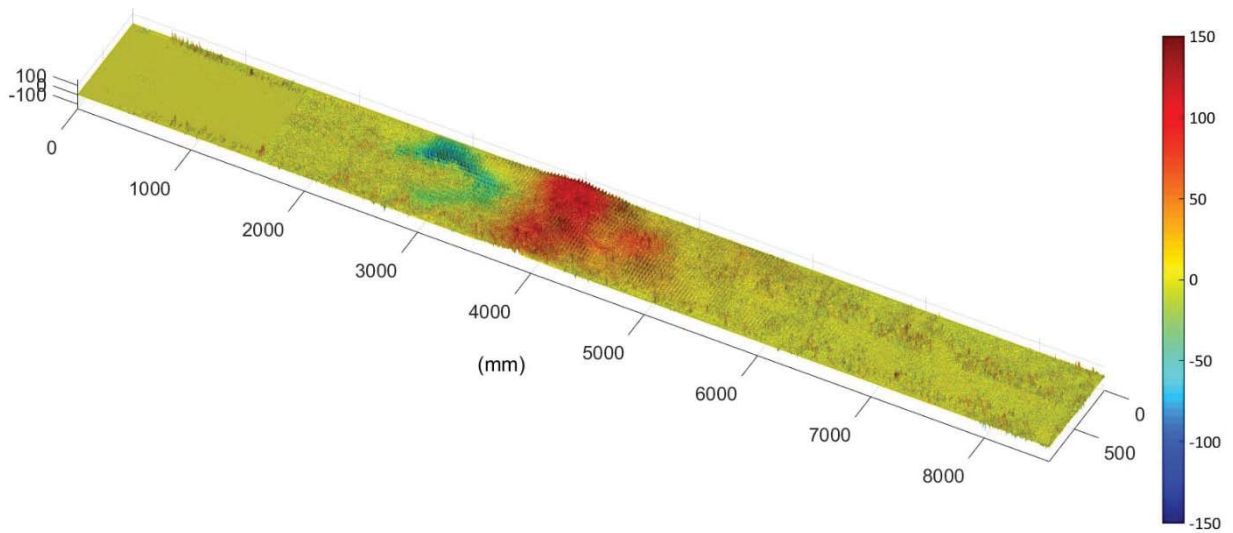


Figure 4.69. Topographic difference plot from zero to four hours of testing time. Note the large deposition at the toe of the slope and depression upslope of it.

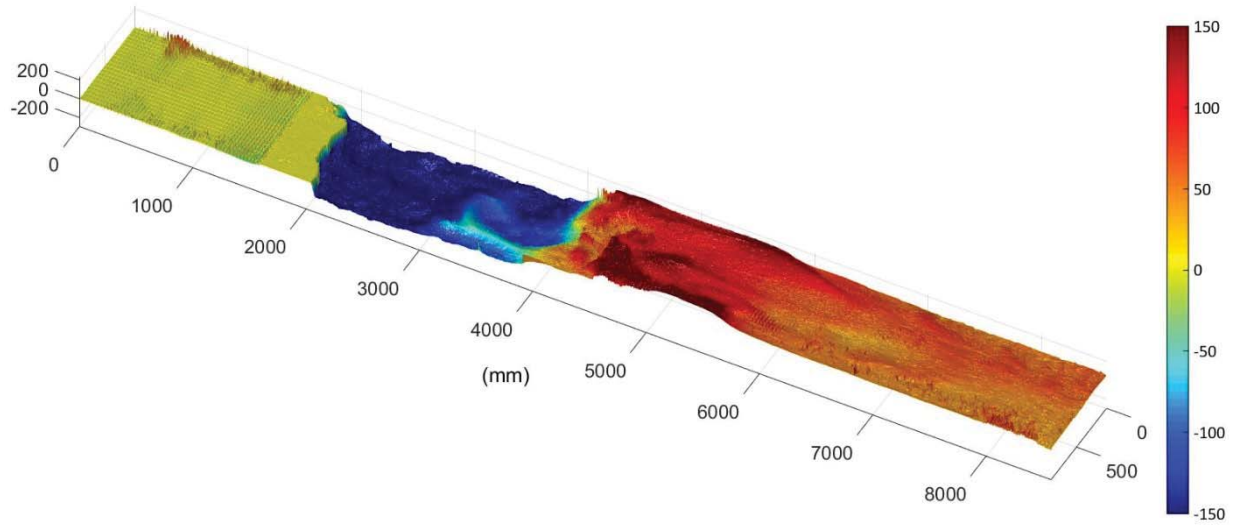


Figure 4.70. Topographic difference plot of initial bare soil vs. final bare soil after 9.5 hours of run time. The upstream slope is still intact. Note that the positive elevation on pavement section is the geogrid that has been flipped back over the surface.

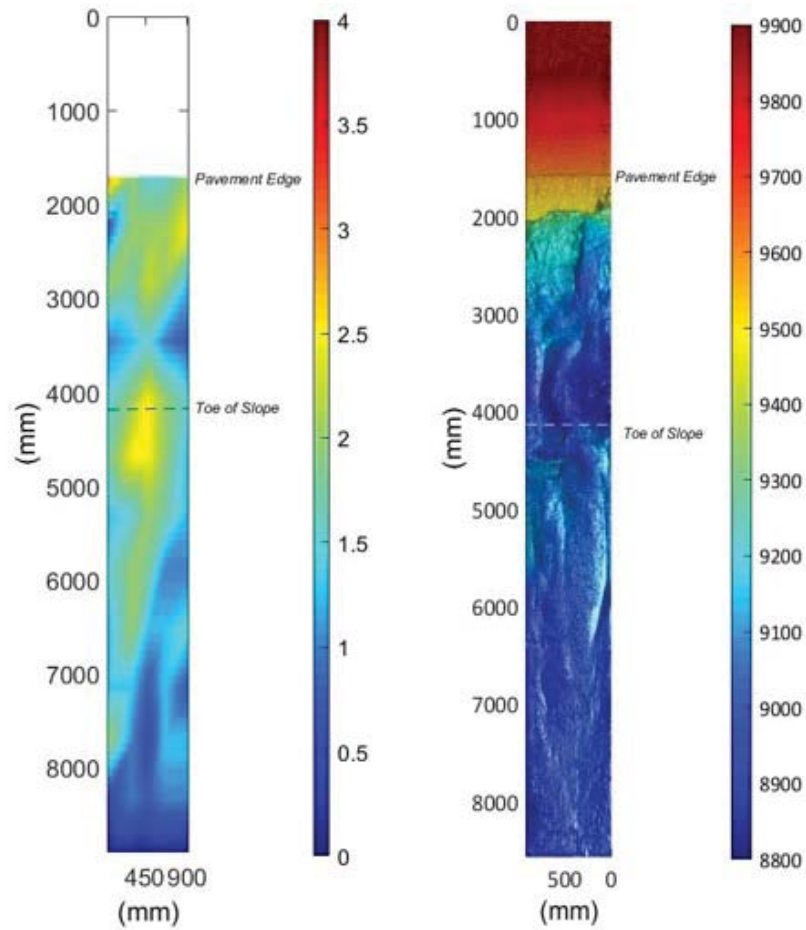


Figure 4.71. (Left). Aerial view of interpolated compaction data on slope with mid-shoulder starting at zero. Compaction measured in tons per square foot. (Right). Aerial view of final bare soil scanned after all sod and geogrid was removed from the slope.

Table 4.18. Statistics of compaction on 4H:1V slope with extended pavement for bare sod testing.

Statistics	On Slope (0-8.9 feet)		On Flat Run-out (10-24 feet)	
	Tons/SF	psi	Tons/SF	psi
Average	1.57	21.8	1.08	15.0
Std Dev	0.61	8.5	0.45	6.2
COV	0.39	5.4	0.41	5.7
Maximum	2.75	38.2	2.00	27.8
Minimum	0.50	6.9	0.25	3.5

4.4 TECHNIQUE 2: TURF REINFORCEMENT MAT WITH FIBER-REINFORCED MATRIX

4.4.1 Technique Summary:

The FRM material that was sprayed onto the TRM and was allowed to cure for 4.5 days on the 4H:1V slope and 6.5 days on the 6H:1V slope before testing. The FRM however did not hold up well; in both tests it quickly washed away, leaving only the TRM to stabilize. Despite this, the TRM performed well on the majority of the slope without any obvious drawbacks. It is most likely that the 6H:1V test failure was due to inconsistent compaction and an area of less compaction than the surrounding soil near the shoulder. In contrast, even though compaction on the 4H:1V slope was not consistent, that slope did not experience any concentrated erosion events.

4.4.2 Test 1. 4H:1V Slope-Quick Test

4.4.2.1 Summary

This stabilization technique consists of two parts: a nylon turf reinforcement mat (TRM) and a hydraulically applied fiber reinforced matrix (FRM). Test 1 was a baseline test of the TRM with FRM. The “quick” test swept through a range of flow discharges to identify the threshold of failure. The total duration of the test was 3.5 hours over 7 individual runs and a maximum overtopping depth of 0.6-ft. Maximum discharge was 7.9 ft³/s, equivalent to a unit discharge of 2.53 ft³/s-ft. Overtopping depth ranged from 0.04-ft to 0.60-ft.

4.4.2.2 Observations

After two hours of run time the fiber reinforced matrix that was sprayed onto the TRM was mostly washed away. The flat runout area past the toe of the slope eroded steadily through the testing process but did not undermine the buried section of the TRM at the toe of the slope. The erosion took place just upstream of the hydraulic jump on the slope and migrated upstream from that point but did not affect the rest of the slope. The upstream transition from the pavement to the slope remained intact throughout the entire testing period.

4.4.2.3 Failure Description

Although the FRM was fully integrated into the TRM it was progressively washed away exposing the TRM mat beneath. Erosion started in the lower third of the slope and slowly migrated upslope. Some soil was deposited beneath the TRM immediately upstream of toe of the slope. Other than several other isolated pockets of erosion the remainder of the slope was essentially free of erosion.

4.4.2.4 Photographs



Figure 4.72. First run on TRM-FRM at 0.89 cfs and 0.5-inches of overtopping.



Figure 4.73. View from upstream after 1 hour of run time, note that some of the FRM has been washed away from the surface of the TRM.

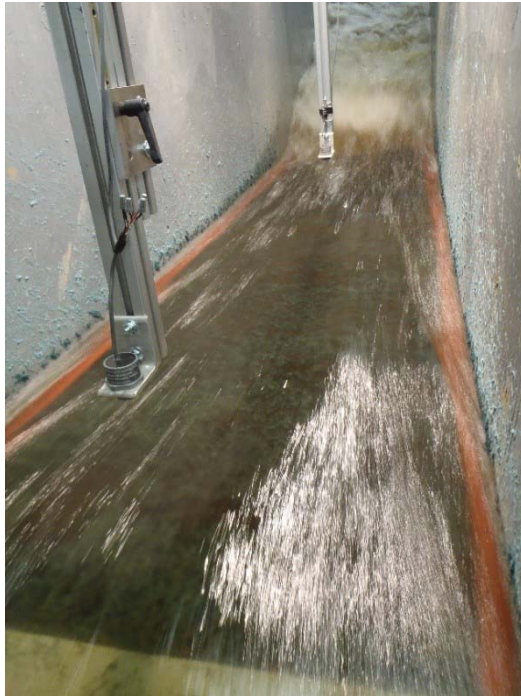


Figure 4.74. View from upstream during 2.5-3.0 hour run. Note that most of the FRM has been washed away at this point.



Figure 4.75. View from downstream after 3.5 hours of run time. Erosion working up the slope from the toe under the TRM.

4.4.2.5 Run Data

Table 4.19. Run data for TRM with FRM, 4H:1V slope "quick" run.

Tech 2: 4H:1V Slope "quick"			Mid-Slope			
Run end time(hr)	Depth Over Crest (ft)	Unit Discharge (ft ³ /s-ft)	Water Depth (ft)	Velocity (ft/s)	Shear Stress, τ (lb/ft ²)	Mannings 'n'
0.5	0.04	0.03	0.02	1.16	0.38	0.054
1.0	0.20	0.46	0.09	4.95	1.45	0.031
1.5	0.30	0.86	0.15	5.92	2.28	0.035
2.0	0.40	1.35	0.17	8.10	2.60	0.028
2.5	0.50	1.93	0.21	9.08	3.32	0.029
2.75 **	0.50	1.93	0.21	9.21	3.27	0.029
3.0 **	0.60	2.52	0.25	9.96	3.95	0.030
3.5	0.60	2.53	0.27	9.28	4.25	0.034

** Note: increased depth mid-run

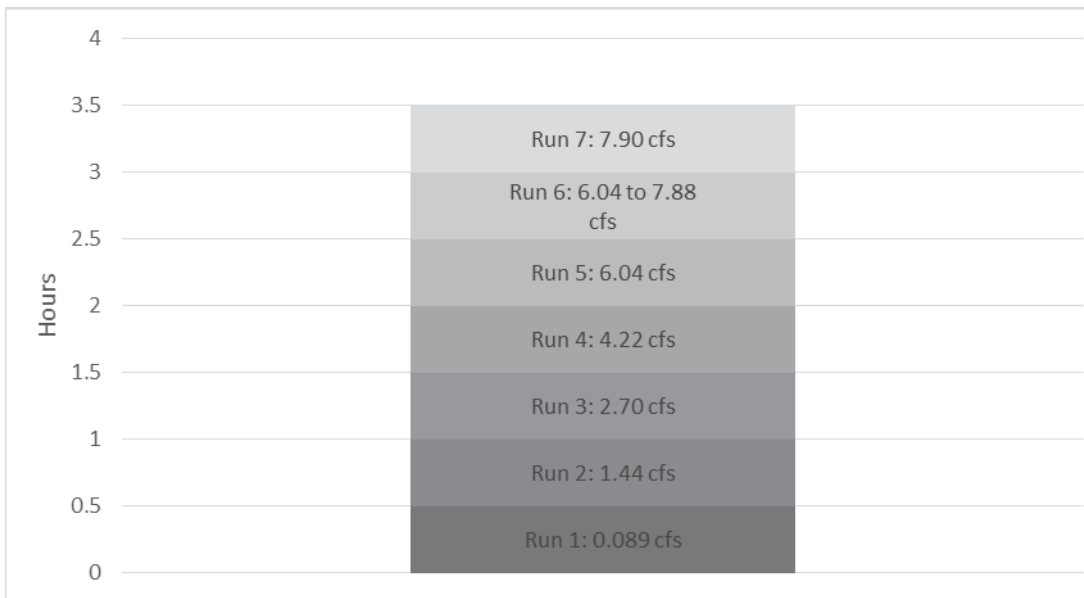


Figure 4.76. Number of runs with flow rate and duration of run time.

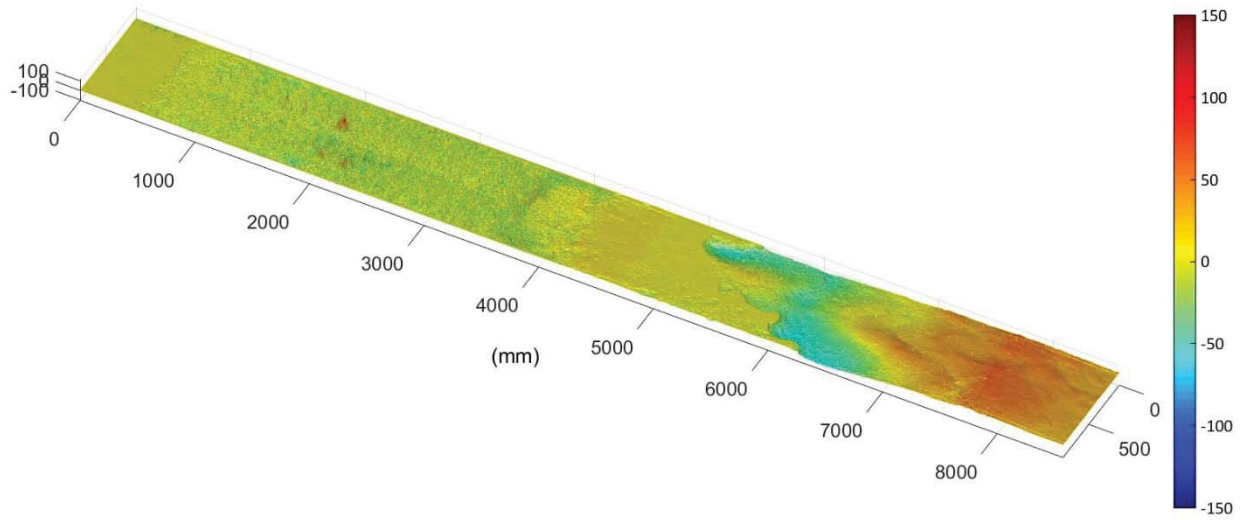


Figure 4.77. Topographic difference plot from zero to 1.5 hours of run time. Note that there is minimal erosion on the slope.

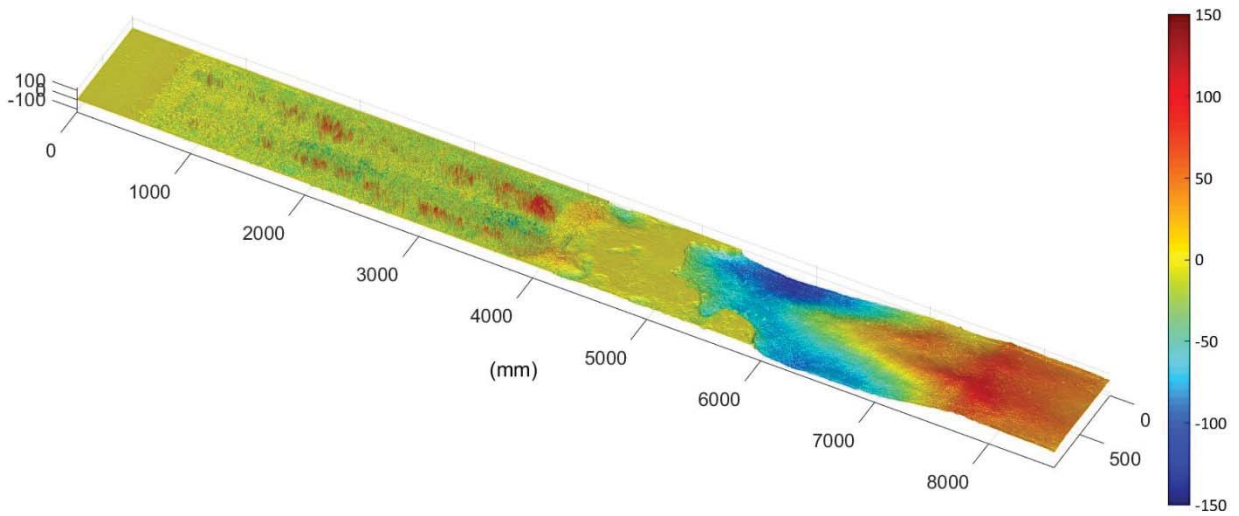


Figure 4.78. Topographic difference plot from zero to 2.5 hours of run time. Erosion and deposition occurring at the toe of the slope.

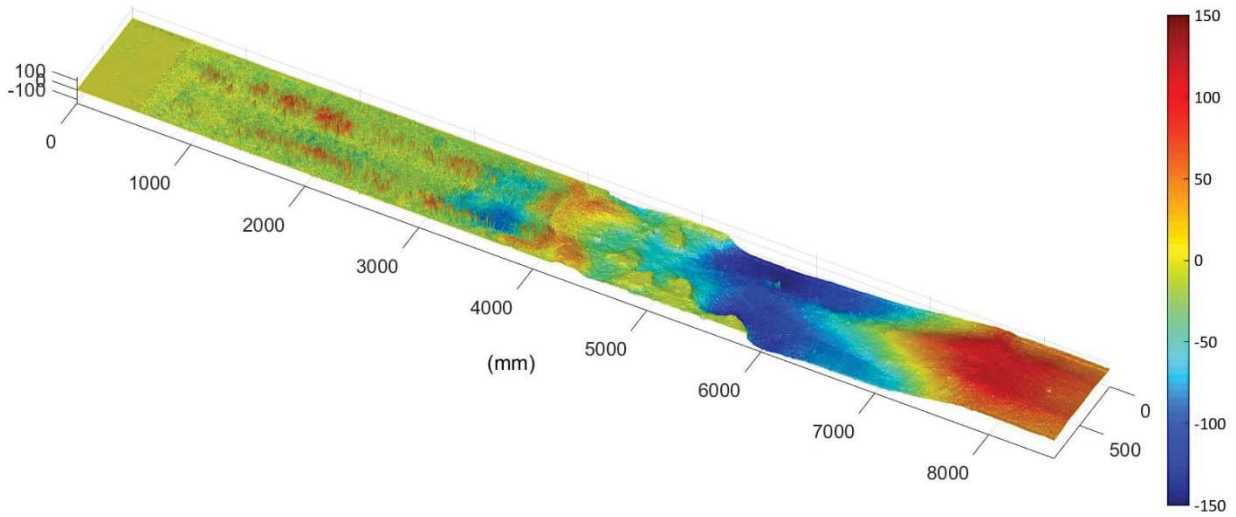


Figure 4.79. Topographic difference plot from zero to 3.5 hours of run time. Extensive erosion at the toe of the slope.

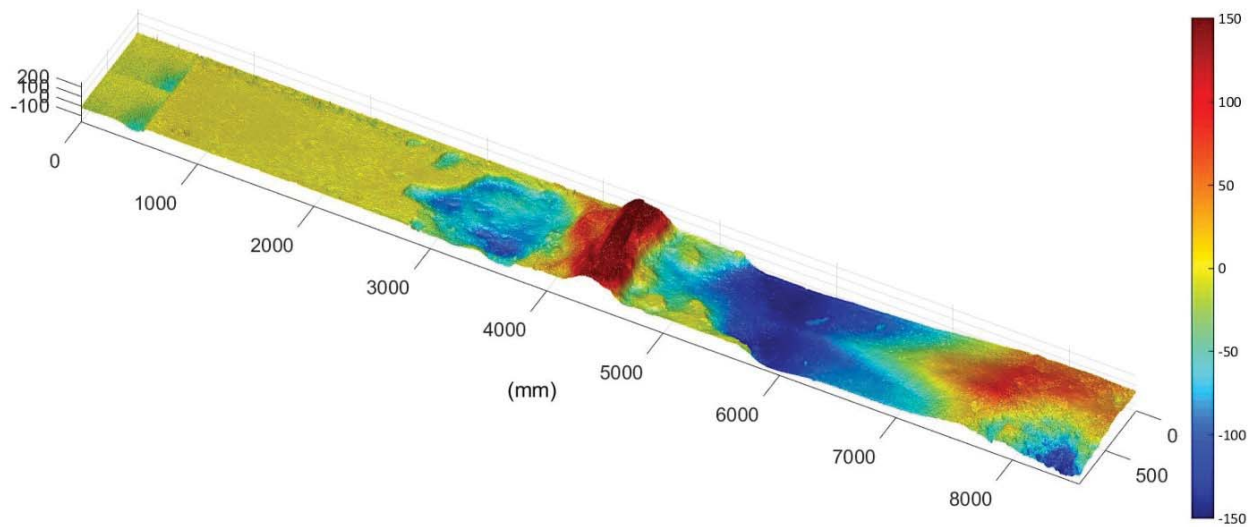


Figure 4.80. Topographic difference plot from initial bare soil vs. final bare soil after 3.5 hours of run time. Substantial erosion near the toe of the slope. The large depositional area at 4300 mm is the TRM after being flipped onto the flat run-out area.

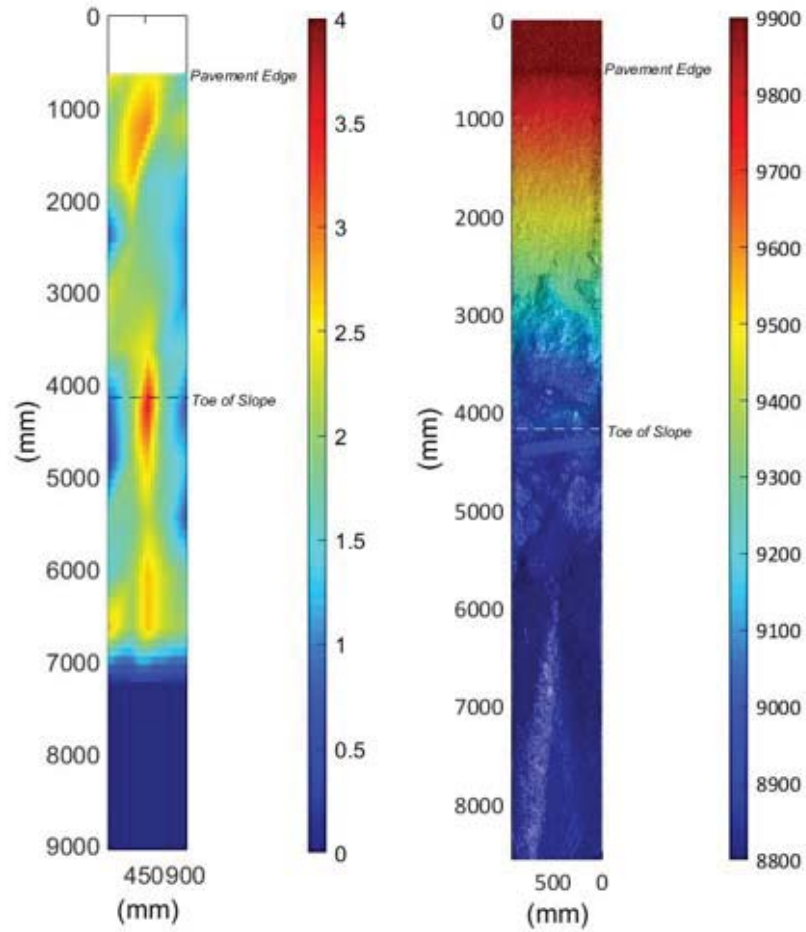


Figure 4.81. (Left). Aerial view of interpolated compaction data on slope with mid-shoulder starting at zero. Compaction measured in tons per square foot. (Right). Aerial view of final bare soil scanned after TRM and FRM was removed from the slope.

Table 4.20. Statistics of compaction on 4H:1V slope for TRM-FRM testing.

Statistic	On Slope (0-12 feet)		On Flat Run-out (14-20 feet)	
	Tons/SF	psi	Tons/SF	psi
Average	1.89	26.3	1.93	26.7
Std. Dev	0.64	8.9	0.62	8.6
COV	0.34	4.7	0.32	4.5
Maximum	3.50	48.6	2.75	38.2
Minimum	0.75	10.4	0.50	6.9

4.4.3 Test 2. 6H:1V Slope

4.4.3.1 Summary

Test 2 was the second experiment on the Turf Reinforcement Mat with Fiber Reinforced Matrix. This test took place on the 6H:1V slope with five runs lasting 8.3 hours and overtopping depths ranging from 0.2 to 0.6 feet. Maximum discharge was $6.86 \text{ ft}^3/\text{s}$, equivalent to a unit discharge of $2.39 \text{ ft}^3/\text{s-ft}$. Overtopping depth ranged from 0.20-ft to 0.60-ft.

4.4.3.2 Observations

As in Test 1, we observe the washout of the FRM material within the first few hours of run however the TRM remained in place. Erosion occurred along the river-right edge of the upstream shoulder. The erosion near the shoulder progressed slowly from 2 hours to 8 hours. During the last run, when the depth over the crest was increased from 0.40ft to 0.60ft, the shoulder gave way after 15 minutes. The remainder of the 6H:1V slope was unaffected during the 8.25 hours of testing time with the exception of a small depression and aggraded area just downstream of the main area of erosion.

The average compaction for the slope was high at $2.59 \text{ tons}/\text{ft}^2$, but the area of failure coincided with the lowest compaction region and may have had some influence. For this experiment, burying the TRM at the toe of the slope did not seem to make any difference in the outcome of the performance. The area where the erosion initiated was between two of the staples fastening the TRM to the slope surface.

4.4.3.3 Failure Description

Within the first two hours a pocket of erosion formed adjacent to the edge of the shoulder. This area slowly grew larger and deeper in the following four runs, until a burst of erosion occurred 15 minutes into the fifth run. The erosion cut deeply along the right flume wall and would have continued to undermine the shoulder. Eroded particles became trapped in a series of small mounds between the deformed TRM and the soil surface where the TRM was anchored with wire staples.

4.4.3.4 Photographs



Figure 4.82. View from downstream during 0-2 hour run. Minimal erosion noticed. FRM is being washed away while TRM is remaining stapled to the slope.

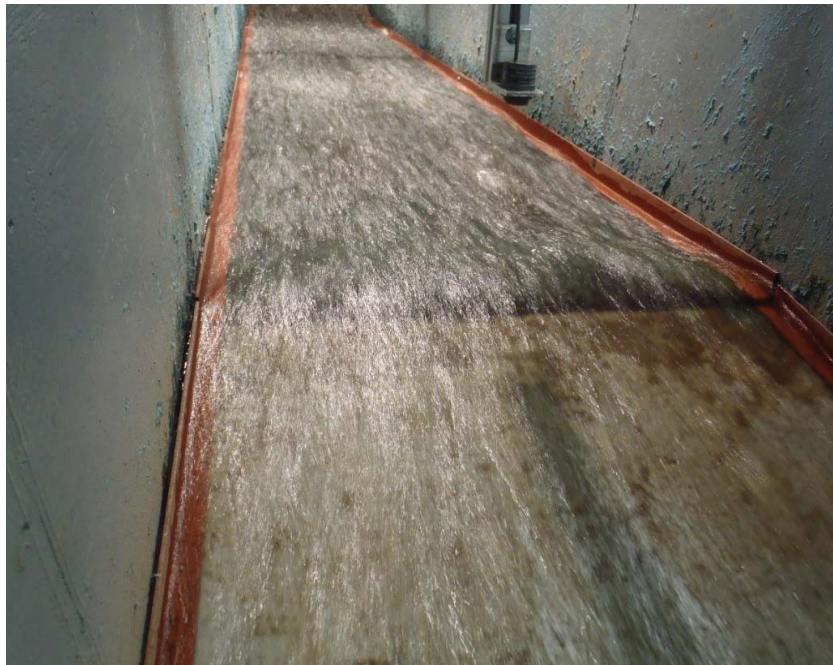


Figure 4.83. View from upstream during 2-4 hour run. Noticeable depression after shoulder along right edge of slope. More of the FRM is being removed from testing.



Figure 4.84. View looking upstream after six hours of run time. Almost all of the FRM has been washed away and the depression near the shoulder has gotten deeper.



Figure 4.85. View looking downstream after 8.25 hours of run time. The large amount of erosion along right wall represents failure.

4.4.3.5 Run Data

Table 4.21. Run data for TRM with FRM, 6H:1V slope.

Tech 2: 6H:1V Slope			Mid-Slope			
Run end time (hr)	Depth Over Crest (ft)	Unit Discharge (ft ³ /s-ft)	Water Depth (ft)	Velocity (ft/s)	Shear Stress, τ (lb/ft ²)	Mannings 'n'
2.0	0.20	0.47	0.13	3.52	1.38	0.045
4.0	0.20	0.45	0.12	3.71	1.27	0.040
6.0	0.40	1.28	0.22	5.78	2.31	0.039
8.0	0.40	1.29	0.22	5.77	2.33	0.039
8.3	0.60	2.39	0.36	6.56	3.78	0.047

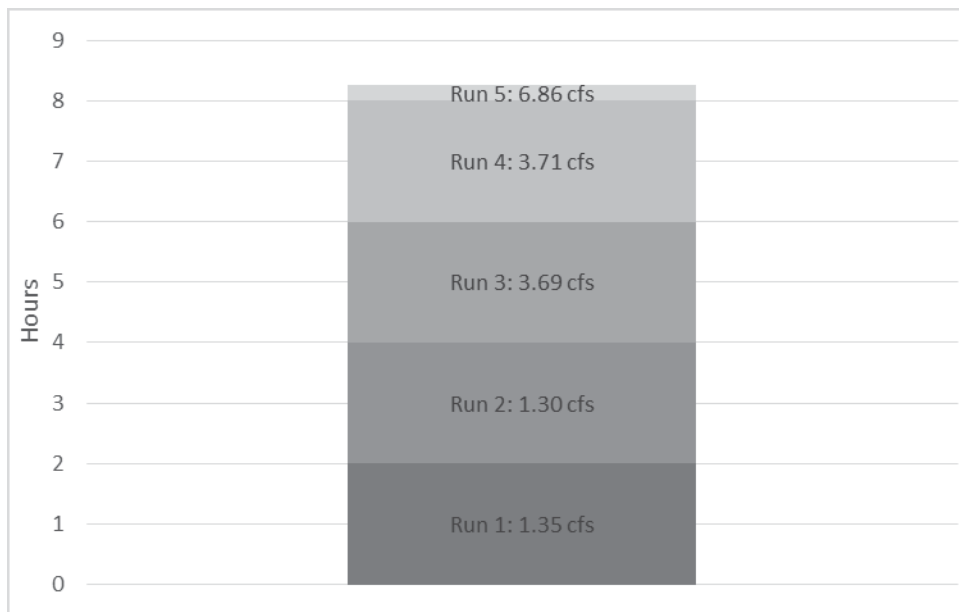


Figure 4.86. Number of runs with flow rate and duration of runtime.

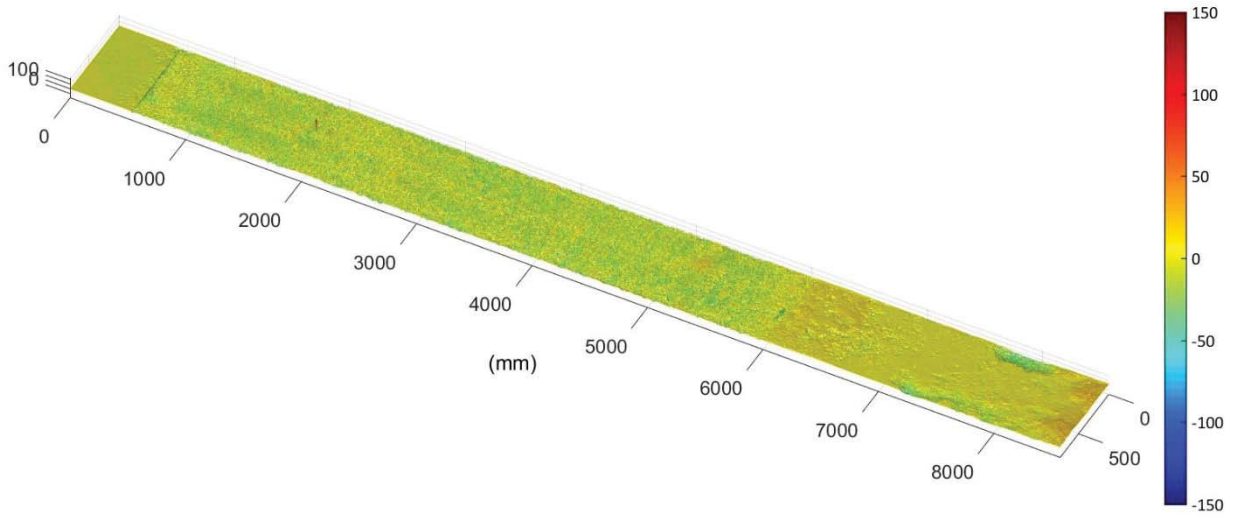


Figure 4.87. Topographic difference plot from zero to four hours of run time. Note that there is little noticeable erosion with the difference plot.

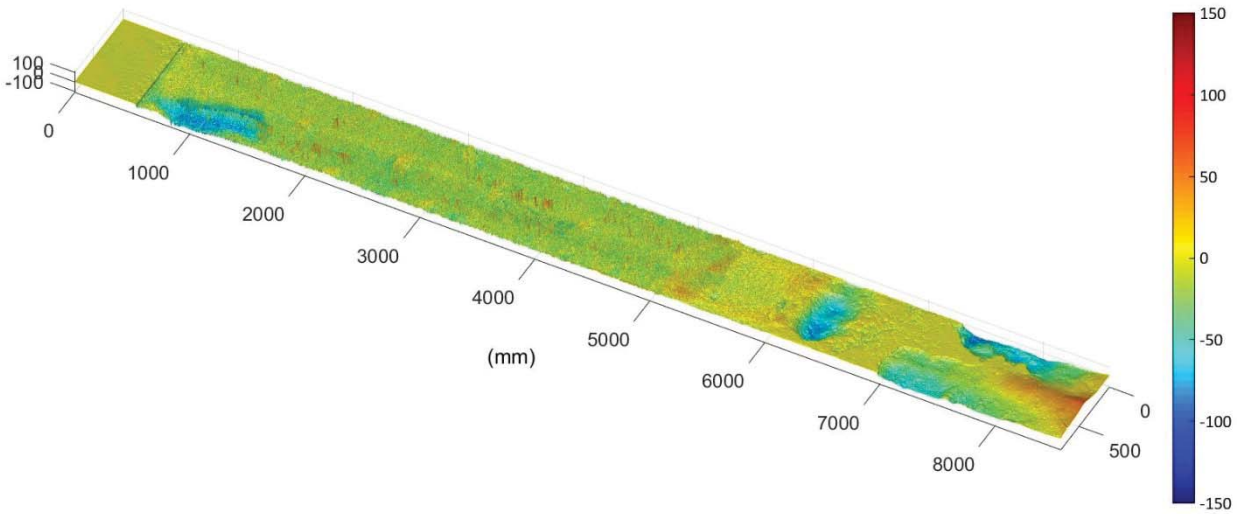


Figure 4.88. Topographic difference plot from zero to eight hours of run time. The start of erosion near the shoulder is detected.

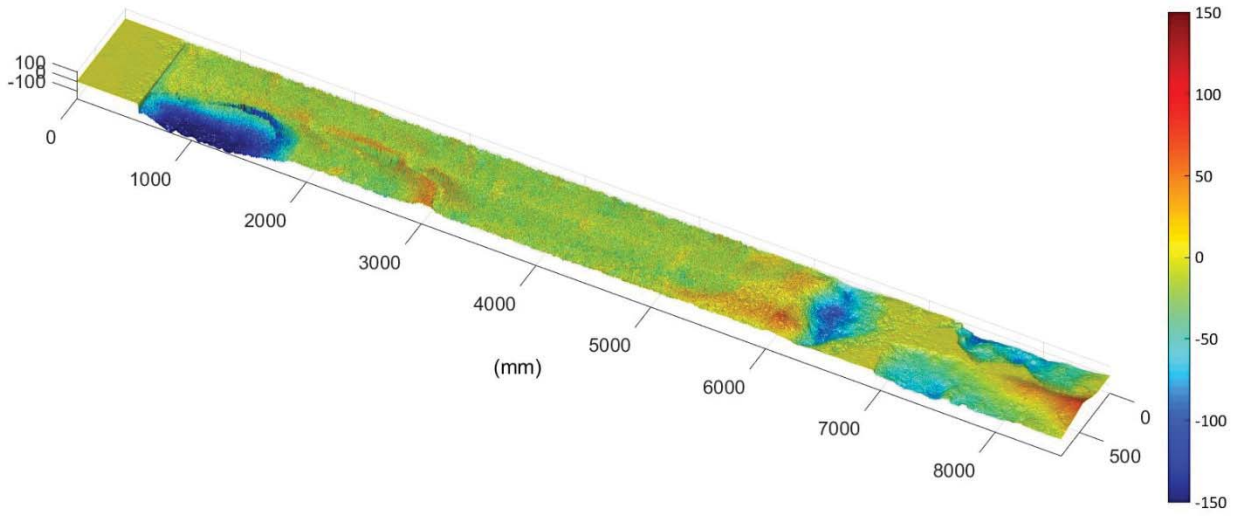


Figure 4.89. Topographic difference plot from zero to 8.25 hours. Erosion quickly expanded near the top of the slope leading to failure.

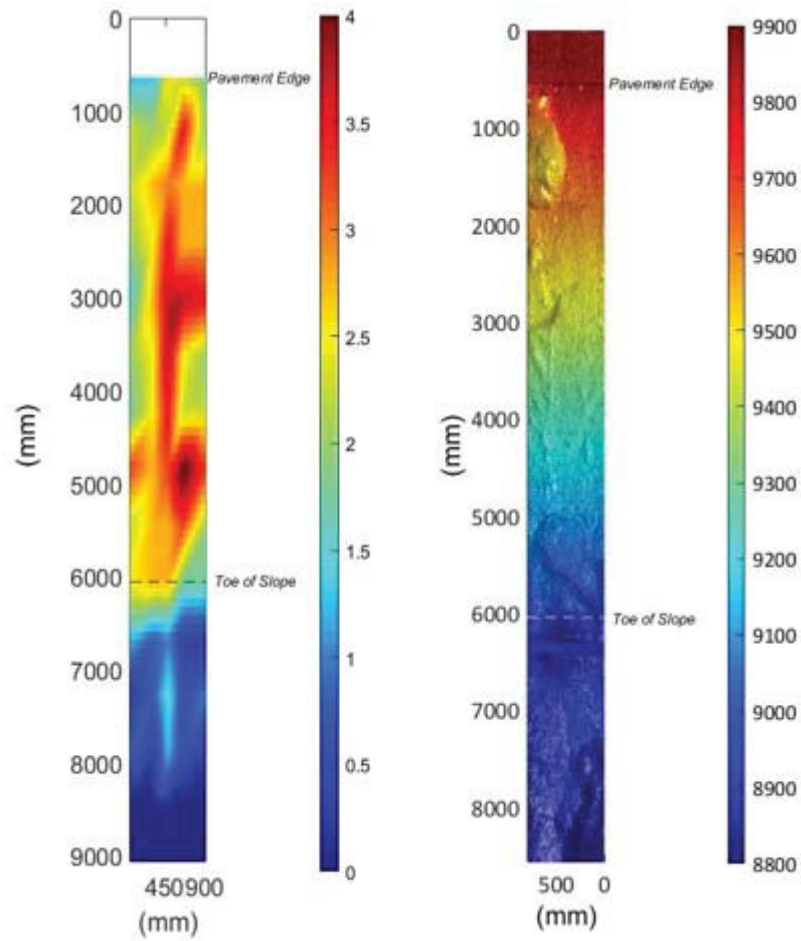


Figure 4.90. (Left). Aerial view of interpolated compaction data on slope with mid-shoulder starting at zero. Compaction measured in tons per square foot. (Right). Aerial view of final bare soil scanned after TRM and FRM was removed from the slope.

Table 4.22. Statistics of compaction on 6H:1V slope for TRM-FRM testing.

Statistic	On Slope (0-12 feet)		On Flat Run-out (14-24 feet)	
	Tons/SF	psi	Tons/SF	psi
Average	2.59	36.0	0.70	9.7
Std Dev	0.68	9.5	0.42	5.9
COV	0.26	3.7	0.61	8.4
Maximum	4.25	59.0	1.50	20.8
Minimum	1.25	17.4	0.25	3.5

4.5 TECHNIQUE 3: FLEXIBLE CONCRETE GEOGRID MAT

4.5.1 Technique Summary

This technique was the most labor intensive to install, especially in the confined flume. The Flexamat[®] Plus performed well during testing of both the 4H:1V and 6H:1V slopes by protecting the soil slopes even under the highest discharges possible in the facility. In the last 4H:1V test, which ran much longer after the first sign of erosion than any previous tests, the slope did not end up having any substantial localized erosion but instead we observed a minor erosion over the entire slope surface.

4.5.2 Test 1. 4H:1V Slope- Quick Test

4.5.2.1 Summary

Test 1 was a baseline test of the flexible concrete geogrid mat. The “quick” test swept through a range of flow discharges to identify the threshold of failure. The test had a total duration of 1.5 hours with overtopping depths up to 0.5-ft and a maximum discharge of 6.04 ft³/s and unit discharges up to 1.93 ft³/s-ft.

4.5.2.2 Observations

Flow over the flexible concrete geogrid is different from the other techniques in that it has a very rough surface. The other techniques were relatively flat or planar whereas this treatment has both small scale roughness in the unfinished concrete and form in the individual blocks with the mat. At low discharge the flow was aerated and turbulent. As far as erosion, the upper portion of the slope remained intact despite erosion at mid-slope. The eroded area correlated with lowest values of measured compaction. The test illustrated well the growth of cyclic scour holes and how these features are linked and grow over time.

4.5.2.3 Failure Description

The first two runs, 0.4-inches and 3 inches of overtopping, resulted in only minor erosion. During the third run, a small scour hole and depositional mound became noticeable about 66% of the way down the slope. This void grew in size and at about 1.5 hours a second scour hole and depositional mound was observed downstream of the first. The experiment was then ended.

4.5.2.4 Photographs



Figure 4.91. Image from Run 1 with discharge set at $0.9 \text{ ft}^3/\text{s}$. There was no noticeable erosion over entire 30 min run.



Figure 4.92. View looking downstream from the shoulder during 1 to 1.5 hour run with flow of $2 \text{ ft}^3/\text{s}$ and overtopping depth of 3 inches. The flow was aerated and very turbulent.



Figure 4.93. Looking upstream at slope near end of 1.5 hour run. Aeration near mid-slope and erosion/deposition areas stepping down the slope.

4.5.2.5 Run Data

Table 4.23. Run data for Flexible Concrete Geogrid Mat, 4H:1V slope "quick" run.

Tech 3: 4H:1V Slope "quick"			Mid-Slope			
Run end time (hr)	Depth Over Crest (ft)	Unit Discharge (ft ³ /s-ft)	Water Depth (ft)	Velocity (ft/s)	Shear Stress, τ (lb/ft ²)	Mannings 'n'
0.5	0.03	0.03	0.01	2.10	0.21	0.020
1.0	0.25	0.64	0.24	2.74	3.67	0.104
1.5	0.50	1.93	0.37	5.25	5.74	0.073

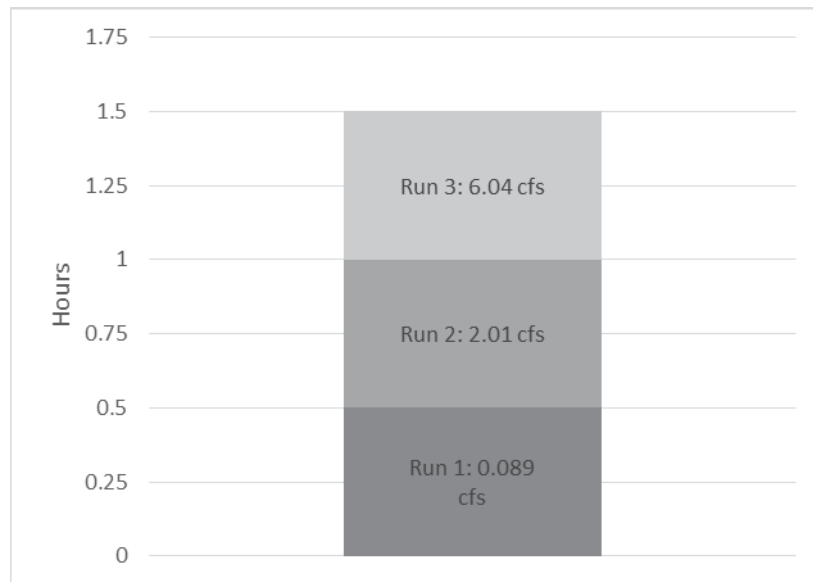


Figure 4.94. Number of runs with flow rate and duration of run time.

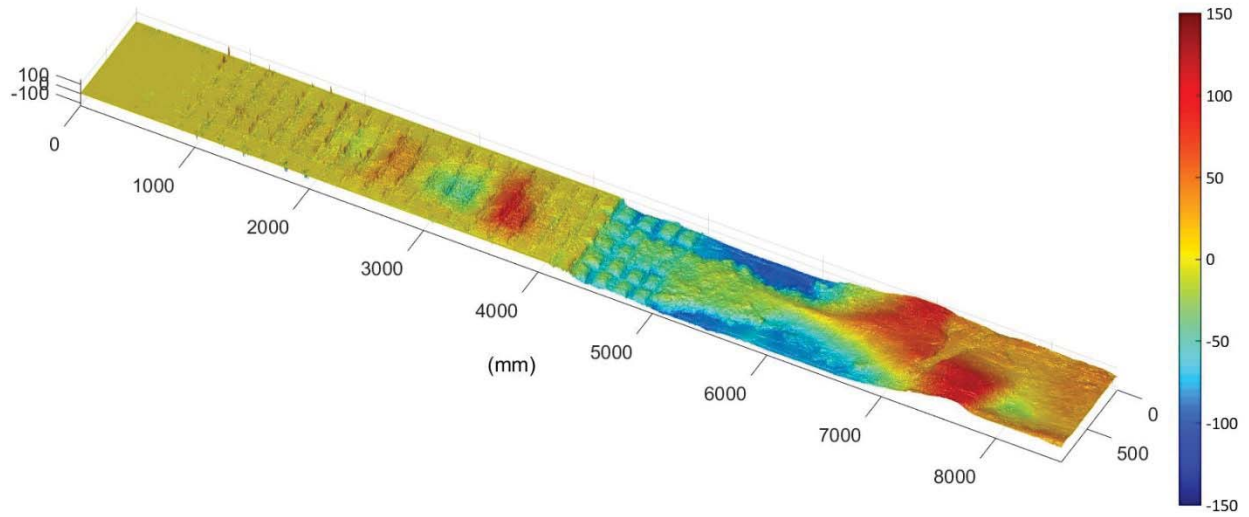


Figure 4.95. Topographic difference plot from zero to 1.5 hours of run time. Note the erosion in a stepped fashion with two depressions and two deposition areas in the middle of the flume.

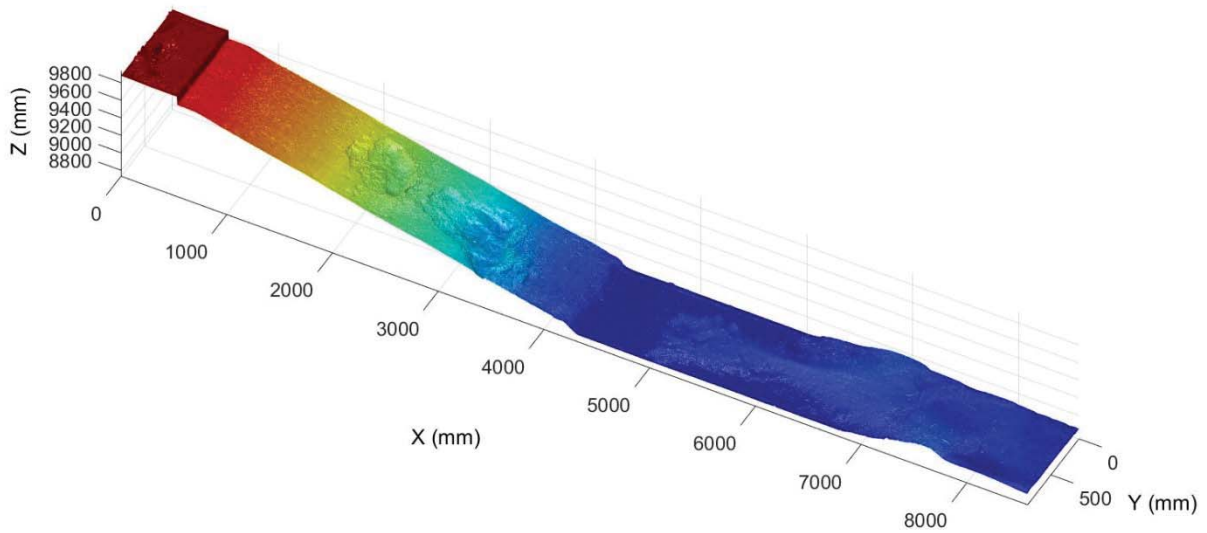


Figure 4.96. Scan of the final bare soil after the Flexamat® was removed. Two large depressions are shown here, similar to what is seen in the difference plot of zero vs 1.5 hours of run time, but more prevalent when seen without the Flexamat® covering it.

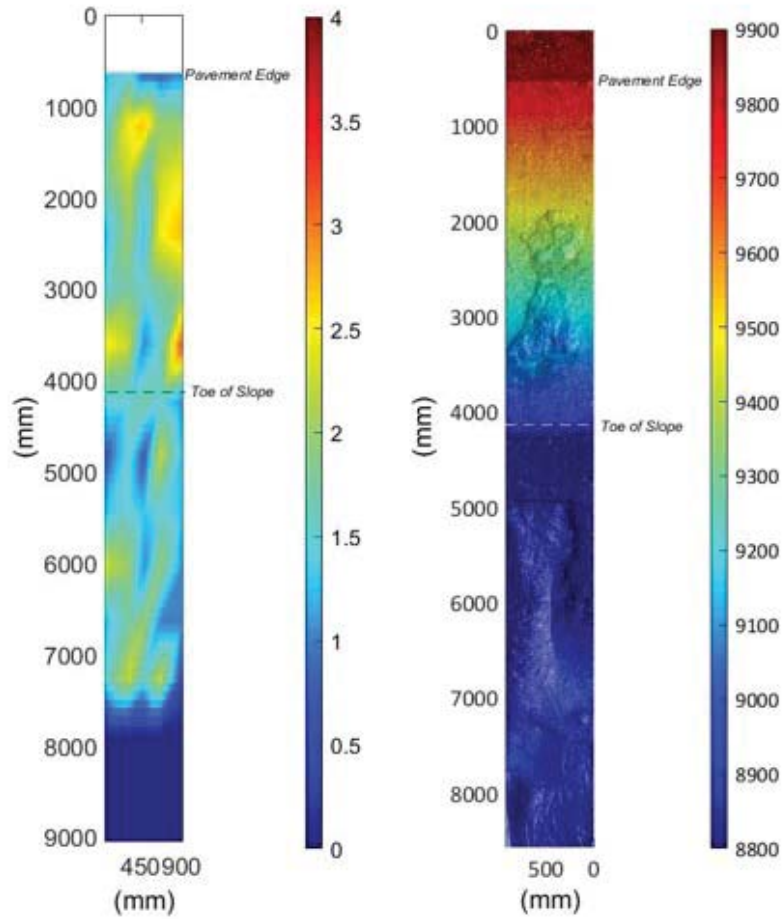


Figure 4.97. (Left). Aerial view of interpolated compaction data on slope. Compaction is presented in units of tons per square foot. (Right) Aerial view of final bare soil scanned after Flexamat[®] Plus was removed from slope.

Table 4.24. Statistics of compaction on 4H:1V slope for Flexamat[®]-Plus testing.

Statistic	On Slope (0-12 feet)		On Flat Run-out (14-22 feet)	
	Tons/SF	psi	Tons/SF	psi
Average	1.78	24.7	1.46	20.3
Std. Dev	0.61	8.4	0.52	7.2
COV	0.34	4.7	0.36	4.9
Maximum	3.25	45.1	2.25	31.3
Minimum	0.75	10.4	0.50	6.9

4.5.3 Test 2. 6H:1V Slope

4.5.3.1 Summary

This was a test of the flexible concrete geogrid mat on the 6H:1V slope. The test involved 13 separate 2 hour runs with flows ranging up to 14.6 ft³/s and overtopping depths ranging from 0.15-0.98 feet. Total run time was 30 hours. Maximum unit discharge was 4.64 ft³/s-ft.

4.5.3.2 Observations

This stabilization technique showed the strongest performance of all techniques. The test were conducted on the lower slope 6H:1V and Flexamat® Plus was able to protect the soil embankment with minimal erosion on the slope.

4.5.3.3 Failure Description

Testing was completed at maximum flume capacity of one foot over the crest of the road. The soil under the Flexamat® Plus did not experience any significant erosion; only shallow and disconnected areas of surface erosion were apparent after removal of the stabilization material. This test resulted in the least erosion among the experimental set.

4.5.3.4 Photographs



Figure 4.98. View from shoulder after Flexamat[®] Plus installation and before testing.



Figure 4.99. View from shoulder looking downstream during 10-12 hour run. No noticeable erosion on the slope.

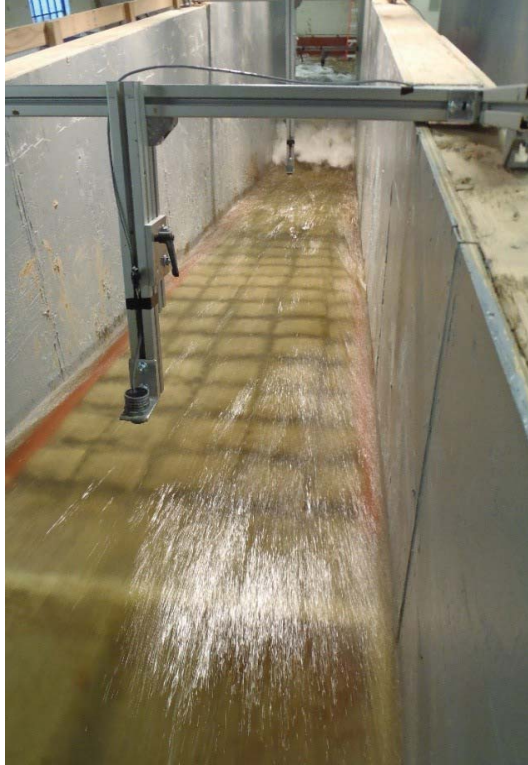


Figure 4.100. View from shoulder looking downstream during 22-24 hour run. No noticeable erosion, smooth water surface to about mid-slope.

4.5.3.5 Run Data

Table 4.25. Run data for Flexible Concrete Geogrid Mat, 6H:1V slope.

Tech 3: 6H:1V Slope			Mid-Slope			
Run end time(hr)	Depth Over Crest (ft)	Unit Discharge (ft ³ /s-ft)	Water Depth (ft)	Velocity (ft/s)	Shear Stress, τ (lb/ft ²)	Mannings 'n'
2.0	0.15	0.29	0.09	3.26	0.94	0.038
4.0	0.15	0.30	0.12	2.46	1.28	0.061
6.0	0.30	0.85	0.15	5.61	1.57	0.031
8.0	0.30	0.85	0.15	5.71	1.55	0.030
10.0	0.45	1.56	0.21	7.40	2.19	0.029
12.0	0.45	1.56	0.21	7.48	2.17	0.029
14.0	0.60	2.43	0.27	8.84	2.85	0.029
16.0	0.60	2.43	0.28	8.66	2.92	0.030
18.0	0.75	3.43	0.42	8.17	4.37	0.042
20.0	0.75	3.44	0.38	9.13	3.91	0.035
22.0	0.98	5.08	0.45	11.38	4.64	0.031
24.0	0.98	5.08	0.43	11.74	4.50	0.030
30.0	0.92	4.64	0.41	11.31	4.26	0.030

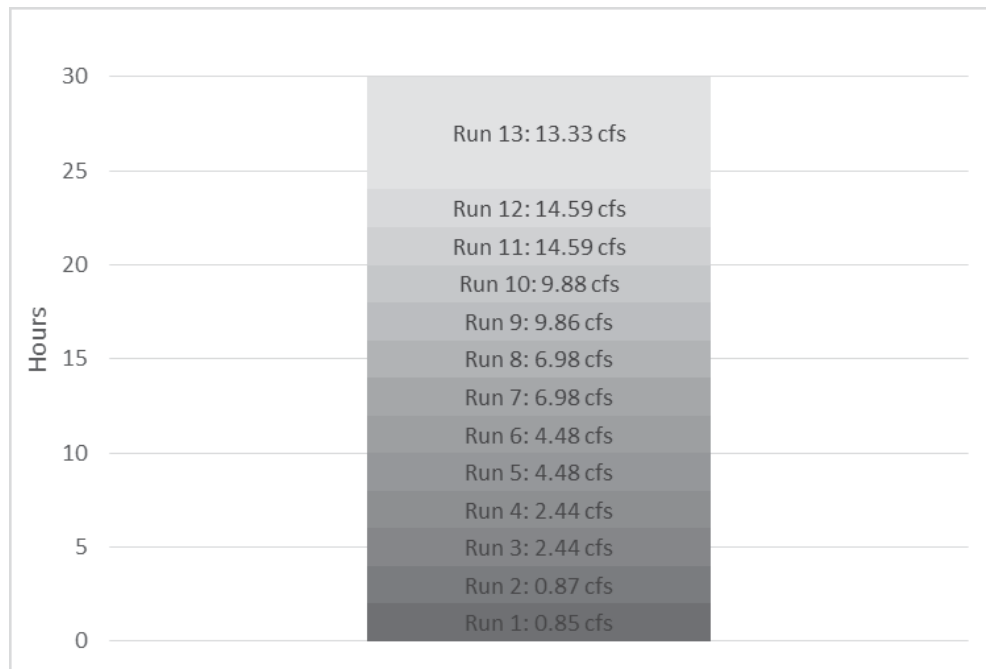


Figure 4.101. Number of runs with flow rate and duration of run time.

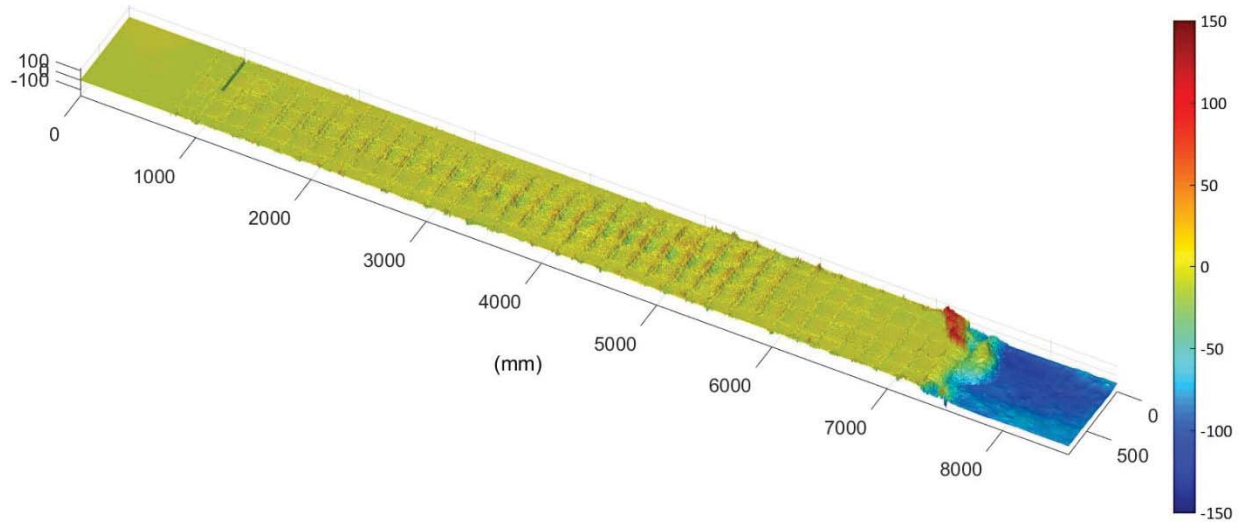


Figure 4.102. Topographic difference plot from zero to 18 hours of run time. No erosion noticeable on the slope.

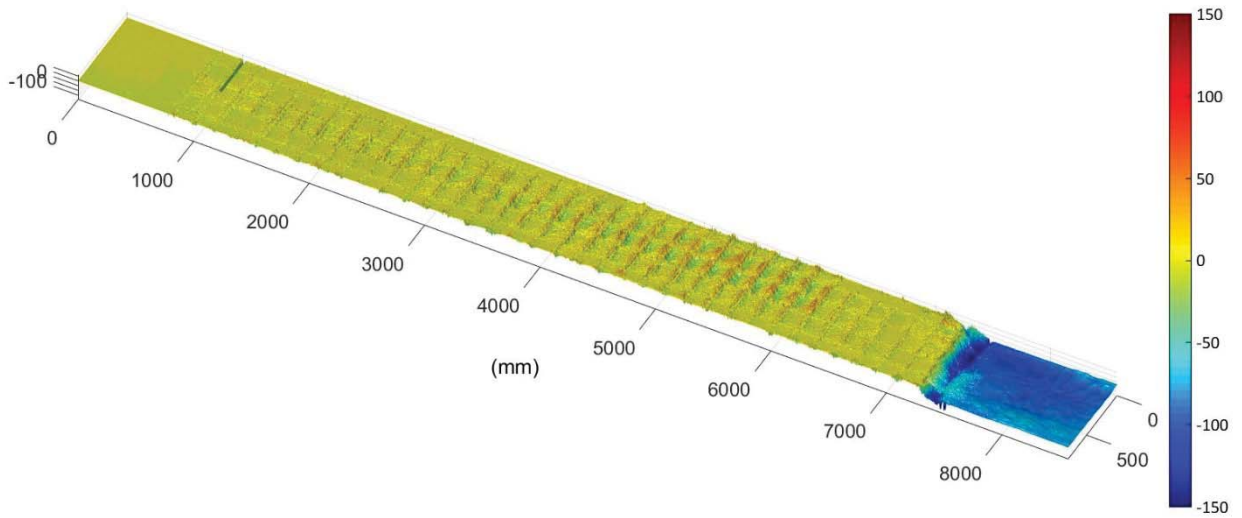


Figure 4.103. Topographic difference plot from zero to 30 hours of run time. Apparent differences shown are due to concrete blocks shifting downslope of their original resting place.

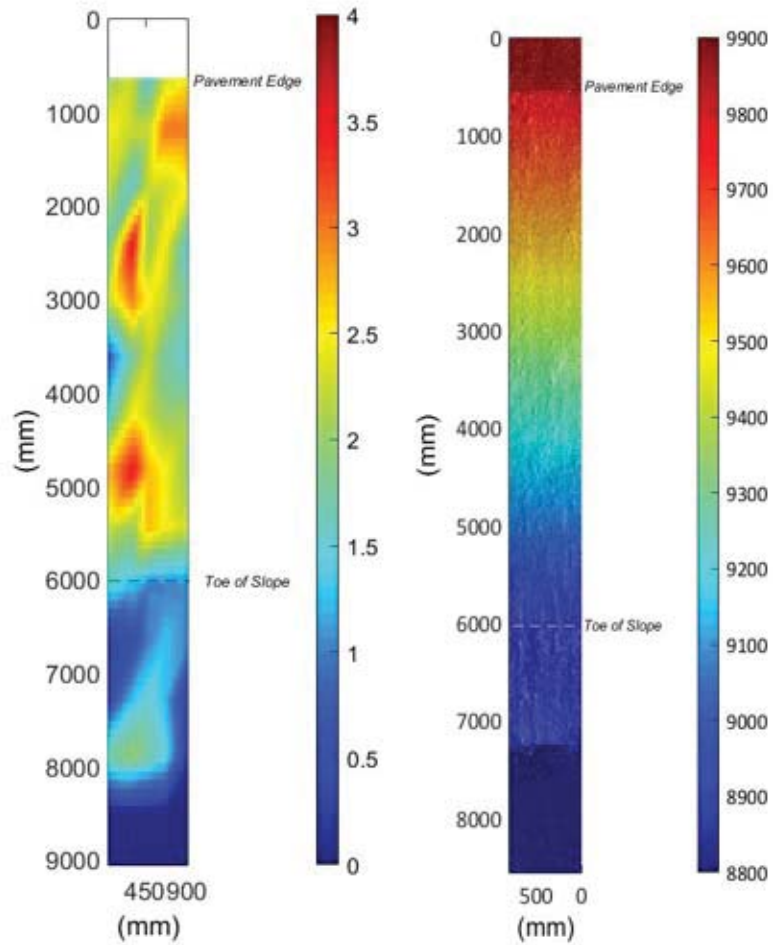


Figure 4.104. (Left) Aerial view of interpolated compaction data on slope with mid-shoulder starting at zero. Compaction measured in tons per square foot. (Right) Aerial view of final bare soil scanned after Flexamat[®] Plus removed from slope.

Table 4.26. Statistics of compaction on 6H:1V slope for Flexamat[®] Plus testing.

Statistic	On Slope (0-12 feet)		On Flat Run-out (14-24 feet)	
	Tons/SF	psi	Tons/SF	psi
Average	2.13	29.6	1.07	14.8
Std. Dev	0.61	8.4	0.59	8.2
COV	0.28	4.0	0.56	7.7
Maximum	3.50	48.6	2.00	27.8
Minimum	0.75	10.4	0.25	3.5

4.5.4 Test 3. 4H:1V Slope

4.5.4.1 Summary

This was a test of the flexible concrete geogrid mat on the 4H:1V slope. The total duration for this test was 25.3 hours and included 10 separate runs. Overtopping depths ranged from 0.15-.72 feet and discharge was up to 13.3 ft³/s or a unit discharge of 3.17 ft³/s-ft.

4.5.4.2 Observations

As with previous tests with this technique, the water surface is very turbulent and aerated during low flow state (Figure 4.106). It is not clear if this hydraulic condition initiates the erosion process. The topographic scan data showed erosion forming mid-slope after 4 hours of run time and fairly low discharge. The run was continued for 25.3 hours total and discharge was increased. During this period, the extent and depth of erosion continued under the mat. The mat did not wash out but was held in place however soil was able to erode and wash away from underneath the mat. The erosion scour and deposition was observed to translate downslope during the test.

4.5.4.3 Failure Description

Erosion was first detected in the topographic elevation data after four hours of run time. Each time the flow rate increased, interesting sequences of erosion followed by periods of stabilization characterized the test. The distinct erosion events propagated downstream starting at mid-slope and translating down to the toe of the slope over 25 hours of run time.

4.5.4.4 Photographs



Figure 4.105. View from shoulder looking downstream during first two hour run. Highly turbulent flow but no noticeable erosion on slope.



Figure 4.106. View from downstream looking up at slope during 24.35 to 25.33 hour run. Mid-slope mound has been eroded and flat upper slope has stabilized and new mound at toe of slope is causing aeration.



Figure 4.107. View from downstream looking up at slope during 4-6 hour run. Note the depression and subsequent aggradation at mid-slope causing aeration.



Figure 4.108. View from downstream looking up at slope during 17.25-20.25 hour run. The slope did not drastically change over 10 hours of run time from the first sign of erosion.

4.5.4.5 Run Data

Table 4.27. Run data for Flexible Concrete Geogrid Mat, 4H:1V slope

Tech 3: 4H:1V Slope			Mid-Slope			
Run end time(hr)	Depth Over Crest (ft)	Unit Discharge (ft ³ /s-ft)	Water Depth (ft)	Velocity (ft/s)	Shear Stress, τ (lb/ft ²)	Mannings 'n'
2.0	0.15	0.29	0.13	2.29	1.98	0.082
4.0	0.30	0.90	0.19	4.64	3.04	0.054
6.0	0.30	0.87	0.18	4.96	2.73	0.047
8.0	0.30	0.88	0.29	3.02	4.54	0.108
10.8	0.30	0.88	0.21	4.16	3.29	0.063
17.3	0.30	0.88	0.21	4.24	3.23	0.062
20.3	0.45	1.62	0.28	5.70	4.42	0.056
22.3	0.45	1.62	0.23	7.06	3.58	0.040
24.3	0.60	2.57	0.29	8.93	4.49	0.036
25.3	0.72	3.17	0.32	9.76	5.07	0.036

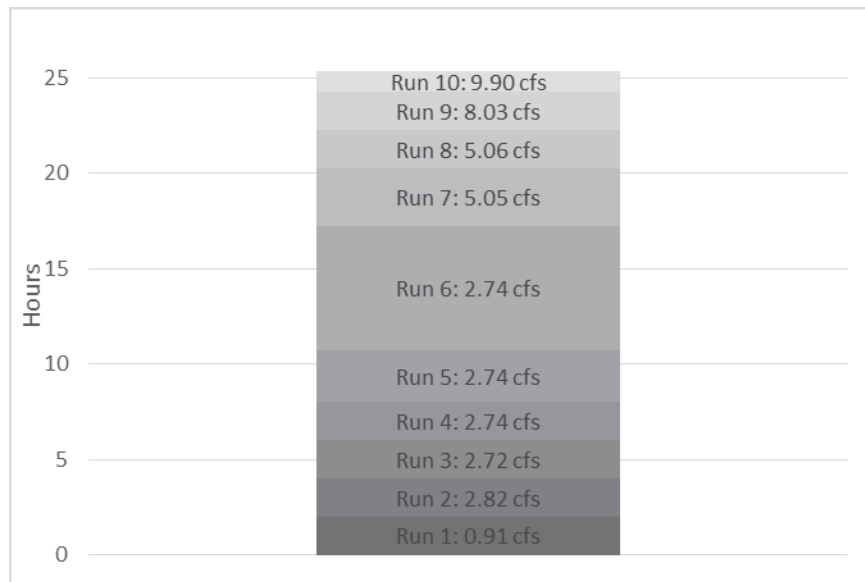


Figure 4.109. Number of runs with flow rate and duration of run time.

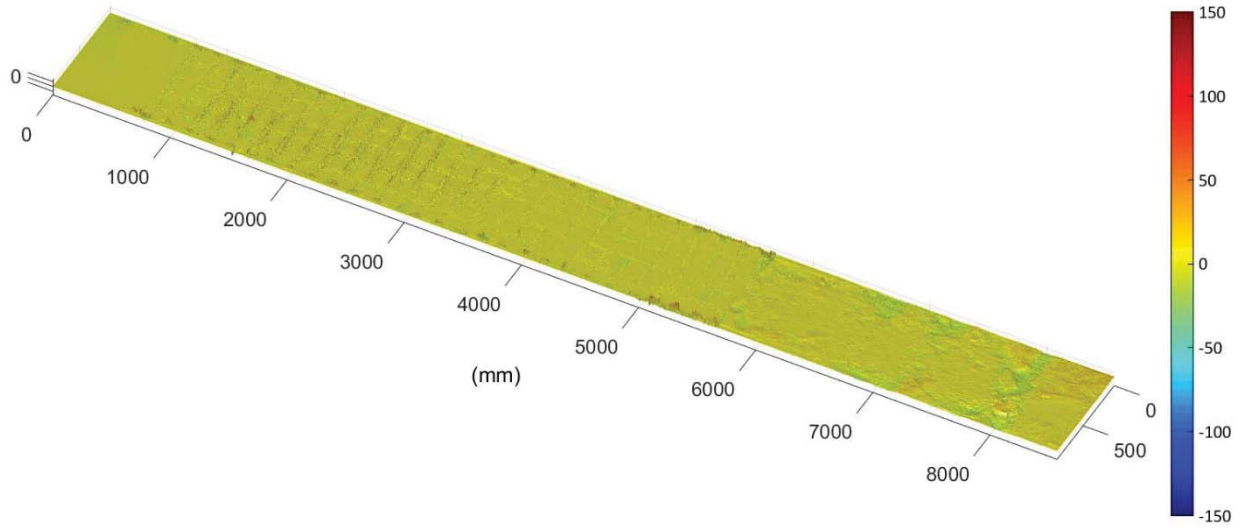


Figure 4.110. Topographic difference plot from zero to two hours of run time. No noticeable erosion on the slope.

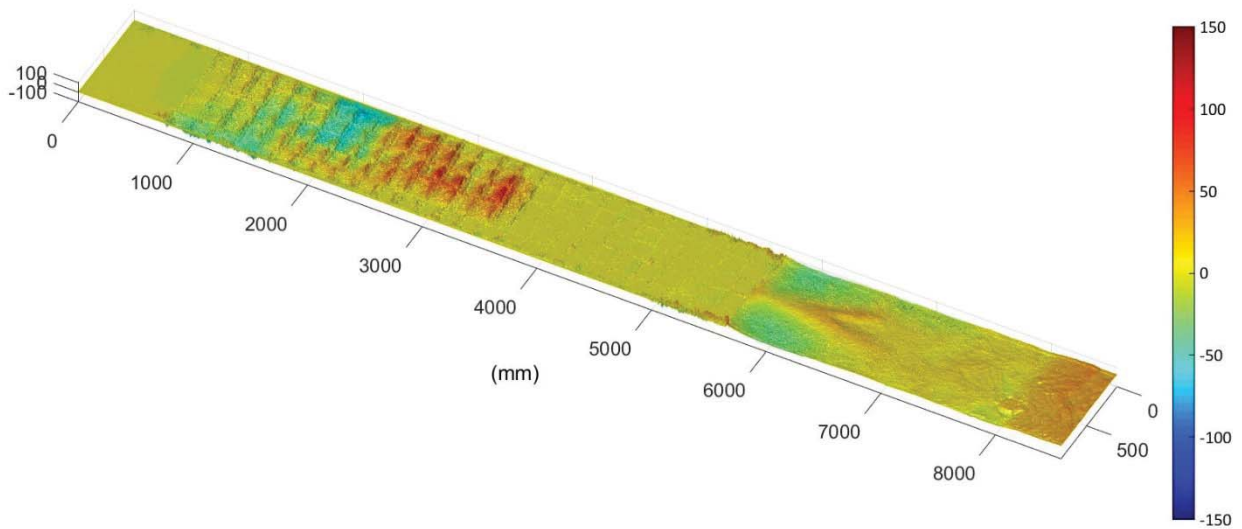


Figure 4.111. Topographic difference plot from zero to four hours of run time. This increments saw a measurable change in slope elevation with a depression at mid-slope and aggradation immediately after.

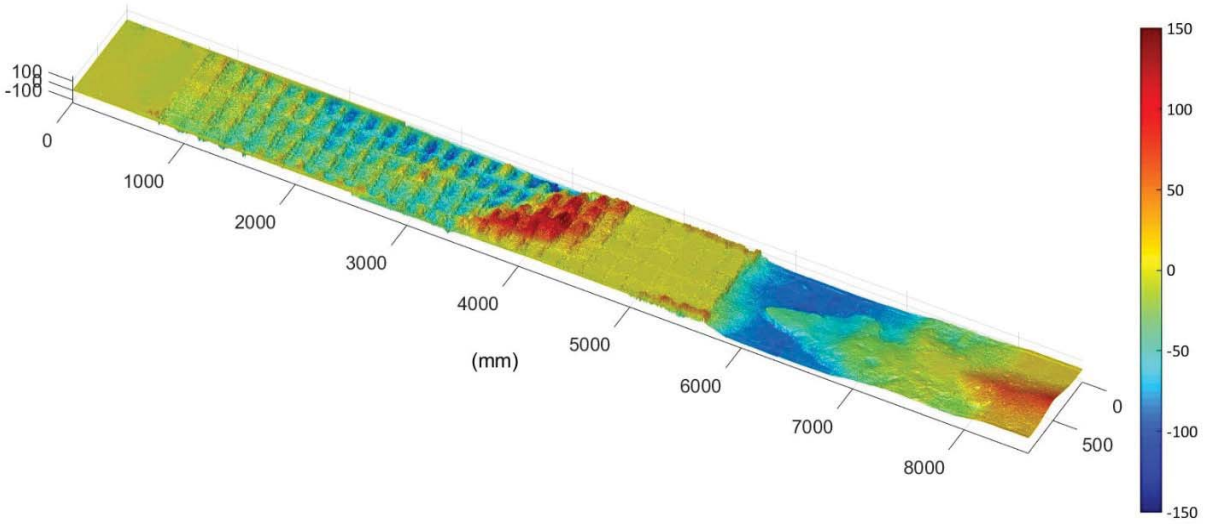


Figure 4.112. Topographic difference plot from zero to 25.33 hours of run time (end of test).

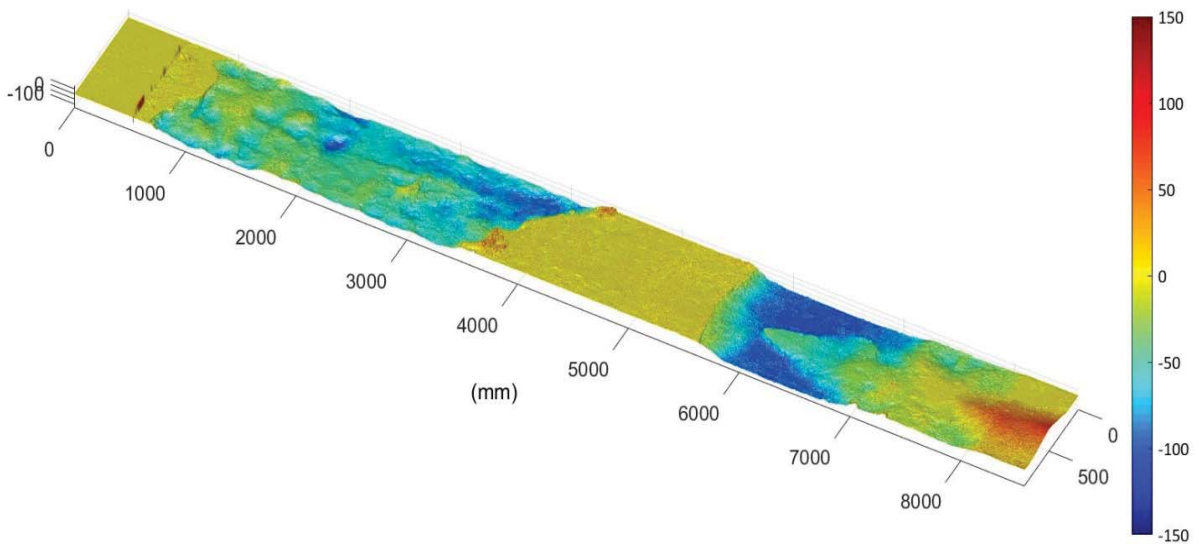


Figure 4.113. Topographic difference plot from initial bare soil vs. final bare soil after 25.33 hours of run time. Note the similarity to the previous figure in the location of the depression and the intact portion of the soil near the shoulder-slope transition.

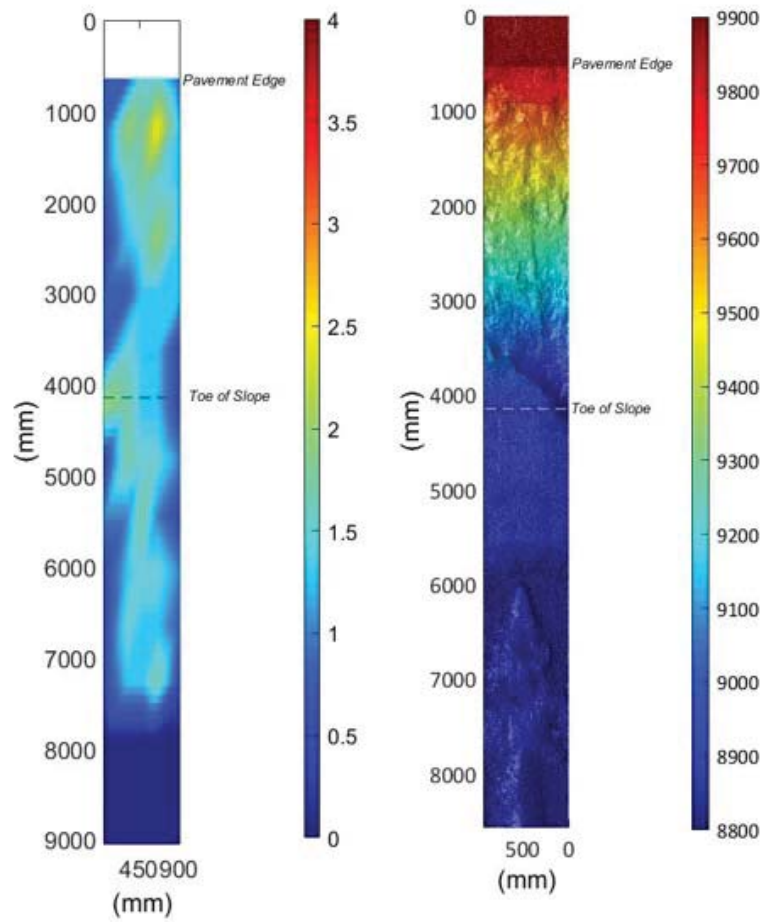


Figure 4.114. (Left) Aerial view of interpolated compaction data on slope with mid-shoulder starting at zero. Compaction measured in tons per square foot. (Right) Aerial view of final bare soil scanned after Flexamat[®] Plus was removed from slope.

Table 4.28. Statistics of compaction on 4H:1V slope for Flexamat[®] Plus testing.

Statistic	On Slope (0-12 feet)		On Flat Run-out (14-28 feet)	
	Tons/SF	psi	Tons/SF	psi
Average	1.26	17.5	1.11	15.4
Std. Dev	0.49	6.8	0.43	6.0
COV	0.39	5.4	0.39	5.4
Maximum	2.50	34.7	1.75	24.3
Minimum	0.50	6.9	0.50	6.9

CHAPTER 5: FIELD CAMPAIGN SUMMARY

5.1 ROADWAY OVERTOPPING FIELD MONITORING SCOPE, PROCEDURES, AND EQUIPMENT

The University's subcontractor, Wenck Engineering, Inc., conducted site monitoring and inspection out of a field office located near the Red River watershed. Site monitoring involved recording flood stage at several roadway locations during overtopping events. Post flood inspections were conducted to evaluate the failure modes observed under natural conditions. Monitoring and inspection sites were selected based on their likelihood of overtopping and use of scour protection systems, if present.

At each chosen road crossing, water level or flood stage was monitored with HOBO U20 submersible pressure transducers manufactured by Onset Computer Corporation, Bourne, Massachusetts. On site these instruments continuously logged absolute pressure. The roadway centerline elevation profile and cross section were surveyed. For the 2013 monitoring, a site logger was attached to a post driven into the ground in the right-of-way upstream of the roadway. A second instrument located on high ground continuously logged barometric pressure to allow the conversion of absolute pressure to water levels. In 2014 additional loggers were purchased to record water levels both upstream and downstream of each roadway thus allowing calculation of the water surface drop across the roadway embankment.

5.2 SUMMARY OF 2013 AND 2014 MONITORING SEASONS

During the 2013 monitoring season from April to August, loggers were deployed at two locations in Norman County and one location in Marshall County. Approximate locations are shown in Figure 1-Figure 3, Appendix A. The only overtopping event captured was at the Marshall County site, where water flowed over County State-Aid Highway 3 for approximately 14 days in early May at depths up to 1.5 feet (refer to Figures 4 and 5, Appendix A in the 2013 monitoring report). No significant erosion was noted at this site. Refer to the 2013 monitoring report in Appendix A for further details.

After the limited results of the 2013 monitoring season, two additional and expanded seasons of monitoring were planned. Additional loggers were purchased and deployed at a total of six locations in April 2014. The same two locations in Norman County were monitored as well as four locations in Kittson County. Approximate locations are shown in Figure 5.1. In 2014 only Kittson County locations 4 and 5 experienced overtopping.

Location 4 was on County Road 57 at Middle Branch Two Rivers, and was subject to of water over the roadway for approximately 15 days in mid-April at depths to just over 10 feet, as shown in Figure 5 in the 2014 monitoring report in Appendix A. Despite the depth, very little erosion occurred but some roadway gravel was moved and deposited on the downstream embankment. Comparison with hydrographs from Red River gauges upstream and downstream of the local site illustrate that the water was due to backup from the Red River and not the local stream. There was very little difference between upstream and downstream water levels, hence there was minimal driving head that would lead to erosion.

Location 5 was on Kittson County Road 58 over the North Branch Two Rivers. Here the roadway was subject to up to 8.5 feet of water during a 13 day overtopping period. This location proved to be very similar to Location 4, and also experienced flooding from the Red River and minimal erosion. Refer to the 2014 monitoring report in Appendix A for further details.

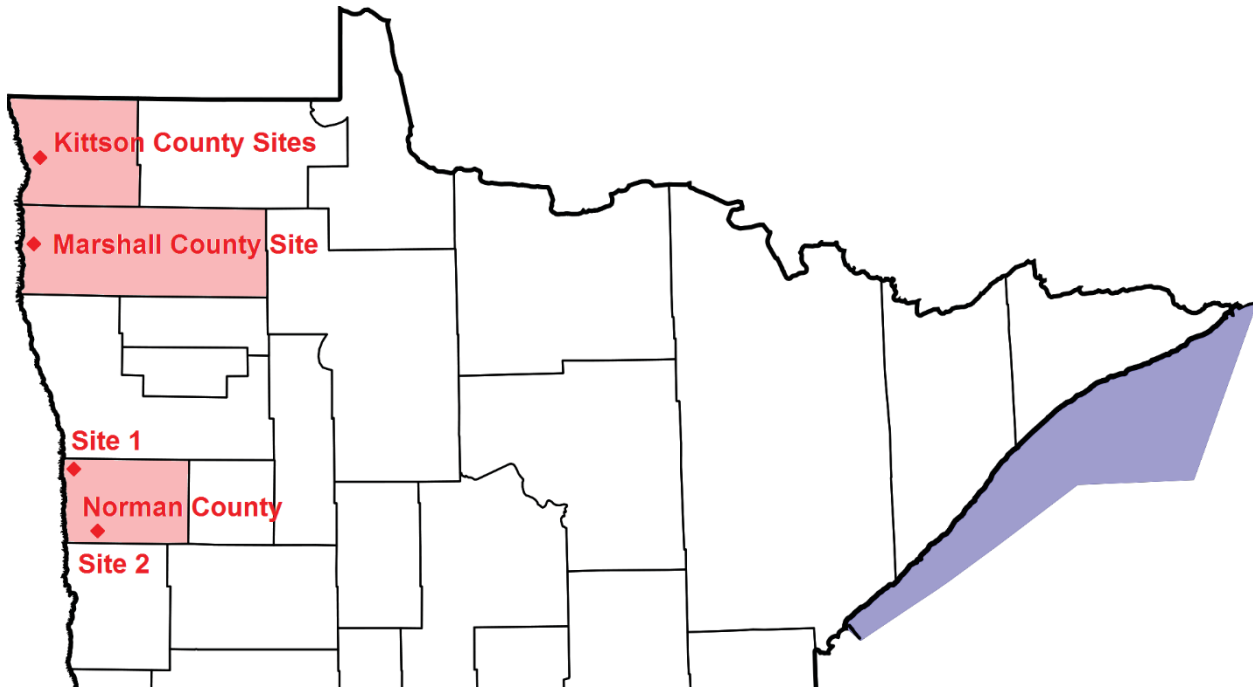


Figure 5.1. Field monitoring site locations on a map of northern Minnesota counties.

In early 2015 there appeared to be little chance of flooding in the Red River valley, so the Technical Advisory Panel, University, and subcontractor decided to forgo Spring 2015 monitoring and wait until the next year. In 2016, similar conditions prevailed and again there was no flooding. At this time, the decision was made that instead of deploying the monitoring equipment, Wenck Associates would prepare a set of instructions for use of the data loggers for roadway overtopping monitoring. The report titled, “Notes for Use of Hobo Pressure Transducer Data Loggers for Road Overtopping Research”, is included at the end of Appendix A, and was supplied to the MnDOT Hydraulics division along with the loggers in spring 2016.

5.3 FIELD MONITORING DISCUSSION

In the three cases of observed roadway overtopping, the difference in water surface elevation (head) between the upstream and downstream sides of the roadway embankment was relatively small. The 2014 data show this was due to area-wide backwater effects. Shear stress is directly proportional to both the depth (d) of water, which in this situation is relatively large, and the slope (S) of the energy grade line, which is very small due to the small head difference. For the monitored sites, the resulting shear stress were low and relatively little erosion occurred.

In the flume study detailed in Chapters 3 and 4, overtopping depths were limited by the available flow rate and ceiling height of the laboratory space, and a “low” tailwater was modeled as a worst-case for erosion potential. The flume experimental parameters created conditions more severe than those observed during this project’s field monitoring, but overtopping conditions with more erosion potential do occur, such as the flow pattern shown in the photograph of Figure 1.1 and 1.4. Other phenomenon that could create conditions with higher erosion potential include a quickly rising or quickly falling hydrograph, where there is a temporary large head difference between upstream and downstream of the roadway embankment.

Comparison of the field and laboratory observations confirms that there is a strong correlation between higher erosion potential and larger head difference across the embankment from upstream to downstream. Where this type of flooding is likely, embankment stabilization is necessary. Conversely, if the only overtopping occurs in the backwater of a river such that the head difference is negligible, it is possible that no additional protective measures are required.

The monitoring methodology developed for the 2014 season should be useful to MnDOT and other researchers studying roadway overtopping in the field. Having both upstream and downstream water level logger locations provided a better understanding of the site dynamics than a single logger alone. The chosen loggers and installation techniques proved to be robust. If a topographic survey is made and water level loggers deployed as recommended in the procedure at the end of Appendix A, the likelihood of gathering useful data is increased. However, as demonstrated in this project, capturing a roadway overtopping event is weather-dependent and requires advance planning. An understanding of the local area hydraulics during flooding, for instance by comparing recorded water levels to nearby river gauges, is also very helpful to understanding the dynamics of the overtopping event.

CHAPTER 6: FINDINGS/DISCUSSION

6.1 STABILIZATION TECHNIQUE PERFORMANCE

Summary data on hydraulic conditions, performance, and circumstances of failure for each of the embankment slope stabilization techniques tested is summarized in Tables 6.1 to 6.4, following the discussion of each tested technique.

6.1.1 Armored Sod (Techniques 1 and 1A)

In this series of tests, one of the primary experimental parameters was the ability of the geogrid to stabilize and hold in place vegetation on the slope. Due to the previously mentioned difficulty and time consuming nature of growing vegetation in the laboratory, two materials were selected to stand in for vegetation: erosion control blanket (ECB) and bluegrass sod.

The ECB beneath the geogrid (Technique 1) was intended to mimic the effect of vegetation; however, this appears to have been only partly successful. While the excelsior (aspen wood) fibers of the ECB had some similarity to a tangled root and stem mat structure, the critical missing component was the depth of contact roots have with the soil. During and after the overtopping flows, the ECB did not degrade and remained intact as a cohesive layer. However, despite the relative flexibility of the material fibers, there was often bridging of the blanket over soil, resulting in erosion occurring beneath.

Despite the limitations, the ECB with geogrid was effective in reducing erosion versus a comparable bare soil slope. For instance, referring to Table 6.1, for the 4H:1V slope “quick” test, the flow per unit width at the first noticeable erosion was more than 10 times greater than the comparable bare soil test. As noted in Technique 1-Test 3, the 4H:1V “long” test failed almost immediately due to a failure at the shoulder-slope transition, perhaps as a result of a slope defect. Erosion in the 4H:1V slope tests escalated quickly with more flow, showing no resilience once the initial erosion had taken place. Technique 1 with ECB performed better on the 6H:1V slope, running 12 hours before erosion occurred at $0.86 \text{ ft}^3/\text{s-ft}$. This test was not run long enough for a large erosive failure, but was stopped based on approximately 0.5 inches of average soil loss. Based on these results, the erosion control blanket (ECB) with the biaxial geogrid is only a marginally effective method of slope protection when laid on bare soil for an overtopping event—i.e., when floodwaters rise before vegetation is established—but appears to function better under a lower slope condition.

The bluegrass sod overlain with biaxial geogrid (Technique 1A) did a better job of simulating natural vegetation but had its own performance challenges. The roughness resulting from individual blades of grass had a beneficial effect and were relatively stable even in high flows. However, two negative aspects were: 1) the lack of a root structure between the sod and the soil surface, and, 2) the presence of seams between sod pieces, both parallel and perpendicular to the flow, such that it functioned as discrete pieces of stabilization material. The sod was fastened with staples but the seams were eventually compromised by flow allowing direct contact between water and the soil. The resulting erosion created localized scour holes or depressions (discontinuity in the slope) with a cascading effect

of further erosion beneath the sod pieces. Referring to Table 6.1, the sod performed better than the ECB on the 4H:1V slope in terms of flow duration and severity of erosion. Significantly, in both tests, the sod directly adjacent to the pavement edge remained intact even when the lower slope was eroded, critically buffering the pavement. The progression of failure was slow to moderate, and there was some degree of resilience exhibited by the sod pieces conforming to the eroded slope contours.

Geogrid: Because of the rigidity and shape of the biaxial geogrid, the results suggest it was not a particularly effective material for securing erosion control blankets or reinforcing vegetation. The profile of the web was thin when laid on the ground and can act like a wing or hydrofoil when exposed to flow parallel to the geogrid. This had some effect of creating turbulence and air entrainment. As the water traveled faster over the top of the geogrid than below, it created an uplift force on the geogrid, allowing more water to flow underneath it and push up against the anchors that held down both the geogrid and erosion control blanket. The density of the geogrid was also low and enabled uplift since the material was made of polypropylene. Polypropylene's density is 0.91 g/cm^3 (Glover, 2008), slightly less than water's density, giving it a slight amount of buoyancy which added to the uplifting process as water flowed down the slope. If time allowed vegetation to grow into and root through the geogrid matrix, the ability of the geogrid to hold together the vegetation mass would likely be similar to the design of a turf reinforcement mat (TRM) with larger openings, less flexibility, but ultimately stronger than commercial TRM.

Metal chain link fence: Fencing has been suggested as an alternative to geogrid. Regarding the issue of uplift, chain link fencing—which is denser than water, more flexible than geogrid, and consists of rounded rather than flat-shaped elements—may be a better option for a similar intended function. Metal chain link fence was not tested as part of this project.

6.1.2 Turf Reinforcement Mat and Fiber Reinforced Matrix (Technique 2)

The Turf Reinforcement Mat (TRM) paired with the Fiber Reinforced Matrix (FRM) had some capability to protect the soil surface even after the FRM had been mostly washed away. In testing, the TRM was still a relatively effective method for soil stabilization even without vegetation, but likely would be more effective with a dense root mat grown in place. The TRM was flexible enough to remain in contact with the soil for small deformations but did bridge over deeper scour holes. Localized scour immediately near the staples was observed, in concurrence with the observation of Chen and Anderson (1986) with Enkamat material. Using the 6H:1V test as an example, the erosion began between the outside staples on the right side of the flume, possibly as a result of a discontinuity in the soil surface. As erosion worked upstream, it exposed the staple upslope, allowing the separation of the TRM from the soil, finally working all the way back to the shoulder. The rest of the slope was held intact and seemed to experience little change in topography despite the large adjacent area of erosion. Downstream of the depression, there was re-deposition of soil but not an amount substantial enough to create a large mound, probably due to the porous nature of the TRM tested. The 4H:1V slope's failure at the toe of the slope, though large, did not affect the upper portion of the slope, which remained intact. Curiously, areas adjacent to deep scour were often completely intact, showing negligible erosion. One reason for this behavior may be the presence of soil tackifier in the FRM formulation that remained on the soil

surface even after the fibers washed away. The tackifier may have created a layer of soil that was “glued” together.

6.1.3 Flexible Concrete Geogrid Mat (Technique 3)

The Flexible Concrete Geogrid Mat (Flexamat® Plus) performed well on the 6H:1V slope, showing minimal erosion after 30 hours of testing at full capacity of the test flume. Tests on the 4H:1V slope did not perform as well and experienced erosion events that met failure criteria, even though the shoulder had not been undermined. Both 4H:1V slope tests experienced localized scour followed by a depositional mound starting at approximately 1500mm downstream of the shoulder, with erosion progressing downslope and leaving the upper slope intact. The turf reinforcement mat (Recyclax®) and light excelsior backing layers beneath the concrete blocks were not entirely compressed by the weight of the blocks and allowed some water to flow through these layers near the soil. Once erosion started, the backing layers acted as a filter, capturing soil and leading to the observed mounding. Despite erosion, the system was relatively resilient. The blocks and backing conformed to the changed surface and moved to redistribute stresses. This is a desirable trait in practice as it lessens the likelihood of a rapid, severe failure and the need for immediate maintenance after an overtopping event.

As compared to the other techniques tested, the concrete blocks created a much higher degree of surface roughness. During lower flows when the flow depth was comparable to the block height, the flexible concrete geogrid mat experienced a large amount of turbulence between the blocks of concrete, as shown in Figure 4.105. The result was locally variable flow conditions, likely including some velocity being directed downward at the soil surface. As higher flows submerged the blocks, the flow pattern changed and a less turbulent water surface over the slope was present.

6.1.4 Summary Tables

The results from the all tests are synthesized in the tables below.

Tables 6.1 and 6.2 summarize the time, discharge, average mid-slope velocity, and shear stress at a) the first observation of erosion of the embankment slope (Table 6.1), b) the noted failure point (Table 6.2), and c) final discharge before test was ended (Table 6.2).

Table 6.3 summarizes the observed location of the most serious erosive feature and provides a description of the progression of erosion, whether up- or down-slope, or both. In the fourth column of this table, the “dot” is a visual indication of the initial erosion location, either near the top of the slope, mid-slope, or near the bottom of the slope. The arrow indicates the direction of erosion migration. The initiation location and direction of migration is important because the highest priority of protection is the roadway surface and top of slope; a washout that does not threaten the roadway integrity is less concerning.

In Table 6.4, the condition of the slope when flow testing was stopped is briefly described. The final column describes the probable progression of erosion if the flow would have been continued, which is based on the observations noted during the testing.

Table 6.1. Summary of hydraulic conditions at first noticeable erosion and average measured compaction.

Technique	Slope	Avg Compaction (tons/ft ²)	At First Noticeable Erosion					Shear stress τ (lb/ft ²)
			Time (hr)	Flow, Q (ft ³ /sec)	Unit Discharge (ft ³ /s/ft)	Avg velocity V (ft/s)		
Tech 0 "Bare Soil"	4H:1V	1.71	0	0.089	0.028	No meas.	No meas.	
	4H:1V-EP	1.55	0	0.089	0.028	No meas.	No meas.	
	6H:1V	2.00	0	0.082	0.029	No meas.	No meas.	
Tech 1 "Armored Sod" with ECB	4H:1V-Q	2.24	1.16	1.10	0.35	3.78	1.45	
	4H:1V	2.64	0	1.10	0.35	3.28	1.67	
	4H:1V-EP	1.37	1.5	0.93	0.30	4.90	0.95	
	6H:1V	2.31	12.0	2.47	0.86	5.68	1.57	
Tech 1A "Armored Sod" real sod	4H:1V-Q	1.75	1.5	1.94	0.62	7.00	1.39	
	4H:1V-EP	1.57	3.8	2.80	0.30	3.28	1.43	
Tech 2 "Turf Reinforcement Mat with Fiber Reinforced Matrix"	4H:1V-Q	1.89	3.0	7.88	2.52	9.96	3.95	
	6H:1V	2.59	2.0	1.35	0.47	3.52	1.38	
Tech 3 "Flexible Concrete Geogrid Mat"	4H:1V-Q	1.78	1.33	6.04	1.93	5.25	5.74	
	4H:1V	2.13	4.0	2.82	0.90	4.64	3.04	
	6H:1V	1.26	-	-	-	-	-	



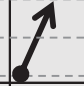


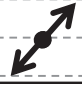


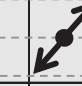
Table 6.2. Summary of hydraulic data at noted "failure" and final flow.

Technique	Slope	At Noted Failure				At Final Flow			
		Time to Failure (hr)	Unit Discharge (ft ³ /s/ft)	Avg velocity V (ft/s)	Shear stress τ (lb/ft ²)	Total Testing Time (hr)	Unit Discharge (ft ³ /s/ft)	Avg velocity V (ft/s)	Shear stress τ (lb/ft ²)
Tech 0 "Bare Soil"	4H:1V	0.13	0.029	No meas.	No meas.	0.13	0.029	No meas.	No meas.
	4H:1V-EP	0.83	0.331	2.85	1.81	0.83	0.331	2.85	1.81
	6H:1V	0.13	0.029	No meas.	No meas.	0.13	0.029	No meas.	No meas.
Tech 1 "Armored Sod" with ECB	4H:1V-Q	1.83	0.87	5.55	2.28	1.93	0.87	5.55	2.44
	4H:1V	0.5	0.35	3.28	1.67	0.5	0.35	3.28	1.67
	4H:1V-EP	3.0	0.30	2.68	1.74	6.0	0.88	2.89	4.76
Tech 1A "Armored Sod" real sod	6H:1V	16.0	1.17	6.45	1.89	16.0	1.17	6.45	1.89
	4H:1V-Q	2.5	1.92	10.67	2.80	4.5	4.27	13.15	5.07
	4H:1V-EP	3.75	0.30	3.28	1.43	9.5	0.90	7.51	1.86
Tech 2 "Turf Reinforcement Mat with Fiber Reinforced Matrix"	4H:1V-Q	3.5	2.53	9.28	4.25	3.5	2.53	9.28	4.25
	6H:1V	8.0	1.29	5.77	2.33	8.25	2.39	6.56	3.78
Tech 3 "Flexible Concrete Geogrid Mat"	4H:1V-Q	1.5	1.93	5.25	5.74	1.5	1.93	5.25	5.74
	4H:1V	25.33	3.17	9.76	5.07	25.33	3.17	9.76	5.07
	6H:1V	-	-	-	-	30.0	5.08	11.38	4.64

Notes:





1. Suffix "Q" indicates quick run, "EP" indicates extended paving from shoulder.
2. Flow, velocity, and shear stresses noted are run averages calculated at mid slope.

Table 6.3. Initial erosion location and description of the progression of erosion

Technique	Slope	Initial Erosion Location		Progression of Erosion	Failure
Tech 0 "Bare Soil"	4H:1V	Near shoulder then entire slope		Entire slope rapidly channelized	Yes
	4H:1V-EP	Entire slope, channels form at bottom		Widespread slope erosion with channels near bottom	Yes
	6H:1V	Near shoulder then entire slope		Entire slope rapidly channelized	Yes
Tech 1 "Armored Sod" with ECB	4H:1V-Q	Mid-slope		Rapidly progressing upslope, beneath ECB	Yes
	4H:1V	Near shoulder		Rapidly across flume immediately downstream of shoulder	Yes
	4H:1V-EP	Across entire flume, 400mm after shoulder		Rapidly across flume slightly downstream of extended paving, then upstream and downstream	Yes
	6H:1V	Mid-Slope, center, 3800mm from shoulder		Slow growth of shallow dip (erosion) and mounds	Moderate
Tech 1A "Armored Sod" real sod	4H:1V-Q	Toe of slope, 2700mm from shoulder		Upslope from toe, detachment of geogrid, soil erosion beneath sod pieces, and removal of sod pieces	Moderate
	4H:1V-EP	Mid-Slope, 1300mm from shoulder		Starting from sod seams, soil erosion beneath sod pieces, detachment of geogrid, and removal of sod pieces	Yes

See notes at end of table

Table 6.3 (Continued) Initial erosion location and description of the progression of erosion

Technique	Slope	Initial Erosion Location		Progression of Erosion	Failure
Tech 2 "Turf Reinforcement Mat with Fiber Reinforced Matrix"	4H:1V-Q	Toe of slope, 3000mm from shoulder		Wide eroded area progressing upstream slowly	Yes
	6H:1V	Near shoulder, right side		Rapid but localized progression downstream from shoulder edge	Yes
Tech 3 "Flexible Concrete Geogrid Mat"	4H:1V-Q	Mid-Slope, 1500mm from shoulder		Formation of second dip and mound system downstream of the first, at 2400 mm from the shoulder	Moderate
	4H:1V	Mid-Slope, 1500mm from shoulder		Dip and mound moved downstream to toe	Moderate
	6H:1V	n/a	n/a	n/a	No

Notes:

1. Suffix "Q" indicates quick run, "EP" indicates extended paving from shoulder
2. In the Failure column, "Yes" means major or rapidly progressing erosion, "Moderate" signifies some soil loss or stabilization material loss of contact, but the test did not continue to the point of major failure.
3. The column with **dot & vector** indicates the location where failure was initiated (dot) and the direction of erosion migration (vector).

Table 6.4. Description of slope condition when testing was stopped and predicted result with continued flow.

Technique	Slope	Failure	Result when Testing Stopped	Predicted Result with Continued Flow
Tech 0 "Bare Soil"	4H:1V	Yes	Undercutting of shoulder, degrading channels	Overall slope degradation, rapid pavement undercutting, eventual failure
	4H:1V-EP	Yes	Slope degraded except for immediately adjacent to extended pavement	Overall slope degradation, eventual but slower extended pavement undercutting and eventual failure
	6H:1V	Yes	Undercutting of shoulder, degrading channels	Overall slope degradation, rapid pavement undercutting, eventual failure
Tech 1 "Armored Sod" with ECB	4H:1V-Q	Yes	Deep channels migrating upstream	Rapid erosion of overall slope, pavement undercutting and failure
	4H:1V	Yes	Trench at top of slope and undercutting of shoulder, shallow eroded pockets on balance of slope	Rapid pavement undercutting and failure
	4H:1V-EP	Yes	Deep eroded trench at top slope, mound slightly downstream, shallow eroded pockets on balance of slope	Rapid erosion slightly downstream of extended paving, leading to rapid pavement undercutting
	6H:1V	Moderate	Several wide, shallow eroded areas, upper slope intact	Slow growth and connection of shallow erosion to cover entire slope
Tech 1A "Armored Sod" real sod	4H:1V-Q	Moderate	Sod partly washed away and lower soil eroded, upper 2/3 of slope intact	Slow erosion progress upslope and loss of sod pieces, eventual undercutting of pavement
	4H:1V-EP	Yes	Deep erosion under sod across slope except directly adjacent to extended pavement	Erosion progress upslope, loss of sod pieces, and eventual undercutting of extended pavement

See notes at end of table

Table 6.4 (Continued) Description of slope condition when testing was stopped, and predicted result with continued flow

Technique	Slope	Failure	Result when Testing Stopped	Predicted Result with Continued Flow
Tech 2 "Turf Reinforcement Mat with Fiber Reinforced Matrix"	4H:1V-Q	Yes	Lower half of slope eroded, upper half intact	Continued erosion at the toe and slow erosion progress upslope
	6H:1V	Yes	Deep erosion near shoulder, balance of slope largely intact	Undercutting of shoulder at erosion location, probably slow erosion of remainder of slope at higher flows
Tech 3 "Flexible Concrete Geogrid Mat"	4H:1V-Q	Moderate	Two sequential dip (erosion) and mound (deposition) sets midslope, upper slope intact	Continued periods of erosion and stabilization (see 4H:1V long test)
	4H:1V	Moderate	Overall soil erosion on the slope, concentrated on the mid to lower slope	Continued periods of erosion and stabilization
	6H:1V	No	Very little soil erosion on slope, some shifting of blocks downstream	Similar erosion / stabilization pattern as 4H:1V slope flows > than flume capacity

Notes:

1. Suffix "Q" indicates quick run, "EP" indicates extended paving from shoulder
2. In the Failure column, "Yes" means major or rapidly progressing erosion, "Moderate" signifies some soil loss or stabilization material loss of contact, but the test did not continue to the point of major failure.

6.2 FAILURE MECHANISMS AND LOCATIONS

6.2.1 Failure location:

Prior to testing, it was expected that the initiation of erosion or scour would occur either: 1) at the top of the slope near the shoulder to slope transition or 2) at the hydraulic jump location. The observations noted in Table 6.2 show that erosion was initiated in all areas of the flume, ranging from the shoulder-slope transition to the mid-slope region, intermittently along the slope, and the toe of the slope. Multiple factors contribute to the likelihood of erosion initiation, making consistent prediction challenging.

6.2.1.1 Top of slope and shoulder transition

The transition zone from pavement to slope is a critical area. Flow accelerates and changes direction from the relatively flat roadway to the steeper inslope. In the laboratory tests, two of the three bare soil runs failed immediately at the transition. Beyond the bare soil runs, the only tests where failure was initiated at the top of the slope adjacent to the paved shoulder were the 4H:1V Armored Sod (Technique 1) and the 6H:1V TRM with FRM (Technique 2). Both failures appear to have resulted from small discontinuities in the soil or protection materials, with lower relative compaction as a secondary cause. Erosion was immediate and proceeded quickly laterally and downslope in the Armored Sod 4H:1V test. The 6H:1V TRM with FRM endured much longer at higher velocities and shear stresses with only localized erosion.

6.2.1.2 Mid-slope

Mid-slope failures were most common among the test performed. A local scour and downstream depositional mound was typical. As an eroded depression formed, soil would deposit immediately downstream forming a mound under the soil protection material. The scour and mound combination had the effect of changing the depth, velocity, and pattern of flow. As the depression on the slope grew, it tended to work upstream eroding towards the shoulder, and the mound of deposited soil from the slope would move further downstream and/or become larger. This was most noticeable in the 4H:1V test of the flexible concrete geogrid mat Figures 4.111 to 4.113. The pattern appears to be a partially arrested form of the cyclic steps observed in the bare soil runs, illustrated in Figure 4.15.

The soil used for testing was typical of roadway embankments in Minnesota and was susceptible to continued disturbance once erosion was initiated. The presence of an erosion control treatment slowed down the development of scour. Generally, it is not possible to control the soil composition of slopes in a field setting, therefore the choice of erosion protection technique for the embankment is important. The TRM with FRM was the only technique in which the mid-slope stayed intact in each run.

6.2.1.3 Toe or base of slope

The toe of the slope was subject to the fastest water velocities and additional turbulence due to the presence of the hydraulic jump. Two failures were initiated at the toe of the slope. For Technique 1A Armored Sod with real sod 4H:1V quick test, hydraulic forces associated with the hydraulic jump caused the downstream end of the sod rolls to become loose and expose the soil embankment underneath. Once the covering protection was removed, water was able to erode the soil and washout the sod. This pattern of uplift of the sod and erosion of soil migrated upstream. If vegetation on the slope (the sod) was rooted into the embankment, this failure would have been less likely as the roots would have resisted uplift. On a natural slope where vegetation has been allowed to grow through the geogrid, this system may be more effective.

The second case of slope failure occurred with the Technique 2 TRM with FRM 4H:1V quick test. In a similar way to the Technique 1A test, the TRM was lifted away from the embankment by the strong hydraulic forces associated with the hydraulic jump. The resulting scour migrated upslope.

6.2.2 Effect of slope continuity, soil contact, and compaction

6.2.2.1 Slope continuity

Any disturbances or discontinuities on the slope surface, including scour holes and depositional mounds that changed the flow pattern, were a location for initiating erosion. These variations caused turbulence, impingement, and asymmetrical flow which accentuated local erosion. Constructing an embankment slope to be as flat as possible, without local depressions, will reduce the chances of erosion regardless of what stabilization material is installed. Precautions should also be taken to not disturb the slope during installation of the protection material, as bridging over the soil surface will leave the bridged area susceptible to erosion. Preventing bridging over ruts, lumps, roots, etc., is a typical recommendation for installation of rolled erosion control products like turf reinforcement mats and should be followed.

6.2.2.2 Soil contact

Ensuring good contact between the soil on the slope and the stabilization technique was crucial for performance. Areas where water flowed between the layers and eroded the slope surface appeared to lack continuous contact. When contact was compromised, flowing water was able penetrate between the erosion protection material and bare soil resulting in local scour and often propagation of erosion. This method of failure was present in many of the experiments. The areas where the material was fastened down properly and stayed in contact with the soil surface were more resistant to erosion. Figure 6.1 shows clearly that locations where protection was closely bonded to the soil surface (e.g. location of staples) had lower erosion.)



Figure 6.1. View from above of the bare soil after the ECB was removed post-testing, 6H:1V slope. Note the indicated holes where the staples were holding down the stabilization material. Flow was from right to left.

A similar lack of contact event occurred on the second 4H:1V test of the flexible concrete geogrid mat (Figure 6.2). The concrete mat separated from the slope surface despite the weight of the concrete block grid. There were no staples fastening the flexible concrete geogrid mat because it was assumed that the weight of the material would hold it against the slope surface. At a high flow of 0.72-ft over the crest, the velocity was fast enough to create uplift and the soil beneath was exposed and eroded near the toe of the slope.



Figure 6.2. Flexible concrete geogrid mat tested on the 4H:1V slope at 9.90 ft³/s and approximately 25 hours of run time. Concrete blocks may be pushed down with a probe rod 3-4 inches before touching the slope surface $\frac{3}{4}$ of the way down the slope.

6.2.2.3 Compaction

Tests show some correlation between location of initiation of erosion and deficiencies in compaction relative to the soil around it, as measured by the penetrometer. It can be inferred from the bare soil tests that there was more erosion in the areas where compaction was relatively low. However, a high absolute compaction was not observed to be as important as consistency in compaction over the slope. The most obvious example of this is the TRM with FRM 6H:1V test. The average compaction was 2.6 tons/ft², higher than other runs, however, erosion started and propagated at the upstream corner where the compaction was only half of the average (Figure 4.90). Although consistent compaction is likely of benefit, it may be difficult to obtain in practice due to factors such as freeze-thaw cycles, errant or maintenance vehicles driving on the slopes, and the effects of burrowing animals.

6.2.3 Slope Angle Comparison: 4H:1V and 6H:1V

Protection of the 6H:1V slope embankment was more effective than the 4H:1V slope embankment. On the 6H:1V slope the flexible geogrid concrete mat performed without failure and the 6H:1V ECB armored sod test resulted in only a very minor failure. The TRM-FRM on the 6H:1V slope experienced localized erosion earlier than the 4H:1V slope but was still able to resist a broader failure longer than the 4H:1V test of the material. Where it is possible, lengthening the embankment slope and decreasing its steepness is likely to reduce erosion. Reduction in slope reduces bed shear stress and also reduces the intensity of the hydraulic jump.

To allow direct comparison between the 4H:1V and 6H:1V slope for three slope protection techniques, some of the tests were designed to target the same discharge per unit width of flume by using the same flow depth over the flume crest (representing the roadway crown) in the 4H:1V and 6H:1V flumes. A summary of results for Techniques 1, 2, and 3 are presented in Tables 6.5, 6.6, and 6.7, respectively, indexed by flow depth over the roadway crest. In each table, the numbers reported are averages of all valid runs for a given slope angle and measured mid-slope depth. From mid-slope depth, average velocity was calculated using the discharge per unit width, and average shear stress was calculated assuming the energy slope was parallel to the embankment slope, as described in Chapter 4, equations 1 and 2. The friction factor 'n' was calculated in a similar fashion using equation 3 in the chapter. Ratios noted are the average value of depth, velocity, shear, or 'n' for the 6H:1V slope divided by the counterpart value for the 4H:1V slope.

Table 6.5. Comparison of 6H:1V and 4H:1V mid-slope data, Technique 1, Armored Sod

Technique 1 Armored Sod	0.17 ft depth over crest			0.24 ft depth over crest			0.30 ft depth over crest		
	0.35 cfs per ft width			0.60 cfs per ft width			0.86 cfs per ft width		
Mid-slope data	6H:1V slope	4H:1V "quick"	6:1 / 4:1 ratio	6H:1V slope	4H:1V "quick"	6:1 / 4:1 ratio	6H:1V slope	4H:1V "quick"	6:1 / 4:1 ratio
Measured Depth (ft)	0.09	0.09	104%	0.12	0.12	100%	0.16	0.16	100%
Calc'd Velocity (ft/s)	3.82	3.78	101%	5.03	4.91	102%	5.45	5.55	98%
Calc'd Shear (lb/ft ²)	0.95	1.45	66%	1.25	1.91	65%	1.65	2.44	67%
Calc'd 'n'	0.032	0.040	81%	0.030	0.037	81%	0.033	0.039	83%

For Technique 1, the "Armored Sod", depths and velocities on the 4H:1V and 6H:1V slopes are similar for all three cases. Shear stress for the 6H:1V slope is about 2/3 of that on the 4H:1V slope. Referring to equation 2 in Chapter 4, shear stress is directly related to slope. Likewise, the calculated Manning's 'n' for the 6H:1V slope is near 81% of the calculated 'n' for the comparable 4H:1V slope case.

Table 6.6. Comparison of 6H:1V and 4H:1V mid-slope data, Technique 2, TRM with FRM

Technique 2 TRM with FRM	0.20 ft depth over crest			0.40 ft depth over crest			0.60 ft depth over crest		
	0.46 cfs per ft width			1.29 cfs per ft width			2.52 cfs per ft width		
Mid-slope data	6H:1V slope	4H:1V "quick"	6:1 / 4:1 ratio	6H:1V slope	4H:1V "quick"	6:1 / 4:1 ratio	6H:1V slope	4H:1V "quick"	6:1 / 4:1 ratio
Measured Depth (ft)	0.13	0.09	139%	0.22	0.17	129%	0.36	0.26	138%
Calc'd Velocity (ft/s)	3.62	4.95	73%	5.78	8.10	71%	6.56	9.62	68%
Calc'd Shear (lb/ft ²)	1.33	1.45	91%	2.32	2.60	89%	3.78	4.10	92%
Calc'd 'n'	0.043	0.031	137%	0.039	0.028	139%	0.047	0.032	147%

For Technique 2, shown in Table 6.6, water depth was 1.3 to 1.4 times greater on the 6H:1V slope than the 4H:1V slope, corresponding to decreased velocity and increased manning's 'n'. Although the velocity on the 6H:1V slope is about 70% of the velocity on the 4H:1V slope on average, the shear stress is only slightly lower (90%) due to the increased weight due to the depth. The lower bulk velocity and lower shear stress are both advantageous for surface protection to prevent erosion.

Table 6.7. Comparison of 6H:1V and 4H:1V mid-slope data, Technique 3, Flexible Concrete Geogrid Mat.

Technique 3 Flex. Conc. Geo. Mat	0.30 ft depth over crest			0.45 ft depth over crest			0.60 ft depth over crest		
	0.9 cfs per ft width			1.6 cfs per ft width			2.5 cfs per ft width		
Mid-slope data	6H:1V slope	4H:1V "quick"	6:1 / 4:1 ratio	6H:1V slope	4H:1V "quick"	6:1 / 4:1 ratio	6H:1V slope	4H:1V "quick"	6:1 / 4:1 ratio
Measured Depth (ft)	0.15	0.21	71%	0.21	0.28	75%	0.28	0.29	95%
Calc'd Velocity (ft/s)	5.66	4.20	135%	7.44	5.70	131%	8.75	8.93	98%
Calc'd Shear (lb/ft ²)	1.56	3.26	48%	2.18	4.42	49%	2.89	4.49	64%
Calc'd 'n'	0.031	0.063	49%	0.029	0.056	52%	0.030	0.036	82%

For the flexible concrete geogrid mat three crest depths were compared in Table 6.7. At shallower flows of 0.3 ft and 0.45 ft over the crest, the flow depth on the 6H:1V slope is about 3/4 of the 4H:1V slope, and the velocity is about 4/3. Shear stress is about half on the 6H:1V slope as the 4H:1V slope, and roughness as indicated by Manning's 'n' is also lower. Due to the height of the blocks, at shallower flows the water surface was influenced by the blocks and was not smooth or uniform. Energy dissipation due to splashing was high, especially on the 4H:1V slope, with calculated 'n' values about double the 6H:1V slope. The 4H:1V slope was subjected to higher shear stress as well as the turbulent forces at lower flows, which have a higher potential to cause erosion.

At 0.6 ft of depth over the crest, a different pattern was observed. The water surface was generally smooth. Depth and velocity were comparable (within 5%) for the 6H:1V and 4H:1V slopes. Lower calculated shear stress for the 6H:1V slope was due primarily to the water surface slope difference, as

was the lower 'n'. In deeper flows, the advantage of the 6H:1V slope in terms of lower shear stress diminishes as compared to the case of shallower flows in Technique 3.

6.2.4 Effect of Extended Shoulder Paving (Inslope Paving)

The extension of pavement past the shoulder and onto the inslope served to improve the road shoulder stability in tests. Observations indicate that the extended paving served to transition and direct the flow from the flatter shoulder (4% slope) to the inslope (4H:1V or 25%) so that flow was essentially parallel to the slope by the downstream end of the extended paving. Relative to all of the erosion control techniques, the paved shoulder was relatively smooth and thus water tended to accelerate over the surface. The primary benefit was in protecting the soil directly adjacent to the extended paving or shoulder. Protection of the adjacent soil was evident in the 4H:1V slope test with bare soil. Where the other bare soil tests immediately experienced erosion directly adjacent to the paved shoulder, the paved slope offered some protection to the “pavement” edge by directing the flow parallel to the slope angle. Conversely, mid-slope erosion was greater in the testing of Techniques 1 and 1A on the 4H:1V slope with extended paving, most likely due to higher “exit” velocities of water coming off the extended paving section.

6.2.4.1 Longevity and Maintenance of Extended Shoulder Paving

As tested the extended paving was fixed (painted plywood) and could not be eroded, which was a reasonable condition for a short test. In actual practice, the bituminous inslope paving is subject to deterioration by natural forces. Inslope paving is challenging to place, compaction is often low or inconsistent leading to cracking and deterioration of the flexible pavement. The field life expectancy may be as short as several years, and installation and maintenance difficulties have been reported (J.T. Anderson, 2016, personal communication).

6.3 OVERTOPPING PROTECTION GUIDANCE

Each technique tested has both strengths and weaknesses which should be considered when weighing design options for embankment overtopping protection. Information on construction costs, installation and maintenance concerns is presented in this section.

6.3.1 Construction Costs

Together with the effectiveness of a given material in preventing serious erosion and the loss of a roadway embankment, cost is a very important factor in the choice of embankment stabilization techniques. Table 6.8 summarizes how estimated construction costs for the tested materials fit into the context of other erosion prevention methods such as stone riprap. The costs listed are meant to represent construction costs only and do not include vegetation establishment, maintenance, or repair costs. An expanded version of this table is located in Appendix B including estimate sources.

Table 6.8. Estimated construction costs of various embankment stabilization techniques

Stabilization Technique	Representative cost per SY	Level of Erosion Protection
Bare Soil	none	negligible
Vegetation	< \$1	variable
Erosion Control Blanket - Category 4	\$1 - 5	temporary
"Armored Sod" (Tech 1) as tested with ECB	\$1 - 5	partial
Turf Reinforcement Mat with Fiber Reinforced Matrix (Tech 2) as tested	\$1 - 5	better
Extended Bituminous Shoulder Paving (Partial Slope Paving)	\$5 - 10	partial
"Armored Sod" (Tech 1A) Real Sod as tested	\$5 - 10	partial
Random Riprap - Class III	~ \$30	"standard"
Matrix Grouted Riprap	~ \$35	substantial
Flexible Concrete Geogrid Mat (Tech 3) as tested	~ \$50	partial
Fully Grouted Riprap	~ \$150	complete coverage

6.3.2 Installation, Maintenance, and Longevity

Construction cost is only one of factors in the choice of stabilization techniques, and should be considered along with the other relevant factors including long term maintenance needs. Inferences drawn from handling and observing the materials during the course of the test program are summarized in Table 6.9.

Table 6.9. Comparison of selected properties for tested stabilization techniques

Criteria for Comparison	Tech 1 Geogrid with ECB	Tech 1A Geogrid with Sod	Tech 2 TRM with FRM	Tech 3 Flex Conc Geogrid Mat
Installation Effort	Moderate	Moderate	High	High
Initial, unvegetated embankment protection	Moderate	Moderate	Moderate - High	High
Survivability - Does erosion stabilize in time?	No	Partly	No	Yes
Speed of soil erosion progress	Rapid	Rapid	Moderate	Mod. - Slow
Apparent susceptibility to damage (mower, vehicle, etc)	Moderate	Moderate	Moderate	Negligible

6.3.2.1 Installation:

The rolled products tested (geogrid, erosion control blanket, and TRM) are relatively light weight and not particularly difficult to handle by hand. These products often require an anchor trench at the top or bottom of the slope or both, with intermediate driven anchors as well. Achieving an adequate anchor density using staples would be time consuming for the geogrid. The integrity of top of slope anchoring was not tested in this study but would be important in a field installation and should be planned and executed carefully. The flexible concrete geogrid mat must be installed with heavy equipment in the field due to its inherent weight. It does not have the same anchoring density requirements as the other techniques, but must be secured per the manufacturer's recommendations. If flows over a roadway embankment are expected to be in one direction only, there is generally no reason to install stabilization materials on the "upstream" slope as this would be typically submerged and subject to minimal erosive force.

Where overtopping flows are expected, a higher level of attention should be paid to the shoulder and inslope construction than is normally afforded these roadway elements. The slope should be graded evenly and consistently with smooth transitions, avoiding local discontinuities that would concentrate flow. Gentler slopes (i.e. 6H:1V may be considered if right-of-way exists. Where right-of-way is limited, a gentler slope is more beneficial near the shoulder than near the toe of slope. Vertical drop-offs at the pavement edge should be avoided, and filled if they occur later.

6.3.2.2 Maintenance:

Once materials are in place for embankment protection, normal maintenance consists of little more than mowing and maintaining vegetation. Catching a mower or other equipment on the geogrid or TRM has the potential of damaging the synthetic material and compromising the erosion protection. Soil contact is vital to the continued functioning of the geogrid-reinforced Armored Sod and the TRM; if these materials become undermined, effectiveness to arrest erosion will be lost. Driving heavy equipment across the embankment may deform and damage the materials, disrupt the anchors, and cause discontinuities in the slope surface. The flexible concrete geogrid mat is less susceptible to these types of damages and can provide a greater degree of protection than the other products when disturbed. Maintenance of inslope paving would be similar to other bituminous paving maintenance but somewhat more difficult due to the degree of slope.

Periodic inspections of embankments to detect damaged materials, material bridging over ruts or erosion, and disruption of anchors will increase the probability of the embankment stabilization techniques functioning as intended. Inspection of protected embankments immediately following flooding is recommended to determine if materials have been damaged by erosion or debris, and to determine what repairs may be needed, if any.

6.3.2.3 Repair:

Fixes may range from installing additional anchors to removing damaged materials, filling and grading smooth the embankment slope and then installing new erosion prevention materials. Special care should be taken to join or overlap areas of repair to avoid discontinuity in the slope or a weak boundary area that would be preferentially eroded.

6.4 LIMITATIONS OF THE RESEARCH AND APPLICATIONS FOR FURTHER STUDY

6.4.1 Limitations of the Research

One of the major limitations of the flume study was the absence of mature vegetation on the embankment slope. Although the test conditions mimic the period immediately after construction but before establishment of substantial vegetation, a fully vegetated condition is normal for much of the lifecycle of an embankment. Redistribution of shear stresses by stems or blades is one area where growing or dormant vegetation would have an effect on the flow. Arguably the most important function of vegetation is the anchoring interaction of the roots with the soil. This function was not well replicated, even when actual vegetation (i.e., sod in Technique 1A) was employed.

This study did not examine the longevity or long-term effectiveness of erosion control products, although some inferences are made in the preceding sections with respect to stability in a partially eroded condition and apparent susceptibility to damage. Long-term field observations may provide a better picture of the durability of any embankment stabilization techniques.

The study was not able to capture the desired field data of actual overtopping events. This was one of the primary objectives of the study; however, the conditions for overtopping did not occur during the project period. This remains a need for effective design of embankment overtopping protection.

6.4.2 Applications for further study

Future studies in this field should investigate other stabilization techniques, the effects of overtopping flows on frozen or thawing ground, effects of through-embankment seepage or piping, cases where a hydraulic jump occurs directly at the shoulder, or the effect of varying soil types on performance. Use of multiple techniques such as partial slope paving over geogrid or a TRM could be studied to optimize overall performance.

Improvements in anchoring is another important area for future research, including comparison of anchor types, spacing, location, or density, and in-situ measurement of uplift forces on anchors, which was researched but found to be not feasible for the current project. Specifically, a study examining anchoring near the shoulder would be helpful.

Ultimately, a decision-making tree or flow chart considering relevant variables and protection types could be developed to aid designers in finding reasonable solutions to prevent washout of

embankments subject to overtopping flows. As always, however, local site conditions and the designer's judgment and experience are critical factors in achieving a positive outcome.

REFERENCES

1. Abt, Steven R., Christopher I. Thornton, Bryan A. Scholl, and Theodore R. Bender, (2013), Evaluation of overtopping riprap design relationships. *JAWRA Journal of the American Water Resources Association* Vol. 49, no. 4, 2013, pp. 923-937.
2. Abt, Steven R., Terry L. Johnson, (1991), Riprap Design for Overtopping Flow. *J. of Hydraulic Engineering*, Vol. 117, No. 8, August, 1991, pp 959-972.
3. Anderson, J.T., Y.H. Lim, (2012), *Protecting Road Embankments from Overtopping Flow*. World Environmental and Water Resources Congress 2012: Crossing Boundaries © ASCE 2012.
4. ASTM Standard D422-63, (2002e2), "Standard Test Method for Particle-Size Analysis of Soils," ASTM International, West Conshohocken, PA, 2002, DOI: 10.1520/D0422-63R07E02, www.astm.org.
5. ASTM Standard D6460-12, (2012), "Standard Test Method for Determination of Rolled Erosion Control Product (RECP) Performance in Protecting Earthen Channels from Stormwater-Induced Erosion," ASTM International, West Conshohocken, PA, 2012, DOI: 10.1520/D6460-12, www.astm.org.
6. Chanson, Hubert, (2015) Embankment overtopping protection systems. *Acta Geotechnica* Vol.10, No. 3, 2015, pp. 305-318.
7. Chen, Y.H., and B.A. Anderson, (1987) *Development of a Methodology for Estimating Embankment Damage due to Flood Overtopping*. FHWA Report: FHWA/RD-86/126. Federal Highway Administration, McLean, Virginia
8. Clopper, Paul E. (1989), *Hydraulic stability of articulated concrete block revetment systems during overtopping flow*. McLean, Va: U.S. Dept. of Transportation, Federal Highway Administration.
9. Clopper, P.E., and Y. Chen, (1988), *Minimizing Embankment Damage During Overtopping Flow*. FHWA Report: FHWA-RD-88-181. Federal Highway Administration, McLean, Virginia
10. Fritz, H.M, and W.H. Hager, (1998), Hydraulics of Embankment Weirs. *J. Hydraulic Engineering*, Vol. 124, No.9, September 1998, pp. 963-971
11. Gilbert, P. A., and S.P. MILLER (1991), *A STUDY OF EMBANKMENT PERFORMANCE DURING OVERTOPPING*. Technical Report, Final Report, No. GL-91-23. 1991.
12. Glover, T. J., (2008), *Pocket Ref. Third Edition*, Sequoia Publishing, Littleton, Colorado, October 2008, p.664
13. Hanson, G.J., K.R. Cook, and S.L. Hunt, (2005), Physical modeling of overtopping erosion and breach formation of cohesive embankments. *Transactions of the ASAE*, 48(5), pp.1783-1794.

14. Khan D and Z. Ahmad (2011), Stabilization of angular-shaped riprap under overtopping flows. *World Academy of Science, Engineering and Technology*, Vol. 5, No. 11, November 2011, pp. 550-554.
15. Lagasse, P.F., L.W. Zevenbergen, J.D. Schall, and P.E. Clopper, (2009), *Bridge Scour and Stream Instability Countermeasures - Experience, Selection, and Design Guidelines, Third Edition*. Report FHWA NHI 09-111, Federal Highway Administration, Hydraulic Engineering Circular No. 23, U.S. Department of Transportation, Washington, D.C.
16. Marr, J.D.G., R.R. Weaver, O. Mohseni, C. Taylor, J. Hilsendager, and S. Mielke. *Matrix (Partially Grouted) Riprap Lab Flume Study. (2015)*. Final Report 2015-15. Minnesota Department of Transportation, St. Paul, Minnesota. April 2015.
<http://www.dot.state.mn.us/research/TS/2015/201515.pdf>
17. Morgan, Scott, Carlos Toro-Escobar, Richard L. Voigt Jr., (1996). *Hydraulic Stability of Channel Lock™ Concrete Block Revetment System During Overtopping Flow*. Rep. No. 396. University of Minnesota, St. Anthony Falls Laboratory, 1996.
18. Morgan, Scott C., Julie A. Tank, and Richard L. Voigt Jr., (1998). *Hydraulic stability of Hand Placed Positive Interlocking Concrete Block Revetment System During Overtopping Flow*. Rep. No. 428. University of Minnesota, St. Anthony Falls Laboratory, 1998.
19. Morgan, Scott C., Julie A. Tank, and Richard L. Voigt Jr., (1999). *Hydraulic Stability of Cable Concrete Revetment System During Overtopping Flow*. Rep. No. 434. University of Minnesota, St. Anthony Falls Laboratory, 1999. MATLAB Release 2014a, The MathWorks, Inc., Natick, Massachusetts.
20. McGee, Hugh W., D. Nabors, P. Baughman, Eds. (2009), *Maintenance of Drainage Features for Safety, A Guide for Local Street and Highway Maintenance Personnel*. Report FHWA-SA-09-024. Appendix A. Federal Highway Administration, Washington, DC. July 2009.
http://safety.fhwa.dot.gov/local_rural/training/fhwasa09024/
21. Minnesota Department of Transportation (2008), *MnDOT Materials Laboratory Manual No. 5-695*, MnDOT, St. Paul, Minnesota. Section 1303, *Liquid Limit Determination* (AASHTO T89), and Section 1304, *Plastic Limit Determination* (AASHTO T90)
22. Minnesota Department of Transportation (2015), *MnDOT Pavement Design Manual*, MnDOT, St. Paul, Minnesota, Chapter 3, July 2015.
http://www.dot.state.mn.us/materials/pvmtdesign/docs/2007manual/Chapter_3-2.pdf
23. Minnesota Department of Transportation (2014), *Seeding Manual 2014 Edition*, MnDOT Office of Environmental Stewardship Erosion Control Engineering Unit, St. Paul, Minnesota
24. Minnesota Department of Transportation (2013), *Standard Specifications for Construction 2014 Edition*, MnDOT, St. Paul, Minnesota.

25. Minnesota Department of Transportation (2015). *Average Bid Prices for Awarded Projects, English Units, Spec Year 14*. April, 2015.
<http://www.dot.state.mn.us/bidlet/avgPrice/142014.pdf>Schall, J.D., P.L. Thompson, S.M. Zerges, R.T. Kilgore, and Morris, J.L. (2012) *HDS-5: Hydraulic Design of Highway Culverts: Third Edition*. U.S. Department of Transportation, Federal Highway Administration Publication Number: HIF-12-026, Washington D.C.
26. Taki, K., and G. Parker, (2005), Transportational cyclic steps created by flow over an erodible bed, Part 1, Experiments, *J. Hydraulic Research*, Vol.43, No.5 (2005),pp.488-501, DOI: 10.1080/00221680509500147
27. Thornton, Christopher I., Steven R. Abt, Bryan N. Scholl, and Theodore R. Bender, (2013), Enhanced Stone Sizing for Overtopping Flow. *Journal of Hydraulic Engineering*, Vol. 140, No. 4, 2013, pp. 06014005.1-06014005.4.
28. US Army Corps of Engineers Waterway Experiment Station (1964), *Stability of Riprap and Discharge Characteristics, Overflow Embankments, Arkansas River, Arkansas, Hydraulic Model Investigation*, Technical Report No. 2-650, June 1964.
29. Voigt, Richard L., Jr., Carlos Toro-Escobar, and Scott Morgan (1998). *Hydraulic Stability of Conlock and Conlock II Concrete Block Revetment System During Overtopping Flow*. Rep. No. 369. University of Minnesota, St. Anthony Falls Laboratory, 1998.

APPENDIX A: FIELD SITE MONITORING AND INSPECTION REPORTS



Wenck Associates, Inc.
1800 Pioneer Creek Center
P.O. Box 249
Maple Plain, MN 55359-0249

800-472-2232
(763) 479-4200
Fax (763) 479-4242
wenckmp@wenck.com
www.wenck.com

November 19, 2013

Shirlee Sherkow
Minnesota Department of Transportation
MS 330
395 John Ireland Blvd
St Paul, MN 55155-1899
Sent via: email

RE: Task 6 Report for Road Overtopping Research

Dear Ms. Sherkow:

The purpose of this letter is to document the results of Task 6, Site Monitoring and Inspection, of the Embankment Overtopping research project. This information is based on the presentation made to Mn/DOT during a meeting on August 8, 2013.

Regional Mn/DOT staff members were asked to locate and rank in order of importance significant overtopping locations in their areas, Norman County and Marshall County. Three pressure transducers with data loggers (Onset HOBO data loggers) were available for installation. Of these locations provided by regional Mn/DOT staff, the top two in Norman County, and the top one in Marshall County were chosen.

The first Norman County location was located on County-State Aid Highway 10 as seen in Figure 1. There is a portion of roadway approximately ½ a mile long in which road overtopping is common during flooding from the Wild Rice River. The second Norman County location was located on County-State Aid Highway 3, west of the town of Shelly as shown in Figure 2. The monitoring location is between the Red River and the Marsh River. The Marshall County site is located on County-State Aid Highway 317 as shown in Figure 3. The section of road is between the Snake River and the Red River.

The equipment was installed on posts driven into the upstream right-of-way near ditch bottom by early April 2013. A barometric logger was placed at the Norman County shop. Barometric pressure is needed to convert the measured pressure to water depth.

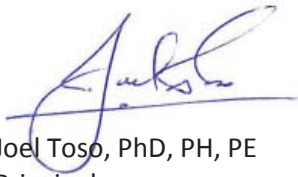
Of the three monitoring locations, only the Marshall County location was overtopped during the monitoring period from April to August 2013. The record is provided in Figure 4. Figure 5 illustrates how the record compares to USGS data collected at Red River gages upstream and downstream of the site.

Shirlee Sherkow
November 19, 2013
Page 2 of 9 including figures

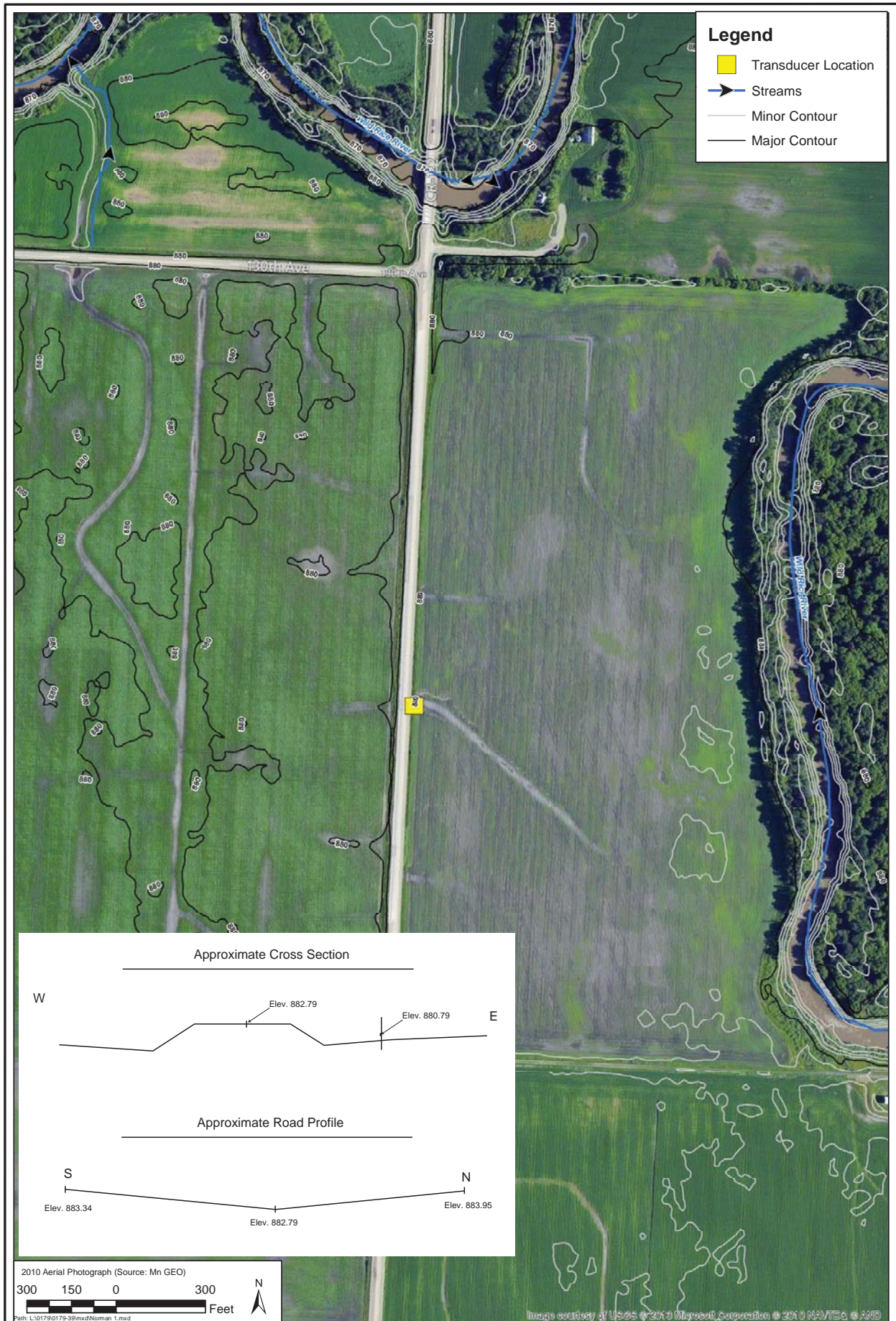
The site was inspected for damage once the flood water receded. Figures 6 and 7 show the site condition on May 23, 2013. There was no significant erosion noted.

Please let me know if you have questions or need more information. I can be reached at 763-479-4231 or jtoso@wenck.com.

Sincerely,
WENCK ASSOCIATES, INC.

A handwritten signature in blue ink, appearing to read "Joel Toso", written over a horizontal line.

Joel Toso, PhD, PH, PE
Principal



UNIVERSITY OF MINNESOTA
Norman County Site 1

Wenck
Engineers - Scientists
Business Professionals
www.wenck.com
1800 Pioneer Creek Center
Maple Plain, MN 55359-0429
1-800-472-2232

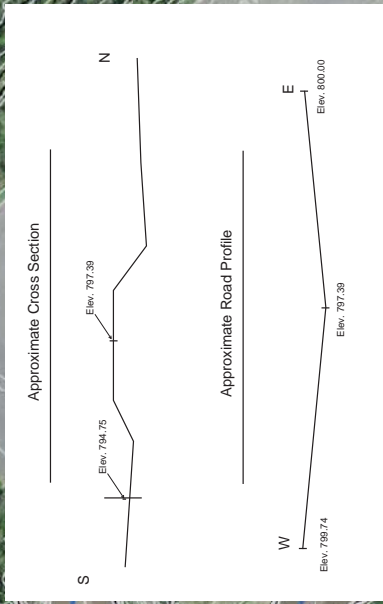
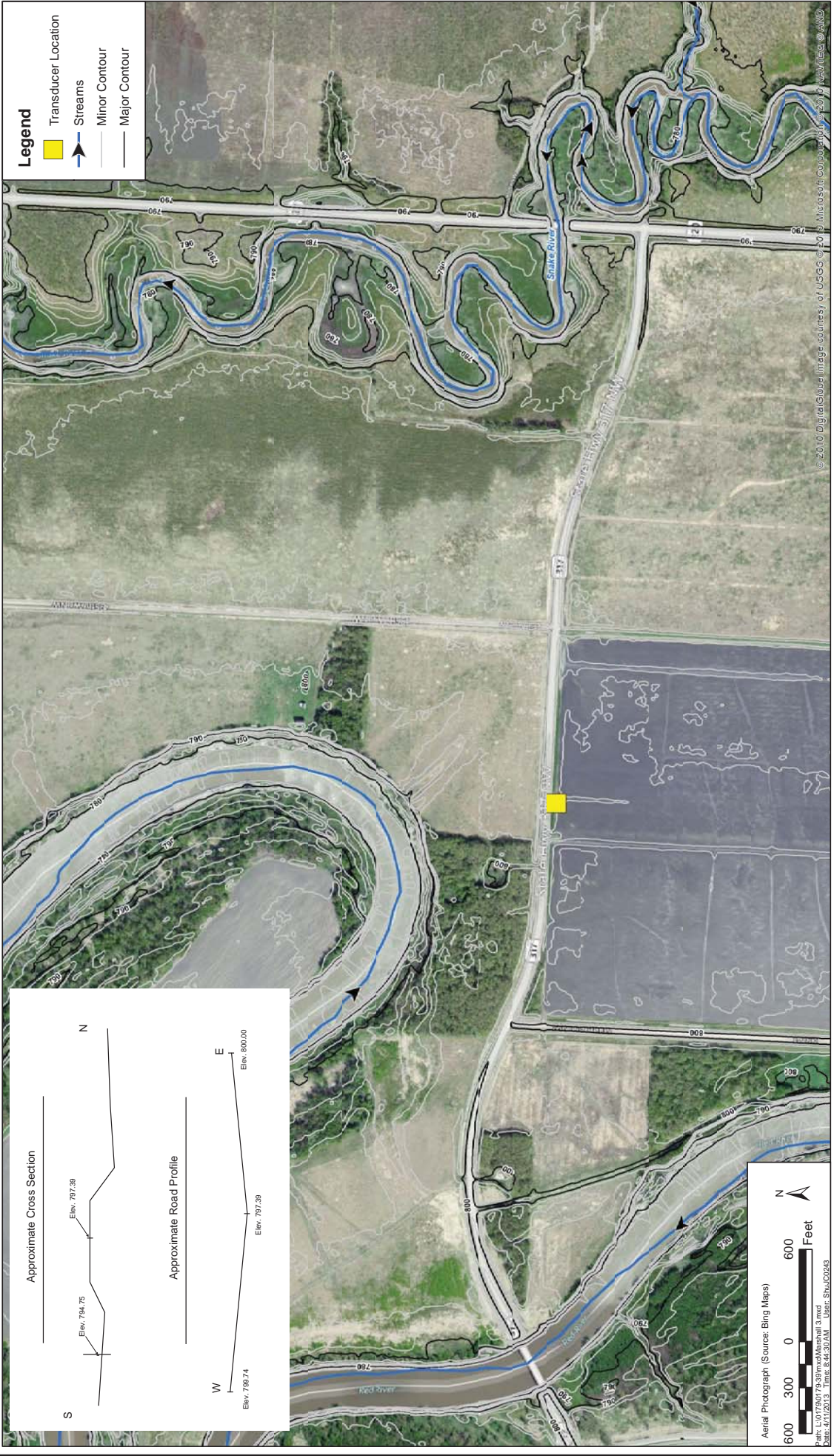
APR 2013
Figure 1



Wenck
 Engineers - Scientists
 Business Professionals
 www.wenck.com

1800 Pioneer Creek Center
 Maple Plain, MN 55359-0429
 1-800-472-2232

UNIVERSITY OF MINNESOTA
 Norman County Site 2



APR 2013
Figure 3

Wenck
 Engineers - Scientists
 Business Professionals
 www.wenck.com
 1-800-472-2232
 1800 Pioneer Creek Center
 Maple Plain, MN 55359-0429

UNIVERSITY OF MINNESOTA
 Marshall County Site 3

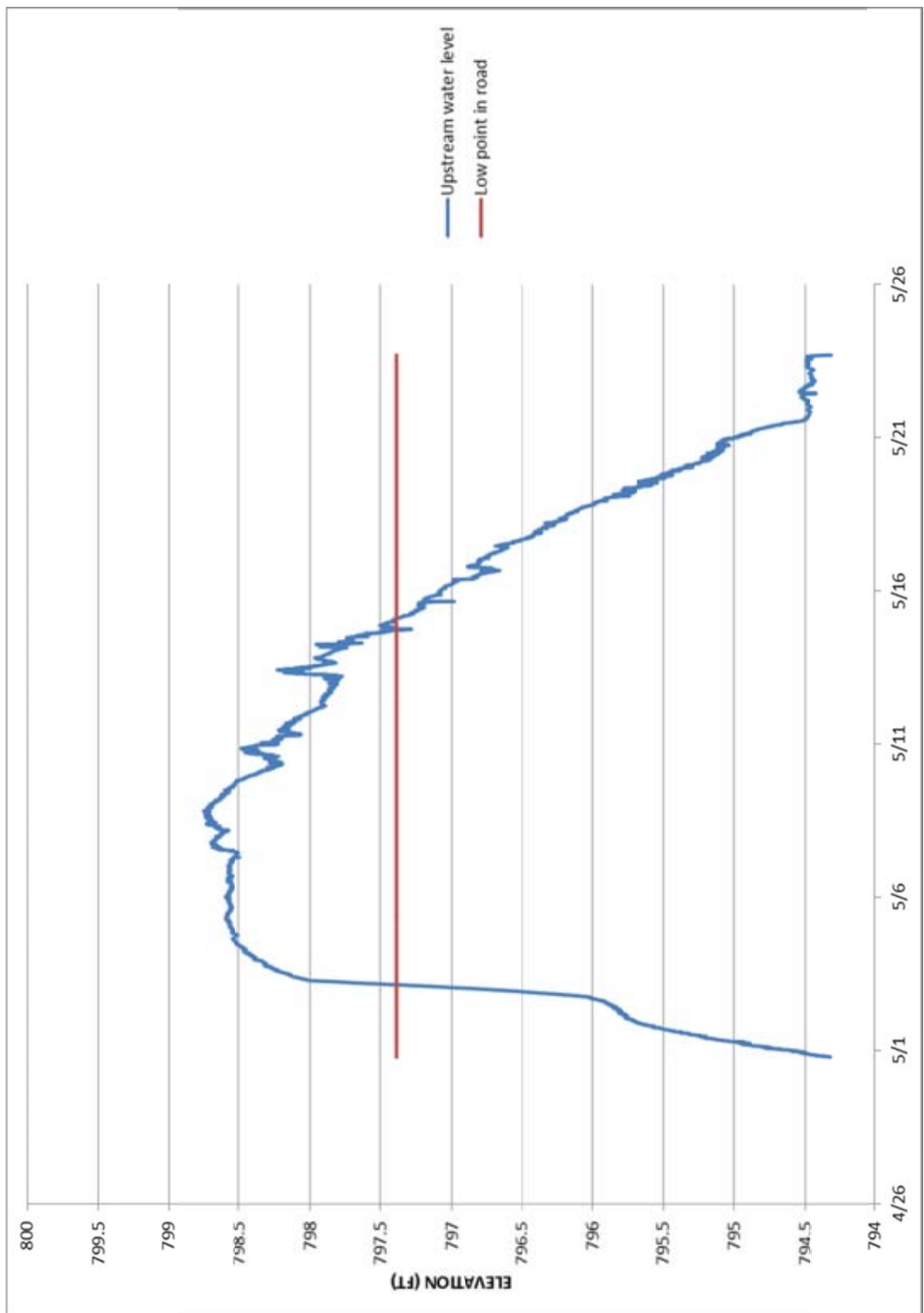


Figure 4. Flood Level Measurements at the Marshall County Site

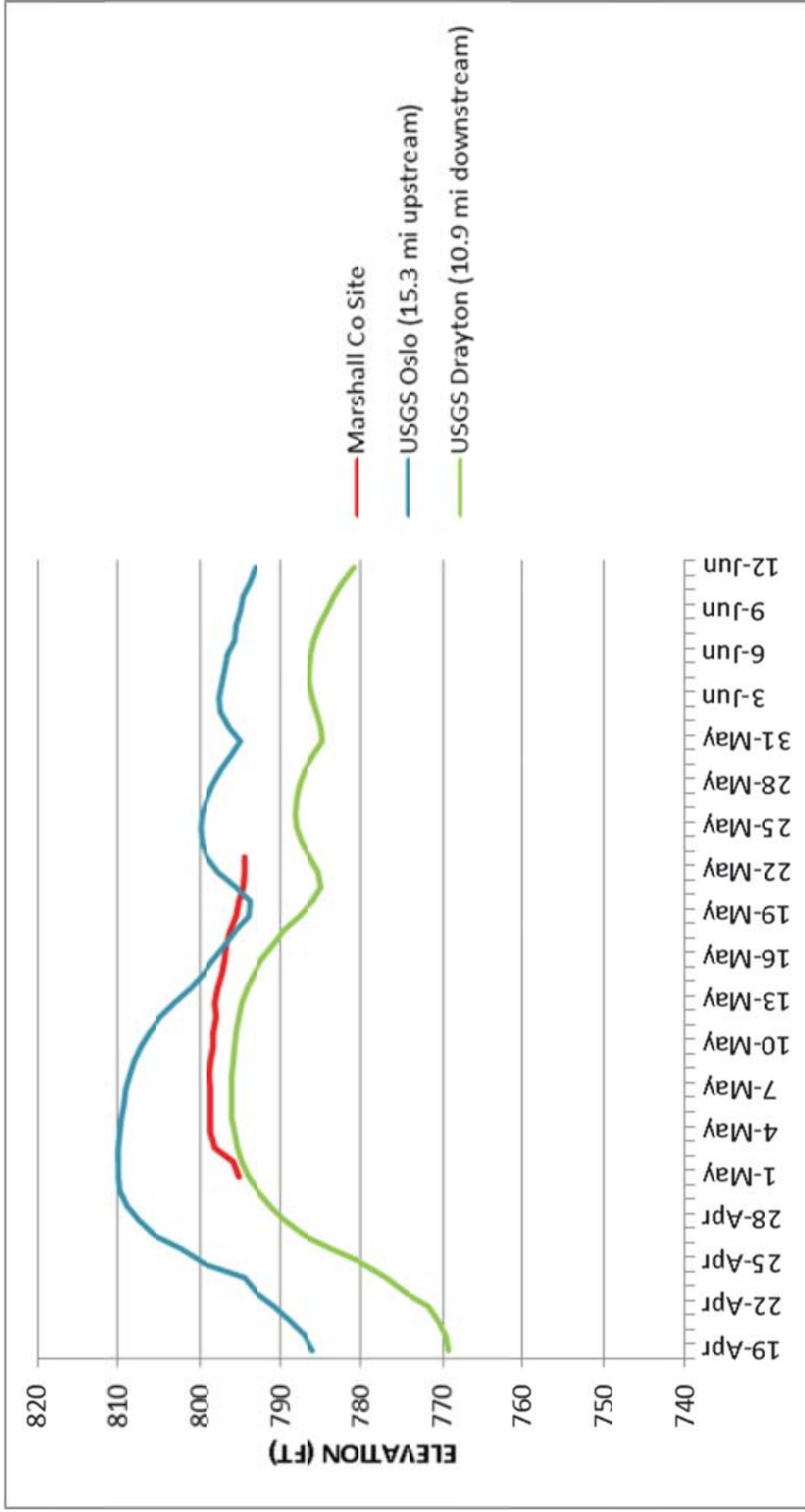


Figure 5. Measurements Compared to USGS Red River Data



UPSTREAM LOOKING EAST

UPSTREAM LOOKING WEST

Figure 6. Inspection – May 23, 2013 at the Marshall County Site



DOWNSTREAM LOOKING EAST

DOWNSTREAM LOOKING WEST

Figure 7. Inspection – May 23, 2013 at the Marshall County Site

To: Sara Mielke, Project Manager, University of Minnesota
From: Joel Toso, Wenck Associates, Inc.
Steve Hegland, Wenck Associates, Inc.
Date: February 16, 2015
Subject: 2014 Road Overtopping Report

This memo is a summary of the results of Task 6, Site Monitoring and Inspection, of the Embankment Overtopping research project completed in 2014. This report is similar to that provided for the 2013 work. Site monitoring was performed from April 8, 2014 until May 1, 2014. The installation report dated April 10, 2014 provides the installation procedures and equipment used during the study.

Installation

On April 8, 2014 fourteen data loggers were installed at six road monitoring locations and two barometric pressure locations. An upstream and downstream pressure logger were installed at each of the road monitoring. Regional Mn/DOT staff members in Norman County and Kittson County were asked to locate and rank in order of importance significant overtopping locations in their areas. Of these locations provided, the top two locations in Norman County, and the top four locations in Kittson County were chosen. The monitoring locations are shown in the attached Figures 1 and 2. Data loggers were also set up at the two county maintenance buildings to record the barometric pressure. Barometric pressure is used to convert absolute pressure to water depths.

Data Download/Information Processing

On May 1, 2015 the data loggers were removed from the monitoring locations. The information was then downloaded from the data loggers and was analyzed.

During retrieval of the devices, the condition of the road embankments were also documented.

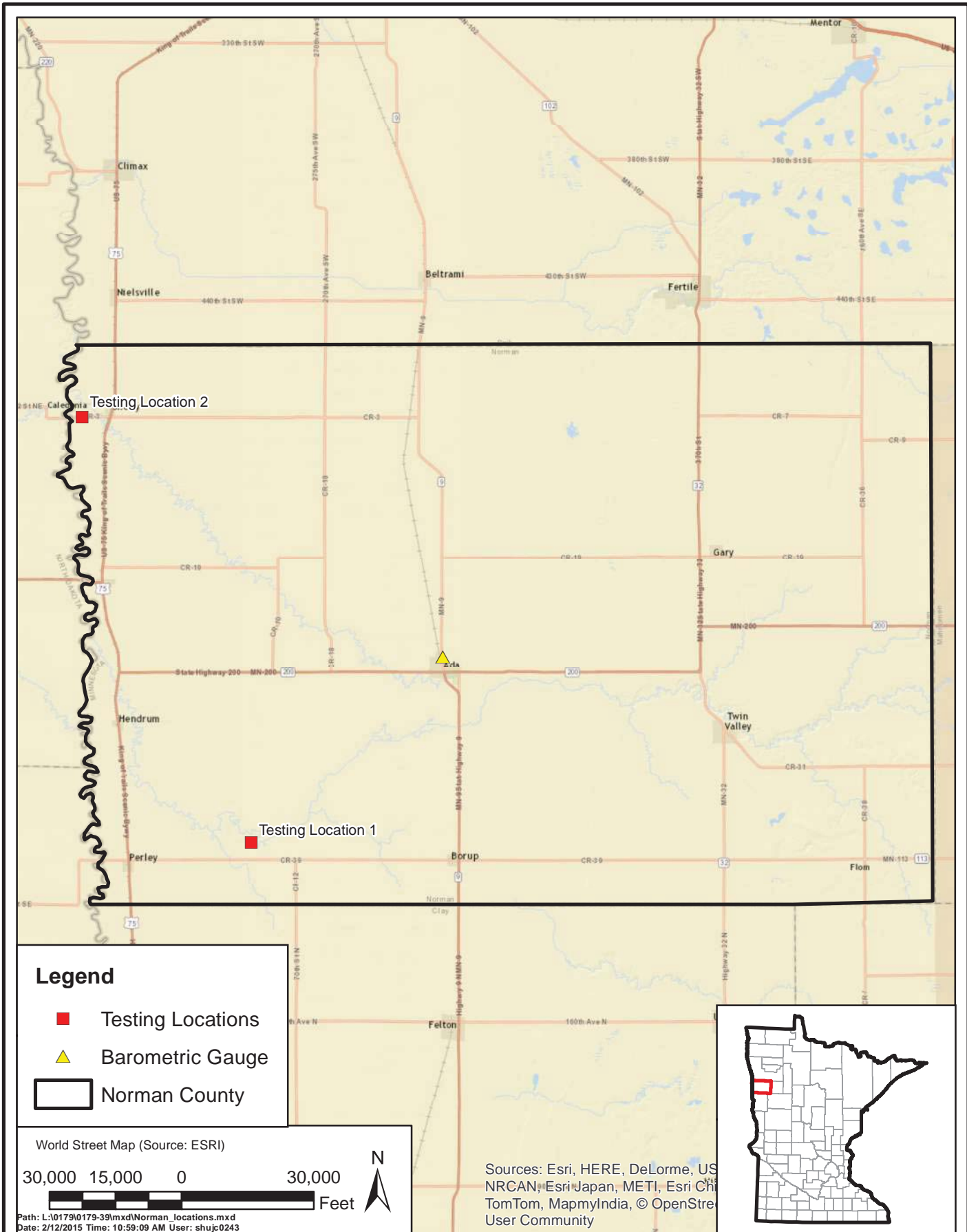
Results

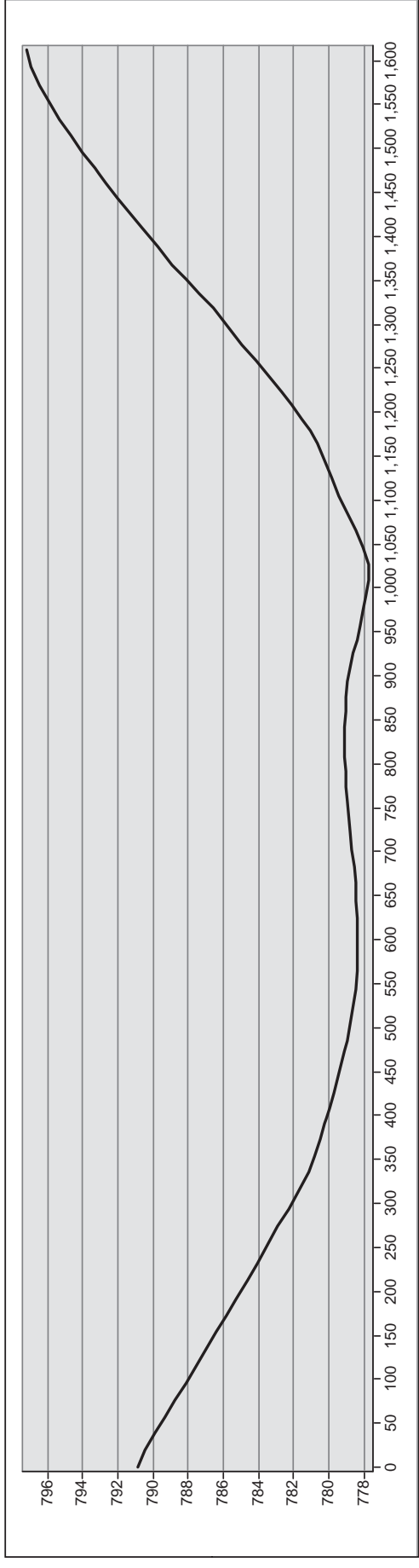
Of the six monitoring locations only two of the locations had road overtopping, Location 4 and 5 in Kittson County (see Figure 2). Location 4 is on County Road 57 of the Middle Branch Two Rivers. Location 5 is on County Road 58 over the North Branch Two Rivers. Road plan and profiles of these locations are provided in Figures 3 and 4. The road profiles allow long sections of roadway to be flooded when overtopping occurs.

The recorded water surface elevations upstream and downstream at Location 4 are shown in Figure 5. Red River levels upstream at Drayton and downstream at Pemina are also provided. Prior to mid-day on April 11th, the dataloggers at Location 4 were dry. After April 11th, the shape of the hydrograph at Location 4 nearly matches that of the Red River. The roadway is overtopped by more than 10 feet of water. Given the depth of flow and timing it is clear that the Red River backs up into the Middle Branch Two Rivers and floods the road way. Road overtopping is not due to the flows in the Middle Branch Two Rivers. The dataloggers show only one or two tenths of a foot difference upstream to downstream indicating low energy, relatively quiescent flow.

Location 5 is very similar to Location 4 (see Figure 6). It is a couple miles northeast on the North Branch Two Rivers. On 4/14 at 12:05 AM it appears that the transducer and stake was knocked over by debris or the flowing water. On 4/17 the transducer was located underwater, righted, and correct water recordings were resumed. Given the depth of flow and timing it is clear that the Red River also backs up into the North Branch Two Rivers and floods the road way. Road overtopping is not due to the flows in the North Branch Two Rivers. Once the transducer and stake were righted there is very little difference between upstream and downstream water surface levels. This low energy flow does not result in erosion of the road surface.

Photographic documentation of the shoulder conditions is provided in Appendix A-1.





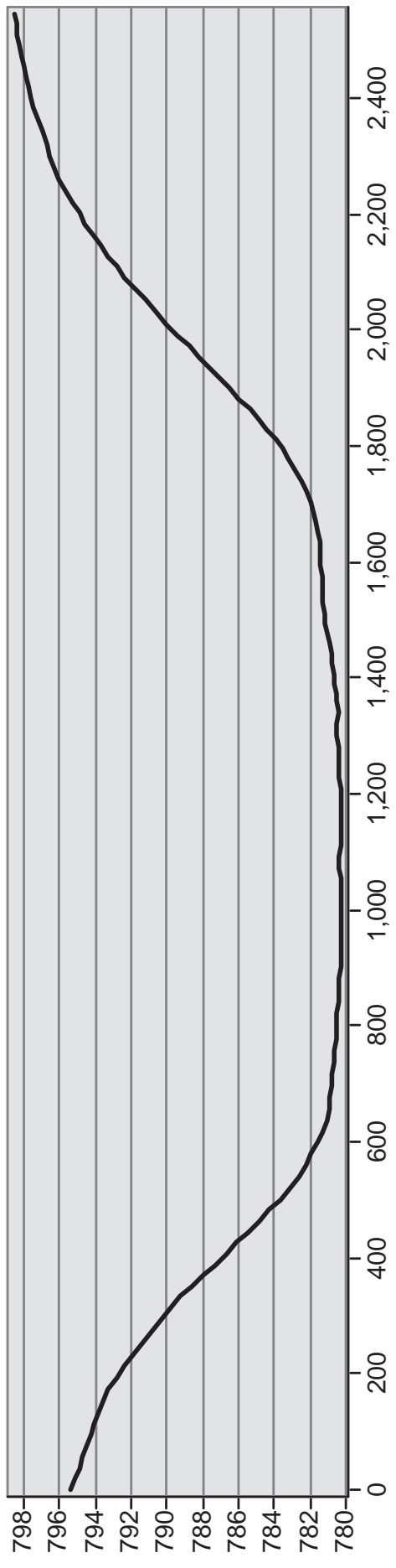
UNIVERSITY OF MINNESOTA

Kittson County Location 4 Plan and Profile

FEB 2015

Figure 3





UNIVERSITY OF MINNESOTA

Kittson County Location 5 Plan and Profile

A-15



FEB 2015

Figure 4

Figure 5
Location 4 Monitoring Results

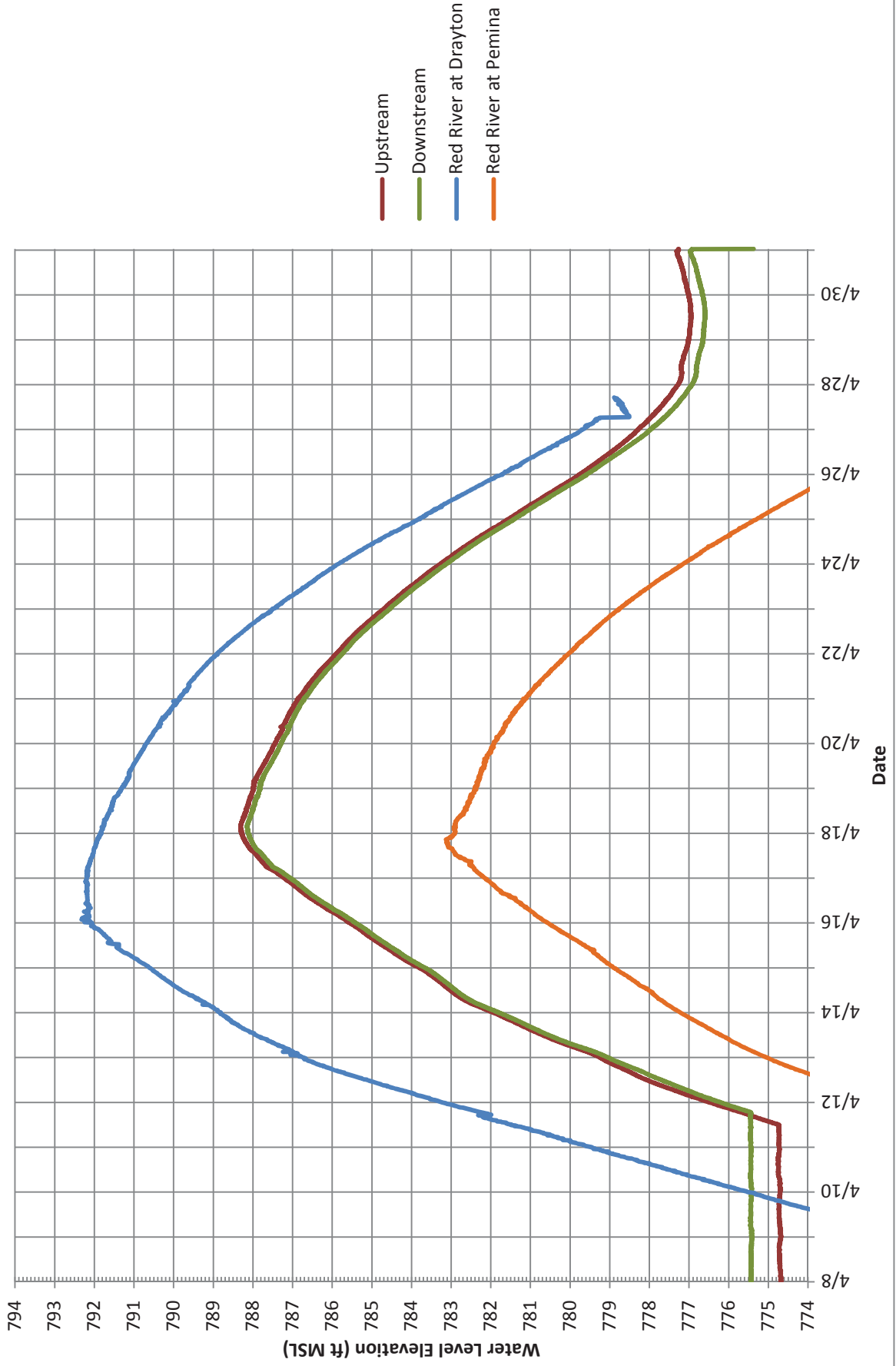
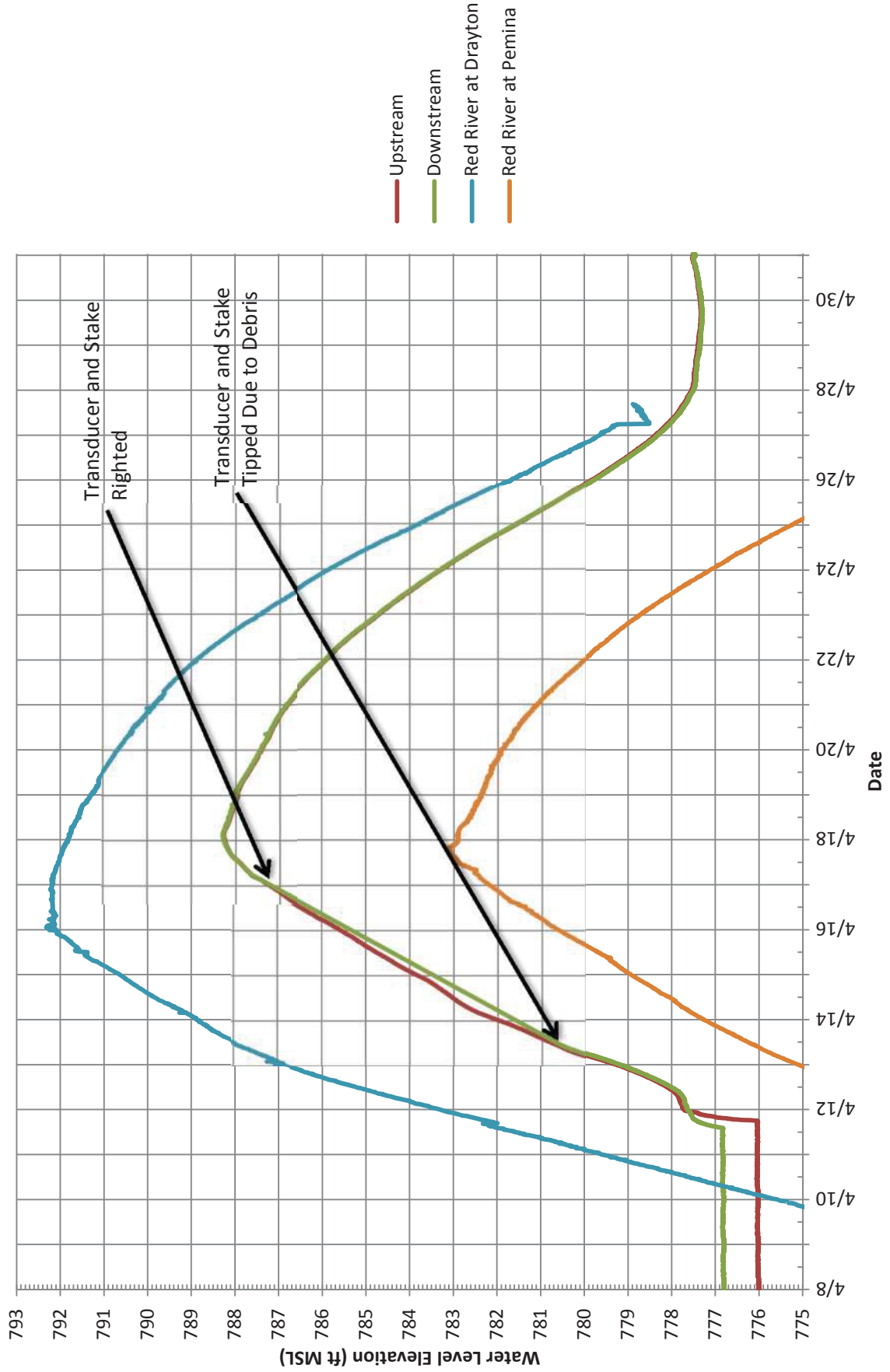


Figure 6
Location 5 Monitoring Results



Appendix A-1



Location 4 Looking west at the upstream shoulder, post-flooding condition

Appendix A-1



Location 4 looking east at minor erosion and deposition on the downstream shoulder, post-flooding condition

Appendix A-1



Location 5 Looking east at the upstream shoulder, post-flooding condition

Appendix A-1



Location 5 looking west at the downstream shoulder, post-flooding condition



Wenck Associates, Inc.
1800 Pioneer Creek Center
P.O. Box 249
Maple Plain, MN 55359-0249

800-472-2232
(763) 479-4200
Fax (763) 479-4242
wenckmp@wenck.com
www.wenck.com

TECHNICAL MEMORANDUM

TO: JT Anderson, MNDOT

COPY: Craig Taylor, Project Manager, University of Minnesota

FROM: Joel Toso, Wenck Associates, Inc.
Steve Hegland, Wenck Associates, Inc.

DATE: April 10, 2014

SUBJECT: Road Overtopping Study, Pressure Transducer Installation

This memo is a summary of the pressure transducer installation completed on Tuesday, April 8, 2014. A brief equipment overview is provided below along with installation methods and individual discussions on each of the installation sites.

Equipment

Twelve (12) Onset HOBO data loggers were used at six locations to collect both upstream and downstream water level elevations. Two (2) data loggers were set up in high ground locations and will log barometric information. Four (4) of the units were reused from last year's study and ten (10) new data loggers were ordered for the 2014 work amendment.

The data loggers used for this study record the absolute pressure over the device. After the data is downloaded, a software program is used to convert the pressure data into hydrostatic water levels by using the barometric data recorded by the barometric gauges.

Installation

The equipment setup was completed on Tuesday April 8th. Data loggers were placed at all six possible flooding locations as well as the barometric gauge at the Norman County and Kittson County Maintenance shops. The loggers are set up to take a reading every 5 minutes. All 14 loggers were launched to start reading at the next corresponding time interval so that all loggers are taking readings on the same schedule. The devices have enough internal storage to read for approximately 72 days.

Steel posts were driven into the ground to provide a structure to attach the devices to if an existing structure was not already present. The posts were approximately 6 feet in length and were driven approximately 2 feet into the ground.

After the posts were driven into the ground, the pressure transducer device was attached to the posts using zip ties. Wenck, consulted with the equipment supplier before installation to ensure this method of attachment would not compromise the data. After the device was attached to the post, the top of the device was surveyed and then the post and device were covered with a perforated PVC pipe. The

Technical Memo

Road Overtopping Study, Pressure Transducer Installation

April 10, 2014

perforated PVC was used to protect the devices from any possible floating debris, but still allow water levels to fluctuate to receive accurate pressure readings. The PVC pipe was not installed over the barometric transducer because it should not need protection from flooding debris. Pictures from the installation are included in Appendix A-2. Because of the recent heavy snowfall in Kittson County, portions of the shoulders were only partly visible. The existing shoulder conditions were still documented with photographs to the extent possible.

Locations

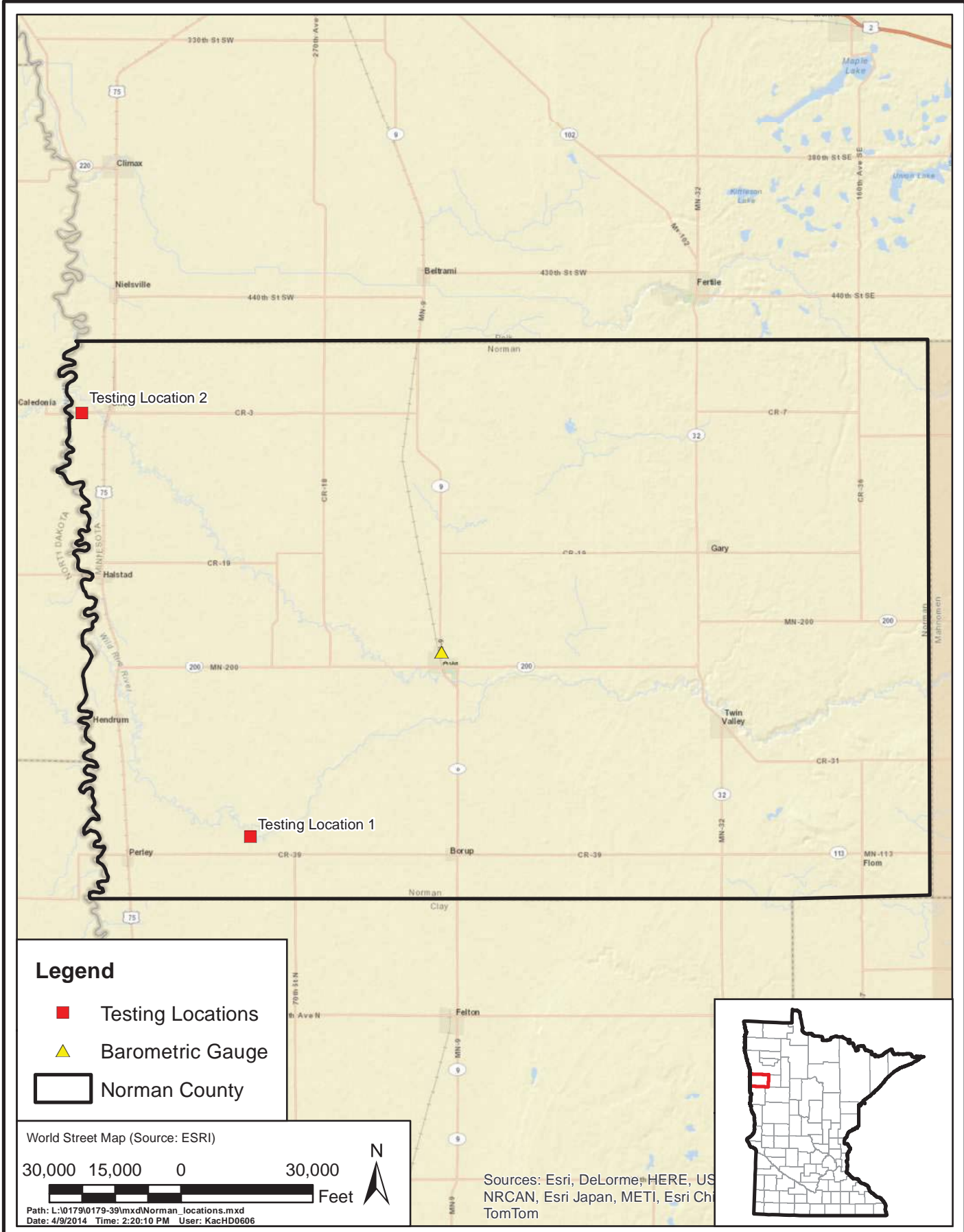
The six locations for the testing were selected based on information provided from the counties in which the devices were installed. Because of the higher probability of flooding in Kittson County vs. Norman County, four locations were selected in Kittson County and only two locations were selected in Norman County. Bob Ramstad at Norman County provided a map detailing locations in which road overtopping is common during the spring flooding as well as ranking the roads. Figure 1 shows the location of the testing Sites 1 and 2. Kelly Bengston from Kittson County provided a map indicated locations within the county in which road overtopping is common during spring flooding and during a phone conversation provided a ranking of the roads to determine testing Sites 3 through 6. Figure 2 shows the location of the Sites 3 through 6.

Setup Mobility

Wenck utilized a member of the Fargo, ND office during the field setup of the equipment. The technician is familiar with the download of the data loggers as well as the deployment of the devices so that if it is determined that a location of one of the field setups should be moved, this can be more easily accomplished from a technician based in the Red River Valley.

Data Download

Once the spring flooding has ceased and the water levels in the testing areas drop to below flooding conditions, the equipment will be collected. The devices will be removed from the posts and the posts and PVC pipes will be removed from the field. The devices will be downloaded immediately and the raw data stored before the software conversion. The person responsible for material removal will record site conditions of both the upstream and downstream condition of the overtopped roadway and will have gps equipment with them to document any information which may be determined useful in the field. The field person will take ample photographs of both the upstream and downstream conditions to accurately characterize the flood impacts.



Legend

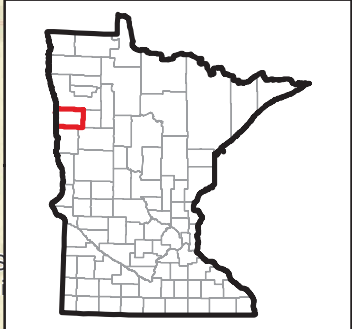
- Testing Locations
- ▲ Barometric Gauge
- Norman County

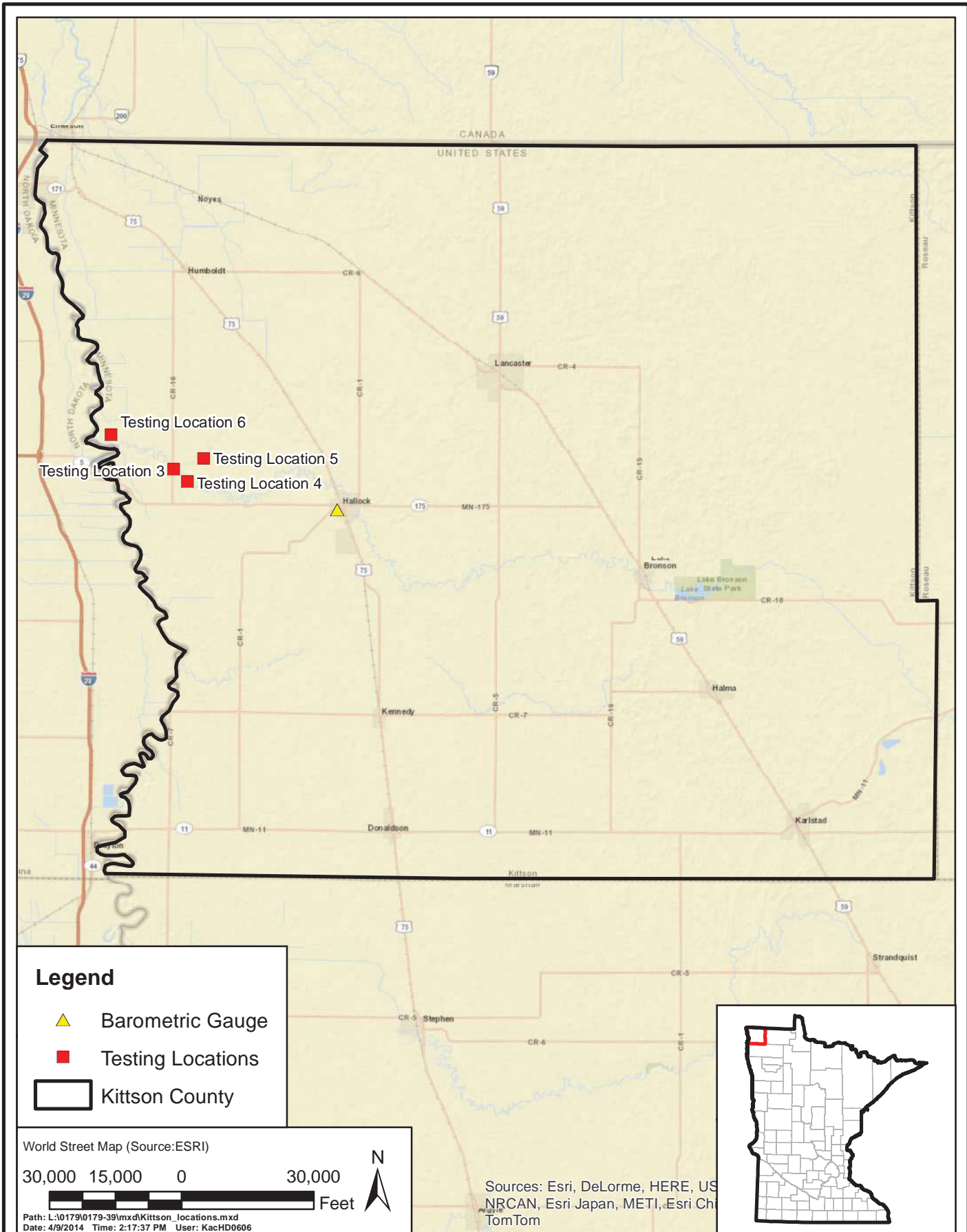
World Street Map (Source: ESRI)

30,000 15,000 0 30,000 Feet




Path: L:\0179\0179-39\mxd\Norman_locations.mxd
 Date: 4/9/2014 Time: 2:20:10 PM User: KacHD0606

Sources: Esri, DeLorme, HERE, US NRCAN, Esri Japan, METI, Esri China, TomTom





Legend

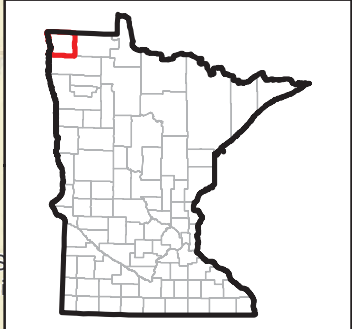
-  Barometric Gauge
-  Testing Locations
-  Kittson County

World Street Map (Source:ESRI)



Path: L:\0179\0179-39\mxd\Kittson_locations.mxd
Date: 4/9/2014 Time: 2:17:37 PM User: KacHD0606

Sources: Esri, DeLorme, HERE, US NRCAN, Esri Japan, METI, Esri China, TomTom



Appendix A-2



Transducer Placed on Stake



Finished Testing Location

Appendix A-2



Existing Shoulder Conditions in Kittson County

2016-03-08 jwt

Notes for Use of Hobo Pressure Transducer Data Loggers for Road Overtopping Research

The purpose of these notes is to pass along information to the next user of the data loggers and make it easier for that person to use them.

There are 14 data loggers from the MnDOT Road Overtopping Research project. These data loggers are accompanied by an optical reader with a USB cable for connection to a computer. There is a CD with software that provides an interface to setup the data loggers, read them, compensate for barometric pressure, and store data. The data loggers record both absolute pressure and temperature. The latter is not really needed for this project, but helps identify day and night periods. The absolute pressure is converted to gage pressure by compensating for atmospheric pressure recorded by one of the data loggers installed in high ground relatively close to the selected project site. Barometric pressure should remain fairly constant over large areas.

The equipment installation is covered in the April 10, 2014 Technical Memo for the project (copy attached). The information below covers the setup, downloading, and processing of the data.

The data loggers are permanently sealed instruments. One is shown to the right of the optical reader in the photo to the right. To setup and/or download the logger, remove the black plastic cap that covers the optical port and insert the logger into the optical reader as shown.

Load the Hobo software on your computer and insert the USB cable of the optical reader into an available port on your computer.

Once the software is installed and running the status of the logger can be seen by clicking on the third icon from the upper left of the menu. An example of the resulting screen for one of the data loggers is shown in Figure 1. The battery state can be checked. The status of the data collection is also noted (collecting data, or stopped). Figure 1 shows that the device with Serial # 10462744 is named P5, it is stopped (not currently collecting data), the battery is good, and other information.



Hobo Data Logger and Optical Reader

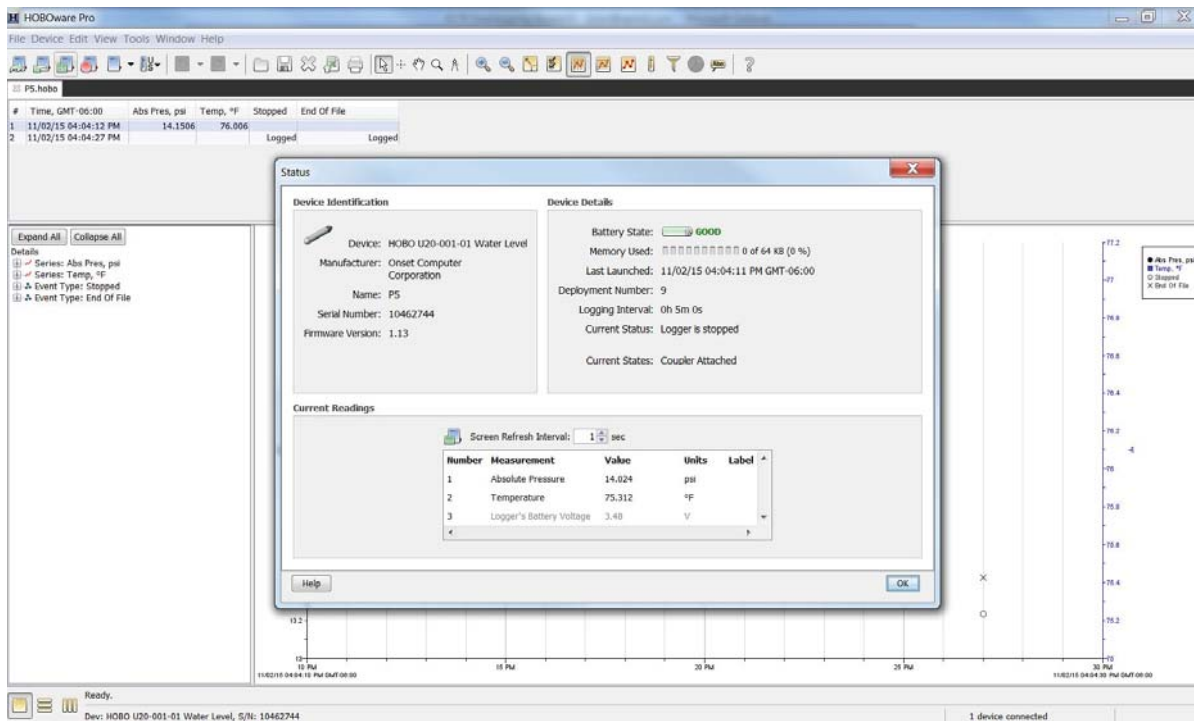


Figure 1 Device Status

To configure and launch the data logger, click on the first icon near the upper left of the menu.

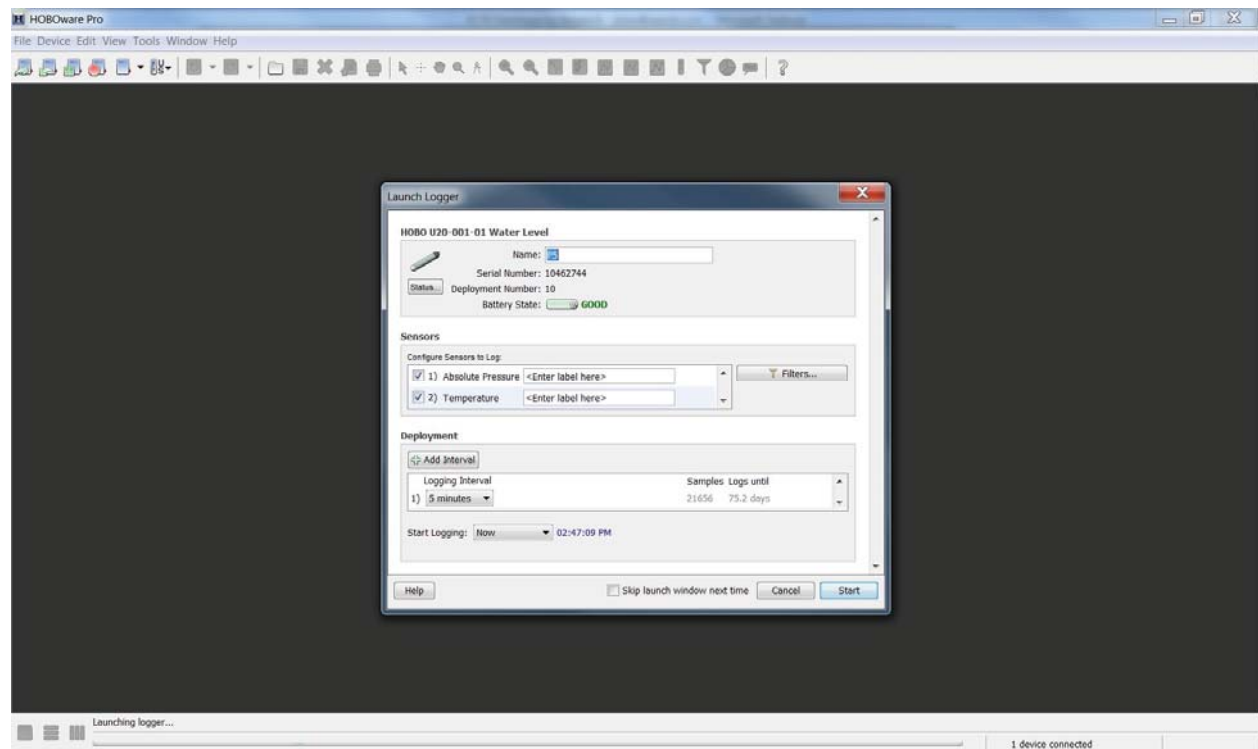


Figure 2 Device Launch

Choose the device name, how often to sample, and when to start sample. There is a start sampling now option, or start sampling at a particular date. It may be best to configure the devices prior to heading into the field to install them. Once configured disconnect the device from the reader and proceed to the next.

To download the data, reconnect the device to the reader and execute the Hobo software. Click on the fourth icon in the upper left of the menu to stop the data collection. Then click on the second icon in the upper left of the menu to download the data. Save the data file in a folder on the computer. The software allows you to plot the data (see example plot in Figure 3).

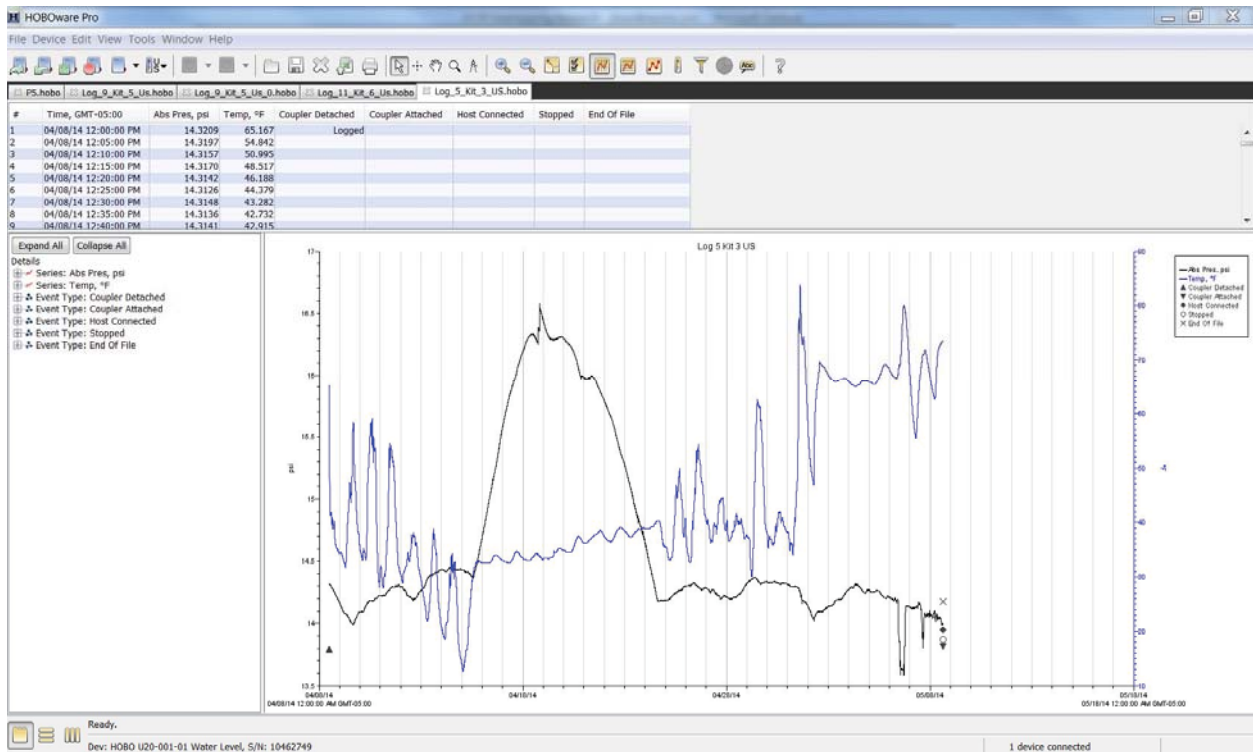


Figure 3 Example data.

To compensate the data for barometric pressure, the data from the barologger (the logger set to measure barometric pressure) should be downloaded and saved in the folder with the other data. Any of the 14 data loggers can be used for the barologger. Once the data from the barologger is saved to the project folder, the absolute pressure from any other data logger may be compensated to gage pressure. The screen below appears after the data is downloaded from the data logger. To compensate it, click on the process button shown in Figure 4 below. Figure 5 shows the resulting screen and Figure 6 provides an example of compensated data.

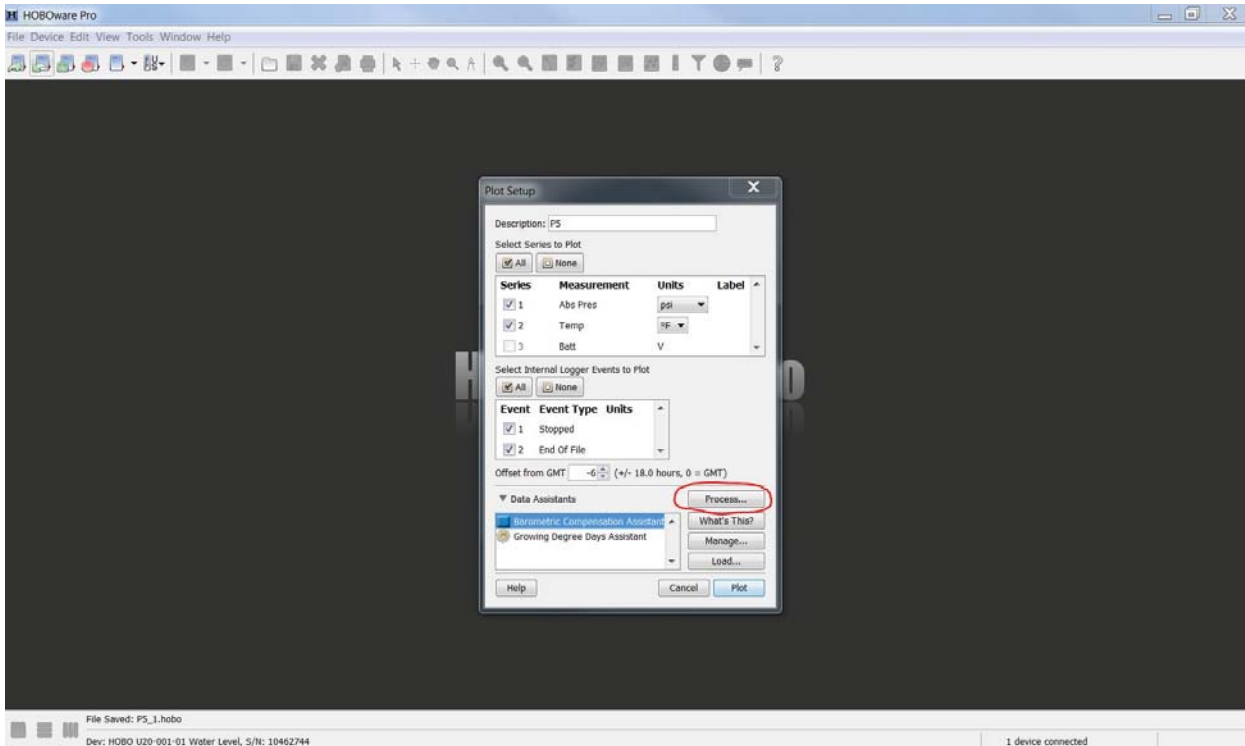


Figure 4 Process to Compensate for Barometric Pressure

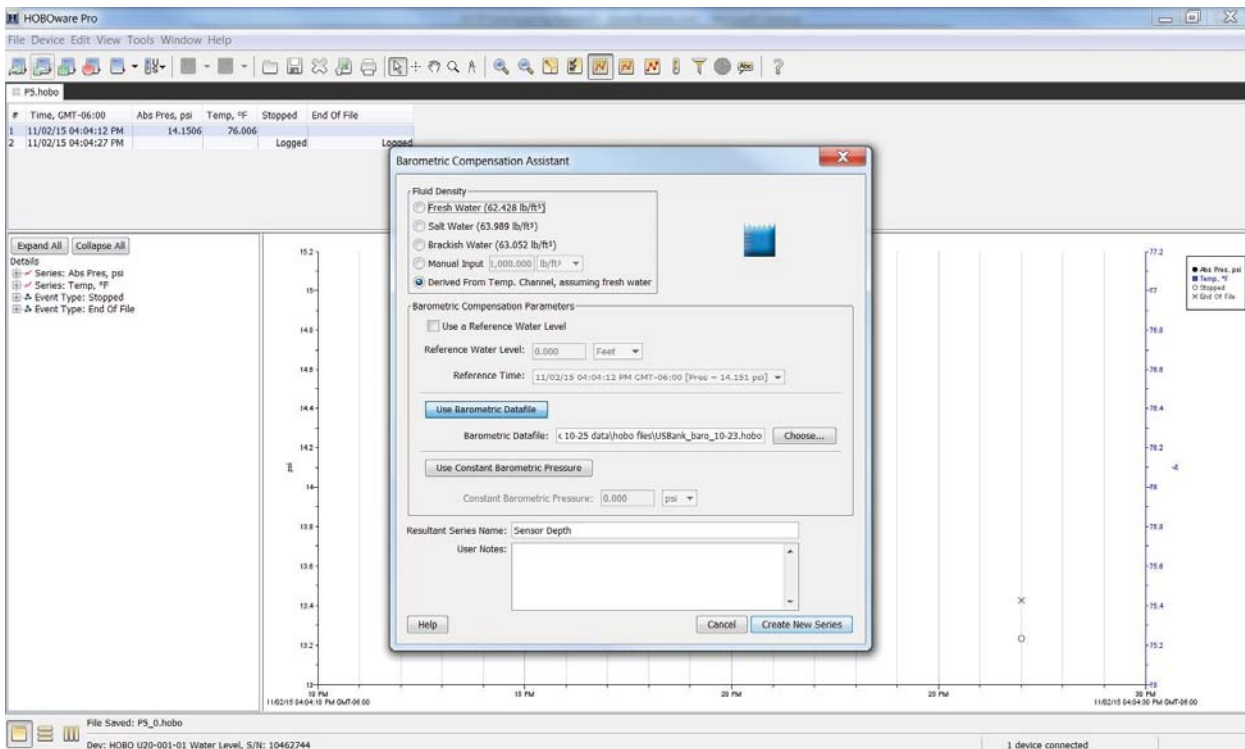


Figure 5 Compensate for Barometric Pressure

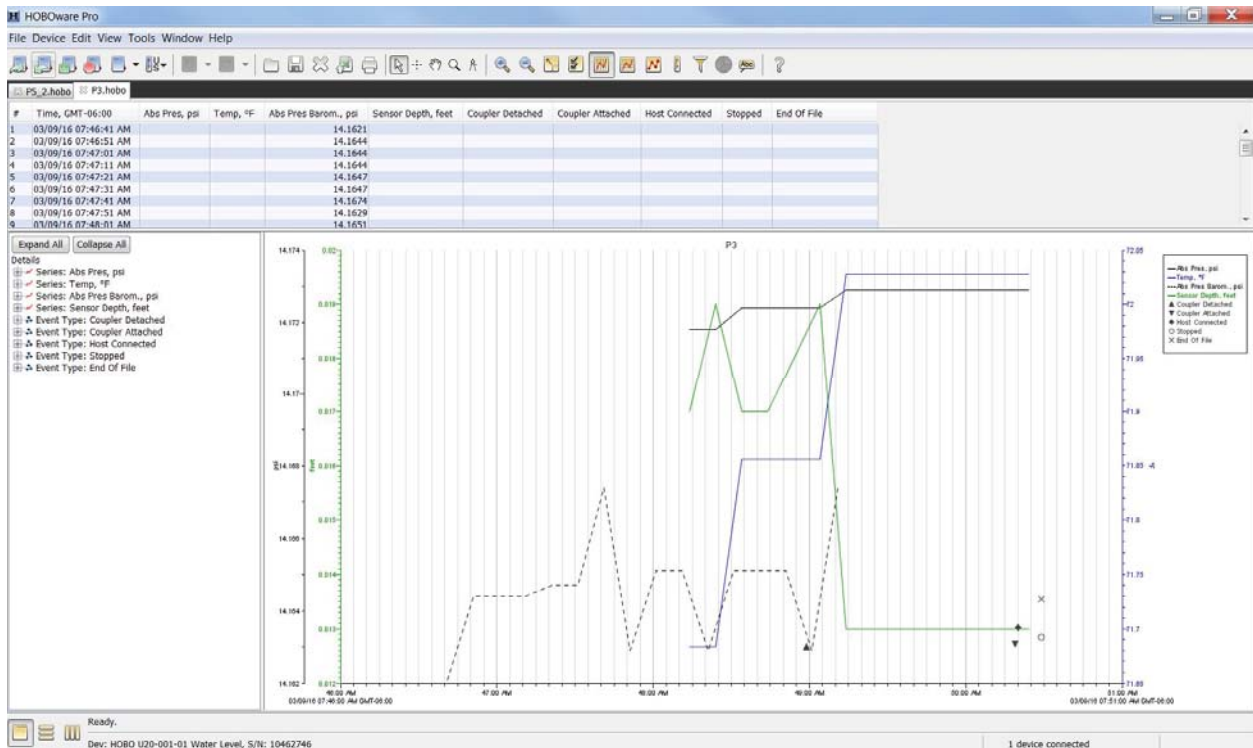


Figure 6 Compensated Data

To export the compensated data to a csv file, click on the export button shown in Figure 7 and the screen shown in Figure 8 appears. Click on Export and save the file to the project directory. The data is now ready to be used in an Excel file for further process and plotting as needed.

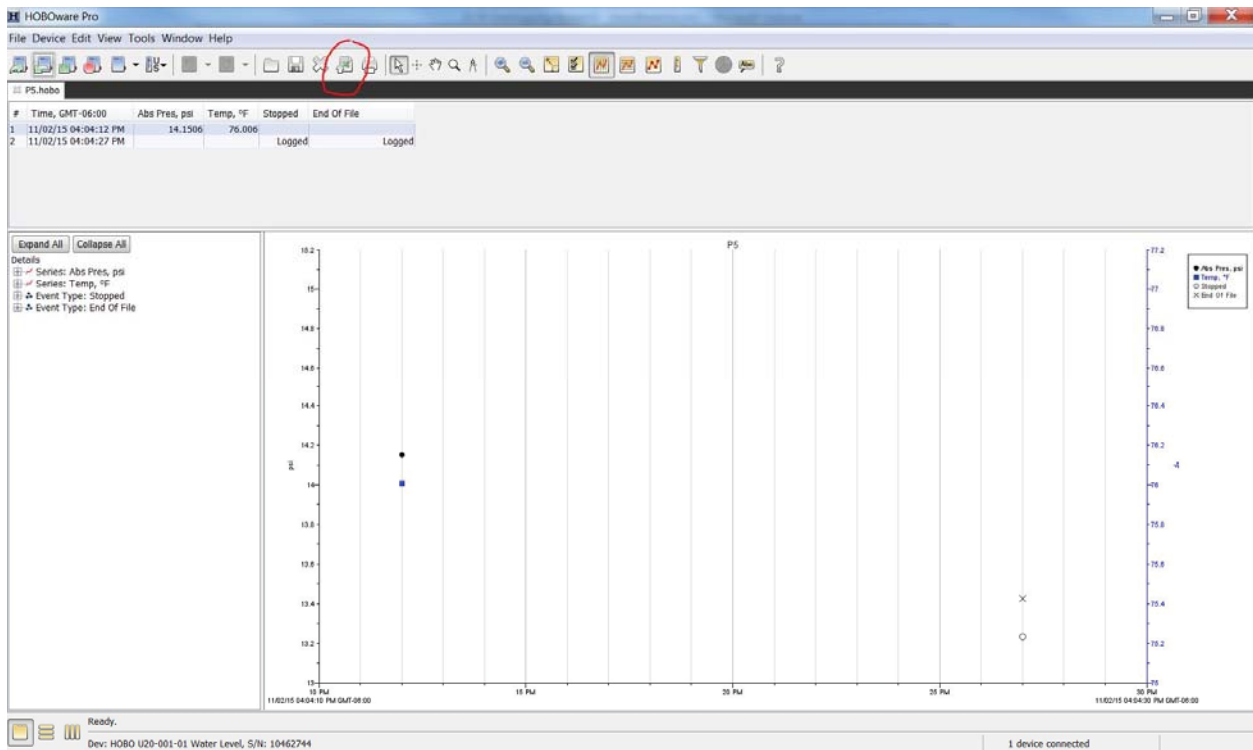


Figure 7 Export Button

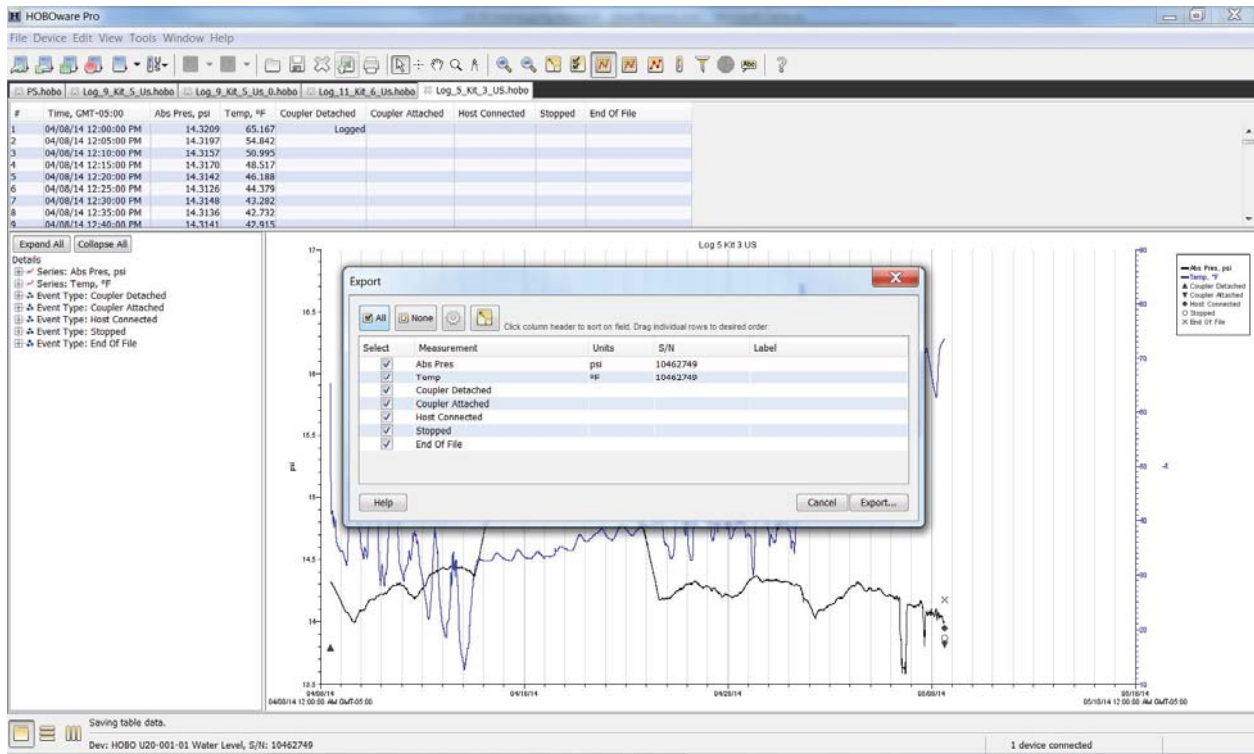


Figure 8 Export Data to CSV

**APPENDIX B: ESTIMATED CONSTRUCTION COSTS OF SELECTED
EMBANKMENT EROSION STABILIZATION TECHNIQUES**

Table B.1. Estimated construction costs of selected embankment stabilization and erosion prevention techniques. Tested techniques are highlighted in light gray. Refer to table end notes.

Stabilization Technique	Cost per SY	Data Sources	Notes
Bare Soil	\$ -	--	Prepared final grade
Vegetation	\$ 0.19	(1)	Per 2014 MnDOT Seeding Manual "Method 1", 2575.502 Seed Mixture 25-141 "Mesic General Roadside" \$4.10/lb @ 59lb/acre, 2575.501 Seeding @ \$190.70/acre, 2575.511 Mulch Type 1 \$178.58/ton @ 2 tons/acre, 2575.508 Fertilizer Type 1 \$0.57/lb @ 200lb/acre
Erosion Control Blanket - Category 3	\$ 1.61	(1)	2575.523 Erosion Control Blanket - Category 3
"Armored Sod" new install without ECB	\$ 2.38	(1), (2), (3), (6)	Geogrid \$1.52/SY, geogrid instal est. \$0.75/SY, "Vegetation" minus mulch
Erosion Control Blanket - Category 4	\$ 1.86	(1)	2575.523 Erosion Control Blanket - Category 4, "Vegetation" minus mulch
Turf Reinforcement Mat - Category 3	\$ 3.45	(1)	2575.525 TRM Category 3, "Vegetation" minus mulch
"Armored Sod" (Tech 1) as tested with ECB	\$ 4.13	(1), (2), (3)	2575.523 Erosion Control Blanket - Category 4, geogrid+installation, "Vegetation" minus mulch

(Continued on the following page)

Table B.1 (Continued)

Stabilization Technique	Cost per yd ²	Data sources	Notes
Turf Reinforcement Mat with Fiber Reinforced Matrix (Tech 2) as tested	\$ 4.63	(1), (3)	2575.525 TRM Category 3, 2575.562 Hydraulic Matrix Type Fiber Reinforced @3,900lb/acre, "Vegetation" minus mulch
Extended Bituminous Shoulder Paving (Partial Slope Paving)	\$ 6.50	(4)	paving the inslope down 4 feet from the shoulder P.I. (est. current from 2012 bid prices)
"Armored Sod" (Tech 1A) Real Sod as tested	\$ 8.58	(1), (2), (3)	Geogrid + install, 2575.505 Sodding Type Lawn
"Armored Sod" alt. Chainlink Fence in place of Geogrid	\$ 20.11	(1)	2557.603 Install Chain Link Fence assume 4ft ht @ \$8.11/LF, 2575.523 Erosion Control Blanket - Category 4, "Vegetation" minus mulch
Random Riprap - Class III	\$ 30.64	(1), (4)	2511.501. Assume 18" thick
Matrix Grouted Riprap	\$ 34.88	(5)	Bid costs 2011-2015, weighted unit costs, assume 18" thick.
Flexible Concrete Geogrid Mat (Tech 3) as tested	\$ 49.23	(6)	"Flexamat Plus"
Precast Articulated Concrete (3604)	\$ 57.65	(4)	3604. 2011 bid price, not adjusted.
Articulated Block Mat Open Cell Type C	\$ 98.49	(1)	2515.501 Articulated Block Mat Open Cell Type C
Concrete Slope Paving	\$134.91	(1)	2514.501 Concrete Slope Paving
Fully Grouted Riprap	\$155.00	(1)	2515.51. Assume 18" thick
<p>Notes:</p> <p>(1) MnDOT "Average Bid Prices for Awarded Projects, English Units - Spec Year 15" dated 4/28/2015, http://www.dot.state.mn.us/bidlet/avgPrice/142014.pdf</p> <p>(2) Installation cost estimated</p> <p>(3) Supplier invoice for project (qty. 1 roll each)</p> <p>(4) Personal communication (email) from J.T. Anderson, MnDOT, 3/11 & 3/22/2016</p> <p>(5) Personal communication (email) A. Hendricks, MnDOT, 3/28/2016</p> <p>(6) Brock White online catalog 6/10/2016</p>			